Dissertation zur Erlangung des Doktorgrades
der Fakultät für Chemie und Pharmazie
der Ludwig-Maximilians-Universität München

Development and Thermo-analytical Studies of New Environmentally Friendly, High-Performance and Stable Solid Propellant Formulations Based on New High-Energy Dense Oxidizers

Mohamed Abdelghany Abdelhameed Mohamed Hussien

Aus

Kairo, Ägypten

2018

Erklärung

Diese Dissertation wurde im Sinne von §7 der Promotionsordnung vom 28. November 2011 von Herrn Prof. Dr. Thomas M. Klapötke betreut.

Eidesstattliche Versicherung

Diese Dissertation wurde eigenständig und ohne unerlaubte Hilfe erarbeitet.

München, den 4. Dezember 2018

_____

Mohamed Hussien

Dissertation eingereicht am	12.10.2018
1.Gutachter:	Prof. Dr. Thomas M. Klapötke
2.Gutachter:	Prof. Dr. Konstantin Karaghiosoff
Mündliche Prüfung am	28.11.2018

Danksagung

Zunächst möchte ich mich bei Professor Dr. Thomas M. Klapötke bedanken, der mir die Möglichkeit gegeben hat, in seiner Gruppe an meiner Doktorarbeit zu arbeiten, und für seine Unterstützung und seine unkomplizierte Art, alle Probleme ohne Schwierigkeiten zu lösen.

Diese Arbeit stellt nicht nur meine eigene Arbeit dar, sie ist ein Meilenstein in der langjährigen Forschung in den Energetischen Materialien der Arbeitsgruppe von Prof. Dr. Klapötke an der Ludwig-Maximilians Universität München. Die Ziele meiner Forschungsarbeit und der damit verbundenen Publikationen wurden durch die wertvolle Anleitung und Unterstützung meines Betreuers Prof. Dr. Thomas M. Klapötke und der anderen Gruppenmitglieder sowie einiger anderer Freunde aus Algerien und Ägypten ermöglicht.

Ich danke Oberst Dr. Ahmed I. Elbeih aus Ägypten für seine Unterstützung und für viele Anregungen zu wissenschaftliche Arbeiten und für unsere intensiven wissenschaftlichen Diskussionen.

Professor Dr. Konstantin Karaghiosoff "Conny" danke ich sehr, dass er als “Co-Schiedsrichter” dieser Arbeit zur Verfügung steht. Ich bin sehr dankbar für die zahlreichen Abende, die er beim Röntgen verbrachte, um die endlose Anzahl von Kristallen zu messen.

Mein Dank gilt auch Prof. Dr. Andreas Kornath, Prof. Dr. Ingo-Peter Lorenz, Prof. Dr. Jürgen Evers und Prof. Dr. Christian Ochsenfeld, die mir als Prüfer zur Verfügung stehen.

Mein besonderer Dank gilt Dr. Jörg Stierstorfer für seine Hilfe und Unterstützung bei der Anwendung der High-Speed-Kamera und der thermogravimetrischen Analysetechnik sowie für seine seriöse und unkomplizierte Art, die Probleme zu lösen.

Vielen Dank auch an Dr. Burkhard Krumm für seine Vorschläge und die Durchführung der NMR, sowie die Zusammenarbeit an einer gemeinsamen Publikation.
Ich möchte auch Frau Irene S. Scheckenbach dafür danken, dass sie die beste Sekretärin der Welt ist und für ihre Hilfe bei jeder Art von Bürokratie.

Im Einzelnen möchte ich mich bei Ihnen bedanken:

- Dr. Marc Bölter für all seine Unterstützung und Hilfe im Labor und im normalen Leben. Er ist einer der besten Kollegen, die mir in meinem Leben begegnet sind. Ich werde ihn nie vergessen.

- Dr. Johann Glück für eine unvergessliche harte Zeit beim Skifahren in Österreich zusammen mit Dr. Bölter.
- Max Born für seine Unterstützung und hilfreiche Anregungen, die mir bei der Lösung einiger Vorbereitungsprobleme geholfen haben.
- Das tolle Team von D3. 110: Marc Bölter, Max Born, Maurus Völkl und Jelena Reinhardt für die tolle Atmosphäre in unserem Labor.
- Stefan Huber für die Messung von Empfindlichkeitswerten unzähliger Proben und für die Versorgung mit Chemikalien.
- Die ganze Arbeitsgruppe und alle Freunde in der Chemieabteilung. Ich danke euch alle für die tolle Zeit! Vor allem möchte ich mich bei meinen Eltern und meiner Familie bedanken, die nie aufgehört haben, an mich zu glauben und für ihre kontinuierliche Unterstützung in allen Bereichen meines Lebens.

Ich kann nicht mit Worten beschreiben, wie dankbar ich bin!

Acknowledgement

First of all, I would like to express my great thanks to Professor Dr. Thomas M. Klapötke, for giving me the opportunity to undertake my PhD thesis within his group, as well as for all his support and his uncomplicated manner of solving problems without any difficulties.

This thesis represents not only my own work; it is a milestone in many years of research in the Energetic Materials of the group of Prof. Dr. Klapötke in Ludwig-Maximilians-University of Munich. The objectives of my research work and related publications have been achieved thanks to the valuable guidance and support from my supervisor Prof. Dr. Thomas M. Klapötke and the other group members. Some friends from Algeria and Egypt have also helped me a lot.

I am indebted to Col. Dr. Ahmed I. Elbeih from Egypt for his support to giving me many suggestions for several scientific papers, as well as for our scientific discussions.

I am grateful to Professor Dr. Konstantin Karaghiosoff "Conny" for agreeing to act as the co-referee of this thesis. I am very thankful for the numerous evenings; he spent at the X-ray diffractometer measuring endless numbers of crystals.

I am also indebted to Prof. Dr. Andreas Kornath, Professor Dr. Ingo-Peter Lorenz, Professor Dr. Jürgen Evers and Professor Dr. Christian Ochsenfeld for agreeing to act as examiners in my defense.

I would like to give a special thanks to Dr. Jörg Stierstorfer for all his help and support using the High-Speed Camera and Thermogravimetric Analysis technique and for his professional and efficient manner in solving problems.

Many thanks also to Dr. Burkhard Krumm for his suggestions and for measuring NMR samples, as well as for his co-operation on a co-author paper.

I would also like to thank Ms. Irene S. Scheckenbach for being the best secretary in the world and for her help with every kind of bureaucracy.

In addition, I would like to express my thanks to:

- Dr. Marc Bölter for all his support and help in the laboratory and in normal life. He is one of the best colleagues that I have encountered in my life. I will never forget him.

- Dr. Johann Glück for the unforgettably hard time during skiing in Austria together with Dr. Bölter.
- Max Born for his support and useful suggestions that helped me to solve some synthesis problems.
- The great team of D3.110: Marc Bölter, Max Born, Maurus Völkl and Jelena Reinhardt for the all-time great atmosphere in our lab.
- Stefan Huber for measuring the sensitivity values of countless samples and for ordering chemicals.
- The whole work group and all my friends in the chemistry department. Thank you all for a really great time! Above all, I would like to say “thank you” to my parents and my family who never stop believing in me and for their continuous support in every aspect of my life.

I cannot describe in words how grateful I am!

Contents

List of Figures

Figure No. **Title** **Page No.**

List of Tables

Table No. **Title** **Page No.**

Nomenclatures

Symbols

A	Pre-exponential factor
E_a	Activation energy
***f*(α)**	Differential form of reaction models
g(α)	Integral form of reaction models
k	Rate constant
m_f	Sample mass at the end of reaction
m_o	Initial sample mass
m_t	Sample mass at time t
n	Order of reaction
R	Universal gas constant (J/mol.K)
t	Time
T	Temperature
α	Extent of reaction
β	Heating rate

Abbreviations

AN	Ammonium nitrate
AP	Ammonium perchlorate
BCHMX	1,3,4,6-tetranitrooctahydroimidazo-[4,5-d]imidazole
BTNEOx	Bis(2,2,2-trinitroethyl)-oxalate
CL-20 or HNIW	2,4,6,8,10,12-hexanitro-2,4,6,8,10,12-hexaazaisowurtzitane
CSRP	Composite Solid Rocket Propellants
CTPB	Carboxy terminated polybutadiene
DMA	Dynamic Mechanical Analysis
DOA	Dioctyl adipate
DOS	Dioctyl sebacate
DOZ	Dioctyl azelate
DSC	Differential Scanning Calorimetry
DTA	Differential Thermal Analysis

DTG	Differential Thermogravimetry
GAP	Glycidyl Azide Polymer
HMDI	Hexamethylene Diisocyanates
HMX	1,3,5,7-Tetranitro-1,3,5,7-tetrazocane
HTPB	Hydroxyl-terminated polybutadiene
IPDI	Isophorone diisocyanate
KAS	Kissinger-Akahira-Sunose
MAPO	Tris-1-(2,MethylAziridinyl) Phosphine Oxide
RDX	1,3,5-Trinitro-1,3,5-triazinane
TDI	Toluene diisocyanate
TGA	Thermogravimetric analysis
TMA	Thermo-mechanical Analysis
TNENC	2,2,2-trinitroethyl-nitrocarbamate
TNEF	2,2,2-trinitroethyl formate

Preliminary Objectives of this Thesis

Energetic materials (Explosives, Propellants and Pyrotechnics) are used extensively in civil as well as military fields and have a wide range of applications [1-4]. Research and development in the field of energetic materials focuses on different aspects in order to fulfill the requirements, which depend on the use of the energetic material in different applications. Initially development started by searching for better performing substances, and later, also energetic materials with reduced sensitivity had to be taken into account. Over the past decades, a large number of high-energy materials for various applications have been developed, which show improved performance and lower sensitivity [5]. Nowadays, there are strict requirements for energetic materials, which must show better performance, lower sensitivity and higher thermal stability, as well as being environmentally friendly and also safe to handle during manufacturing and usage. However, these requirements are somewhat mutually exclusive. The energetic materials having high performance usually exhibit high sensitivity and bad thermal stability and vice versa.

This thesis focuses on solid propellants, which have a wide range of applications in tactical rockets, intercontinental- and submarine-based ballistic missiles, space launcher boosters, airplane ejection seats, and even amateur hobby rockets. Solid propellants typically fall into one of two broad categories namely, *homogenous* (double-base) propellants and *heterogeneous* (composite) propellants. Double-base propellants consist of nitrocellulose (NC) as a fuel plasticized with nitroglycerine (NG) as an oxidizer. Composite propellants consist mainly of an oxidizer (normally, ammonium perchlorate AP) that is bound by a polymeric matrix and some metallic fuel (normally aluminum powder Al). The investigation of new high-energy dense oxidizers (HEDOs), specifically with the aim of finding a suitable candidate that can overcome the tremendous impact sensitivity of NG and the toxicity of $HCl_{(g)}$ (which is produced from the combustion of AP) was the main objective of this thesis. In addition, a further goal was to study the thermal behavior of its propellant formulations. It was not easy to find a suitable candidate, which fulfilled all of these requirements.

Introduction

1 Definition of Energetic Materials

When many people hear or read the words “energetic materials”, the first things that come to their minds are war and destruction. Other people however think about satellites and how the missile can overcome gravity, and they dream about flying to the moon and discovering the universe. Other people think about festivals and the wonderful colors and shapes of fireworks that are often used on such occasions. Based on these different points of view, it can be concluded that energetic materials have different applications and consequently have different definitions.

Politzer and Murray defined energetic materials as follows: “*Energetic materials encompass different classes of chemical compositions of fuel and oxidant that react rapidly upon initiation and release large quantities of force (through the generation of high-velocity product species) or energy (in the form of heat and light)*” [6]. While the American Society of Testing and Materials (ASTM) defines energetic materials as “*a substance or a mixture of substances which contains the oxidizer and the fuel at the same time and is therefore capable to react readily under the liberation of large amounts of heat and gaseous reaction products without any external reaction partner*” [7].

Baily and Murray state that the legal definition in Great Britain is given in the Explosives Act of 1875, where an explosive is “*a substance used or manufactured with a view to produce a practical effect of explosion*” such as gunpowder, nitroglycerin and TNT [8]. Meyer and Köhler gave the following definition to an explosion itself “*An explosion is a sudden increase in volume and release of energy in a violent manner, usually with generation of high temperatures and release of gases. An explosion causes pressure waves in the local medium in which it occurs*” [4]. Many people think that energetic materials are just explosives, however the definition of Politzer and Murray is a more comprehensive definition of energetic materials.

2 History of Energetic Materials

It is widely reported that the first people who discovered energetic materials were the Chinese people, who are said to have discovered black powder as early as 200 A.D. The earliest record however, can be found in the Chinese military manual "Wu Jing Zong Yao" dated 1044 A.D [6]. Black powder is an energetic material formulation, which consists of

charcoal, potassium nitrate and sulfur. The Chinese formula reached Europe in the 13th century, and by 1327 A.D., the Europeans were firing bombards. Francis Bacon, who published the formula in the West, was so impressed by its awesome power that he speculated man would give up starting wars when he saw the terror of black powder [6]. Although the first use of black powder was as a war tool, in the 1600's, black powder was used for the first time in Hungary for mining [9]. Black powder was the standard formulation in use for a couple of centuries. However, it had some disadvantages such as the production of large amounts of smoke during combustion. By the mid-nineteenth century, nitration reactions had been discovered and the combination of alcohols with mixed acid (sulfuric and nitric) resulted in the formation of highly flammable, if not explosive, species [10].

Braconnot discovered nitrocellulose (NC) or "gun cotton" in 1833, which was subsequently patented by Schonbein in 1846. Sobrero tried to nitrate liquid glycerin using nitric acid in 1846 and he found that a true reaction took place. Hence, nitrocellulose (NC) and nitroglycerin (NG) were discovered within a decade of each other, but neither found widespread use until the 1860's when methods of stabilizing them were devised [6, 11]. Due to the extreme sensitivity and danger of nitroglycerin, Sobrero believed that his invention couldn't be used commercially. However, Alfred Nobel who had good personal contact with Sobrero searched for a solution to overcome the sensitivity of nitroglycerin. Nobel found a way to reduce the sensitivity of NG by adsorbing it on the surface of diatomaceous earth and called it "Dynamite" [2]. This invention was as a revolution in the field of energetic materials and made Nobel a rich man. He thought that his invention would help the people and cause an industrial revolution through the use of dynamite in the coalmines and railway tunnels. However, after seeing the disastrous results of his invention, he decided to collect all his money and found a prize that is given to people, who have helped humankind the most in the previous year, which is called now the "Nobel Prize" [12].

In 1880, Hepp prepared pure 2,4,6-Trinitrotoluene (TNT) as a pure substance by the nitration of toluene with mixed nitric and sulfuric acid. Claus and Becker were able to determine its structure in 1883. In the early 20^{th} century, TNT became the standard explosive during WW I [2]. The reputation of TNT has also spread widely in the civil filed, especially in the field of mining and in the construction of roads between the mountains. It has become the most famous and extensively used explosive. TNT has a large difference in its melting and decomposition temperatures, which gives it the advantage of being able to be used easily in different kinds of munitions using the casting technique [13, 14]. Unfortunately, TNT shows

some stability problems during storage since it usually contains some other isomers and impurities which are not easy to remove. This makes that it does not comply with modern insensitive munition (IM) requirements [2]. For this reason, the development and synthesis of new energetic materials has become the main target for many researchers to improve both the thermal stability and sensitivity of the final charges, but without affecting the performance [15-18]. Many new energetic materials have been synthesized like, for example but not limited to, 1,3,5-trinitro-1,3,5-triazinane (RDX), 1,3,5,7-tetranitro-1,3,5,7-tetrazocane (HMX), 2,4,6,8,10,12-hexanitro-2,4,6,8,10,12-hexaazaiso-wurtzitane (CL-20), 1,3,3-trinitroazetidine (TNAZ), cis-1,3,4,6-tetranitro-octahydroimidazo-[4,5-d]imidazole (BCHMX) and dihydroxylammonium 5,5′-bistetrazole-1,1′-diolate (TKX-50) [4, 19-28] and the competition still continues.

3 Classification of Energetic Materials

Energetic materials can be classified into three main categories, which are Explosives, Propellants and Pyrotechnics. Each category can be further divided into sub-classes as shown in Figure 1.

3.1 Primary Explosives

These materials are characterized by:

- Detonation reaction with moderate velocity, about 4000 m s^{-1} but with very high acceleration.
- High sensitivity (easily initiated) to different initiating impulses (flame, impact, friction,...).
- Used to initiate other explosive materials of low sensitivity. Hence they are used for the production of all types of initiators, primers, primer screw, detonators, detonating capsules,…etc.
- Examples:

  $Hg(CNO)_2$.....Mercury fulminate $Pb(N_3)_2$…….Lead Azide

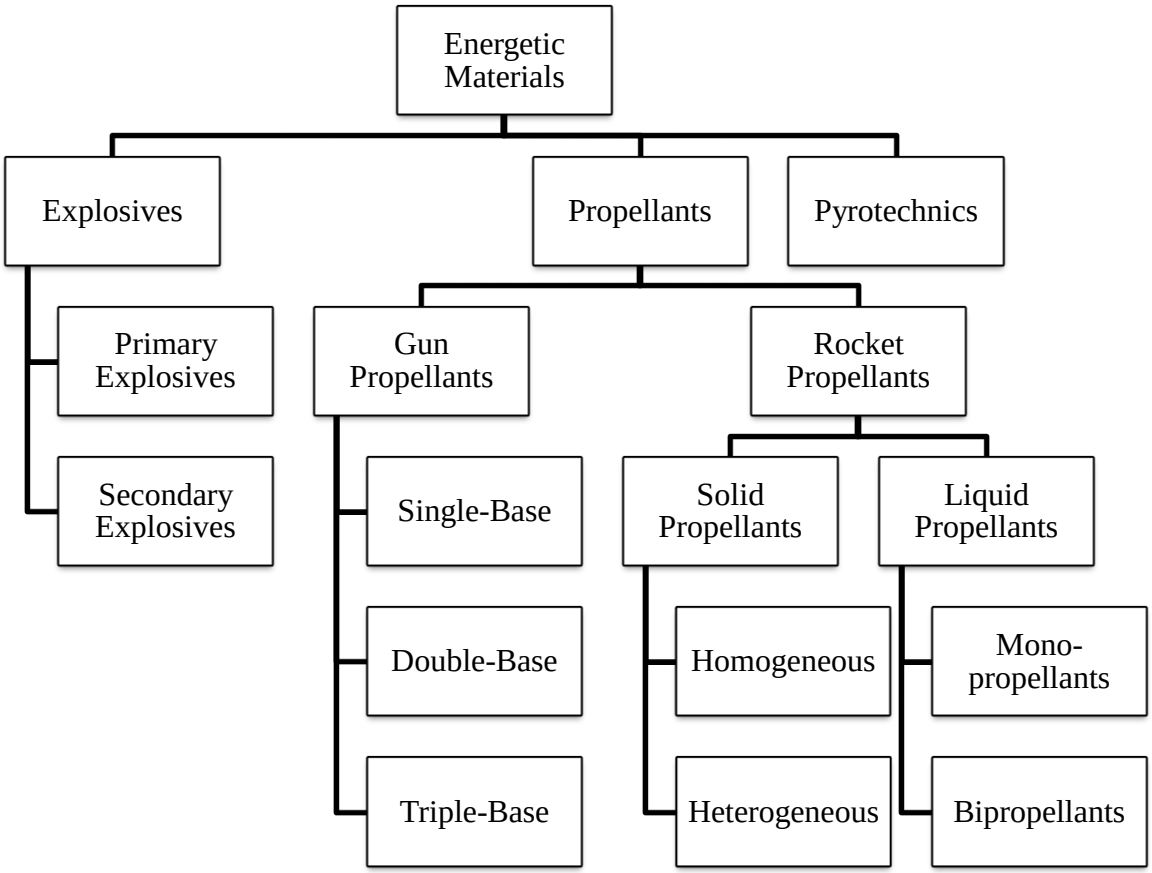

Figure 1. Classification of Energetic Materials.

3.2 Secondary Explosives (High Explosives)

These materials are characterized by:

- Very strong detonation reaction.
- Velocity of detonation about 5-10 km s^{-1}.
- Act as a source of highly energetic gases.
- Less sensitive towards external stimuli.

High explosives can be used in military and industrial applications. The industrial high explosives are used in blasting work or demolition in both the military and civilian sectors. They are used for the blasting of rocks (mine work, bench blasting, tunneling, digging of trenches,...) and common examples are Dynamite, Ammonium Nitrate/Fuel Oil (ANFO) and TNT [29-32]. The military high explosives are used for filling all types of artillery shells, rocket warheads, hollow charge ammunitions, all types of mines, and for the production of blasting charges and detonating fuses. These materials can be used in the pure state, in phlegmatized state, and as mixtures with other energetic components [33, 34]. Hexogen,

1,3,5-trinitro-1,3,5-triazinane (RDX), which is also known as cyclonite, is currently one of the most important high explosives worldwide for both military and civil applications [35]. HMX (1,3,5,7-tetranitro-1,3,5,7-tetrazocane) is an explosive with a high melting point and molar mass of 296.2 g mol^{-1}, which exists in four polymorphic modifications (α, β, γ, δ) which are most likely conformational modifications. Each of the four can be obtained by crystallization from a different solvent while maintaining a different rate of cooling of the solution [36].

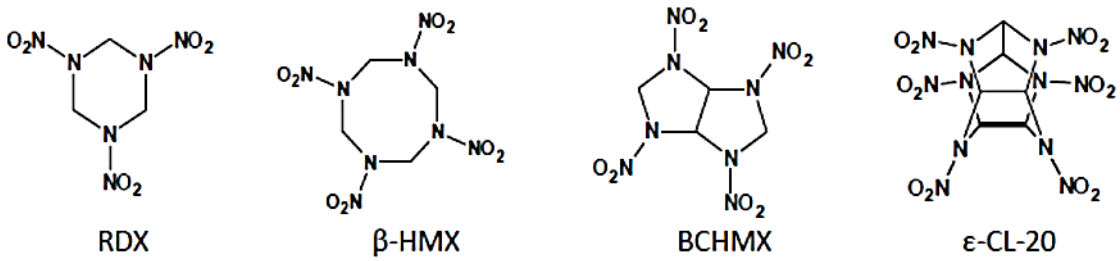

Figure 2. Molecular structure of some cyclic nitramines.

Currently, polycyclic nitramines are increasingly gaining importance as prospective highly energetic materials. The main features of importance are their high density and high performance, but with no significant increase in their sensitivity to mechanical stimuli. BCHMX (cis-1,3,4,6-tetranitrooctahydroimidazo-[4,5-d]imidazole) is one example of such a promising compound and which is predicted to possess a higher density than HMX [37]. During the 1980's very intense efforts were dedicated to find an economically feasible chemical procedure to obtain this energetic material in larger amounts. Despite the extensive work which was undertaken, it was only possible to prepare small quantities of BCHMX by a 5-stage process involving expensive reagents and offering very low yields [38, 39]. Recently, BCHMX has been obtained by an unpublished, novel, two-stage method, which produces BCHMX in fair yields with >98% purity (checked by HPLC) [40]. Within the last few years, much research has been published which investigates the application of BCHMX as a highly energetic material. It has been shown that the replacement of PETN by BCHMX in Semtex explosives results in a decrease in the friction sensitivity, enhanced thermal stability of Semtex 10, while the impact sensitivity remains approximately the same [41]. BCHMX has been studied as explosive filler with PIB binder (C4, polyisobutylene plasticized by dioctyl Sebacate, DOS, and oily material) to replace RDX [16], and with Viton

A to replace HMX [42]. Furthermore, the thermal behavior and decomposition kinetics of BCHMX with different thermoplastic polymeric matrices were studied [43-49].

In view of its superior performance, 2,4,6,8,10,12-hexanitro-2,4,6,8,10,12-hexaza-isowurtzitane (HNIW), popularly known as CL-20, is considered today to be the most powerful explosive. It belongs to the family of polycyclic-cage nitramines, and has four stable polymorphs (α, β, ε, γ) which are known to exist under ambient conditions [22]. The ε-polymorph has high symmetry and has the highest density (2.04 g cm^{-3}) among the four polymorphs. Due to its high detonation parameters and performance [50, 51], it can be regarded as a next generation high-energy material. The high performance of CL-20 can be traced to its strained cage structure which has six -NO_2 substituents. Hence CL-20 is 20% more powerful than HMX [52].

Table 1. Characteristic properties of some high explosives

Explosives	RDX [4]	HMX [4]	BCHMX [44]	CL-20 [4]
Chemical Formula	$C_3H_6N_6O_6$	$C_4H_8N_8O_8$	$C_4H_6N_8O_8$	$C_6H_6N_{12}O_{12}$
Oxygen Balance (ΩCO_2)	-21.6	-21.6	-16.3	-9.5
Density (g cm^{-3})	1.82	1.91	1.86	2.04
Impact Sensitivity (N m)	7.5	7.4	2.98	4
Friction Sensitivity (N)	120	120	88	48
Detonation velocity (m s^{-1})	8750	9100	9050	9800

A new class of high explosive compositions known as “Plastic Bonded Explosives, PBXs” has found use and a wide field of application in the production of “Insensitive High Explosive munitions”. A PBX is an explosive material bound by a polymeric material and other ingredients. The resulting PBX mixture shows very low sensitivity to different types of impulses, as well as to battle field dangers (bullets, fragments, detonation wave shock, fire,…). The first PBX was developed in Los Alamos National Laboratory in 1947. In this PBX, the binders that were used contained a plasticizer to improve the mechanical properties of the product. Polyurethanes are the most widely used polymers in current PBX formulations. PBXs are insensitive and good processing explosives that can be safely formed into different shapes with the required dimensions.

3.3 Pyrotechnics

This class of energetic materials is characterized by a burning reaction which usually produces a small amount of gases. It is a heterogeneous mixture of fuel (metal powder, metal alloy or organic matter) and inorganic oxidizer. These compositions have different military and civilian applications and can be used as: Tracers, Flares, smock agents, incendiaries, delay elements, heating mixtures, illuminating compositions, signaling shots,….etc [53-55].

3.4 Propellants

Propellants are a class of energetic materials, which are used in the production of a pressurized gas that is subsequently used to propel a vehicle, projectile, or other object. Common propellants consist of a fuel and an oxidizer. Usually propellants are burned (or otherwise decomposed) to produce the propellant gas. Some rare examples of propellants are simply liquids that can readily be vaporized to produce thrust [56]. Propellants can be divided into two groups: Gun propellants, which mainly have military applications, and rocket propellants, which have many civilian and research applications in addition to military applications [1, 57, 58]. Gun propellant (Powder) charges are ignited and burned completely and instantaneously in the cartridge case (Figure 3), which remains inside the barrel, and produce large amounts of gaseous products, which give the projectile (Bullet) a high kinetic energy, to deliver it from the barrel to its target as is shown in Figure 4. On the other hand, Rocket propellant charges are burned layer by layer and produce gaseous products, which exit the missile combustion chamber from the nozzle, during the flight of the missile on its trajectory.

Gun propellants are all based on Nitrocellulose (NC) as the basic energetic ingredient in the powder. There are three main types of gun propellants (powders):

- Single-base powder (SBP).
- Double-base powder (DBP).
- Triple-base powder (sometimes called cold powder) (TBP).

Table 2 illustrates the composition of these powders.

Table 2. Compositions of NC-Powders [59]

Component	Designation			
	IMR	M1	M2	M15
Nitrocellulose, NC (13.15 N%)	93.3	85.0	77.5	20.0
Nitroglycerine, NG	---	---	19.5	19.0
Nitroguanidine, NGu	---	---	---	54.0
Stabilizer (Diphenylamine)	0.7	1.0	0.6	6.0
Dinitrotoluene	---	10.0	---	---
Other additives	6.0	4.0	2.4	1.0

IMR Single-base powder
M1 Single-base powder (+DNT; if DNT is considered to be an explosive, it could be considered to be a DBP)
M2 Double-base powder (NC+ NG)
M15 Triple-base powder (NC+ NG+ NGu)

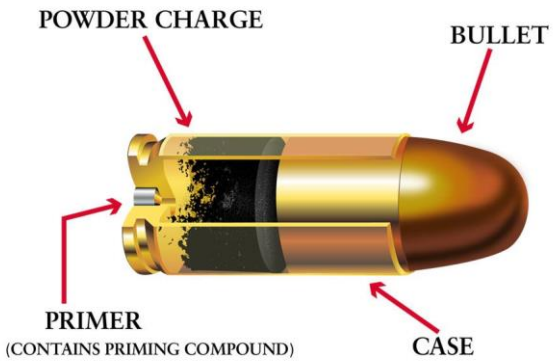

Figure 3. Construction of Bullet 9 mm Pistol [60].

Figure 4. Gun Propellants (Powders) firing mechanism [61].

Rocket Propellants can be divided into solid and liquid rocket propellants. Liquid propellants can be further sub-classified into monopropellants and bipropellants as shown in Figure 1. A monopropellant is a single liquid that contains both the oxidizer and fuel [62]. Despite its

high toxicity, hydrazine (N_2H_4) is the most commonly used monopropellant nowadays [63]. Bipropellants consist of two separately stored liquids (fuel and oxidizer), which in a react hypergolic manner when they come into contact with each other. For this system, two separate storage tanks are required, and the fuel and oxidizer are injected into a combustion chamber continuously in a controlled manner but only when the motor is fired. Therefore, it is possible to control the propulsion by controlling the amount of liquids, which are sprayed into the combustion chamber. This is considered to be one of the big advantages of liquid propellants. However, the complicated system design and the large space that the tanks require inside the rocket engine are considered to be big disadvantages.

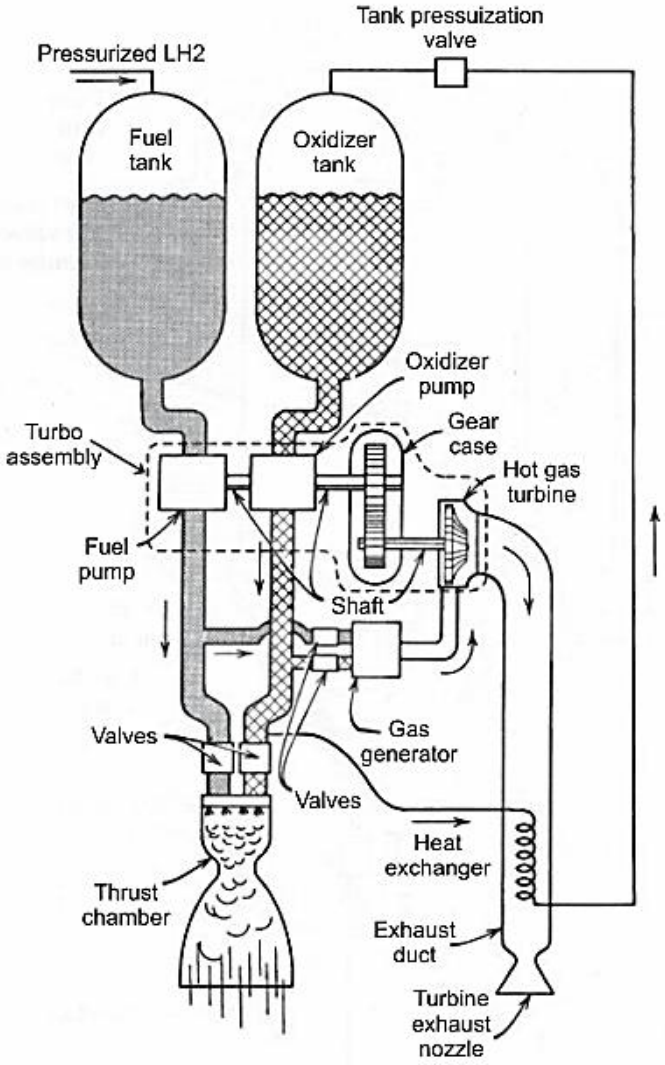

Figure 5. Simple diagram of liquid propellant engine containing a turbo-pump feed system and gas generator [64].

Solid rocket propellants are preferred over liquid and hybrid propellants, because of their reliability, simplicity, ready-to-use system availability and the lower costs of the propulsion

system [65, 66]. Solid rocket propellants can be categorized into homogeneous (double-base) propellants and heterogeneous (composite) propellants. Homogeneous (double-base) rocket propellants mainly consist of an energetic polymer (nitrocellulose, NC) plasticized with a nitric ester (nitroglycerin, NG). Unfortunately, this propellant formulation undergoes continuous slow decomposition. The decomposition products released in the decomposition process increase the decomposition rate and lead to self-accelerating behavior. Chemical stability additives (stabilizers) e.g. diphenylamine (DPA) are added to prevent this autocatalysis process. Some additives are also added to simplify the manufacture usually a plasticizer is added in the range of about 0-10% (e.g. dioctyl phthalate (DOP)) to NG in the casting solvent as it reduces the friction and impact sensitivity. Other additives for specific operations (flash suppressant additives e.g. zirconium oxide, zirconium silicate) can also be added. The manufacturing process of double-base rocket propellants occurs by one of two production methods: Casting or Extrusion processes [67, 68].

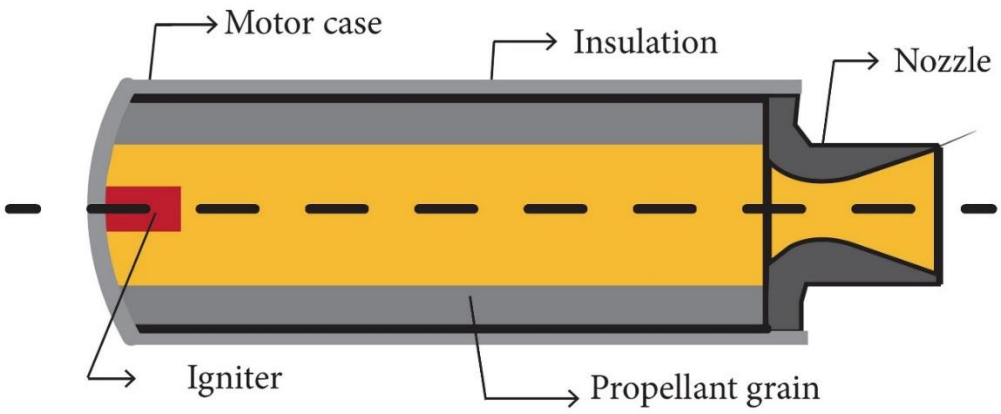

Figure 6. Solid propellant thrust system [69].

Since it is sometimes necessary to increase the energy level of the propellants in order to fulfill some special needs and requirements, some energetic additives, such as ammonium perchlorate (AP), Aluminum powder (Al) or some nitramines such as RDX or HMX can also be added to form so-called composite modified double-base propellants (CMDB) propellants [70].

Heterogeneous (composite) propellants (or so-called composite solid rocket propellants (CSRP)) mainly consist of an oxidizer (ammonium perchlorate, AP) bonded by a polyurethane matrix based on hydroxyl-terminated polybutadiene (HTPB) and a metallic fuel (aluminum, Al) powder [71]. In 1972, a new series of what is called energetic binders

such as glycidyl azide polymer (GAP), poly 3-nitratomethyl-3-methyloxetane (poly NIMMO) and poly 3, 3-Bis 3-azidomethyl oxetane (Poly BAMO), appeared enhancing the properties of composite rocket propellants to a great extent [72]. Table 3 shows the typical ingredients of composite solid rocket propellants.

Table 3. Typical ingredients of composite solid rocket propellants [73]

Type		Weight (%)	Examples
Oxidizer		0-70	Ammonium perchlorate (AP) Ammonium nitrate (AN)
Metal fuel		0-30	Aluminum (Al)
Burning rate modifiers		0.2-3.0	Iron oxide
Fuel Binder	Prepolymer	0-18	Hydroxy terminated poly butadiene (HTPB) Carboxy terminated poly butadiene (CTPB) Glycidyl azide polymer (GAP)
	Curing agent	1.0-3.5	Isophoron Diisocyanate (IPDI) Hexamethylene Diisocyanate (HMDI)
	Plasticizer	0-7	Dioctyl azelate (DOZ) Dioctyl sebacate (DOS) Dioctyl adipate (DOA)
	Bonding agent	> 0.5	Tris-1-(2,MethylAziridinyl) Phosphine Oxide (MAPO) Toluene Diisocyanate (TDI)

Metal fuel: The most commonly used metallic fuel is Al (although it does not give the highest energy), since the propellants containing Al are safer than other metallic fuels during handling and transportation. In addition, Al is cheap and readily available in comparison with other fuels. The main disadvantage of Al containing propellants however are the smoke exhausts and the presence of some solid particles in the plume.

Burning rate modifier: These additives accelerate the decomposition of the oxidizer by lowering its decomposition temperature. Iron oxides, copper chromite and organic by-products of copper, iron, chromium, or boron are used as accelerators [74]. ***Prepolymer:*** Prepolymers are viscous liquid substances. The prepolymer must be a liquid during the preliminary phase of preparation. Binder elements must have low volatility in order to

withstand the high vacuum during mixing. Furthermore, they must be chemically compatible with the oxidizer, in order not to cause a temperature increase that would result in an exothermic reaction leading to the unwanted auto-ignition of propellant. Once it is cured, the binder should lend its properties to the propellant. ***Curing agent:*** Curing agents are used to form longer chains of the prepolymer as well as to interlock the formed chains, and therefore affect the mechanical properties of the produced propellants. The most commonly used curing agents are IPDI and HMDI [73]. ***Plasticizer:*** Plasticizers are used to reduce the viscosity in order to facilitate processing, and also affect the mechanical properties of the produced propellant (increasing strain). The most commonly used plasticizers are dioctyl azylate (DOZ), dioctyl sebacate (DOS) and dioctyl adibate (DOA), and these should be compatible with the prepolymer [73]. ***Bonding agent:*** The main task of the bonding agent is to improve the mechanical properties, and to prevent the settling of solid ingredients of the composite solid rocket propellant. The most commonly used bonding agent is Tris-1-(2, Methyl Aziridinyl) Phosphine Oxide (MAPO). A good bonding agent must satisfy the following demands; Ability to rapidly coat the solid particles, compatibility with the crosslinking agent used and enhancement of the mechanical properties [73]. ***Oxidizer:*** They should supply oxygen to burn the binder and the metal fuel. The most commonly used oxidizer in CSRP is ammonium perchlorate (AP), which has a high oxygen balance, is readily available, cheap and is thermally highly stable [75-78]. Although AP has all these advantages, AP-based propellants contaminate the atmosphere by releasing hydrochloric acid (HCl) as an exhaust product. Moreover, the soluble perchlorate anion (ClO_4^-) is considered to be a contaminant source. Ammonium perchlorate has long been used in the defense industry as an oxidant in solid propellants and explosives. The primary sources of soil and groundwater contamination with perchlorate are related to the production of the compound for aerospace and military applications [79]. The United States Food and Drug Administration has detected perchlorate in food crops and milk [80]. Perchlorate is highly soluble in water, and relatively stable and mobile in surface and subsurface aqueous systems [81]. The low volatility and high solubility of perchlorate make many treatment technologies such as ultra-filtration, air stripping, carbon adsorption, and advanced oxidation either ineffective or uneconomical. Furthermore, the smoke trail caused by AP is a very serious tactical disadvantage, because it adversely affects guidance and control systems [82]. A consequence of all these disadvantages is that many researchers worldwide are working intensively to develop new replacement oxidizers for AP, which fulfill the increasing

requirements expected of solid rocket propulsion systems such as: enhanced performance, improved thermal stability and negligible environmental effects during manufacture, processing, handling, transport, storage, usage and disposal.

4 New High Energy Dense Oxidizers

The currently most promising chlorine-free oxidizers are ammonium dinitramide (ADN), which was first synthesized in 1971 in Russia, as well as the nitroformate salts hydrazinium nitroformate (HNF) and triaminoguanidinium nitroformate (TAGNF) [83]. Although ADN would solve the toxicity problems of AP, since ADN has completely green (chlorine-free) decomposition products, its lower thermal stability constitutes another challenge. ADN thermally decomposes at 127 °C and melts at 91.5 °C [84]. Ammonium nitrate (AN) proved to be a very interesting oxidizer to many researchers and scientists [85, 86]. AN begins decomposition at the melting process at 169.9 °C with complete decomposition at 210 °C [86]. The new big challenge with AN is that it is hygroscopic and shows phase transitions from one polymorph to another at -16.9 °C, 32.3 °C, 84.2 °C and 125.2 °C [2]. To overcome these phenomena and problems, researchers and scientists have invested much time and effort to search for other suitable replacement candidates that can achieve these requirements.

5 Thermal Analysis Techniques

Thermal analysis focuses on the effect of changing the temperature on different properties of a given material, including the mass, dimension, volume ...etc. The thermal decomposition provides an important and valuable reference when investigating the stability and safety of energetic materials [87]. Thermal analysis techniques can also be used to compare the stability of different types of energetic materials [46-49, 88]. The thermal behavior and decomposition kinetics of energetic materials can be determined either isothermally or non-isothermally using different thermal analysis techniques. A list of the most common thermal analysis techniques is presented in Table 4.

Table 4. Common thermal analysis techniques

Technique	Abbreviation	Detected Property	SI units
Thermogravimetric Analysis	TGA	Mass (mass loss)	mg
Differential Scanning Calorimetry	DSC	Enthalpy (heat flow)	mW
Differential Thermal Analysis	DTA	Temperature (temperature difference)	K
Thermomechanical Analysis	TMA	Mechanical properties (length variation)	mm
Dynamic Mechanical Analysis	DMA	Mechanical properties (elasticity)	Pa

5.1 Thermogravimetric Analysis (TGA)

TGA is a technique in which the mass of a substance is measured as a function of temperature while the substance is subjected to a controlled temperature program. Materials can be heated in the temperature range from ambient to 1600°C at rates of fractions of a degree per minute up to 100°C min^{-1}. Samples are usually 1-20 mg in weight. Different atmospheres can be used, from inert gases such as nitrogen, to reactive gases such as oxygen, hydrogen and air [89]. TGA can be used for studying the mass changes, adsorption, absorption, dehydration, vaporization, sublimation, oxidation, reduction, solid-gas reactions or the general thermal decomposition. TGA can be employed using two experimental approaches, namely isothermal and dynamic (non-isothermal) approaches. The isothermal approach involves rapid heating of the material sample to a specific temperature and monitoring the mass change as a function of time while maintaining the temperature constant. On the other hand, for the dynamic approach, the sample is heated at a constant rate over the decomposition reaction temperature range. In differential thermogravimetry (DTG) the actual measurement signal appears as a derivative plot of the weight loss or gain which aids in the accurate assignment of the end and beginning points for overlapping reactions which often appear as combined peaks in TGA.

5.2 Differential Scanning Calorimetry (DSC)

DSC is a technique in which the difference in energy input into a substance and a thermally inert reference material is measured as a function of temperature, while the substance and reference materials are subjected to a controlled temperature program. DSC operating temperatures range from -180 °C to 750 °C. Some of the monitored physical changes are melting, crystallization, fusion, liquid crystal transitions, vaporization, sublimation and polymer glass transition [89]. Chemical changes, which can be monitored are dehydration, decomposition, oxidative reactions, solid-state reactions, combustion, polymerization, curing and catalyzed reactions.

5.3 Differential Thermal Analysis (DTA)

DTA is a technique in which the temperature difference between the substance and a thermally inert reference material is measured as a function of the operating temperature. The tested substance and the reference material are subjected to a controlled temperature between -120°C and 1800°C. Physical and chemical changes (processes) are monitored [90].

5.4 Thermomechanical Analysis and Dynamic Mechanical Analysis (TMA & DMA)

TMA measures the changes in the physical dimensions of the sample as a function of temperature under a given fixed external load or stress. The dimensional change is generally measured in one direction (the length of the sample) with respect to the applied load [91]. In the absence of the external load, the changes in dimensions can be related to the thermal expansion coefficients. TMA can therefore be used to measure the expansion, compression, softening point, bending properties and extension of the tested material. DMA employs an oscillating load. Deformations of the sample are measured as a function of the time, temperature, load, and frequency. Tension or extension probes are used for measuring extension or shrinkage in thin films and fibers. The tension holder consists of a pair of grips, clamps or hooks. One of them is fixed and the other is moveable to pull the sample in tension under load. The range of loads is 0.1–200 g, forces of 0.1–100 N may be selected and the furnace temperatures may be programmed from -150 °C to 1000 °C. Samples of various sizes and shapes may be tested (length: 1-50 mm and diameter: ~ 10 mm). These instruments must be calibrated for both temperature and dimensional motion.

6 Theoretical Study of Decomposition Kinetics

Many transformations may occur when a sample of solid energetic material is heated, such as melting, sublimation, polymorphic transformation and degradation. The transformations involving weight or enthalpy changes are of high interest as their kinetics can be studied by the common thermal analytical methods. When a process involves a weight loss, the kinetics can be studied via the thermogravimetric analysis (TGA). When heat is evolved or consumed kinetic evaluation could be done via the differential scanning calorimetry (DSC) or the differential thermal analysis (DTA); the weight loss or the heat flow data can be converted to a normalized form by calculating the fractional conversion (α) which varies from 0 to 1 and expresses the reaction progress. For the isothermal processes, the fractional conversion at any time can be defined as follows:

$$\alpha_t = \frac{m_0 - m_t}{m_0 - m_f} \quad (1)$$

Where, m_0 is the initial sample weight, m_t is the sample weight at time, t, and m_f is the final sample weight. For the non-isothermal processes the fractional conversion at any temperature can be defined as follows:

$$\alpha = \frac{m_0 - m_T}{m_0 - m_f} \quad (2)$$

Where, m_T is the sample weight at temperature T.

There are two different computational methods that can be used for analyzing the solid-state decomposition kinetics data, the namely model-fitting and the isoconversional (model-free) methods as is illustrated in Figure 7.

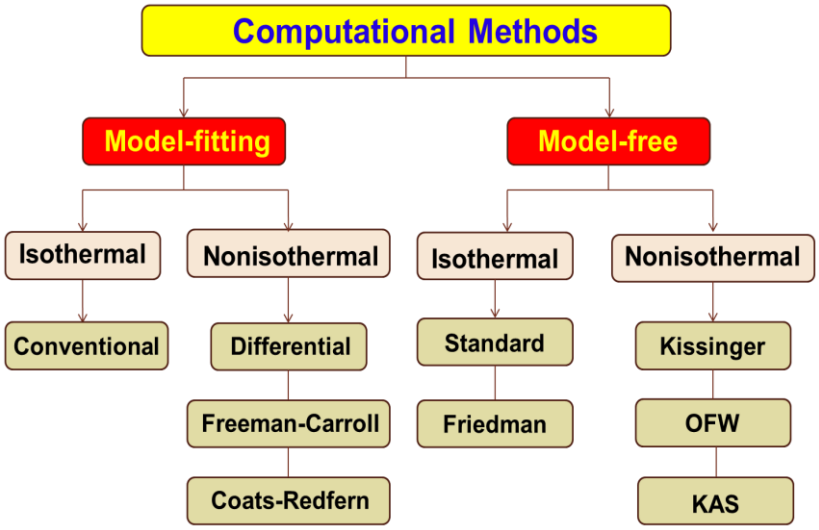

Figure 7. Computational methods for studying solid-state kinetics.

6.1 Model-fitting Methods

There are many models, which can be applied to the collected data to select the model giving the best statistical fit. The activation energy (E_a) and frequency factor (A) can be subsequently calculated. The conventional isothermal model-fitting method involves two types of fit: the first, determines the rate constant (k) according to the model of the best fit with eq. (3), while the second determines the conventional kinetic parameters such as the activation energy (E_a) and the frequency factor (A) according to the Arrhenius equation as written in eq. (4).

$$g(\alpha) = kt \tag{3}$$

$$k = Ae^{\frac{-E_a}{RT}} \tag{4}$$

6.2 Isoconversional (model-free) Methods

In these methods, the frequency factor is grouped with the model and the slope leads only to the activation energy (E_a). These methods require several kinetic curves to perform the analysis and therefore have been called “multi-curves” methods [92, 93]. Calculations from several curves are performed at the same value of conversion (α), thus the name isoconversional. As a result, the activation energy at each conversion point ($E_{a\alpha}$) is obtained. The isoconversional plot (E_a vs. α) can be used to analyze both the isothermal and the nonisothermal data as follows:

Isothermal isoconversional Methods

These methods utilize the isothermal rate law and include the following isoconversional methods:

- **Standard Isoconversional Method**

This method can be derived by taking the logarithm of the isothermal rate law and rearranging it to give:

$$-\ln t = \ln\left(\frac{A}{g(\alpha)}\right) - \frac{E_a}{RT} \quad (5)$$

The plot of -ln t versus 1/T for each α results in the activation energy corresponding to values of "α" regardless of the kinetic model adopted [94, 95].

- **Friedman Isoconversional Method**

This method is a differential method and was one of the first isoconversional methods. The logarithm of the isothermal rate law gives:

$$\ln(\frac{d\alpha}{dt}) = (\ln(Af(\alpha)) - \frac{E_a}{RT} \quad (6)$$

ln (dα/dt) is plotted versus 1/T for each α and the corresponding activation energy is to be found from the slop [96].

Nonisothermal Isoconversional Methods

Unlike isothermal data, the nonisothermal data involve the use of the temperature integral. The following methods of analysis are used in this work:

- **Kissinger Method**

Kissinger proposed a method for analysis of the reaction-order models ($f(\alpha)=(1-\alpha)^n$). According to this method, the maximum reaction rate occurs when the second derivative is zero and therefore;

$$\frac{E_a\beta}{RT_m^2} = A(n(1-\alpha)_m^{n-1})e^{\frac{-E_a}{RT_m}} \quad (7)$$

Where, β is the heating rate, T_m and α_m are the values corresponding to this rate.

The peaks of DSC or DTG indicate this condition. Taking the natural logarithm of (eq. 7) and rearranging, the following equation can be obtained;

$$\ln\frac{\beta}{T_m^2} = \ln\left(\frac{AR\left(n(1-\alpha)_m^{n-1}\right)}{E_a}\right) - \frac{E_a}{RT_m} \quad (8)$$

The activation energy (E_a) can be obtained by plotting the left-hand side of eqn. (8) versus $1/T_m$ for a series of runs at different heating rates.

It is worth noting that Kissinger's method can be considered as one of the model-free methods since it does not require any modelistic assumptions to calculate the activation energy (E_a). However, it is not an isoconversional method as it does not calculate E_a values at selected values of α, but only assumes a constant activation energy, and therefore cannot detect reaction complexities [97-99].

- **Ozawa, Flynn and Wall (OFW) Method**

Ozawa, Flynn and Wall independently developed an isoconversional calculation method for analyzing the nonisothermal data. It is commonly referred to as the OFW method. Taking the common logarithm of the nonisothermal rate law and rearranging it, the following equation can be obtained:

$$\log\beta = \log\frac{AE_a}{g(\alpha)R} - 2.315 - 0.457\frac{E_a}{RT} \quad (9)$$

A plot of ln β versus 1/T for each α yields E_a at the selected α regardless of the model [100, 101].

- **The Modified Kissinger-Akahira-Sunose (KAS) Method**

The modified (KAS) method is more accurate than the mentioned Kissinger method [102]. In this method the value of E_a is estimated from the following equation:

$$\ln\left(\frac{\beta}{T^{1.92}}\right) = const - 1.0008\frac{E_a}{RT} \quad (10)$$

A plot of the left hand side of eqn. (10) versus 1/T at each α yields E_a at that α, regardless of the model.

In comparison with the Ozawa-Flynn-Wall (OFW) method, the modified KAS method offers a significant improvement in the accuracy of the E_a values which are obtained. It has been stated that each of the components of a kinetic triplet is associated with some fundamental theoretical concept. E_a is associated with the energy barrier, A with the frequency of vibrations of the activated complex [103], and $f(\alpha)$ or $g(\alpha)$ with the reaction mechanism [104].

7 Summary

The investigation of different new high-energy dense oxidizers in order to find new candidates, which are suitable to replace nitroglycerin (NG) in homogeneous (double-base) propellants to form new smokeless double-base propellant formulations with high performance characteristics, high thermal stability, long shelf-life, environmentally friendly and safe during manufacturing, handling, transportation, safe and operational use was undertaken. Moreover, candidates suitable to replace ammonium perchlorate (AP) in heterogeneous (composite) solid propellants to form new green (chlorine-free) and high performance composite solid rocket propellant formulations were also investigated. Three promising candidates, namely Bis(2,2,2-trinitroethyl)-oxalate (BTNEOx), 2,2,2-trinitroethyl-nitrocarbamate (TNENC) and 2,2,2-trinitroethyl formate (TNEF), were selected based on a literature survey and theoretical calculations by the EXPLO5 V_6.03 code.

Synthesis of the three high-energy dense oxidizers (HEDOs) was performed according to the literature, with the incorporation of some new modifications to the synthetic method in order to improve the purity, increase the yield and decrease the reaction time.

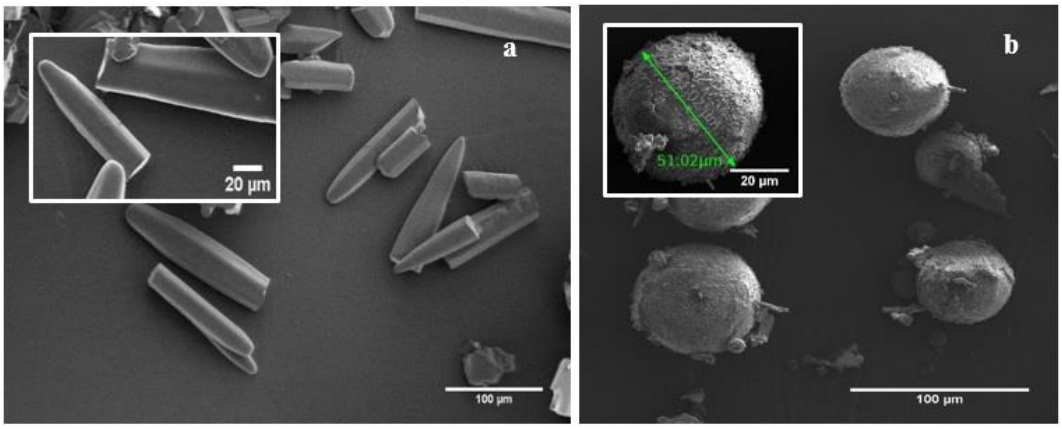

Figure 8. SEM of TNEF a) before and b) after recrystallization.

Preparation of different new smokeless double-base propellant formulations based on nitrocellulose (NC) and the selected oxidizers using casting method was performed. Moreover, preparation of different new green (chlorine-free) composite propellant formulations based on the selected oxidizers and different binder systems, Hydroxyl-terminated polybutadiene (HTPB) and energetic binder glycidyl azide polymer (GAP) has been done.

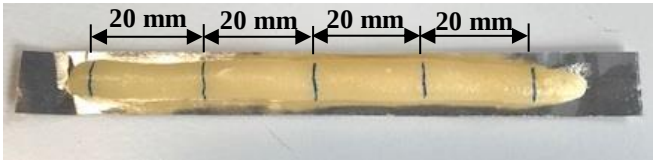

Figure 9. Prepared propellant sample.

The thermal behavior and decomposition kinetics of pure samples of the selected oxidizers and all of the prepared propellant formulations using different thermal analysis techniques and calculation methods were also established.

All the three of the oxidizers showed great results in the formulations for double-base propellants. They formed completely homogeneous propellant formulations and a smokeless burning process. Furthermore, they also demonstrated great thermal stability with decomposition temperatures ~ 202 °C and high performance characteristics. In the case of composite solid rocket propellant formulations, BTNEOx and TNENC showed incompatibility with the binder system due to decomposition and ignition processes, which occurred during the curing process. TNEF however, showed very good results in terms of its compatibility with the two different binder systems, high thermal stability with a decomposition temperature of 210 °C, high burning rate, high activation energy, high performance characteristics and green (chlorine-free) gaseous decomposition products.

Figure 10. Burning of three different new formulations of smokeless double-base propellants.

References

[1] A. Sikder, N. Sikder, *J. Hazard. Mater.* **2004**, 112 (1), 1-15.

[2] T.M. Klapötke, *"Chemistry of High-Energy Materials"*. Berlin: Walter de Gruyter GmbH & Co KG, **2017**.

[3] P.W. Cooper, *"Explosives Engineering"*. New York: Wiley-VCH, **1996**.

[4] R. Meyer, J. Köhler, A. Homburg, *"Explosives"*. Germany: Wiley-VCH, **2007**.

[5] R.W. Shaw, T.B. Brill, D.L. Thompson, *"Overviews of Recent Research on Energetic Materials"*. Singapore: World Scientific, **2005**.

[6] P. Politzer, J.S. Murray, *"Energetic Materials: Part 1. Decomposition, Crystal and Molecular Properties"*. Amsterdam: Elsevier, **2003**.

[7] A. International. (2017). *https://www.astm.org*.

[8] A. Bailey, S. Murray, *"Explosives, Propellants and Pyrotechnics"*. London: Potomac Books Incorporated, **2000**.

[9] T.L. Davis, *"Chemistry of Powder and Explosives"*. New York: John Wiley & Sons, **1941**.

[10] M. Berthelot, *"Explosives And Their Power"*. London: John Murray, **1892**.

[11] B.W. Brodman, M.P. Devine, S. Schwartz, **1977**, US4033798.

[12] G.S. Conway, M. Davies, A. Merry, *Health*, **1996**, 348 1014-16.

[13] S. Thiboutot, P. Brousseau, G. Ampleman, D. Pantea, S. Cote, *Propellants Explos. Pyrotech.*, **2008**, 33, 103-108.

[14] M.L. Chan, A.D. Turner, **1991**, US5009728.

[15] S. Zeman, *J. Hazard. Mater.*, **2006**, 132 (2), 155-164.

[16] A. Elbeih, J. Pachman, W. Trzcinski, S. Zeman, Z. Akstein, J. Selesovsky, *Propellants Explos. Pyrotech.*, **2011**, 36(5) 433-438.

[17] Q.-L. Yan, S. Zeman, R. Svoboda, A. Elbeih, J. Málek, *J. Therm. Anal. Calorim.*, **2013**, 112 (2), 837-849.

[18] A. Elbeih, J. Pachman, S. Zeman, P. Vavra, W. Trzcinski, Z. Akstein, *J. Energ. Mater.*, **2011**, 30 (4), 358-371.

[19] C.W. An, F.S. Li, X.L. Song, Y. Wang, X.D. Guo, *Propellants Explos. Pyrotech.*, **2009**, 34 (5), 400-405.

[20] T.A. Douglas, M.E. Walsh, C.J. McGrath, C.A. Weiss, *J. Environ. Qual.*, **2009**, 38 (6), 2285-2294.

[21] N. Fischer, D. Fischer, T.M. Klapötke, D.G. Piercey, J. Stierstorfer, *J. Mater. Chem.*, **2012**, 22 (38), 20418-20422.

[22] R.L. Simpson, P.A. Utriew, D.L. Ornellas, G.L. Moody, K.J. Scribner, D.M. Hoffman, *Propellants Explos. Pyrotech.*, **1997**, 22 (5), 249-255.

[23] S. Bircher, P. Mader, J. Mathieu, in *29th Int. Annu. Conf. ICT*, Karlsruhe, Germany, **1998**, pp. 1-14.

[24] A. Sikder, N. Sikder, B. Gandhe, J. Agrawal, H. Singh, *Def. Sci. J.*, **2002**, 52 (2), 135-146.

[25] A.K. Sikder, N.R. Sikder, B.R. Gandhe, *J. Hazard. Mater.*, **2004**, 113, 35-43.

[26] A. Elbeih, J. Pachman, S. Zeman, P. Vávra, W.A. Trzciński, z. Akštein, *J. Energ. Mater.*, **2012**, 30 (4), 358-371.

[27] T.M. Klapötke, T.G. Witkowski, Z. Wilk, J. Hadzik, *Propellants Explos. Pyrotech.*, **2016**, 41 (1), 92-97.

[28] J.L. Gottfried, T.M. Klapötke, T.G. Witkowski, *Propellants Explos., Pyrotech.*, **2017**, 42 (4), 353-359.

[29] S. Meyers, E.S. Shanley, *J. Hazard. Mater.*, **1990**, 23 (2), 183-201.

[30] W.B. Sudweeks, *Indust. Eng. Chem. Prod. Res. Develop.*, **1985**, 24 (3), 432-436.

[31] B.T. Fedoroff, O.E. Sheffield, *"Encyclopedia of Explosives and Related Items"*. USA: Picatinny Arsenal Dover, **1960**.

[32] L.K. Gustavsson, N. Klee, H. Olsman, H. Hollert, M. Engwall, *Environ. Sci. Pollut. Res.*, **2004**, 11 (6), 379.

[33] W. Cocroft, D. Jones, S. Wright, E. McAdam, *"Dangerous Energy: The Archaeology of Gunpowder and Military Explosives Manufacture"*. UK: English Heritage Swindon, **2000**.

[34] J.P. Agrawal, *"High Energy Materials: Propellants, Explosives and Pyrotechnics"*. Weinheim, Germany: WILEY-VCH, **2010**.

[35] P.P. Vadhe, R.B. Pawar, R.K. Sinha, S.N. Asthana, A.S. Rao, *Combust. Explos. Shock Waves*, **2008**, 44 (4), 461-477.

[36] T. Urbanski, *"Chemistry and Technology of Explosives"*. Oxford: Pergamon Press, **1984**.

[37] R. Gilardi, J.L. Flippen-Anderson, R. Evans, *Acta Crystallogr.*, **2002**, 58, 0972-0974.

[38] G. Eck, M. Piteau, **1997**, US556032.

[39] J.P. Agrawal, R.D. Hodgson *"Organic Chemistry of Explosives"*. New Delhi: Willey&Sons, **2007**.

[40] D. Klasovity, S. Zeman, A. Ruzicka, M. Jungova, M. Rohac, *J. Hazard. Mater.*, **2009**, 164, 954–961.

[41] A. Elbeih, J. Pachman, S. Zeman, Z. Akštein, *8th Int. Arm. Conf. Sci. Asp. Arm. Safety Technol.*, **2010**, 2, 7-16.

[42] A. Elbeih, J. Pachman, S. Zeman, W. Trzcinski, M. Suceska, *Propellants Explos. Pyrotech.*, **2013**, 38 (2), 238-243.

[43] A. Elbeih, J. Pachman, S. Zeman, W. Trzcinski, Z. Akstein, M. Suceska, *Cent. Eur. J. Energ. Mater.*, **2010**, 7 (3), 217-232.

[44] Q.-L. Yan, S. Zeman, R. Svoboda, A. Elbeih, *Thermochim. Acta*, **2012**, 547, 150-160.

[45] Q.-L. Yan, S. Zeman, J. Selesovsky, R. Svoboda, A. Elbeih, *J. Therm. Anal. Calorim.*, **2013**, 111 (2), 1419-1430.

[46] Q.-L. Yan, S. Zeman, F.-Q. Zhao, A. Elbeih, *Thermochim. Acta*, **2013**, 556, 6-12.

[47] Q.-L. Yan, S. Zeman, A. Elbeih, *Thermochim. Acta*, **2013**, 562, 56-64.

[48] Q.-L. Yan, S. Zeman, T.-L. Zang, A. Elbeih, *Thermochim. Acta*, **2013**, 574, 10-18.

[49] Q.-L. Yan, S. Zeman, A. Elbeih, A. Zbynek, *Cent. Eur. J. Energ. Mater.*, **2013**, 10 (4), 509-528.

[50] S.S. Samuder, U.R. Nair, G.M. Gore, R.K. Sinha, A.K. Sikder, S.N. Asthana, *Propellants Explos. Pyrotech.*, **2009**, 34, 145-150.

[51] U. R. Nair, R. Sivabalan, G. M. Gore, M. Geetha, S. N. Asthana, H. Singh, *Combust. Explos. Shock Waves*, **2005**, 41 (2), 121-132.

[52] X. Jiang, Q. Jiao, H. Ren, T. Sun, *J. Explo. Propellants*, **2011**, 34, 21-24.

[53] J.A. Conkling, C. Mocella, *"Chemistry of Pyrotechnics: Basic Principles and Theory"*. Boca Raton: CRC press, **2010**.

[54] G. Steinhauser, T.M. Klapötke, *Angew. Chem. Int. Ed.*, **2008**, 47 (18), 3330-3347.

[55] H. Ellern, *"Military and Civilian Pyrotechnics"*. New York: Chemical Publishing Company, **1968**.

[56] N. Kubota, *"Propellants and Explosives: Thermochemical Aspects of Combustion"*. Weinheim, Germany: Wiley-VCH, **2015**.

[57] A. Götz, C. Mäding, L. Brummel, D. Haeseler, in *37th Joint Propul. Conf. Exhibit*, Salt Lake City, UT, USA, **2001**, p. 3546.

[58] B. Andrea, F. Lillo, A. Faure, C. Perut, *Acta Astronaut.*, **2000**, 47 (2-9), 103-112.

[59] E. C. Meyer, P.T. Smith, *"General Ammunition"*. Washington, USA: Headquarters, Department of the army, **1969**.

[60] T. Pinsta. **(2017)**. *An Introduction to Rifle and Pistol Ammunition*, Available: http://www.thepinsta.com

[61] M.Scott, **(2012)**. *A Simple Blog About the Kel-Tec P-3AT 380 Semi-Automatic Pistol*, Available: https://keltec-p3at.blogspot.com

[62] P.B. Weill, P.L. Darby, **1977**, US4047988.

[63] Y. Zhang, J.M. Shreeve, *Angew. Chem.*, **2011**, 50 (4), 935-937.

[64] G.P. Sutton, O. Biblarz, *"Rocket Propulsion Elements"*. New Jersey: John Wiley & Sons, **2016**.

[65] L.T. DeLuca, in *"Chemical Rocket Propulsion"*. Switzerland: Springer, **2017**, pp. 1015-1032.

[66] H. Singh, in *"Chemical Rocket Propulsion"*. Switzerland: Springer, **2017**, pp. 127-138.

[67] C.E. Johnson, P.F. Dendor, E.R. Csanady, **1978**, US4102953.

[68] V.R. Grassie, **1960**, US2946673.

[69] A. Adami, M. Mortazavi, M. Nosratollahi, *J. Aeros. Tech. Manag.*, **2017**, 9 (1), 71-82.

[70] L.P. Arthur, **1975**, US3878003.

[71] S. Dixon, B. Tunick, E. Brown, **2004**, US0094250.

[72] A. Provatas, **2000**, (DSTO-TR-0966 Australia).

[73] A. Davenas, *"Solid Rocket Propulsion Technology"*. New York: Pergamon Press, **1992**.

[74] S. Krishnan, R. Jeenu, *J. Propul. Power*, **1992**, 8 (4), 748-755.

[75] N.K. Memon, A.W. McBain, S.F. Son, *J. Propul. Power*, **2016**, 32 (1), 682-686.

[76] Y.-H. Wang, L.-L. Liu, L.-Y. Xiao, Z.-X. Wang, *J. Therm. Anal. Calorim.*, **2014**, 119 (3), 1673-1678.

[77] T. Kuwahara, *Propellants Explos. Pyrotech.*, **2015**, 40 (5), 765-771.

[78] L. Zhang, R. Tian, Z. Zhang, *Aeros. Sci. Tech.*, **2017**, 62, 31-35.

[79] S. Kannepalli, K.W. Farrish, *Inter. J. Environ. Bioremed. Biodegrad.*, **2016**, 4 (3), 68-79.

[80] C.W. Murray, S.K. Egan, H. Kim, N. Beru, P.M. Bolger, *J. Expos. Sci. Environ. Epidem.*, **2008**, 18 (6), 571-580.

[81] US Environmental Protection Agency (USEPA), **(2011)**. *Region 9. Perchlorate in the Pacific Southwest*. Available: www.epa.gov/region9/toxic/perchlorate

[82] W.E. Motzer, *Environ. Foren.*, **2001**, 2 (4), 301-311.

[83] M. Göbel, T.M. Klapötke, *Z. Anorg. Allg. Chem.,* **2007**, 633 (7), 1006-1017.

[84] D.E. Jones, Q.S. Kwok, M. Vachon, C. Badeen, W. Ridley, *Propellants Explos. Pyrotech.,* **2005**, 30 (2), 140-147.

[85] M. Kohga, K. Okamoto, *Combust. Flame,* **2011**, 158 (3), 573-582.

[86] J.C. Oxley, J.L. Smith, E. Rogers, M. Yu, *Thermochim. Acta,* **2002**, 384 (1-2), 23-45.

[87] W. Zhang, Y. Luo, J. Li and X. Li, *Propellants Explos. Pyrotech.,* **2008**, 33, 177-181.

[88] Q.-L. Yan, S. Zeman, A. Elbeih, *Thermochim. Acta*, **2012**, 537, 1-12.

[89] R.A. Meyers, *"Encyclopedia of Analytical Chemistry"*. Chichester: John Wiley & Sons, **2000**.

[90] G.D. Christian, J.E. Reilly, *"Instrumental Analysis"*. Boston: Allyn and Bacon, **1986**.

[91] J.W. Robinson, E.S. Frame, G.M. Frame II, *"Undergraduate Instrumental Analysis"*. New York: Marcl Dekker, **2005**.

[92] J. Zsako, *J. Therm. Anal. Calorim.*, **1973**, 5, 239-251.

[93] J. Zsako, *J. Therm. Anal. Calorim.*, **1996**, 46, 1845–1864.

[94] S. Vyazovkin, *Thermochim. Acta,* **2000**, 355, 155–163.

[95] A. Khawam, D. Flanagan, *Thermochim. Acta*, **2005**, 429, 93–102.

[96] H. Friedman, *J. Polym. Sci. Part C,* **1964**, 6, 183–195.

[97] H.E. Kissinger, *Res. Nat. Bur. Stand.*, **1956**, 57, 217–221.

[98] H.E. Kissinger, *Anal. Chem.*, **1957**, 29, 1702-1706.

[99] S. Vyazovkin, C. Wight, *Thermochim. Acta,* **1999**, 341, 53-68.

[100] T. Ozawa, *Bull. Chem. Soc. Jpn.,* **1965**, 38, 1881-1886.

[101] J.H. Flynn, L.A. Wall, *J. Polym. Sci. Part B,* **1966**, 4, 323–328.

[102] T. Akahira, T. Sunose, *Res. Report Chiba Inst. Technol. (Sci. Technol.),* **1971**, 16, 22-31.

[103] M. Starink, *Thermochim. Acta,* **2003**, 404 (1), 163-176.

[104] M.E. Brown, *"Introduction to Thermal Analysis: Techniques and Applications"* New York: Kluwer Academic Publishers, **2001**.

A Review on Differential Scanning Calorimetry Technique and its Importance in the Field of Energetic Materials

Book Chapter © 2018 Walter de Gruyter GmbH, Berlin/Boston.
Published in *Physical Sciences Reviews* **2018**, 3(4), pp. -. (DOI: 10.1515/psr-2017-0103)

Abstract: Differential scanning calorimetry (DSC) helps to follow processing conditions, since it is relatively easy to fingerprint the thermal behavior of materials. DSC instrument nowadays became a routine technique, which can be found virtually in every chemical characterization laboratory. The sample can be analyzed over a wide temperature range using various temperature programs under isothermal and non-isothermal conditions. It is appropriate to determine the kinetic parameters under non-isothermal conditions. The sample can be in many different physical forms and in various shapes (powder, granules, fiber, etc.). A lot of characterization (step/glass transition, melting, and decomposition temperature, etc.) data can be obtained by easy way and within short time. DSC is very helpful in analysis of energetic materials due to very small amount of material is enough to run the experiment.

Introduction

The branch of material science which known as thermal analysis (TA) is the study of the effect of temperature change on the properties of materials through the investigation of the sample behavior as a function of temperature. Different properties are studied using this method including mass, dimension, stiffness, heat transfer and temperature. TA has a great ability to characterize, quantitatively and qualitatively, a huge variety of materials over a considerable temperature range, which gave it the chance to be accepted as an analytical technique. Many scientists and engineers all over the world use TA in the basic researches and other applications. Many TA books, general and specific, have been published [1-11]. When conducting experiments with thermal analysis, the temperature generally is controlled in a standardized format. This is achieved by keeping, increasing or decreasing the temperature at a constant rate or working with predetermined different temperatures.

Environment is a major key in correctly conducting thermal analysis. The surrounding atmosphere of the element being researched can have strong effects on the technical results.

Most of the common thermodynamics study use an inert gas such as nitrogen, Argon or helium as a surrounding atmosphere for the studied samples, which allow the minimum effect on the heat transfer results within the study. The temperature is controlled in a predetermined way by either a continuous raise or decrease in temperature at a constant rate (linear heating/cooling) or by running a series of determinations at different temperatures (stepwise isothermal measurements). More advanced techniques have been developed which use an oscillating heating rate (Modulated Temperature Thermal Analysis) or modulate the heating rate response to the changes in the system's properties (Sample Controlled Thermal Analysis). In addition to controlling the sample temperature, it is also important to control its surrounding atmosphere.

Differential Scanning Calorimetry (DSC) is one of the most common TA techniques, which has been widely used in various fields all over the world in the last decades. At present, it is very difficult to find ordinary substances and industrial products that have not yet been the purpose of thermal analysis. DSC is a relatively new technique; the first DSC has existed since 1963 by Perkin–Elmer under the name of DSC-1. According to the ASTM standard E473, DSC is a thermoanalytical technique in which the heat flowrate difference into a sample and a reference is measured as a function of temperature, while the sample and reference are maintained at nearly the same temperature throughout the experiment. The acronym DSC can be said on the technique (differential scanning calorimetry) or the measuring device (differential scanning calorimeter). As will be seen from this chapter, there are two different techniques of *DSC, **power compensation DSC***, which was created by Gray and O'Neil at the Perkin-Elmer Corporation in 1963, and ***heat flux DSC,*** which was grew out of differential thermal analysis (DTA) that originates from the works of Le Chatelier 1887, Roberts Austen 1899, and Kurnakov 1904.

The main applications of the DSC technique are in the fields of polymer and pharmaceutical, but also organic and inorganic chemistry have benefited dramatically from the existence of DSC. Some of this applications (not all, but examples) are the easy and fast determination of the degree of purity, glass transition temperature, melting and crystallization temperatures, heat of fusion, heat of reactions, and kinetic determination of chemical reactions, such as curing, thermal degradation, and the kinetics of polymer crystallization [12-15]. Recently, specific DSC instruments are developed for the new DSC users, which are food industry and biotechnology [16-20].

The choice of thermal analysis by DSC is very useful when only a limited amount of sample is available, as only milligram quantities, generally 0.1–10 mg, are needed for the measurements. With development nowadays, newer techniques are introduced within DSC itself, such as; pressure DSC, fast scan DSC, and modulated temperature DSC. Wide range of temperature measurements are also available, which the experiment can be operated at temperatures from -180°C to 700°C with a special liquid nitrogen cooling accessory to achieve the very low end of the temperature range. The heating and cooling processes in DSC must be able to be in a controlled manner. In the modern DSC instruments, automatic intelligent sample changers are available, which permit the unattended analysis of as many as 50 samples or more.

Energetic materials that mainly consist of carbon, hydrogen, oxygen, and nitrogen exposed to slow decomposition processes through the slowly breaking down of the nitro, nitrate, nitramines, etc., in the energetic material molecules. Due to the low-temperature kinetics, as well this influence of other mechanisms gives energy to the molecule such as heat (high temperature storage conditions), light, infrared and ultraviolet radiation, etc. That's make the scientists and researchers to be very interested in the thermal analysis of the energetic materials [21]. The investigation of the thermal behavior and decomposition kinetics of the energetic materials are very necessary and important for the research and development to be able to determine the complicated decomposition reaction mechanism and to find suitable new materials. Thermal analysis is considered the best process to study the thermal decomposition of energetic materials. Nowadays, many scientists and researchers use the most common thermal analysis techniques such as thermogravimetric analysis (TGA), differential thermal analysis (DTA) and differential scanning calorimetry (DSC) isothermally and non-isothermally in the study of the thermal behavior and decomposition kinetics of the energetic materials [22-30].

Theory

The theory of DSC depends on measuring the difference in the heat flow rate ($mW = mJ\ s^{-1}$) between a sample and an inert reference as a function of time and temperature. There are two main instrumentation types of DSC, ***heat flux DSC*** and ***power compensated DSC***. In the heat flux instrument, the same furnace heats both the sample and the reference. The pans of the sample and reference put on a heated thermoelectric disk, made of a Cu/Ni alloy (constantan). The attached thermocouples to the bottom of the sample and reference

positions on the thermoelectric disk are monitoring the differential heat flow into the sample and reference during the changing in the temperature, which is directly proportional to the difference in the thermocouple signals.

The sample temperature that is measured by the alumel/chromel thermocouple under its position is an estimated temperature, because the thermocouple is not inserted into the sample itself, so this temperature accuracy will depend on the thermal conductivity of the sample and its pan, the heating rate, and other factors. Figure 11 shows the schematic of a heat flux DSC with a sample and empty reference pans. The process of the heat flux DSC is based on a thermal equivalent of Ohm's law, which states that current equals the voltage divided by the resistance, so for the thermal analog one obtains:

$$\dot{Q} = \frac{\Delta T}{R} \quad (1)$$

Where $\dot{Q}$ is the heat flow rate, ΔT is the temperature difference between the sample and reference, and R is the thermal resistance of the heat disk.

The DSC heat flow signal is depending on other parameters according to the following equation:

$$\frac{dH}{dt} = C_p \frac{dT}{dt} + f(T,t) \quad (2)$$

Where dH/dt is the DSC heat flow signal, C_p is the sample heat capacity, dT/dt is the heating rate and *f (T,t)* is the heat flow that is function of time at an absolute temperature.

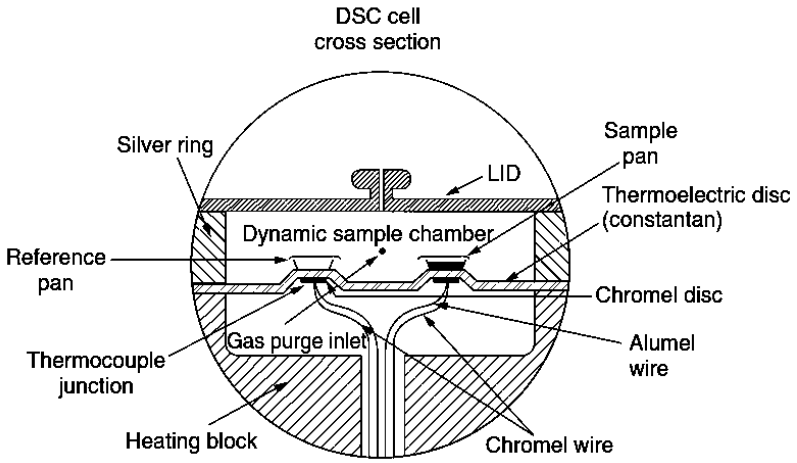

Figure 11. Schematic of a heat-flux DSC. (Courtesy of TA Instruments).

The main difference in power compensated DSC instruments is that there are two separate heating elements are used for the sample and the reference. The sample and reference stay at the same temperature and any change in the temperature between the sample and the reference acts as a signal to "turn on" one of the heaters. When a reaction, phase change, glass transition or similar things occurs in the sample. It becomes a different in temperature of the sample and reference, this leads to an extra power to be directed to the cell at the lower temperature in order to heat it to keep the temperature of the sample and the reference cells as constant ($\Delta T = 0$) throughout the experiment. In this way, the power and the temperatures of the sample and reference are measured accurately and continuously using Pt resistance sensors, shown in Figure 12. The power input difference is plotted vs. the average sample and reference temperature. Power compensation instrumentation provides high sensitivity, high calorimetric accuracy, and high precision, which permit analysis of very small samples.

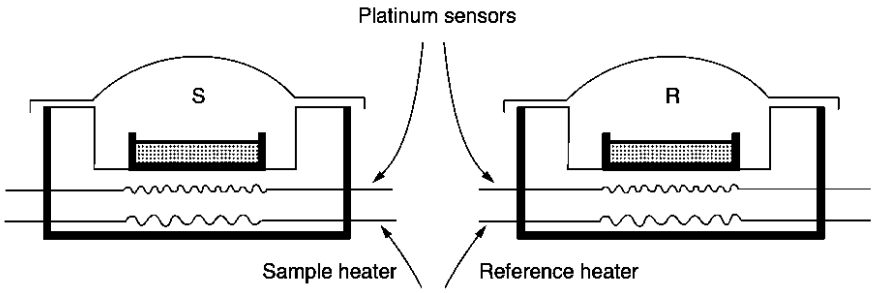

Figure 12. Schematic of a power-compensated DSC (Courtesy of PerkinElmer).

The DSC peak area must be calibrated. The National Institute of Standards and Technology NIST in the US discussed many types of high purity metals and salts that are used to calibrate DSC instruments. As an example, NIST SRM 2232 is a piece of 1 g of high purity indium metal for calibration of DSC and instruments. The fusion temperature of indium SRM is certified to be 156.5985°C ± 0.00034°C and it has a certified enthalpy of fusion equal to 28.51 ± 0.19 J g^{-1}. A range of similar standards is also offered by NIST, these materials and their certified values can be found on the NIST website at www.nist.gov. Other similar reference materials are offered by the government standards organizations in other countries.

Sample Preparation

As mentioned above, using of DSC is very useful in case of only small or limited amount of samples (milligram quantities) are available, a sample of 0.1 – 10 mg is sufficient to run the

experiment. Therefore, it is the best choice for thermal analysis of energetic materials, which minimize the potential risks during the study of the thermal behavior of energetic materials. Preparation of good sample carefully is the first step to obtaining good data. Preparation of samples must account for the fact that these materials are reactive, and care must be taken to avoid premature or unwanted reaction. It is recommended to use fresh prepared samples. The sample should be encapsulated in some kind of a DSC pan that made of high-purity metal (Al, Pt, Au, Ag, Cu, or stainless steel), which is determined according to the sample type. Normally, hermetically sealed pan (Al pan closed with a special pin hole Al lid and crimper cold-welds the bottom and top parts of the pan) is the most common type for various types of energetic materials experiments with a small sample mass (<10 mg), at ambient up to (0.2 MPa) pressure and a temperature range -180°C to 600°C. Pt and gold pans are used when a higher temperature range is required -180°C to 750°C. For the high pressure experiments (up to 20 MPa), thick stainless steel pans and lids with a gold plated copper disk seals "with a special high pressure pan kit" are used in a temperature range of ambient to 300°C (see Figure 13).

Figure 13. Different types of used DSC pans and lids.

The heavy weight of these types of capsules is its main disadvantage; since there are no two capsules have the same mass and the baseline in case of using these capsules is often heavily sloped. Therefore, it is recommended firstly to run a baseline with an empty capsule. The gold platted copper ring and the top should be simply placed on the bottom part without screwed together, then the same pan should be used for the sample run, and the baseline should be subtracted. On the other hand, other special types of capsules are available, such as high-volume DSC capsules, or pans made of other materials, such as graphite pans, which are used for evaluating materials that might alloy with the various metal pans in a temperature range of -180°C to 750°C. Non-oxidizing purge gas (such as Nitrogen) must be used while using such this types of pans.

Figure 14. Hand press kit for DSC pans (Courtesy of TA Instruments).

A dry sample of the required tested energetic material should be precisely weight using four digits analytical balance in a weight range of 0.1 to 10 mg (1-3 mg is recommended for the energetic materials), then it has to be pressed into a suitable pan type accourding to the experiment conditions, as mentioned above, by means of a hand press (see Figure 14). It is very recommended to keep the sample thickness as thin as possible and to cover as much as the bottom of the pan as possible. The upper part of the die set tool is inserted into the upper part of the hand ress kit, then the bottom part of the die set tool is inserted into the bottom part of the hand press kit. The pan with the sample is put on the bottom part of the set tool and the lid is put on it, then press on the hand of the pressing kit one time to make what is called the cold-weld process. The hand of the press kit is returned to its original place and the lower die set is removed with the welded pan.

Current Generation Machines (Not all, but Examples)

Perkin-Elmer as the first company that presented the first DSC device to the light under the name of DSC-1 did not stop at this stage. It keeps to going forward to improve and develop this valuable device, to present nowadays DSC 4000 system, DSC 6000, DSC 8000 and LAB SYS-DSC 8500, which make it to be one of the fiercest competitors in the field of thermal analysis (see Figure 15).

Figure 15. Current different Perkin-Elmer DSC devices.

The DSC 4000 system is one of the current generation machines presented by Perkin-Elmer, which has a temperature range of -100°C to 450°C, and its typical applications are: undergraduate teaching practical, evaluating additives for plastic lifetime optimization and ideal for oxidation induction test. DSC 6000 offers a wide range of temperature from -180°C to 450°C with a scanning rates up to 0.1°C to 100°C that gives it more typical applications such as: Characterizing materials during product process development, trouble-shooting product quality issues and for academic research and post-graduate studies. The more advanced DSC 8000 with a temperature range of -180°C to 750°C and the controlled heating and cooling for the most accurate results give it more advanced typical applications such as: isothermal kinetic studies, process and product improvement "demanding industrial and academic research" and UV curing in polymers. The typical applications for LAB SYS-DSC 8500 are: characterization of pharmaceutical materials, polymorph characterization in pharmaceuticals, process studies in pharmaceuticals and process simulation in plastics. For the thermal study of the energetic materials, it is recommended to use DSC 8000 or higher.
TA Instruments is one of the most important and effective companies in the field of thermal analysis and presents a large variety of thermal analysis techniques such as DSC, TGA, STA, DMA, TMA and VSA. TA Instruments' patented Tzero™ DSC technology, is a revolutionary and fundamentally more accurate way of measuring heat flow. It provides significant improvements in baseline flatness, transition resolution and sensitivity. Tzero™ technology allows direct measurement of heat capacity, and makes Modulated® DSC experiments both faster and more accurate. TA Instruments presents now a new generation of DSC, which is DSC25, DSC250 and DSC2500 (see Figure 16).

Figure 16. Current different TA Instruments DSC devices.

All the three devices offer a wide range of temperature scan from -180°C to 725°C. This is quite enough for the thermal study of the energetic materials, with a differences in temperature accuracy form ± 0.1°C for DSC25 to ± 0.025°C for DSC2500, also the temperature and enthalpy precision which are ± 0.01°C and 0.1% for DSC25 and ± 0.005°C and 0.04% for DSC2500, respectively. No baseline subtractions required for these devices. The main advantage of using these devices is the very high accuracy. DSC2500 also has an advantage of the direct C_p measurement ability, which is not available through other two devices.

Figure 17. Discovery DSC 25P (TA Instruments).

Another new DSC device which are presented by TA Instruments that provides heat flow measurements on pressure sensitive materials is Discovery DSC 25P (see Figure 17). It has a narrower temperature range than the other three devices. From -130°C as a lowest possible temperature that can be reached "with a special cooling accessory" and 550°C as a maximum temperature, but in the same time it offers a pressure range up to 7MPa or 1000PSI, and a

wide varieties of purge gas (N_2, air, O_2, Ar, CO_2, CO, H_2). The Discovery DSC 25P is used to study thermal transitions, chemical reactions and oxidative stability/ decomposition under vacuum, standard atmospheric pressure and elevated pressures. It measures a materials' heat flow in a variety of inert, oxidizing or reducing atmospheres.

In 1873, NETZSCH is founded by Thomas NETZSCH and his brother Christian in Selb/Upper Franconia, Germany. The first products are pump wagons for extinguishing fires and agricultural machines. Now, it grows up and has many branches all over the world Italy, France, USA, Japan, Switzerland, Singapore, Spain, China, Argentina, etc. Now it offers various DSC models (see Figure 18), covering a broad temperature range from -180°C to 1750°C according to the used furnace type (silver, copper, steel, platinum, silicon carbide, rhodium or graphite) and the cooling system (liquid nitrogen, forced air or chilled water).

Figure 18. Current different NETZSCH DSC devices.

All these different DSC instruments operate based on the respective instrument standards as well as application or material testing specifications, including ISO 113587, ASTM E968, ASTM E793, ASTM D3895, ASTM D3417, ASTM D3418, DIN 51004, DIN 51007 and DIN 53765. They work in accordance with the heat-flux principle and feature high detection sensitivity and long service lives, which are ideal conditions for successful application in research and academia, material development and quality control.

DSC 404 *F1 Pegasus* and DSC 404 *F3 Pegasus* are high-temperature DSC instruments, which can be operated from -150°C to 1750°C with heating rates of 0.001 K min^{-1} to 50 K min^{-1}. DSC 204 *F1 Phoenix* can be operated in a temperature range of -180°C to 700°C with a wider range of heating rates from 0.001 K min^{-1} to 200 K min^{-1} and maximum cooling rates 200 K min^{-1}, which make it more suitable for the thermal study of energetic materials. The NETZSCH Photo-DSC 204 *F1 Phoenix* is used mainly for UV curing and its main advantage of light-curing system is their fast reaction time. Monomer solutions that are mostly free of solvents can be cured within only a few seconds and already at low temperatures. That makes it very helpful in studying of plastic bonded explosives (PBXs). The DSC 204 *HP Phoenix* is a high-pressure DSC device, which can be operated under a wide pressure range from vacuum up to 15MPa and within temperature range of -150°C to 600°C, which has varied applications such as determination of vapor pressure and evaporation heat, curing of thermosets and oxidation stability. DSC 214 *Polyma* is more specified for polymer characterization, which operates at very low temperature -170°C, and wide range of heating and cooling rates from 0.001 K min^{-1} to 500 K min^{-1}.

Figure 19. SHIMADZU DSC-60 Plus.

SHIMADZU also is one of the oldest companies that started the manufacture of educational physics and chemistry instruments in Kyoto 1875. Now SHIMADZU DSC-60 Plus competes in the international DSC market, it can be operate under temperature range from -140°C to 600°C with using liquid nitrogen (see Figure 19).

Capabilities

The DSC instruments have a wide capabilities and applications in different fields such as:

- Characteristic temperatures (melting, crystallization, polymorphous transitions, reactions, glass transition).
- Melting, crystallization, transformation and reaction heats (enthalpies).
- Crystallinity of semi-crystalline substances.
- Decomposition, thermal stability.
- Oxidative stability (oxidative induction time OIT and oxidation onset temperature OOT).
- Degree of curing in resins, adhesives, etc.
- Purity determination of low molecular mass compounds.
- Specific heat (c_p).
- Compatibility between components.
- Influence of aging.
- Distribution of the molecular weight (peak form for polymers).
- Impact of additives, softeners or admixtures of re-granulates (for polymer materials).

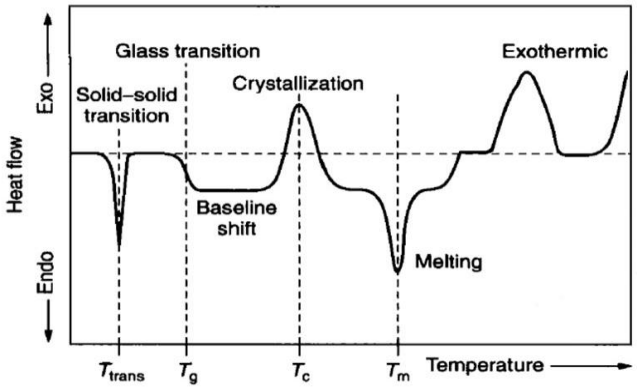

Figure 20. Typical Transitions in a DSC thermogram.

Recently, a lot of scientists and researchers in the field of energetic materials used the DSC to study the thermal behavior and decomposition kinetics of energetic materials through the thermolysis [31-42]. Energetic materials can be existed in different phases; solid, liquid and polymeric matrices like Propellants and PBXs. Studying of thermal behavior and decomposition kinetics of the energetic materials is very important for good characterization and for safety processing and storage. The thermal decomposition kinetics of many PBXs and solid propellant formulations were studied [43-46]. This study became easier by using DSC, which has all the above capabilities (see Figure 20). Moreover, the decomposition kinetic study using DSC technique and different methods of calculations for the decomposition kinetic parameters.

Costs

The price of the device is the most expensive part in the DSC thermal analysis, which is normally starts from €30000, this price is getting higher according to the manufacture company (brand), specifications, and the accessories. Moreover, the price of the pans and lids which are available for one use only. The price of pans and lids is different according to their material. The cheapest and most common pans and lids which are made of Aluminum cost about €200 for the package (100 Al pan & 100 Al lid), which make the DSC sample analysis is more expensive than other thermal analysis techniques like TGA which operate the experiment by one reusable crucible.

Brands

The most common brands in manufacturing of DSC instruments are:

- LINSEIS Thermal Analysis
- TA Instruments
- Perkin-Elmer
- NETZSCH
- SHIMADZU
- Mettler Toledo
- Setaram Instrumentation
- Microcal/Malvern Instruments

Practical Information – "How to perform the technique"

- ***Keeping the DSC cell clean***

One of the first steps to ensuring good data is to keep the DSC cell clean. DSC cell could be contaminated by decomposing samples during DSC runs, samples spilling out of the pan or transfer from bottom of pan to sensor. DSC cell can kept clean by:

- Don't decompose samples in the DSC cell (run TGA to determine the decomposition temperature and stay below that temperature).
- Make sure that the bottom of pans stay clean.
- Use lids.
- Use hermetic pans if necessary "recommended for energetic materials".
- Brush gently the cell if necessary (see Figure 21).
- Blow out any remaining particles.

Figure 21. Cleaning of DSC cell.

- ***Sample Shape***

The shape of the sample in the pan is very important for accurate results; the sample shape should be (see Figure 22):

- Thin as much as possible.
- Cover as much as the bottom of pan as possible.
- Cut sample to make thin, don't crush.
- If pellet, cut cross section.
- If powder, spread evenly over the bottom of the pan.

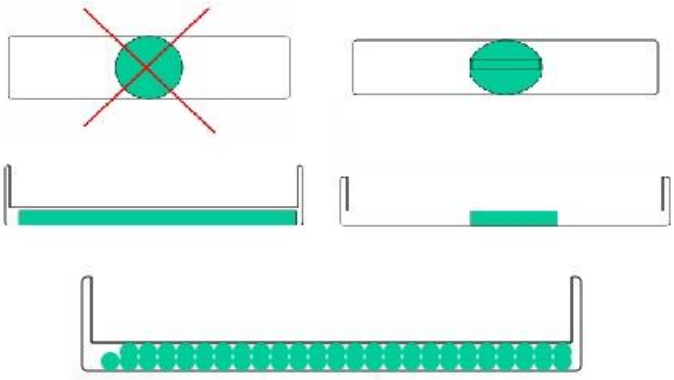

Figure 22. DSC sample shape.

- ***Sample Press***

During sample press, some defects should be avoided:

- Don't over crimp when using crimped pans.
- Bottom of pan should remain flat after crimping (see Figure 23).
- Hermetic pans are sealed by forming a cold-wield on the Aluminum pans.

Figure 23. DSC pan sample press.

- ***Sample Size***

Choosing the sample size is an important factor to get good results; larger samples will increase sensitivity but on the other hand will decrease resolution. The goal is to have heat flow of 0.1 – 10 mW going through a transition. Sample size depends on what you are measuring, so:

- For extremely reactive samples (primary or high explosives), <1mg is much recommended for running sample.
- For other energetic materials, up to 3 mg could be a good choice.
- For organic materials and pharmaceuticals, 1-5 mg is recommended.
- For polymers (inert, e.g. not PBXs), ~ 10 mg is recommended.
- For composites, 15-20 mg is recommended.

- ***Purge Gas***

Purge gas should always be used during DSC experiments to provide dry and inert atmosphere, ensure even heating and help sweep away any off gases that might be released, the most common used purge gases are:

  - Nitrogen: is the most common used purge gas (recommended for energetic materials) with typical flow rate of 50 ml min^{-1}.
  - Helium: has high thermos-conductivity and used with upper temperature limited to 350 °C and typical flow rate of 25 ml min^{-1}.
  - Air or Oxygen: is used to view oxidative effects with typical flow rate of 50 ml min^{-1}.

- ***Sample Temperature Range***

Choosing of experiment temperature range is important for choosing the type of pan and for saving the time. So the instrument temperature range doesn't mean that it should be the same range of the experiment (i.e. if the instrument has a temperature range of -90 °C to 550 °C, it doesn't mean that you need to cool every sample to -90 °C and heat it to 550 °C).

- ***Heating Rate***

Experiment heating rate is very important in each used method due to its effecting on the sensitivity and resolution, that faster heating rates increase the sensitivity but on the other hand, it decreases the resolution. For normal experiments to study the thermal behavior of energetic materials, it is recommended to start the experiment with heating rate of 5 °C min^{-1}, but on the other hand, for deep kinetic study of energetic materials lower heating rates are recommended. For non-energetic materials thermal behavior study, 10 °C min^{-1} is good starting point.

Data Analysis – "How to interpret the results"

The typical DSC curve (thermogram) presents the transition processes for the sample as shown in Figure 20. The first endothermic peak on the thermogram present the solid-solid transition of the material, followed by small endothermic step of glass transition temperature (T_g), then an exothermic peak of crystallization. Most of these transition processes for different energetic materials lies below room temperature. The melting endothermic peak

that is the temperature at which the solid material is melts (T_m) is very important result for characterization of any material and especially for the energetic materials, which can be easily extracted from the DSC thermogram. In most cases, the exothermic peak that followed the endothermic melting peak for pure energetic materials is the decomposition temperature ($T_{dec.}$), and for some polymers, it has a cross-linking (curing) exothermic peak before the exothermic decomposition peak.

The software interfaces nowadays became easier, although each device (brand) has its own software, but also all of these devices software include all the required equations and calculation methods (integration, extrapolation, etc.) to calculate different required parameters. We cannot explain every software, but we take the universal analysis (UA) software that is used by "TA Instrument" as a case study with some screen shots to clarify how to interpret the results.

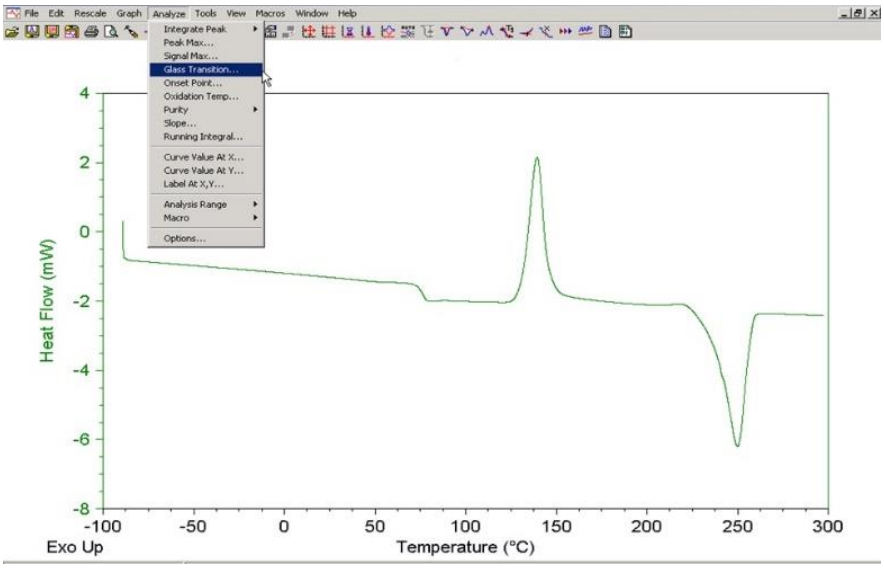

Figure 24. DSC thermogram clarification using UA software (case study).

If we look at Figure 24, we can see a DSC thermogram for a sample with three different changes to the material sample, which from left to right are step/glass transition, exothermic crystallization peak and endothermic melting peak. Let us know how to analyze these phenomena. The step/glass transition analyses are used to calculate the onset, end, inflection and signal change of a step/glass transition in the curve. As shown in Figure 25, the onset is the intersection of the first and second tangents, the inflection is the portion of the curve between the first and third tangents with the steepest slope, and the end is the intersection of the second and third tangents.

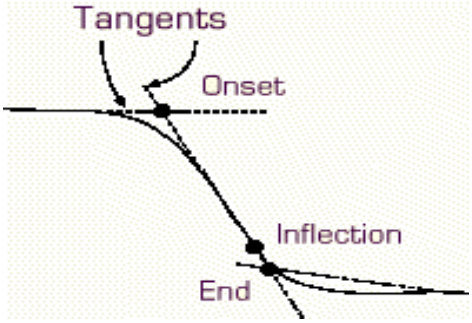

Figure 25. Step/Glass transition analysis.

We can start the analysis by clicking on the analyze icon from the toolbar then click on the glass transition as shown in Figure 24. Then the software take us to pick the limits, which can be easily picked by moving the cursor on the curve and click on the first limit (before the step) and the end limit (after the step). By accepting the limits through clicking on the right mouse button after picking the limits, the glass transition temperature will appear immediately on the curve as shown in Figure 26.

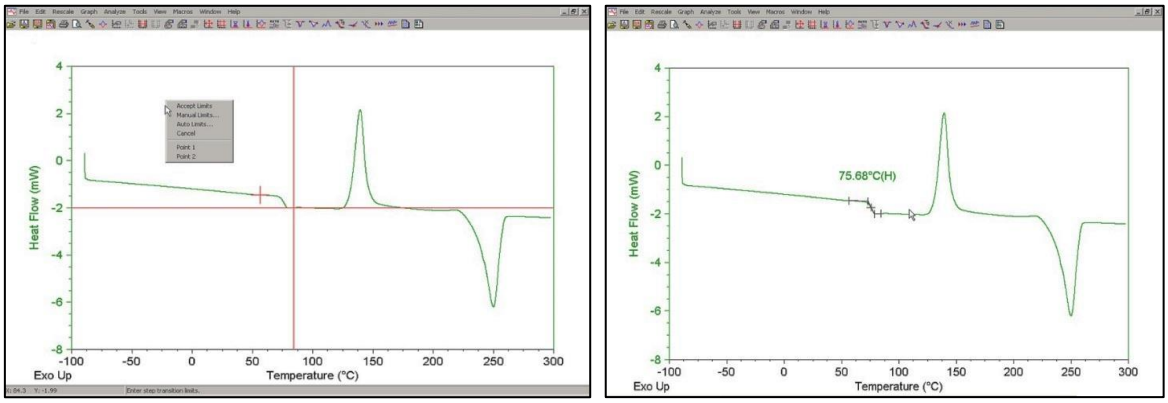

Figure 26. Pickup and accept the limits for step/glass transition.

The steps of analyzing the other two different peaks, which are exothermic crystallization and endothermic melting peaks are in the same way. Starting by clicking on the analyze button on the toolbar and choose the integrate peak then click on linear to take you to the pick and accept limits page on the curve which is doing by the same way as mentioned above and as shown in Figure 27.

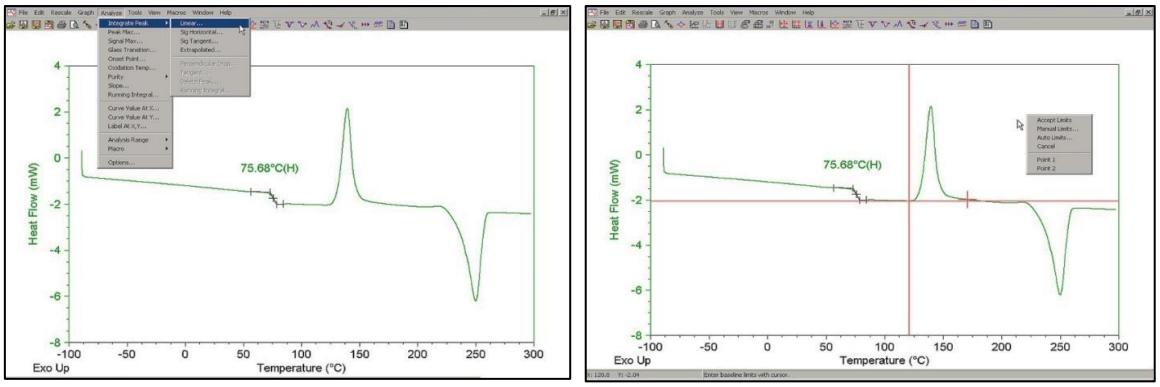

Figure 27. Pickup and accept the limits for peaks.

By clicking on the accept limits button, the peak temperature and the change in enthalpy due to the process will appear on the curve. The change in enthalpy is calculated by integration of the area under the curve and presents in the unit of J g^{-1}. The analyzing of endothermic melting peak can be easily determined by repeating the same steps, which was done for the exothermic crystallization peak. Finally, all the analysis results present on the curve, and then by clicking on the file button, we can choose to save analysis and print it as pdf file from the export data file list as shown in Figure 28.

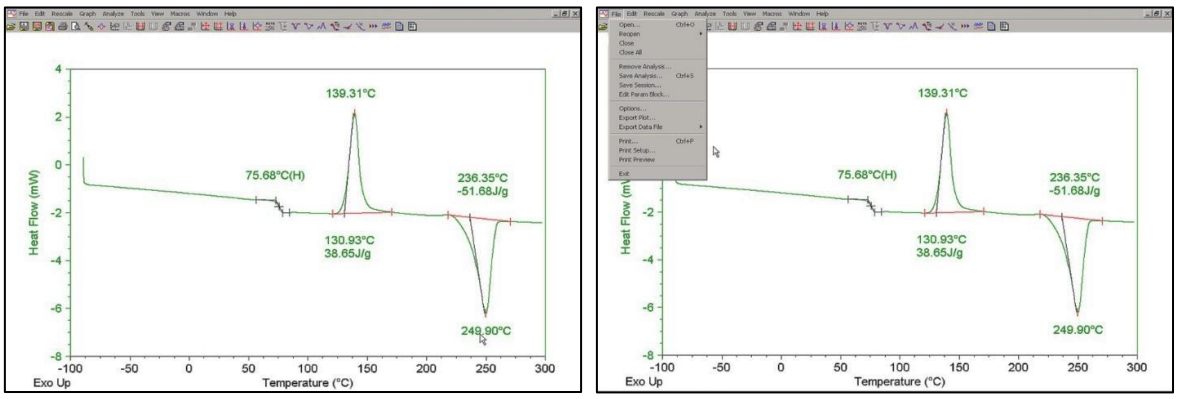

Figure 28. Get results and saving.

The DSC thermogram for one of a relatively new energetic materials which is cis-1,3,4,6-tetranitroocta-hydroimidazo-[4,5-d] imidazole (BCHMX) from a literature study is presented in Figure 29. A solid 0.912 mg sample of BCHMX was spread on an Al DSC pan bottom and was covered by an Al pinhole lid and measured under a dynamic nitrogen atmosphere of 0.1Mpa with heating rate 5°C min^{-1} in a temperature range of 50°C to 300°C. It is shown that there is only one exothermic peak with a peak temperature 249.8°C, which refers to its decomposition, and ΔH=2816 J g^{-1}, with no any endothermic melting peak.

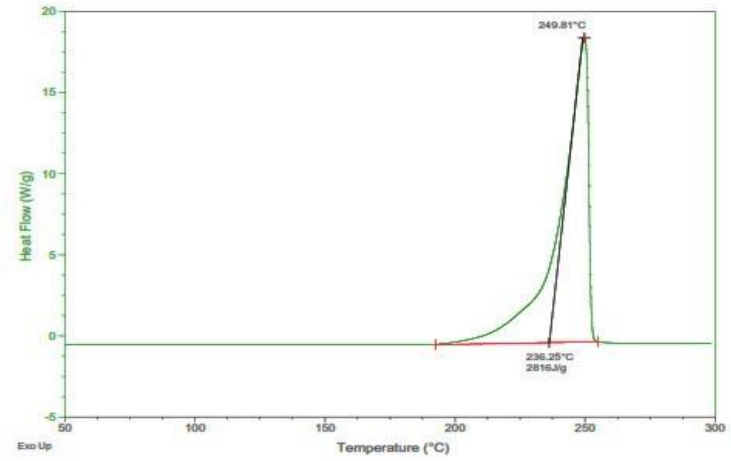

Figure 29. DSC thermogram of BCHMX.

For more deep study, the thermal study should be at a wider range of temperature to determine if there is any other phenomenon for this compound. For the kinetic study, lower heating rates should be used.

Summary

This chapter is designed to provide a general information on differential scanning calorimetry (DSC) and a variety of its applications with focusing on the energetic materials. It includes the theory of working, how to prepare the sample for a good measurement and some examples of the current generation machines. Moreover the device capabilities, average cost for the device and other requirements such as pans and lids, brands and companies that interested in the manufacturing of the DSC devices. Furthermore the experimental procedure and important practical information which should be considered (before, during and after) the run and finally data analysis and explanation of a case study with screen shots to clarify how to interpret the results.

Conclusions

DSC helps to follow processing conditions, since it is relatively easy to fingerprint the thermal behavior of materials. DSC instrument nowadays became a routine technique, which can be found virtually in every chemical characterization laboratory. The sample can be analyzed over a wide temperature range using various temperature programs under isothermal and non-isothermal conditions. It is appropriate to determine the kinetic

parameters under non-isothermal conditions. The sample can be in many different physical forms and in various shapes (powder, granules, fiber, etc.). Many characterization (step/glass transition, melting and decomposition temperature, etc.) data can be obtained by easy way and within short time. DSC is very helpful in analysis of energetic materials due to very small amount of material is enough to run the experiment.

References

[1] W.W. Wendlandt, *"Thermal Methods of Analysis"*. New York: Wiley-Interscience, **1974**.

[2] H.E. Bair, W. Bessey, R. Chartoff, P. Gallagher, A. Hale, M. Jaffe, *"Thermal Characterization of Polymeric Materials"*. London: Academic Press, **1984**.

[3] F. Paulik, *"Special Trends in Thermal Analysis"*. Chichester: John Wiley & Son, **1995**.

[4] R.B. Kemp, *"Handbook of Thermal Analysis and Calorimetry: From Macromolecules to Man"*. New York: Elsevier, **1999**.

[5] T. Hatakeyama, F. Quinn, *"Thermal Analysis: Fundamentals and Applications to Polymer Science"*. Chichester: John Wiley & Son, **1999**.

[6] M.E. Brown, *"Introduction to Thermal Analysis: Techniques and Applications"*. London: Springer, **2001**.

[7] V.S. Ramachandran, R.M. Paroli, J.J. Beaudoin, A.H. Delgado, *"Handbook of Thermal Analysis of Construction Materials"*. New York: William Andrew, **2002**.

[8] B. Wunderlich, *"Thermal Analysis of Polymeric Materials"*. Berlin: Springer, **2005**.

[9] P. Gabbott, *"Principles and Applications of Thermal Analysis"*. Indiana, IN: John Wiley & Sons, **2008**.

[10] P.J. Haines, *"Thermal Methods of Analysis: Principles, Applications and Problems"*. Dordrecht: Springer, **2012**.

[11] S. Gaisford, V. Kett, P. Haines, *"Principles of Thermal Analysis and Calorimetry"*. Cambridge: Royal Society of Chemistry, **2016**.

[12] H.E. Kissinger, *Anal. Chem.*, **1957**, 29, 1702-1706.

[13] E.S. Freeman, B. Carroll, *J. Phys. Chem.*, **1958**, 62, 394–397.

[14] J. Šesták, G. Berggren, *Thermochim. Acta*, **1971**, 3 (1), 1-12.

[15] D. Patil, T. Brill, *Combust. Flame*, **1991**, 87 (2), 145-151.

[16] S. DeCordt, I. Avila, M. Hendrickx, P. Tobback, *Biotechnol. Bioeng.*, **1994**, 44 (7), 859-865.

[17] M.P. Buera, S. Rossi, S. Moreno, J. Chirife, *Biotechnol. Progr.*, **1999**, 15 (3), 577-579.

[18] J. Gajdoš, K. Galić, Ž. Kurtanjek, N. Ciković, *Polym. Test.*, **2000**, 20 (1), 49-57.

[19] M.L. Meste, D. Champion, G. Roudaut, G. Blond, D. Simatos, *J. Food Sci.*, **2002**, 67 (7), 2444-2458.

[20] S. Tripathi, G. Mehrotra, P. Dutta, *Int. J. Biol. Macromol.*, **2009**, 45 (4), 372-376.

[21] P.W. Cooper, *"Explosives Engineering"*. New York: Wiley-VCH, **1996**.

[22] M. Abd-Elghany, T.M. Klapötke, A. Elbeih, S. Zeman, *J. Anal. Appl. Pyrolysis*, **2017**, 126, 267-274.

[23] Y.-H. Wang, L.-L. Liu, L.-Y. Xiao, Z.-X. Wang, *J. Therm. Anal. Calorim.*, **2014**, 119 (3), 1673-1678.

[24] Q.-L. Yan, S. Zeman, F.-Q. Zhao, A. Elbeih, *Thermochim. Acta*, **2013**, 556, 6-12.

[25] Q.-L. Yan, S. Zeman, T.-L. Zang, A. Elbeih, *Thermochim. Acta*, **2013**, 574, 10-18.

[26] A. Elbeih, M. Abd-Elghany, T.M. Klapötke, *Propellants Explos. Pyrotech.*, **2017**, 42 (5), 468-476.

[27] Q.-L. Yan, S. Zeman, R. Svoboda, A. Elbeih, *Thermochim. Acta*, **2012**, 547, 150-160.

[28] Q. Wang, L. Wang, X. Zhang, Z. Mi, *J. Hazard. Mater.*, **2009**, 172 (2), 1659-1664.

[29] Q.-L. Yan, S. Zeman, A. Elbeih, *Thermochim. Acta*, **2012**, 537, 1-12.

[30] M. Abd-Elghany, T.M. Klapötke, A. Elbeih, S. Hassanein, T. Elshenawy, *Chin. J. Explos. Propellants*, **2017**, 2 (4), 24-32.

[31] J.-S. Lee, C.-K. Hsu, *Thermochim. Acta*, **2002**, 392, 153-156.

[32] J.-S. Lee, C.-K. Hsu, C.-L. Chang, *Thermochim. Acta*, **2002**, 392, 173-176.

[33] M.A. Bohn, *Thermochim. Acta*, **2003**, 401 (1), 27-41.

[34] M. Abd-Elghany, A. Elbeih, S. Hassanein, *Cent. Eur. J. Energ. Mater.*, **2016**, 13 (3), 349-356.

[35] A.K. Burnham, R.K. Weese, *Thermochim. Acta*, **2005**, 426 (1), 85-92.

[36] K. Xu, J. Song, F. Zhao, H. Ma, H. Gao, C. Chang, Y. Ren, R. Hu, *J. Hazard. Mater.*, **2008**, 158 (2), 333-339.

[37] A. Elbeih, M. Abd-Elghany, T. Elshenawy, *Acta Astronaut.*, **2017**, 132, 124-130.

[38] M. Kohga, K. Okamoto, *Combust. Flame*, **2011**, 158 (3), 573-582.

[39] V.P. Sinditskii, V.Y. Egorchev, G.F. Rudakov, A.V. Burzhava, S.A. Filatov, L.D. Sang, *Thermochim. Acta*, **2012**, 535, 48-57.

[40] Q.-L. Yan, S. Zeman, P. Sánchez Jiménez, T.-L. Zhang, L. Pérez-Maqueda, A. Elbeih, *J. Phys. Chem. C*, **2014**, 118 (40), 22881-22895.

[41] Q.-L. Yan, S. Zeman, A. Elbeih, A. Zbynek, *Cent. Eur. J. Energ. Mater.*, **2013**, 10 (4), 509-528.

[42] R. Turcotte, M. Vachon, Q.S. Kwok, R. Wang, D.E. Jones, *Thermochim. Acta*, **2005**, 433 (1), 105-115.

[43] M. Abd-Elghany, T.M. Klapötke, A. Elbeih, *Propellants Explos. Pyrotech.*, **2017**, 42 (12), 1373-1381.

[44] S. Pisharath, H.G. Ang, *Thermochim. Acta*, **2007**, 459 (1), 26-33.

[45] X. Li, X. Liu, Y. Cheng, Y. Li, X. Mei, *J. Therm. Anal. Calorim.*, **2014**, 115 (1), 887-894.

[46] M. Abd-Elghany, T.M. Klapötke, A. Elbeih, *J. Anal. Appl. Pyrolysis*, **2017**, 128, 397-404.

Recent Advances in Green Oxidizers for Solid Rocket Propulsion

Published in *Green Chemistry* **2017**, 19(20), 4711-4736 (DOI: 10.1039/c7gc01928a)

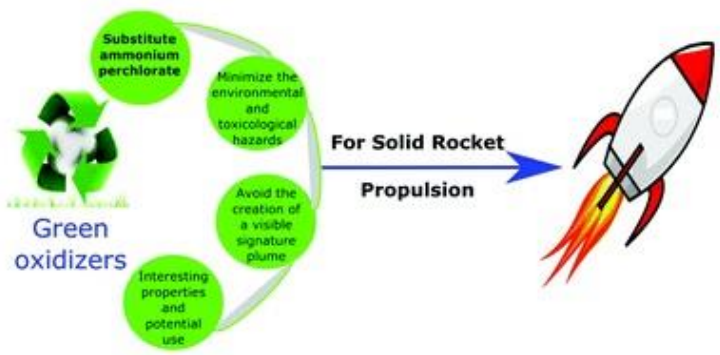

Abstract: Ammonium perchlorate (AP), the workhorse of oxidizers in solid rocket and missile propellants, exhibits various environmental issues resulting from the release of perchlorate into ground water, which have been directly linked to thyroid cancer. Furthermore, the generation of hydrochloric acid causes the depletion of the ozone layer and leads to high concentrations of acid rain. Nowadays, considerable efforts have been devoted to developing solid propellants using green oxidizers which demonstrate less hazards and environmentally friendly chlorine free combustion products. Although many candidates for AP replacement have been identified, most of them are far from being practically employed in the real applications because of a number of severe difficulties, including cost. In this review, the potential green chemicals for use as oxidizers are highlighted and these reveal interesting physicochemical properties and performance. After a quick definition of green solid propellants and their main ingredients, the current status of AP propellants issues is discussed in light of possible substitution with potential green ingredients. Particular attention will be paid to the recent advances of the green oxidizers and their characteristic properties. The advantages and shortcomings of various green oxidizers for specific and potential propellant uses are also discussed together with the attempts made to overcome these problems. As a consequence, efforts will certainly continue to seek AP alternatives and efficient green oxidizers for solid rocket propulsion in the near future.

Introduction

Solid rocket motors (SRMs) are distinguished from other kinds of propulsion systems (nuclear, electric and radiant) by the fact that their propellants are stored in solid form as a mixture of ingredients, which eject hot gases at high speeds to deliver a payload (*e.g.* satellite, warhead). Fundamentals and historical overviews on SRMs have been reported elsewhere [1-6]. Solid propellants find a wide range of applications in tactical rockets, intercontinental- and submarine-based ballistic missiles, space launcher boosters, airplane ejection seats, and even amateur hobby rockets, to name a few. They are preferred over liquid and hybrid propellants, because of their reliability, simplicity, ready-to-use system availability, lower cost of propulsion system and compactness [7, 8]. Solid rocket propellants typically fall into one of two broad categories namely, homogenous (double-base) propellants, which contain their oxidizer and fuel in the same molecule, and heterogeneous (composite) propellants, which consist of mechanical mixtures of separate ingredients. These energetic materials liberate their energy through slow deflagration processes and it may take up to several seconds to reach complete combustion [9, 10]. The present review will be limited to numerous types of ingredients used as oxidizers and their effect on the performance and environmental concerns of composite solid propellant formulations.

Composite propellants, based on ammonium perchlorate (AP, NH_4ClO_4) and aluminum (Al), have been extensively employed for both military and civilian applications for more than 60 years [7]. However, they specifically pose various environmental issues in three main areas: (i) ground-based impacts ranging from groundwater contamination to accidents caused by inopportune processing and handling of propellants, (ii) atmospheric impacts broadly coming from the interaction of the exhaust combustion products with the surrounding atmosphere including the ozone layer; and (iii) biological impacts that encompass toxicity and corrosiveness of propellants [11-13]. For example, AP is thought to affect the function of the thyroid gland. AP-based propellants contaminate the atmosphere by releasing hydrochloric acid (HCl) as an exhaust product. The launch of a large space vehicle engenders about 580 tons of HCl in addition to heavy toxic metal oxides, what pollute the stratosphere including land and water sources. The launch of six Titan class vehicles can lead to ozone depletion of the order of 0.024% and stratospheric acidic rain of the order of 0.01% [8]. Also, although the compounds of aluminum, for example, aluminium oxide (Al_2O_3), are not considered harmful, their release as small particles as an Aerosol may present a potential toxic effect to humans, animals and plants [14].

Researchers are exploring several approaches to fulfill the increasing requirements of solid rocket propulsion systems that impart enhanced performance, improved mechanical properties, prolonged life span, less vulnerability, and negligible environmental effects during manufacture, processing, handling, transport, storage, usage and disposal. Efforts are being made all over the world to develop modern/futuristic propellants meeting the previously mentioned challenges. In developing new propulsion systems, optimal compromises are often sought that are achievable through synthesis or producing new compounds [15-18], modifying or combining known compounds [19, 20], testing of new formulations [21-23], experimental characterization and precise theoretical evaluation [24, 25]. The development of green energetic materials for propulsion purposes is an emerging area of materials chemistry stimulated by a worldwide need to substitute the propellants currently used, because of the environmental considerations and safety requirements, while at the same time ensuring high performance. This new generation of energetic materials has to meet various standards in order to become largely accepted. In addition to the performance characteristics, other desired criteria are stability, compatibility, reasonable cost, favorable classificatio hazards as well as the new or adapted technologies to be mastered to bring such green materials into use in 'real' aplications.

Green chemistry has been widely used in several industrial sectors such as aerospace, energy, automobile, pharmaceutical, cosmetic, electronics, and propulsion field [11, 26-29]. A more fundamental definition of green chemistry involves reducing or eliminating the utilization or generation of hazardous substances in the design, manufacture, and application of chemical products [30]. It is worth noting, however, that the new class of eco-friendly advanced solid propellants is not totally clean, because its constituting compounds can engender an environmental effect in one way or other [8, 31]. Nevertheless, a green propellant is viewed as an energetic composition that seeks to minimize or mitigate the environmental and toxicological hazards associated with currently used materials.

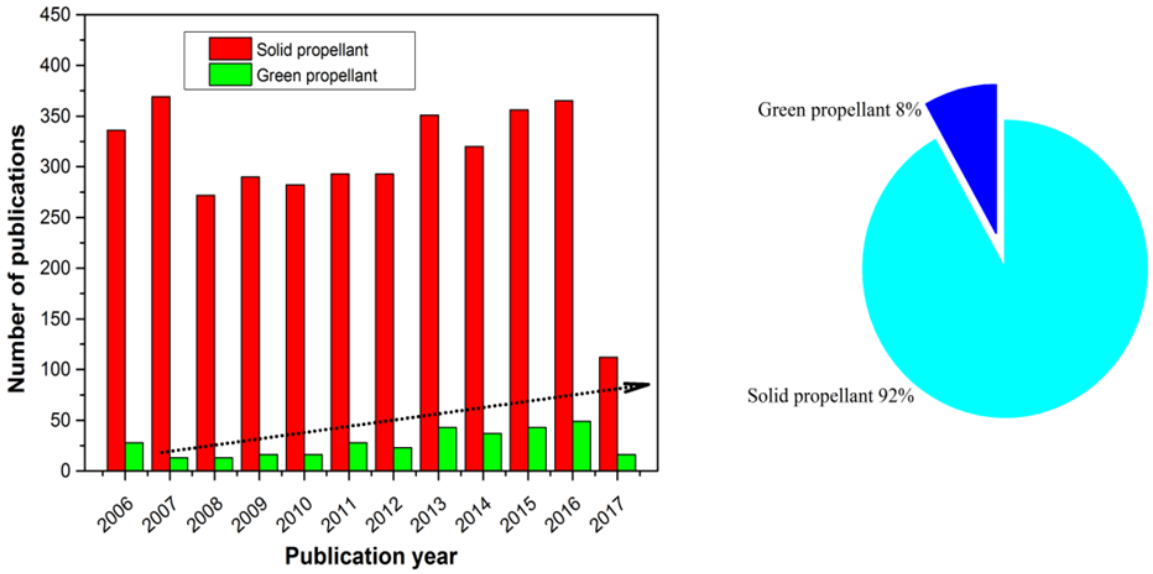

Figure 1. Illustration of the annual number of scientific publications since 2006, using the search terms "solid propellant and green propellant".Data analysis completed using Scopus search system in June 2017.

Significant advances have been made in the synthesis, production, characterization and development of green energetic compounds for their employment in solid propellant formulations. Figure 1 shows that the investigations on green energetic materials for solid rocket propulsion are increasing with a greater number of scientific papers being published in this field. Although many green propellant formulations have been tested, most of them are far from being practically usable in the near future because of a number of difficulties, including cost considerations, and consequently further effort is needed to produce mature green propulsion systems. Currently work is continuing worldwide to overcome the existing problems and to find reasonable solutions. Several reviews [14, 30-36], books [6, 11, 13, 15] and patents [37, 38] have been published in the last two decades covering numerous aspects related to green energetic materials for solid rocket propulsion, including, synthesis procedures, theoretical evaluation, characterization, propellant formulation, processing and testing. However, the focus of the present paper differs from the published literature and where suitable, specific points covered in the published literature are summarized and/or referenced to the relevant paper/patent/book. This review paper firstly provides an overview of the green chemistry principles followed by the main ingredients used in composite solid propellants showing the potential green substances that could be substituted for the current ones. Furthermore, a critical and analytical examination is offered of the advantages and disadvantages of the various oxidizers developed so far.

Green Chemistry and Propulsion

The concept of green chemistry is not new, and dates back in the 1960s, but it has only received urgent attention over the last 25 years, and this continues today, with the focus on minimizing the environmental impact of manufacturing processes through the control of products, energy and wastes. The 12 principles of green chemistry, as described by Anastas and Eghbali [29], provide useful context to highlight self-evidence challenges related to the chemical production and utilization, where several sectors of industry are associated encompassing various scientific disciplines [28, 29, 39]. These principles demonstrate a multidimensional matrix to guide the manufacturing process and the design of individual components, and to make a process eco-friendlier. They will help the chemical engineers / technologists / scientists carry out their work in safer and cleaner manner [14]. The essential factors that should be considered in the area of energetic materials for propulsion systems are: (i) the substitution of the current energetic materials that generate polluting combustion substances with others, which exhibit green characteristics and comparable performance, (ii) the development of safer and cleaner methods for synthesis of substances (*e.g.*, utilization of supercritical carbon dioxide (CO_2), enzymatic procedure, microwave, ionic liquids, ultrasound) or formulation manufacturing (*e.g.*, solventless methods, clean solvents), (iii) efficient monitoring of the life-cycle during manufacturing, storage, testing and disposal, and (iv) reduction of costs to determine whether the processes can be commercialized [7, 11, 14, 31, 32, 34, 36, 40, 41]. The development of green propellants is under a significant cost pressure, because it is problematical for emergent products to compete with the relatively low cost of well-developed conventional formulations. Currently, green energetic materials are 100 times more expensive to produce than conventional ones [14]. Therefore, green energetic materials for propulsion purposes require further government and other external support to succeed and address all of the previously mentioned challenges. Perhaps this review paper can convey part of this process by providing an overview of some of the challenges in this domain and their potential solutions.

It is worth noting that recent research efforts have been made towards environmentally friendly and non-toxic composite solid propellants. Nonetheless, adopting green energetic materials for solid propulsion does not mean that these propellants are totally clean without any impacts on the environment, because the combustion of the so-called green propellants generate exhausts which may typically encompass alumina, nitrogen oxides, water vapor, CO_2, inorganic chlorine, sulfates, and soot [8, 42]. Thus, these green formulations do impact

on the environment but at a relatively lower level. Recently, many activities have been conducted through several projects worldwide to develop green propellants. Various candidates such as green composite solid rocket propellant ingredients have appeared and continue to be developed in different laboratories and research centers all over the world.

Composite Solid Rocket Propellant Formulations

Propellants are considered the most influential factor in the design of rockets, missiles and launch vehicles. These energetic materials generate mainly hot gaseous products ejected at high velocity from the gas dynamic nozzle to produce forward thrust to the vehicles. Solid rocket propellants consist, in one form or another, of a blend of fuels and oxidizers with some structural rigidity [2, 5, 6]. They are prepared as a slurry, and are commonly cast and cured into the motor as a solid mass known as the grain. The engineered geometry of the grain is a crucial parameter that determines the thrust level and profile of the motor.

Modern rockets and missiles broadly employ composite propellants which are essentially made up of an oxygen-rich solid oxidizer (65% - 90%) that provides oxygen (O_2) for oxidation purposes, an organic polymer that serves as both binder and gas fuming combustible (8% - 15%), and a metal fuel (10% - 20%) that generates additional thermal energy to increase the propellant performance [35, 43, 44]. In addition to these primary ingredients, other minor substances such as plasticizers, cross linking agents, curing catalysts, antioxidants, bonding agents, process aids, and burning rate catalysts are added to the propellant formulation. The following sections will especially focused on composite solid propellants oxidizers. They will give detail on substitutes for traditional toxic compounds such as AP. Recent advances on green ingredients used as new propellant oxidizers are also presented and discussed.

Green Oxidizers

The main oxidizer that has been consistently utilized in all rocketry until now is the AP [45, 46]. Because of its oxygen balance of 34%, high density, high thermal stability, low sensitivity to shock, good compatibility and long shelf-life, this oxidizer is used for application in amateur rocketry, airbag inflators, aircraft injection seat, and pyrotechnic devices such as warning flares [6, 10, 47]. The greatest benefit of using AP is the huge experience and widely available information on AP-based propellants collected over many decades, which gives a sound confidence in this ingredient [48-51]. Unfortunately, this low

cost salt has some toxic issues, especially when considering its good solubility. Perchlorate anions (ClO_4^-) have been detected in drinking water supplies throughout the south-western United States, where it is mistakenly taken up in place of iodide leading to dysfunction and affecting both growth and development of humans and animals. Furthermore, amphibians' normal pigmentation and growth is altered by the exposure to AP [6]. This oxidizer might be also toxic to various marine life forms. Further problems are generated by AP-based solid propellants during their combustion. For example, the burning of the space shuttle boosters produces a huge amount of exhaust products containing mainly HCl and other compounds which are highly toxic and corrosive in nature. It is estimated that each flight of the Ariane 5 space launcher liberates about 270 tons of concentrated HCl as well as alumina, thereby polluting the atmosphere and causing ozone depletion in the stratosphere. Acid rains can be caused by this enormous quantity of HCl emission [10, 35]. Additionally, for military applications, the smoke trail caused by AP is a very serious tactical disadvantage, because it adversely affects guidance and control systems.

Currently, AP has no suitable alternatives; this is why intensive efforts have been devoted and continue to be made to produce eco-friendly propellants with a reduced component of such pollutants or altogether free from them. The most important benefit of developing chlorine-free propellants is that they eradicate smokes formed by the condensation of atmospheric water vapor and exhaust plume, and avoid the creation of a visible signature plume (Fig. 2). Several promising candidates as oxidizers to substitute AP have been developed such as phase- stabilized ammonium nitrate (PSAN), ammonium dinitramide (ADN), hydrazinium nitroformate (HNF), hexanitrohexaazaisowurtzitane (HNIW or CL-20), some molecules containing the trinitromethyl functionality or fluorodinitromethyl derivatives, polynitro-substituted pyrazoles and triazoles, polynitroazoles, tetrazole derivatives, carbamate derivatives and tetranitroacetimidic acid [6, 41, 52-54].

These chlorine-free alternatives, which at present are in testing procedures, can overcome most of the previously mentioned shortcomings, but at the same time bring up new challenges as it will be described later in the paper. Some properties of conventional and advanced oxidizers, which have been investigated in the present review, are given in Table 1.

Figure 2. Smokeless and smoky exhaust products of solid propellant during combustion. Reprinted from ref. 8 with permission. Copyright © 2017, Springer International Publishing, Switzerland.

Table 1. Properties of some green and conventional oxidizers from various sources

Oxidizer[a]	Chemical Formula	Oxygen Balance (%)	Molar Mass (g mol^{-1})	Density (g cm^{-3})	ΔH_f (kJ·mol^{-1})	Environ. Impact	Ref.
AP	NH_4ClO_4	+34.00	117.50	1.95	-295.8	ClHNO	[55]
HNF	$N_2H_4HC(NO_2)_3$	+25.00	183.00	1.86	-71.0	CHNO	
AN	NH_4NO_3	+20.00	80.04	1.73	-367.5	HNO	[56]
ADN	$NH_4N(NO_2)_2$	+25.80	124.10	1.81	-134.6	HNO	[1]
CL-20	$(NNO_2)_6(CH)_6$	-10.90	438.20	2.04	+372.0	CHNO	
FOX-7	$C_2H_4N_4O_4$	+43.20	148.10	1.88	-134.0	CHNO	[57]
TNAA	$C_2HN_5O_9$	+30.00	239.10	1.87	-322.6	CHNO	[53]
NTNAA	$C_2HN_5O_9$	+30.00	239.10	2.03	-415.3	CHNO	[58]
TNENCA	$C_3H_3N_5O_{10}$	+32.70	269.08	1.73	+343.9	CHNO	[59]
TNEF	$C_7H_7N_9O_{21}$	+30.40	553.18	1.81	-519.0	CHNO	[151]
BTNEO	$C_6H_4N_6O_{16}$	+30.80	416.12	1.84	-688.0	CHNO	[151]
TKX-50	$C_2H_8N_{10}O_4$	-27.10	236.15	1.92	+446.6	CHNO	[60]
HADNMNT	$C_2H_8N_8O_7$	+6.35	256.15	1.87	+299.4	CHNO	[153]
DNDNT	$C_2N_{18}O_8$	+15.84	404.00	1.95	+1210.0	CHNO	[61]
TTBTE	$C_2H_2N_{20}O_8$	+11.06	434.00	1.92	+1274.0	CHNO	
ANNPA	$C_5H_4N_{11}O_{10}$	+14.85	378.23	1.82	+491.7	CHNO	[52]
DNNPDA	$C_5H_6N_9O_{10}$	+11.40	354.57	1.81	+124.1	CHNO	
DNPDN	$C_3H_4N_6O_4$	-8.51	188.04	1.82	+173.0	CHNO	
NNTAA	$C_4H_5N_8O_8$	+10.95	292.00	1.79	+160.6	CHNO	

[a] The acronyms are identified in the respective sections in the text.

Phase Stabilized Ammonium Nitrate (PSAN)

Ammonium nitrate (AN, NH_4NO_3) is one of the most important ammonium chemicals in the agricultural and chemical industries [10, 62, 63]. It has been widely employed as a fertilizer component and as an industrial explosive ingredient, as well as an oxidizer for solid propellants, gas generator systems and emergency starters because of its low cost, availability, chemical stability, low sensitivity to friction and impact, releases almost 100% gaseous products during decomposition, and has a positive oxygen balance [54, 62]. Although it plays the role of a source of ammonia and nitrate ion vital to plants in the form of nitrogen fertilizer, in industrial explosives and propellants the nitrate ion is considered as a source of oxygen [56]. AN is broadly produced by the neutralization reaction of synthetic ammonia and nitric acid (HNO_3), followed by evaporation to the melt that is subsequently treated by a prilling process or a granulator to generate the commercial product in the form prills (pellets or granules) [64]. These high density prills are frequently used in the fertilizer industry. However, their low liquid absorption means they cannot be used in energetic material compositions [65]. Subsequently, Kim *et al.* have developed a process, for manufacturing spherical AN particles with a uniform distribution, which is the melt spray [66]. The AN particles are considered to be better for energetic material compositions because of their morphology, surface roughness, uniformity and particles size.

Much has been published about the physicochemical properties of AN, its thermal decomposition, its coating, the effect of additives, its applications, its disasters and the different challenges associated with its practical uses. For a more complete view of this green energetic oxidizer, there are many excellent review papers [56, 64, 67-69] and books [10, 62, 63] that have been published in recent years. In this section, this will not be repeated but the most important aspects applicable to AN as oxidizer for solid rocket propellants will be mentioned. However, this review will concentrate on providing recent progress in using AN as a replacement of AP in solid propellant formulations.

In spite of its hygroscopic nature, low performance, low burning rate, and the near room temperature polymorphic transitions involving a volume change, AN is actually considered as one of the most attractive oxidizer [20, 54, 70-72]. Recently, there has been renewed and growing interest in developing smokeless, chlorine-free, and environmentally benign propellants based on AN, because much progress has been achieved in surmounting the previously mentioned shortcomings. The hygroscopicity of AN has been recognized as the main cause for caking and has been considered as the most serious obstacle for its utilization

in solid propellants. Many researchers have suggested various surface modification methodologies based on successful coating to decrease this hygroscopicity. These methods can be physical, chemical or encapsulating coatings (Table 2), and have been described well in the recent reviews by Elzaki & Zhang, and Jos & Mathew [54, 67].

Table 2. Advantages and drawbacks of different coating methods of AN [67]

Method	Advantages	Disadvantages
Physical coating	1. Simple. 2. Convenient and easy to manufacture. 3. Improves the stability of the particles. 4. Safety. 5. Enhances the compatibility of particles with other materials.	1. Uses a large amount of coating agent. 2. Thickness of coating layer not easy to control. 3. Large difference of interfacial tension between the surface coating layer and the polarity of AN.
Chemical coating	1. Small dosage of coating agent. 2. Strong binding force. 3. The hydrophobic group made the thin layer on the surface prevents hygroscopicity.	1. The surfactant and coupling agent have low molecular weight. 2. The surfactant has a small solubility in water. 3. Low hygroscopicity properties.
Encapsul-ation coating	1. Improves the physical properties of coated particles on the surface. 2. Protects the particles from external moisture. 3. Polymer hygroscopicity was zero. 4. Coating layer is thin.	1. The brittle polymer is susceptible to cracking during the drying process. 2. There are sticky polymer adhesives not dispersed. 3. Polymer polarity low is difficult to stick on surface of AN particles.

Another major drawback of AN is the presence of temperature dependent phases at atmospheric pressure that are characterized by continuously more motion freedom of the NH_4^+ and NO_3^- ions. The phase transformation which occurs around room temperature can be accompanied by a substantial volume contraction and expansion which gives rise to undesirable crack formation in the propellant grains. AN shows at least five polymorphic transitions below its melting point at atmospheric pressure (Fig. 3) [73]. Among the phase transformations of AN, IV–III phase transition happens at ambient temperature is followed by a volume change of about 3.8%. Therefore, many research activities have been devoted to preventing such phenomenon.

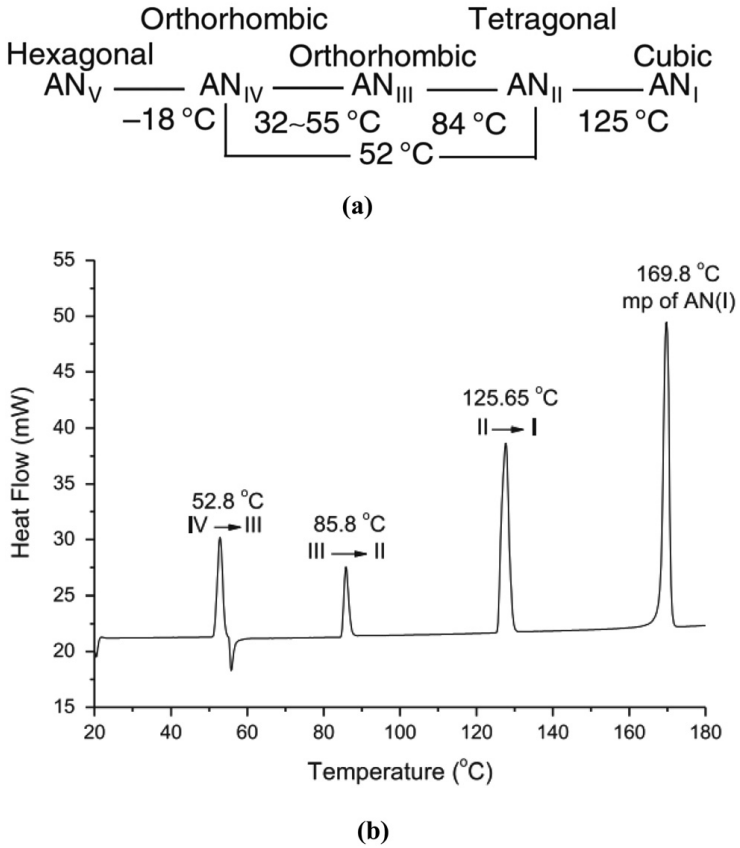

Figure 3. (a) Phase transitions of ammonium nitrate. Reprinted from ref. 155 with permission. Copyright © 2017, Springer Science; (b) low-temperature differential scanning calorimetry identification-test thermograms of ammonium nitrate, showing the different phase transitions. Reprinted from ref. 67 with permission. Copyright © 2013, Elsevier Limited.

It is commonly achieved by adding organic or mineral modifiers into the AN crystal lattice. For example, diamine complexes of transition metals, alkali metal salts, potassium salts and magnesium nitrate, potassium ferrocyanide, copper nitrate, potassium nitrate (KNO_3), poly(vinyl pyrrolidine), poly(ethylene oxide), poly(acrylamide), trioxy purine and crown ethers have been extensively used to phase-stabilized AN [10, 54, 64, 70]. Phase stabilization of AN with metal oxides is demonstrated to be beneficial with respect to burning rate, ignition, and hygroscopicity [56]. Furthermore, in spite of the stability of AN at ambient temperature, a small amount of ammonia can be evolved, leaving the salt slightly acidic [56]. It is worth noting that the thermal decomposition of AN strongly depends on temperature, pressure, sample purity, state of confinement, monitoring techniques, and amount of additives, and experimental conditions such as sample size, sample mass and heating rate [54, 74]. It is noticeable that no simple mechanism can be used to elucidate all of the aspects of its decomposition features. It is broadly accepted that the thermal decomposition of AN

is initiated by an endothermic proton transfer reaction, followed by an exothermic reaction at around 200–230 °C [56]. Other reactions may be undergone under different conditions. During decomposition, several products may appear such as water (H_2O), nitrogen (N_2), nitrous oxide (N_2O) and HNO_3. Other minor by-products could be detected such as nitric oxide (NO) and nitrogen dioxide (NO_2) [54]. Recently, Cagnina *et al.* studied the gas phase decomposition mechanism of AN using CBS–QB3 *ab initio* calculations [75]. Scheme 1 displays the mechanism of the formation of decomposition products H_2O, N_2, O_2, OH, HNO and NO_3^-. The authors proposed, as a first step, the dissociation of AN into ammonia and HNO_3. It was suggested that the hemolytic breaking of NO bond in HNO_3 engendered hydroxyl radicals and NO. The reaction between hydroxyl radical and ammonia generated amidogen radical. The successive reaction of amidogen radical with NO led to the final decomposition products of AN. Other detailed mechanisms, kinetics and the thermal decomposition of AN, and the effect of different additives have been widely investigated, and some comprehensive reviews have been written[56, 64, 69].

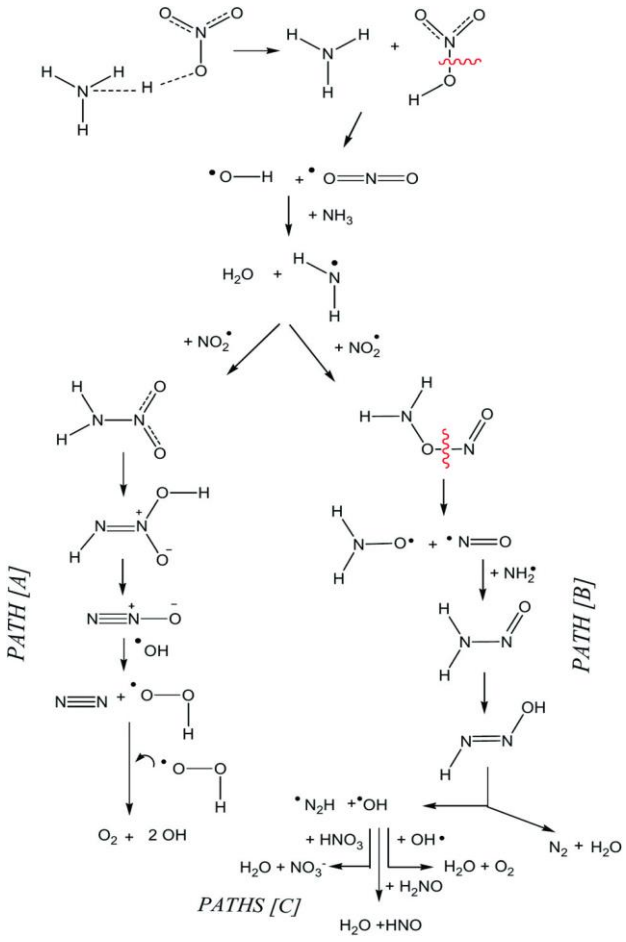

Scheme 1. Reaction paths for the decomposition of ammonium nitrate. Reprinted from ref. 69 with permission © 2013, The Royal Society of Chemistry.

In order to surmount the low reactivity and low energetics of AN in a propellant formulation, different approaches have been adopted. The first concerns the incorporation of additives to enhance the thermal decomposition of AN. Some inorganic salts such as chromium nitrate, iron nitrate, aluminum nitrate and iron salts have been revealed to promote the thermal decomposition of AN because of the high charge to radius ratio of the metal ions [76]. Some monometallic catalysts such as platinum (Pt), copper (Cu), zinc (Zn) and iron (Fe) supported on silica doped alumina shifted the endothermic decomposition of AN into exothermic decomposition [77]. Other transition metal oxides such as MOx (M = manganese (Mn), cobalt (Co), nickel (Ni), Cu) acted on the endothermic decomposition as well [54]. Some nanocatalysts such as nano titanium dioxide (TiO_2) and nano copper oxide (CuO) have been tested by Vargeese's group[70, 72, 78]. The incorporation of TiO_2 to AN led to the decrease of the activation energy and the plausible mechanism for the catalyzed AN is depicted depicted in Fig. 4a. The reaction starts by the dissociation of AN (step1) followed by the adsorption of ammonia (NH_3) on TiO_2 (step 2). The dissociation of HNO_3 produced from AN generates OH and NO_2 (step 3), that subsequently dissociates to NO and O_2 (step 4), which interacts with TiO_2 as well (step 5). Like TiO_2, the addition of nano CuO into AN also reduced the activation energy of the thermal decomposition. As presented in Fig. 4b, the authors demonstrated that the CuO nanorods provide Lewis acid and/or active metal sites, enabling the elimination of AN decomposition inhibition species such as NH_3 and thereby improve the rate of decomposition. More recently, some nanocomposites such as CuO or copper iron oxide ($CuFe_2O_4$) anchored on graphene oxide (GO) sheets have been tested as catalysts [79]. It was shown that the decomposition temperature and the activation energy were notably decreased when CuO/GO was added to AN, whereas no synergetic effect was found when $CuFe_2O_4$/GO was added. However, the effect of carbonaceous materials on the thermal decomposition of AN has been widely investigated. Lurie and Lianshen deduced that incorporation of carbon black into AN, augmented the AN decomposition rate intensely [80]. It is caused by the reduction of HNO_3, produced from the dissociation of AN, to HNO_2 by the carbon black and the following reactions generate N_2. Recently, Atamanov *et al.* have revealed that the addition of 5 mass% of dextran (acting as a catalyst) reduces the activation energy of AN to 64 kJ mol^{-1} [81].

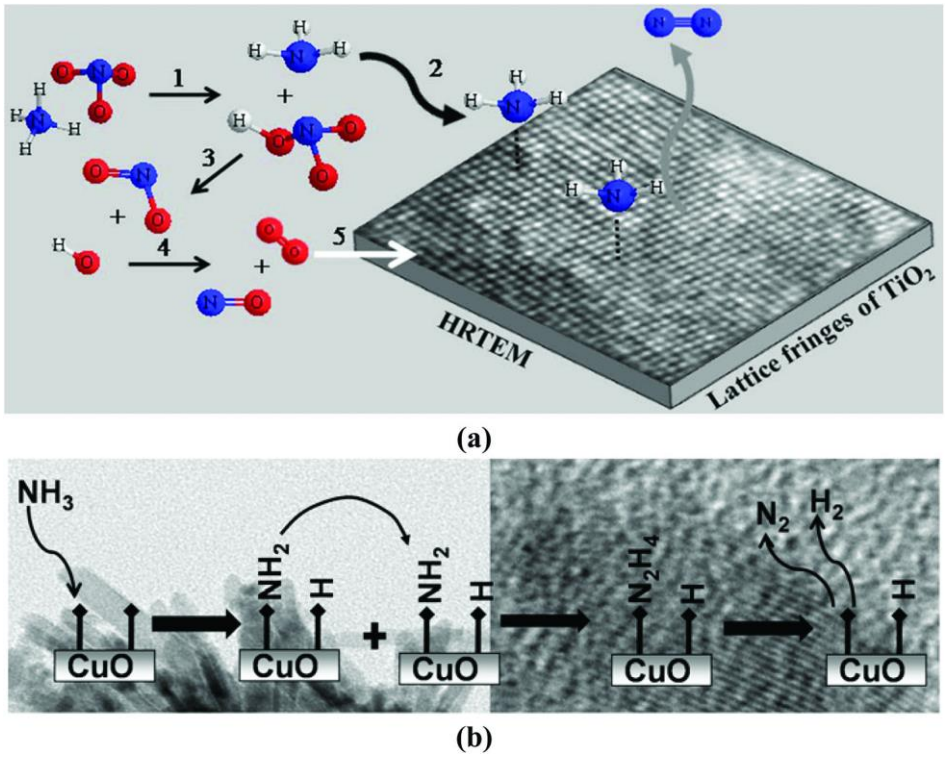

Figure 4. (a) Mechanism of catalytic decomposition of ammonium nitrate. Reprinted from ref. 72 with permission. Copyright © 2011, Elsevier Limited; (b) the possible mechanism of the adsorbed ammonia surface reactions. Reprinted from ref. 64 with permission. Copyright © 2012, Elsevier Limited.

The second approach consists of the use of dual oxidizers to increase the performance of AN-based propellants. Chaturvidi and Dave other [56] have shown that AN-based composite propellants are attractive due to the clean burning and smokeless exhaust. However, this propellant present some drawbacks such as poor ignition and low burning rate. AP-based composite propellants, however, have outstanding ignition and burning characteristics, although the combustion gases contain HCl. It was anticipated that an AN/AP dual oxidizers-based propellant would have an acceptable performance for practical applications because each oxidizer would compensate for the flaw of each other [56]. In another work, propellant formulations using double-oxidizers such as (PSAN+AP)/hydroxyl terminated polybutadiene (HTPB)/Al (40+28)/14/18, with PSAN in turn including 5% phase stabilizer, were also tested by DeLuca's group [82]. The measured burning rates fall in the low range 5 to 8 mm s^{-1} at 7 MPa, with a pressure sensitivity n = 0.58-0.64. Recently, Kohga and Handa [83, 84] studied the thermal decomposition behaviors and burning rate characteristics of composite propellants prepared using combined AP/AN particles. They tested two methods to combine both oxidizers (physical and freeze-drying) before propellant formulation. They

deduced that the burning characteristics of the propellants produced with the combined AP/AN samples varied from those of the propellants manufactured by physically mixing AP and AN particles. The burning characteristics of some of the propellants produced by physically mixing AP and AN particles exhibited unsteady combustion, whereas the propellants manufactured with the combined AP/AN samples burned steadily. The use of the combined AP/AN particles reduced the heterogeneity of the combustion wave of an AP/AN propellant. In a separate work, Kumar *et al.* [20] prepared a mixture of AN and potassium dinitramide (KDN) using a co-crystallization method. The authors revealed that KDN presents an excellent phase stabilizing effect on AN and has a positive effect on the burning characteristics. The thermal analyses of different co-crystals of AN/KDN have shown that the ratio 50/50 is the best one, since the KDN play a double role as both a phase stabilizer and an energy enhancer. The morphology of the different prepared propellants is shown in Fig. 5.

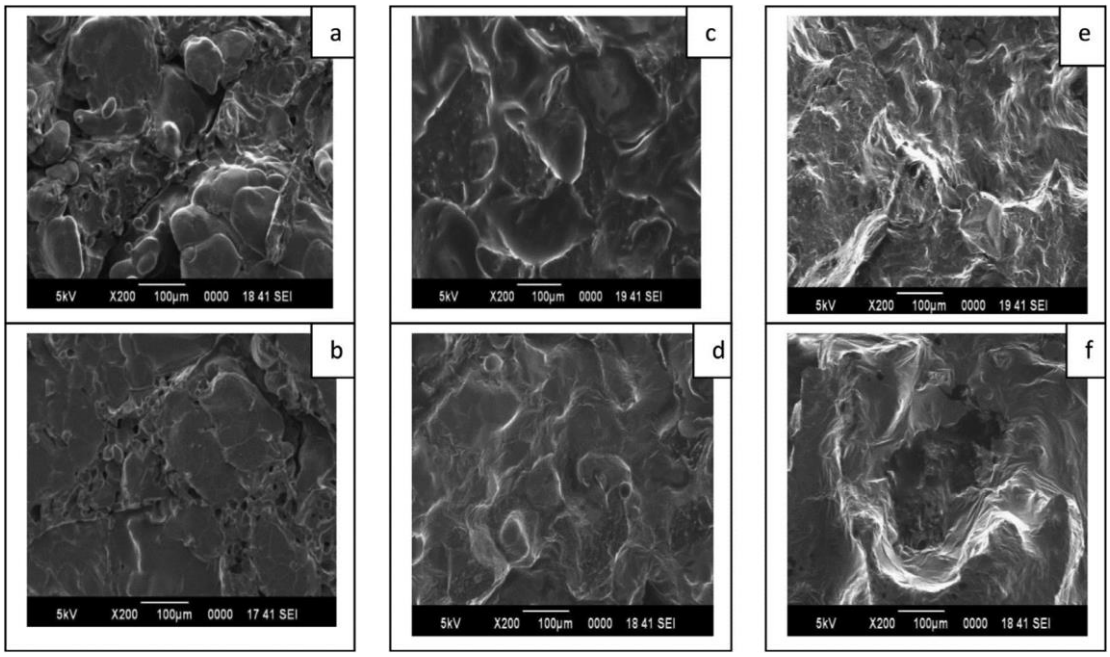

Figure 5. Scanning electron microscopy images of: (a) pure AN propellant, (b) AN + Cu–Co* propellant, (c) AN/KDN (75/25) + CuO propellant, (d) AN/ KDN (75/25) + Cu–Co* propellant, (e) AN/KDN (50/50) + CuO propellant, and (f) AN/KDN (50/50) + Cu–Co* propellant. Reprinted from ref. 20 with permission. Copyright © 2016, Elsevier Limited.

It is clear that the morphology differs from one propellant to another, because the composition is different. As depicted in Fig. 6, the combustion characteristics are affected as well. It is revealed that the propellant AN/KDN (50/50)/HTPB/catalyst (copper–cobalt based metal oxides, Cu-Co*) shows the highest burning rate with an acceptable pressure

index (n) value of 0.746, compared to other formulations. The authors concluded that the propellant containing AN/KDN (50/50) is the most promising green formulation.

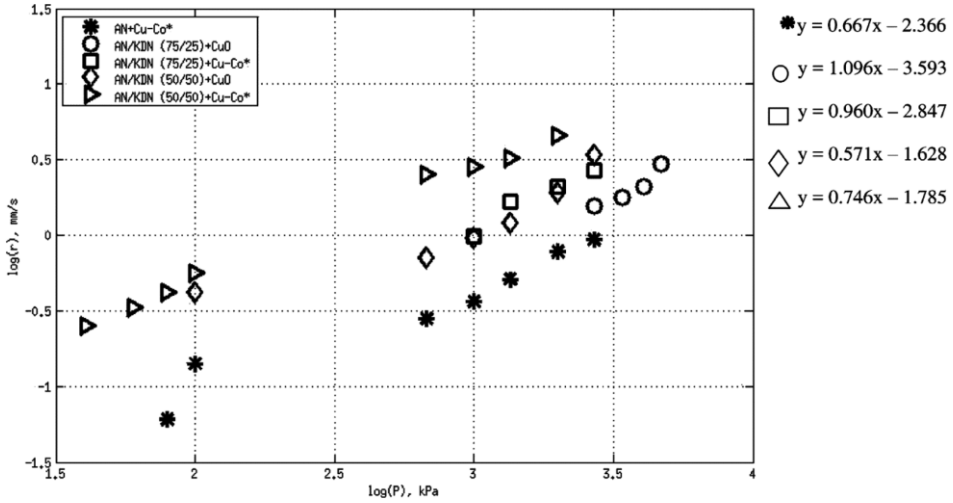

Figure 6. Burning rate vs. pressure for different propellant samples. Reprinted from ref. 20 with permission. Copyright © 2016, Elsevier Limited.

To avoid redundancy, other propellant formulations based on AN as oxidizer have been recently discussed and reviewed [54], where several fillers (cyclohexamethylene trinitramine, cyclotetramethylene tetranitramine, Hexanitrohexaazaisowurtzitane, HNIW), binders [polytetrahydrofuran, poly(3,3-bis(azydomethyl) oxetane)], plasticizers [nitroglycerine, 1,2,4–butanetriol trinitrate, and trimethylolethane trinitrate (TMETN)] and catalysts (Fe_2O_3, Cr_2O_3, MnO_2, SiO_2, PbC, CuC, potassium dichromate, ammonium dichromate, transition metal [Mn(II), Fe (II), Fe(III), Co(II), Ni(II), Cu(II), and Zn(II)] salts of 5–nitro–2,4–dihydro–3H–1,2,4–triaole–3–one, aminoguanidinium 5,5´–azobis–1H–tetrazolate, and triamino guanidine nitrate) have been tested. It was consequently concluded that in spite of the fact that much progress has been achieved in the AN-propellant formulations studies, further endeavor should be undertaken in future research to overcome the remaining shortcomings and offer efficient propulsion systems using AN.

Ammonium Dinitramide (ADN)

Another promising, relatively new, candidate considered as a replacement for hazardous AP in solid rocket propellant is the ammonium dinitramide [ADN, $NH_4N(NO_2)_2$] [6, 10]. This dinitramide was first synthesized in the Soviet Union in the early 1970s, where it was tested in various missile programs, and it has been developed in the western world since 1990s [63, 85, 86]. Its synthesis has been extensively studied and an overview of the different methods

has been given by Venkatachalam *et al.* [87]. These authors deduced that the most practical procedure for scaling up is that invented by Langlet *et al.* (Scheme 2), which is based on the direct nitration of ammonia sulfate derivatives using an ordinary sulfo-nitric acid mixture followed by reaction with NH_3.

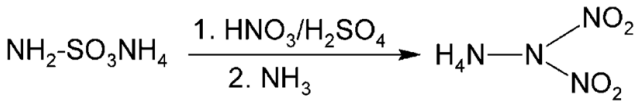

Scheme 2. Synthesis of ammonium dinitramide. Reprinted from ref. 80 with permission © 2004, John Wiley and Sons.

The current commercially available ADN from Eurenco Bofors in Sweden is produced using this method developed and patented by FOI [85, 88]. More recently, Kim *et al.* have used potassium sulfamate as an ADN precursor and have proved that the prepared ADN presents high purity of 99.2% with a high reaction yield of 57.2% [89]. However, the commonly resulting crystals of crude ADN have low purity, high cost, irregular morphology and a high aspect ratio with some agglomerates, which can complicate the processing [6, 88, 90, 91]. Such issues make ADN unsuitable for propellant formulation and the feasibility of the compositions are greatly compromised because of the large increase in viscosity as well as high loading rates are envisaged. In this sense, two methods stand out in re-shaping the ADN crystals, which are spray crystallization and prilling in suspension (Fig. 7) [90, 92]. The disadvantage of the first method is the use of molten ADN that is known to be unstable above its melting point, whereas the second method presents a technical complexity to be scaled-up.

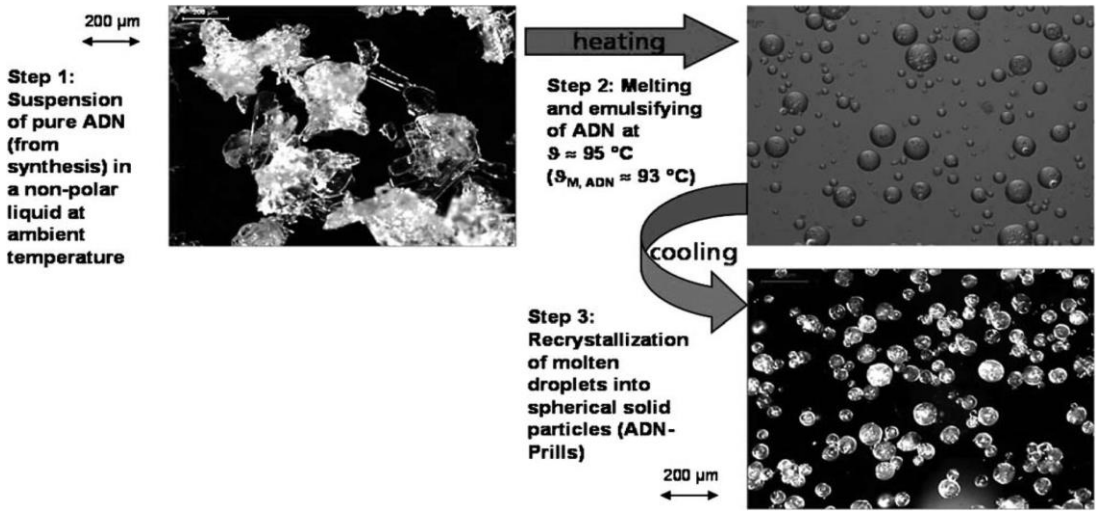

Figure 7. Principal steps of the ADN-prilling process. Reprinted from ref. 85 with permission © 2009, John Wiley and Sons.

To overcome the previously mentioned drawbacks and improve the properties of the final ADN crystals, some researchers have recently patented two other crystallization methods [91, 93]. These methods are not based on converting the crude crystals obtained, but either on crystallization in the presence of an added chemical element (crystal modifier) or on crystallization in solution with controlling nucleation and crystal growth in a high viscosity solvent. It is shown that the first method based on the modified crystallization is a simple, easily comparable operation whose implementation does not necessitate exceptional equipment and does not exhibit any particular pyrotechnic hazard. Furthermore, it can be performed in inexpensive and non-toxic solvents. This crystallization is revealed to be much more valuable than prilling process. On the other hand, it is demonstrated by the second approach that the crystals obtained present a low shape factor of 1 to 1.5 and are perfectly suitable to be used in energetic material formulations.

ADN has attracted attention of researchers, as a solid rocket propellant or liquid monopropellant oxidizer, for many reasons [13]. It combines a positive oxygen balance, high enthalpy of formation, high burning rate, does not evolve chlorine or mimic iodide, clean burning properties, low signature combustion and does not show any phase transition like AN or density modification under temperature stress [94]. Nevertheless, ADN exhibits a moderate thermal stability and high hygroscopicity. It is chemically reactive with some curing systems and this can be problimatic, and it does not exhibit simple ballistic control. Consequently, extensive research has been devoted to understanding its behavior and possibly correct such problems. Benazet and Jacob [95] demonstrated that less hygroscopic ADN crystals can be obtained by optimizing and improving the crystallization process. In another work, Ting *et al.* [96] have successfully applied an alumina coating on the surface of ADN using an atomic layer deposition technology in order to build a water molecule diffusion barrier layer on the surface and improve its stability in humid air. However, the thermal behavior and combustion of ADN have not been adequately elucidated because of the numerous and complex phenomena that can occur. Subsequently, several pieces of research have been conducted and currently continue to be done in various laboratories over the word.

Recently, Ermolin and Fomin [97] have published a comprehensive review on the mechanisms of thermal decomposition of ADN. It was demonstrated that ADN can decompose in either the liquid or solid phase. It was reported that ADN decomposition occurred in the liquid phase proceeds through two paths, where the initial steps are

monomolecular decomposition of the anion over the N–NO_2 bond and equilibrium dissociation of the salt into the acid and base. The second path, however, occurs at 100 °C. In contrast, the path of salt decomposition in the solid phase proceeds through its dissociation into the acid and base. It was shown that the monomolecular decomposition of the anion into NO_3^- and N_2O occurs at a higher rate than in the melt process. In addition to being thermally labile, ADN is also light sensitive [63]. Furthermore, it was found that the synthesis method and conditions may certainly affect the ADN structure and its physicochemical properties.

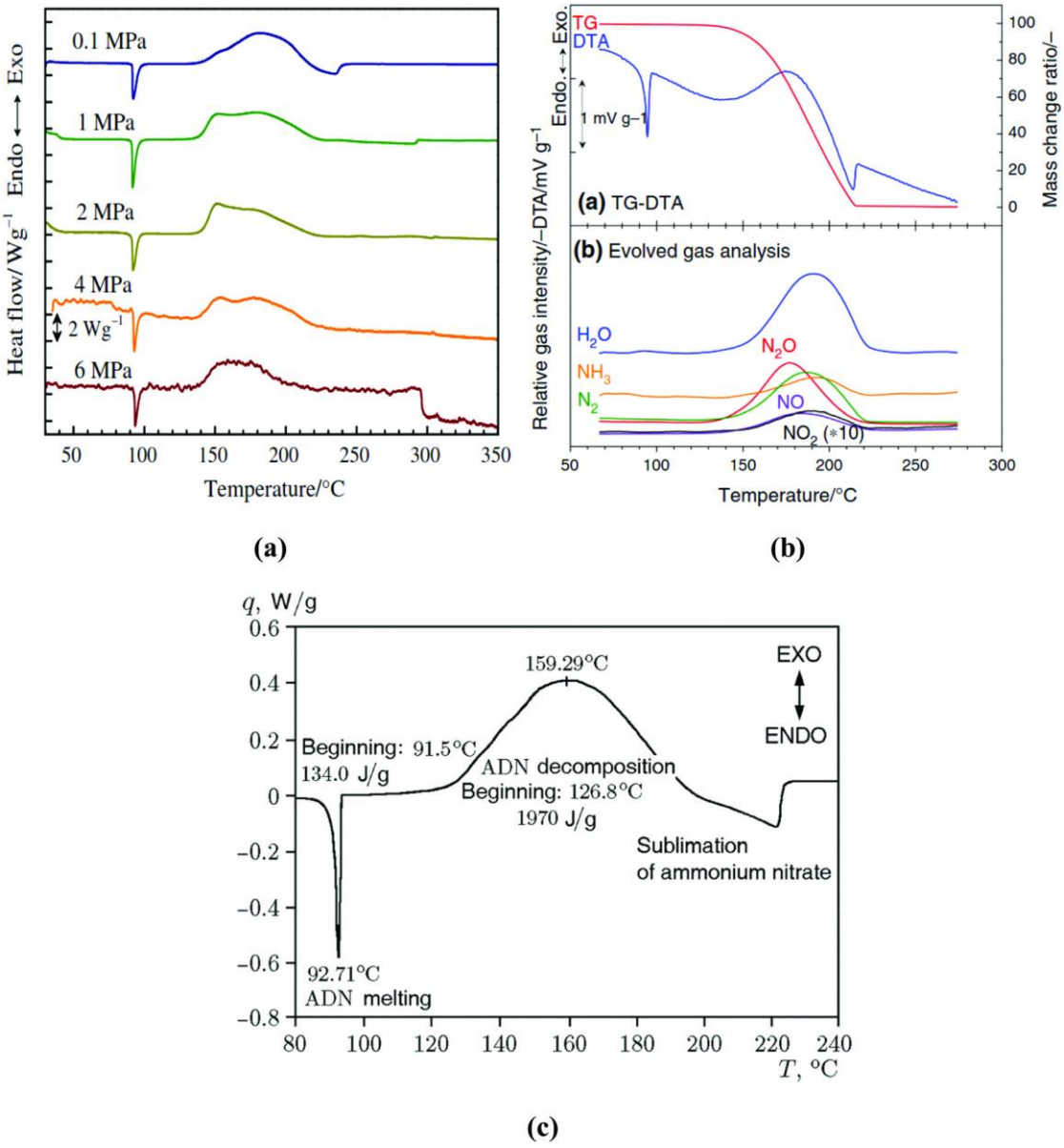

Figure 8. (a) PDSC of ADN. Reprinted from ref. 89 with permission. Copyright © 2014, Springer Science; (b) TG-DTA-MS curves for ADN at a heating rate of 4 k min^{-1}. Reprinted from ref. 90 with permission. Copyright © 2017, Springer Science; (c) DSC measurement of ADN at a heating rate of 0.5 k min^{-1}. Reprinted from ref. 156 with permission. Copyright © 1997, Elsevier Limited.

Matsunaga *et al.* [98] have also studied the thermal decomposition behavior of ADN under pressurized conditions. The pressure differential scanning calorimetry (PDSC) curves of ADN at each pressure value are displayed in Fig. 8a. An endothermic peak was observed at around 92 °C and two exothermic events appeared between 135 °C and 220 °C at each pressure. The melting temperature reported in the literature ranges from 83 °C to 95 °C [63]. This large variation in the published values is most likely to be from impurities, which can significantly affect the thermal behavior of ADN even at very low concentration. The first exothermic peak became more significant with the pressure increase. Raman analysis revealed the formation of AN during the decomposition. The authors found that the AN inhibited the decomposition of ADN at a low decomposition temperature, and contributed to the reaction at high temperature. In a related work, the similar research group has recently investigated the thermal decomposition of ADN using a simultaneous thermogravimetry-differential thermal analysis-mass spectrometry-infrared TG-DTAMS-IR spectroscopy [99]. Figure 8b shows evolving gas and thermal behavior, obtained using the simultaneous analyses. They have shown that the main evolved gases were H_2O, N_2, N_2O and NH_3, and they indicated that the activation energies decreased with increasing progress of the reaction, and the decomposition of ADN exhibited an autocatalytic behavior.

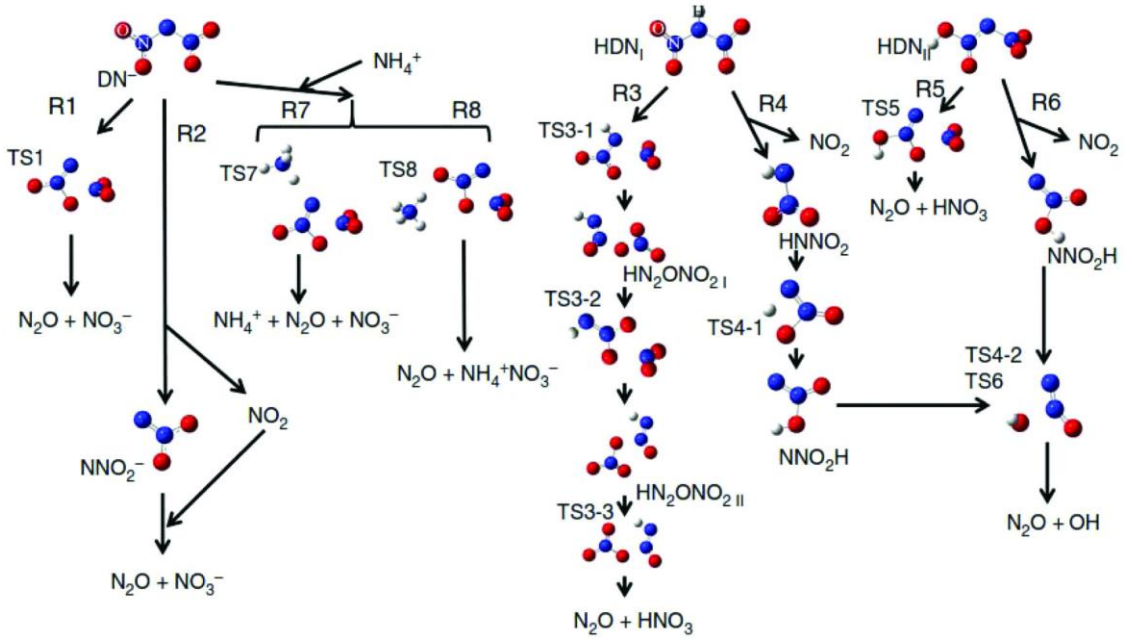

Scheme 3. Reaction mechanism of the decomposition behavior of molten ADN. Reprinted from ref. 90 with permission. Copyright © 2017, Springer Science.

The proposed mechanism of the decomposition reaction of molten ADN is shown in Scheme 3. This intricate decomposition of ADN confirmed the reported results on the complicated combustion behavior of its energetic compositions as discussed and summarized by DeLuca *et al.* [55, 100]. However, a severe chemical instability can be caused by the aggressive oxidizing ability of ADN. The low symmetry structure of the dinitramide anion is one of the main reasons for the reactivity and the instability of ADN. However, AP is nearly not reactive because of the high symmetry and low energy of the tetrahedral structure of the perchlorate anion [6]. Thus, different reactions and compatibility behavior of ADN with other substances that could be added to propellant formulations should be well understood. Also, some stabilizers can be added to ADN to improve its chemical stability [63, 85].

Broadly, ADN does not attack C–H or C–C single bonds, and displays good compatibility with compounds having double-bounded carbon [85]. However, ADN exhibits severe compatibility issues with isocyanates, and it easily reacts and decomposes in their presence [101]. Thus, the polymers that undergo polyurethane bonding (Scheme 4) can negatively affect the compatibility and the chemical stability of the ADN-based energetic composition [102]. Therefore, two main approaches have been adopted to avoid such a problem.

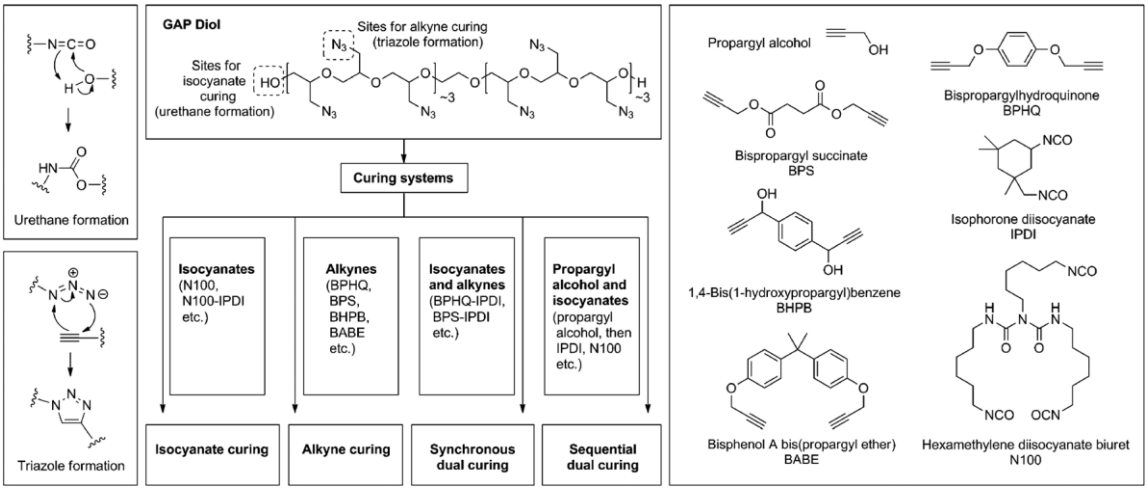

Scheme 4. Overview of curing mechanisms, curing systems, and curing agents for glycidyl azide polymer. Reprinted from ref. 96 with permission © 2015, John Wiley and Sons.

The first one consists of the use of polymeric coating materials to increase the compatibility of ADN with common curing agents used in most binder systems. Several microencapsulating and coating processes have been developed since the first work of Green and Schleicher in 1953 [63]. The technological procedures are widely used in nearly all industrial and commercial fields. Teipel *et al.* [103, 104] have employed a conservation

process according to the core-shell principle. They have utilized ethylcellulose and cellulose acetobutyrate (CAB) as coacervate capsules (Fig. 9). They revealed that the choice of materials is important for a successful microencapsulation process and showed that non-polar organic solvents were suitable for water soluble cores such as ADN and AN. A few years later, Heintz *et al.* [105] developed a coating method based on fluidized bed technology. They demonstrated that the use of polyacrylate, glycidyl azide polymer (GAP) and HTPB were leading to increased compatibility of ADN. The second approach, which consists of the use of free-isocyanate curing systems, was the most explored pathway.

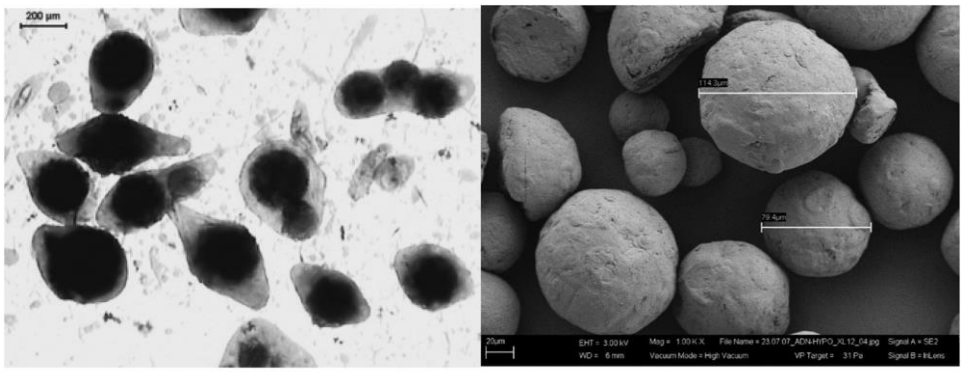

(a) **(b)**

Figure 9. Spherical ADN particles in CAB-containing coacervate capsules. Reprinted from ref. 56 with permission © 2006, John Wiley and Sons; ADN-Prills coated with 5% polyacrylate/silane. Reprinted from ref. 85 with permission © 2009, John Wiley and Sons.

The motivation of this approach was not only to improve the compatibility of ADN in a propellant formulation, but to overcome other flaws as well. Isocyanates are both moisture sensitive and hazardous. They react with moisture to liberate CO_2 and form voids in the cured propellant, leading to poor mechanical properties during storage. In systems including energetic nitrate ester plasticizers, isocyanates generate toxic nitroso derivatives. Some of potential replacements for isocyanate-based curing agents that have been reported are: bispropargylhydroquinone (BPHQ), bisphenol A bis(propargyl ether) (BABE), bis-propargylsuccinate (BPS), 1,4-bis(1-hydroxypropargyl)benzene (BHPB), and other bis(propargyl) aromatic esters and ethers [101, 102, 106, 107].

The development of ADN-based green propellant was driven by civilian requirements for environmental respect in space propulsion systems and by military needs for high performance and minimum smoke propellant in tactical missile applications. Several formulations have been tested to satisfy a number of critical tasks such as compatibility,

performance, curing, mechanical properties and stability. Flon *et al.* [108] have evaluated the substitution of AP by ADN in solid rocket propellants, containing HTPB as binder and Al as fuel, for large space launch boosters. The results from the performance computations revealed that, by replacing AP with ADN, the theoretical specific impulse increases by 3% and the combustion temperature decreases by 4%. The authors deduced the presence of a little reactivity between ADN and HTPB, thus the use of such a formulation needs improvement. To further improve the ADN-based propellant performance, some researchers suggested the utilization of GAP which is an energetic binder, to compensate for the lower oxygen balance of ADN (+25.8%), with respect to AP (+34.04%). Thermodynamic calculations of the theoretical gravimetric specific impulse under frozen equilibrium assumption have been reported for the systems ADN/GAP/Al and AP/HTPB/Al. It was noticed that the gravimetric specific impulse of the system ADN/GAP/Al features higher values with a maximum of 296 s at 59% ADN, 20% GAP, and 21% Al when compared to the system AP/HTPB/Al (maximum 284 s at 68% AP, 12% HTPB and 20 % Al). Even more notable is the fact that the compositions with higher specific impulses are in a region of larger binder contents of 20–30% instead of 10–20% for AP/HTPB/Al and this will permit to manufacture such formulations with better mechanical properties. The combustion behavior of a propellant formulation containing ADN/GAP filled with 16% of aluminum was investigated by Weiser *et al.* [109]. They demonstrated that the combustion of such propellant obeys the Vieille's law with a pressure exponent of 0.58 and a multiplicative factor of 8.82 mm s^{-1}. That is quite high for practical applications and thus further efforts are needed to decrease the absolute burning rate. Cerri *et al.* [110] have studied the aging behavior of several ADN/GAP-based propellant formulations.

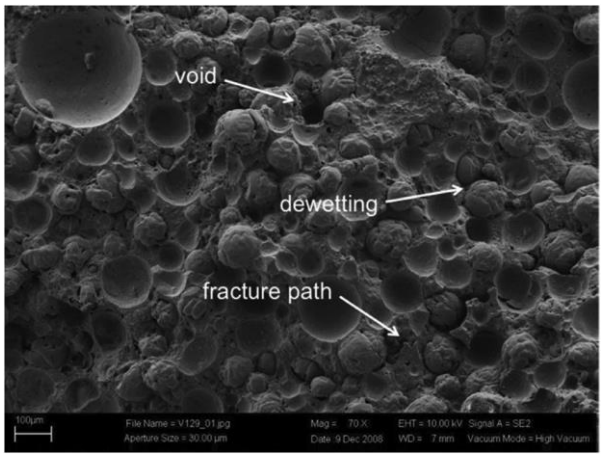

Figure 10. Scanning electron microscopy analysis of the ADN-based propellant after the tensile test. Reprinted from ref. 99 with permission © 2014, John Wiley and Sons.

They revealed that the ADN/GAP-based formulations show evidence of a high porosity of the propellants and strong dewetting phenomena, as shown in Fig 10. Also, the dynamic mechanical analysis measurements revealed a high glass transition of 40 °C to 50 °C, which is higher than the ones of the current HTPB/AP/Al formulations. Thus, it was concluded that they cannot fulfill the NATO specification for the very wide in-service temperature range of –54 °C to +71 °C, which means that intensive efforts should be focused to address such problems. Winborg [111] has recently substituted 1-diamino-2,2-dinitroethene (FOX-7, $C_2H_4N_4O_4$) and guanylurea dinitramide (FOX-12) for ADN to decrease the sensitivity of the ADN/GAP propellant. It was concluded that the amount of FOX should be kept below 30% in order to obtain a reasonable pressure exponent. In a separate work, propellant formulations containing a combination of dual oxidizers AN (coated by KNO_3)/ADN with GAP and HTPB binders have recently been tested [112]. It was shown that varying the ratio of the ADN/AN oxidizer mixture, the burning rate of aluminized propellant can be tuned. For GAP-based propellants; the increase of the content of AN led to a decrease of the burning rate and the impact sensitivity, whereas an increase of pressure exponent to unacceptable values was found for HTPB-based propellant. It was noted that further research is required to solve some compatibility issues as well.

It was reported that any binder normally used in solid rocket propellants could be used allowing for the fact that the curing agent needs to be chemically compatible with ADN. Thus, the utilization of non-isocyanate curing agents is of great interest. Thus, an alternative methodology suggested to exploit the 1,3-dipolar cycloaddition reaction (Huisgen reaction) between azide group of a new generation of energetic binders and triple bond of alkynes forming 1,2,3-triazoles [101]. This is considered as a versatile tool in polymer chemistry for forming crosslinked networks without any side reaction, and thus is a prime example of Click chemistry [113]. In addition to GAP, several other binders can be employed in ADN-based propellants such as poly(3-nitratomethyl-3-methyloxetane) [poly(NiMMO)], poly(glycidyl nitrate) [poly(GLyN)], poly(3,3-bis(azydomethyl)oxetane) [poly(BAMO)] and poly(azidomethyl methy oxetane) [poly(AMMO)] [85]. Consequently, this kind of ADN/binder-propellants may yield enhanced performance in terms of specific impulse as well as produce clean environmentally acceptable combustion products [14].

Hydrazinium Nitroformate (HNF)

A potential eco-friendly oxidizer, hydrazinium nitroformate (HNF, $N_2H_5C(NO_2)_3$), has entered the field of advanced propulsion systems some decades ago [114, 115]. Although HNF has a relatively lower oxygen balance with respect to AP, it has a noticeably superior heat of formation leading to higher specific impulse [116]. Additionally, it undergoes intense exothermic combustion reaction near the burning surface of the HNF-based propellant, giving rise to an effective heat feedback which augmenting the burning rate [14]. This energetic material has further benefits over AP, such as clean combustion, a low signature, non-hygroscopic nature, high density, and ease method of synthesis [35]. Furthermore, the melting point of HNF lies in the range of 115-124 °C depending on its purity and is suitable for processing of propellant formations, because the curing process is commonly performed at high temperature. In Europe, HNF was actively produced in the Netherlands in a pilot plant that had a maximm capacity of 300 kg per year. Today, it is mainly India and China who continue its production. HNF is reported to have been discovered in 1952. The synthesis of HNF involves a two-step process with an acid-base reaction of nitroform (NF) and hydrazine, as shown in Scheme 5 [10].

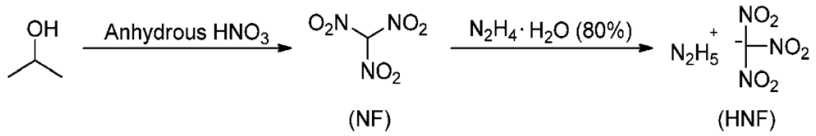

Scheme 5. Synthesis procedure of hydrazinium nitroformate. Reprinted from ref. 109 with permission © 2014, The American Chemical Society.

NF is the key starting material for the preparation of HNF [115]. According to Joo and Min [117], Hantzsch was considered as the pioneer in the production of NF by nitration reaction of acetic anhydride to tetranitromethane, followed by its conversion to NF using sulfuric acid (H_2SO_4) and potassium hydroxide. Several other procedures for the synthesis of NF have been developed by the use of a number of substrates, comprising acetylene, acetone, isopropanol, and acetic anhydride [117-119]. But several production technology methods had to be abandoned because of the environmentally unfriendly substances, high costs and many explosions occurring during the production process [119]. The only efficient procedure for large-scale manufacturing is the reaction of isopropanol and HNO_3. Recently, the reaction conditions were optimized and the NF yield of 53.6% was obtained from isopropanol by Ding *et al.* [120]. More recently, Yan *et al.* [119] have synthesized NF using

acetylacetone as substrate and fuming HNO_3 with acetic acid as the nitrating system. This new synthesis route for NF is expected to be an alternative method for the industrial production of the first step process of HNF manufacturing. This method is considered inexpensive, has mild reaction conditions with a satisfactory yield. Recent different recent procedures of NF synthesis are shown in Scheme 6.

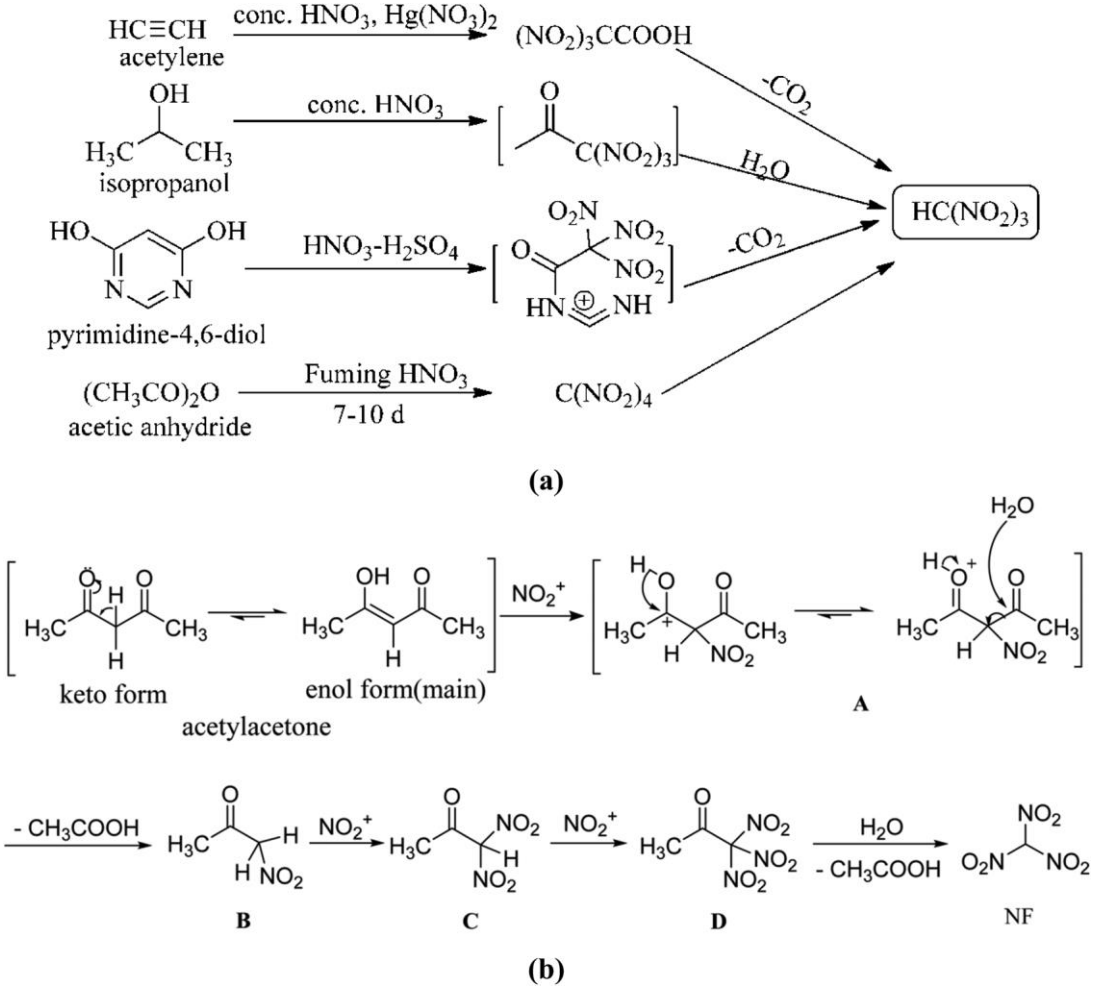

Scheme 6. (a) Synthetic routes for the synthesis of nitroform using different substrates. Reprinted from ref. 157 with permission © 2014, The American Chemical Society; (b) reaction mechanism for the synthesis of nitroform from acetylacetone. Reprinted from ref. 108 with permission © 2016, The American Chemical Society.

However, despite the progress in the last few decades, there are various unresolved issues concerning the thermal stability, and friction and impact sensitivity of HNF. Furthermore, the use of the hydrazinium cation may be critical because of the eventual liberation of highly cancerogenic hydrazine as a consequence of thermal stress or alkaline reaction conditions, but this latter is free of chlorine, thus the combustion reaction is considered to be clean. The purity of the HNF produced is also crucial since the presence of solvents or impurities leads

to serious safety problems during handling, transport and storage [6, 10, 35]. Recently, several production procedures have been optimized to overcome this drawback [119-121]. The incorporation of stabilizers will probably be required to improve the thermal stability of HNF as well [10]. However, it has long been considered that the main problem of HNF was its sensitivity. The large length-diameter ratio (L/D) of HNF was expected to be the reason of its high sensitivity. Several methodologies have been tested to decrease the L/D of HNF crystals, but no important progress was achieved using simple crystallization procedures. Recent research, by several researchers, has developed the industrial manufacturing of HNF crystals, using advanced crystallization or coating methods [120-122]. Athar *et al.* [122], for example, have successfully desensitized HNF by changing its crystal size, shape and coating it with nanocomposites. The authors have employed a number of methods such as mechanical stirring, ultrasound and using crystal shape modifiers. The optimized conditions generate a preferential axial crystals growth, where the long needles with sharp edges and corner, which have a very high L/D and high impact as well as friction sensitivity, have been transformed to near cubic shape crystals with a lower L/D and improved sensitivity, as shown in Fig. 11. They reported that the best coating agent was the hydroxyl-terminated poly(butadiene)-based clay nanocomposites. In 2014, Ding *et al.* have synthesized HNF using NF derived from isopropanol.

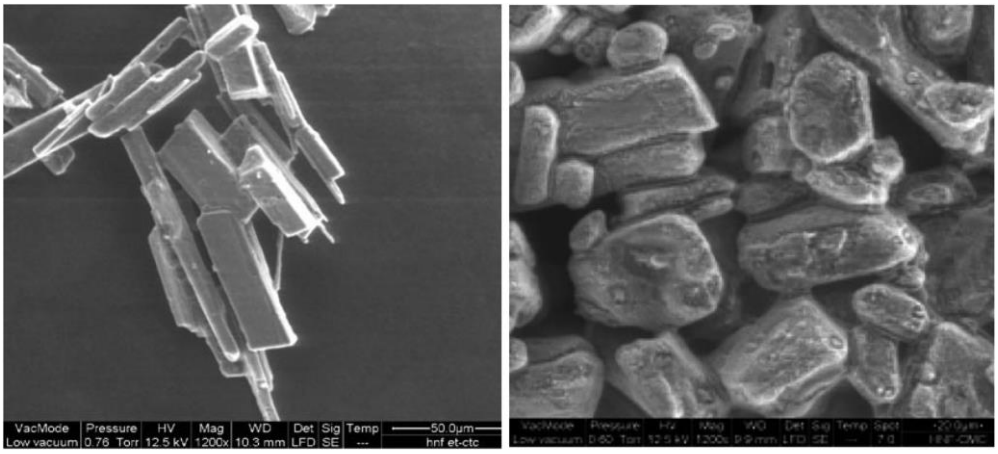

Figure 11. (a) Virgin HNF crystals with sharp edges and corners and very high L/D ~ 6.0, friction/impact sensitivity of 2.0 kg/25 cm; (b) Modified HNF crystals with rounded edges and lower L/D ~ 2.0. Friction/impact sensitivity of 4.0 kg/28 cm. Reprinted from ref. 111 with permission © 2010, John Wiley and Sons.

The morphology of HNF crystals was modified by a number of crystallization procedures to decrease the sensitivity of HNF toward environmental stimulus. The morphology of HNF crystals obtained using different test methods is displayed in Fig. 12. The solvent/non-solvent (S/NS) crystallization using methanol/ dichloromethane displayed crystals with small L/D ration with gentle edges and corners. However, the obtained value of L/D was still comparable with that reported previously. The utilization of sono-crystallization produced promising L/D values, whereas sharp edges and corners still persisted. However. The best L/D value was, provided by the sequential cooling crystallization method leading to uniform crystals with soft edges and corners.

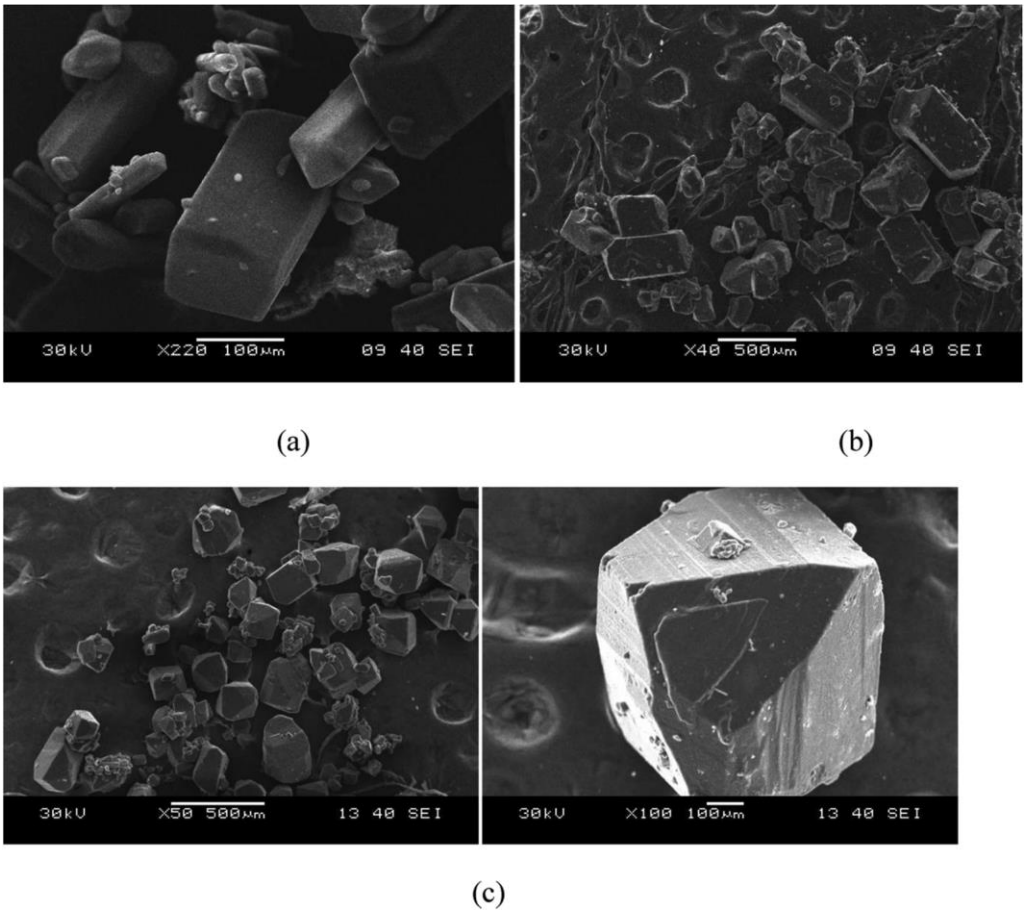

Figure 12. HNF crystals from: (a) antisolvent crystallization using S/NS, acetonitrile /dichloromethane; (b) sono-crystallization; (c) sequential cooling crystallization. Reprinted from ref. 109 with permission © 2014, The American Chemical Society.

The synthesized HNF using the later procedure exhibited lower sensitivity toward friction and impact. Another flaw of HNF, that has been recently resolved, is its compatibility with the most extreme binder which is commercially available and used, which is HTPB. The existence of carbon double bond in the HTPB backbone was reported to be the main cause

of the HNF/HTPB incompatibility, because the carbone-carbone double bond are easily oxidized by HNF leading to a decrease of mechanical properties of the binder [115]. This incompatibility can also be caused by the presence of isocyanates, used as crosslinking agents, where a hydrogen transfer from HNF to nitrogen of the isocyanate group –N=C=O can occur [10]. A more recent patent by Deppert *et al.* [123] showed a new approach to desensitize HNF and to improve its compatibility with HTPB and its curing isocyanate agents. HNF particles have been dispersed in a polymeric binder and there is a bonding agent that plays the role of Lewis acid to form an encapsulating film to at least a portion of the HNF particle surfaces. A bonding agent is a component of propellant formulation that improves processing, mechanical properties, safety, ballistic and stability characteristics, eliminates voids and micro porosity, and enables higher solids loadings [9, 10, 43]. Several bonding agents can be used, such as boron-based compounds, halides, some metals, enone compounds, and any monomer or polymer containing an atom or group that acts as Lewis acid. The bonding agent is added to HNF in an amount of 0.1 to 1.0 mass %. The molecular mass of the binder that holds the two components (HNF and bonding agent) can be in the range between about 600 and 3000 g mol^{-1}. Additional additives can be incorporated into the coated HNF to improve its properties such as other fillers [*e.g.,* cyclotrimethylene trinitramine (RDX)], fuels (*e.g.,* Al), stabilizers (*e.g.,* diphenylamine), and processing aids (*e.g.,* catalysts) [10, 124-126]. Briefly, the hydrazinium cation ($N_2H_5^+$), of the HNF salt, that has a nitrogen atom with alone pair of electrons can play the role of Lewis base. Accordingly, in the presence of Lewis acid, this hydrazinium cation of the HNF salt will donate a pair of electrons to form a Lewis adduct. The procedure developed leads to the chemical reaction of the bonding agent with the surface of the HNF and during the curing step, the bonded oxidizer and other compounds, if present, will react with a polymeric binder to produce the required propellant formulation without compatibility problems [38]. In another piece of research, Sonawane *et al.* [127] have tested a new isocyanate-free curing agent (BPHQ) for GAP and investigated the compatibility of HNF with this curing agent. It was found that isocyanate-free curing system could be more suitable in chlorine-free composite solid propellant formulation and the BPHQ showed good compatibility with HNF.

Unlike HTPB, several pieces of research have shown that HNF is compatible with the recent developed binders such as GAP, poly(NiMMO), poly(GLyN), polynitromethyloxetane (PLN) and poly(BAMO). Potential benefits can be obtained when using this oxidizer, because it not only gives high performance, but also produces an environmentally benign

exhaust as the gases released during combustion are free from chlorine [6, 10, 14, 128]. The friction and impact sensitivity of HNF-based propellants are acceptable with respect to other formulations being used presently [10]. An overview of the HNF-based propellant formulations has been summarized by Dendage *et al.* in their review article [129]. Propellant formulations based on HNF demonstrated a relatively high burning rate (30 mm s^{-1} at 7 MPa). For non-catalyzed HNF-based propellants, the pressure exponent *n* ranged between 0.81–1.12 [35, 128]. The *n* value can be decreased to more acceptable values, *i.e.* $0.4 < n < 0.6$, by using suitable ballistic modifiers or by reducing the mean size of HNF [10, 130]. It is predicted that by utilizing HNF-based propellants, an increase in specific impulse of more than 7% and a payload capacity gain of 10% can be reached [6, 35].

FOX-7 and Its Derivatives

Some of the new energetic materials, which have been prepared during these two last decades, have led to new possibilities not only for military but also for civilian ones, because of environmental considerations and safety requirements while at the same time securing high performance [15, 17, 131]. FOX-7, a relatively new high energetic material, presents high thermal stability, high performance, low sensitivity, high heat of formation, favorable oxygen balance, high density, clean decomposition products and good compatibility with oxidizers, polymers, plasticizers and isocyanates [57, 132]. The synthesis procedures of FOX-7 (Scheme 7), together with its structural, spectroscopic, thermal and explosive properties have been thoroughly reviewed [132-135]. This compound can be used as an insensitive high energy density material because its performance is comparable to the common secondary explosives such as cyclotetramethylene tetranitramine (HMX), RDX and pentaerythritol tetranitrate (PETN). The typical structural features of FOX-7 are established by alternating amino and nitro groups in the solid state.

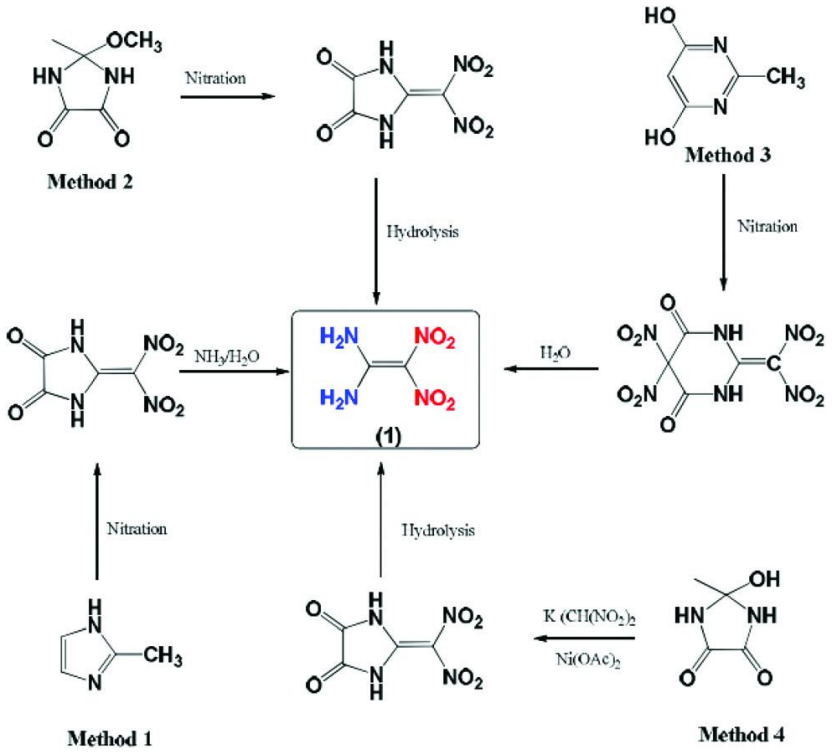

Scheme 7. Typical methods used to synthesize FOX-7. Reprinted from ref. 122 with permission © 2016, The Royal Society of Chemistry.

Since 1998, when FOX-7 was first synthesized by Latypov *et al.* [136], it has caused a great deal of interest and has been considered as one of the potential candidates to be used in solid propellants. Florczak [137] performed thermodynamic calculations and studied the thermochemical and ballistic properties of aluminized composite propellants containing AP/Al/binder with and without FOX-7. The author concluded that the incorporation of FOX-7 instead of AP led to a decreased heat of combustion, burning temperature, specific impulse and burning rate of the propellant. In a separate work, Chen *et al.* [138] investigated the properties of some propellant formulations based on HTPB/FOX-7 using DSC and sensitivity test apparatus. They showed that the apparent activation energy of FOX-7 propellant was about 245.2 kJ·mol^{-1} and the friction sensitivity was less than 68% and the impact sensitivity was over 25.0 J. Compared with RDX propellant formulations, mechanical sensitivities and electrostatic discharges of HTPB/FOX-7 significantly decreased. Recently, Lempert *et al.* [139] have theoretically compared the effect of FOX-7 and HMX on the properties of AP/Al/binder (inert or active) propellant formulations. They reported that the FOX-7-based composites containing an inert binder ($C_{73.17}H_{120}$) had energy characteristics which were too low, as it would be expected in view of the low oxygen content in FOX-7. They demonstrated that the values of specific impulse of propellant

formulations with FOX-7 were lower than those of composites with HMX by 10 s and 4 s at levels of 60% FOX-7 and 30% HMX in the composite, respectively. They concluded, however, that a solid composite propellant formulation, with a specific impulse of 251 s, density of 1.91 g·cm^3, and burning temperature of 3600 K, can be created using 60% FOX-7 and 19% of an active binder ($C_{18.96}H_{34.64}N_{19.16}O_{29.32}$). More recently, Jensen *et al.* [140] showed that FOX-7 is an attractive, but less than ideal, substitute for nitramine in smokeless GAP-RDX composite rocket propellants that exhibit low shock sensitivity and good mechanical properties.

However, because of the abundance of FOX-7 chemical reactivity through acid-base reaction, coordination reaction, reduction reaction, oxidation reaction, acetylate reaction, nucleophilic substitution reaction and electrophilic halogenation reaction, more than 130 derivative compounds of this energetic material have been published (Scheme 8). Recent reviews have comprehensively collected all of these reactions [133-135, 141, 142]. In spite of the numerous reactions involving FOX-7 described in the past ten years, new reactions continue to be found [57, 58, 141]. Derivatives of FOX-7 were not known to act as oxidizers before 2013, and the discovery of this behavior presents a new episode in the chemistry of FOX-7. While these chemicals are not proposed as potential alternatives for current propellant oxidizers, this is a valuable discovery in the chemical life and behavior of FOX-7 [143]. Therefore, finding new oxidizers with desirable properties is needed so that they can be substituted for the currently reported ones (AP, PSAN, ADN, HNF) which are limited in numbers and present many drawbacks in practical application.

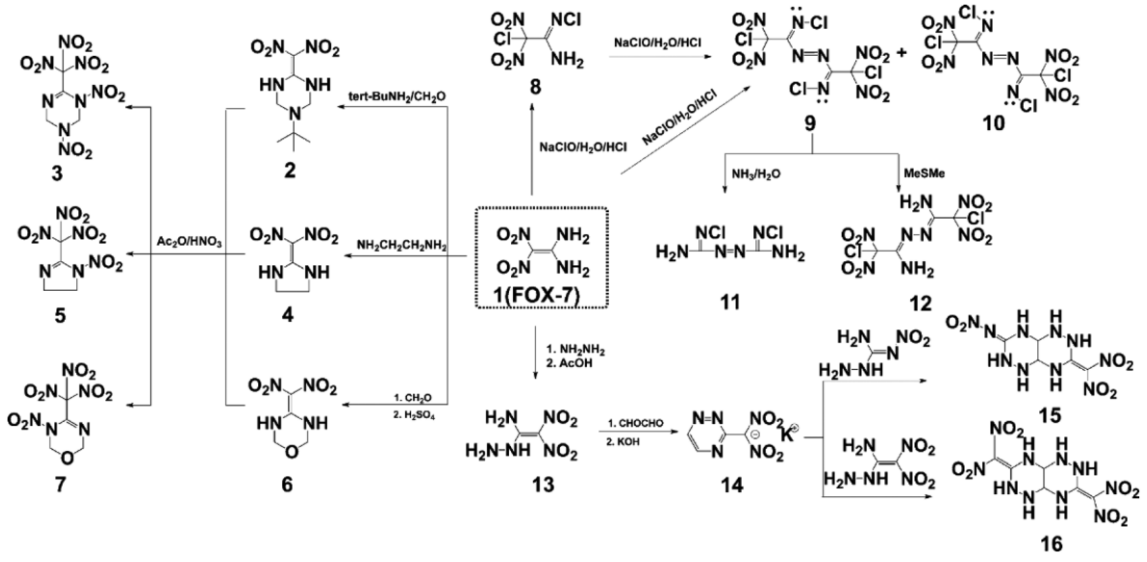

Scheme 8. Selection of FOX-7 derivatives. Reprinted from ref. 121 with permission © 2015, John Wiley and Sons.

Incorporating further nitro groups is a practical strategy to produce energetic FOX-7 derivatives. Nitro groups are essential chemical groups of high energy density materials and their presence in molecules contributes significantly to the overall energetic performance and enhances the density and oxygen balance of energetic materials. The Shreeve group proposed a new oxidizer tetranitroacetimidic acid (TNAA, Scheme 9, **42**) [53, 135]. It was demonstrated that TNAA is a very attractive and promising replacement for AP. Its melting point of 91 °C is comparable to that of ADN (93 °C) and its decomposition temperature of 137 °C is higher than that of HNF (131 °C). Despite its lower thermal stability and friction sensitivity with respect to AP, it presents comparable properties and acceptable stability to that of ADN and HNF, and it can be added to propellant formulations. Compared to AP, TNAA has a considerably enhanced oxygen and nitrogen content and higher positive oxygen balance because of the presence of the trinitromethyl group. A similar research group pointed out that the calculated value of specific impulse of the formulation of HTPB/TNAA/Al (12/68/20) was 261 s. Another very promising candidate compound to be considered as a replacement for AP is the tetranitroacetamide (NTNAA) [58]. It was demonstrated by a computational study that the synthesis of NTNAA from TNAA is thermodynamically possible. Zhang and Gong [58] revealed that NTNAA present properties similar to TNAA, and consequently it could be a potential replacement for AP as oxidizer in composite propellants.

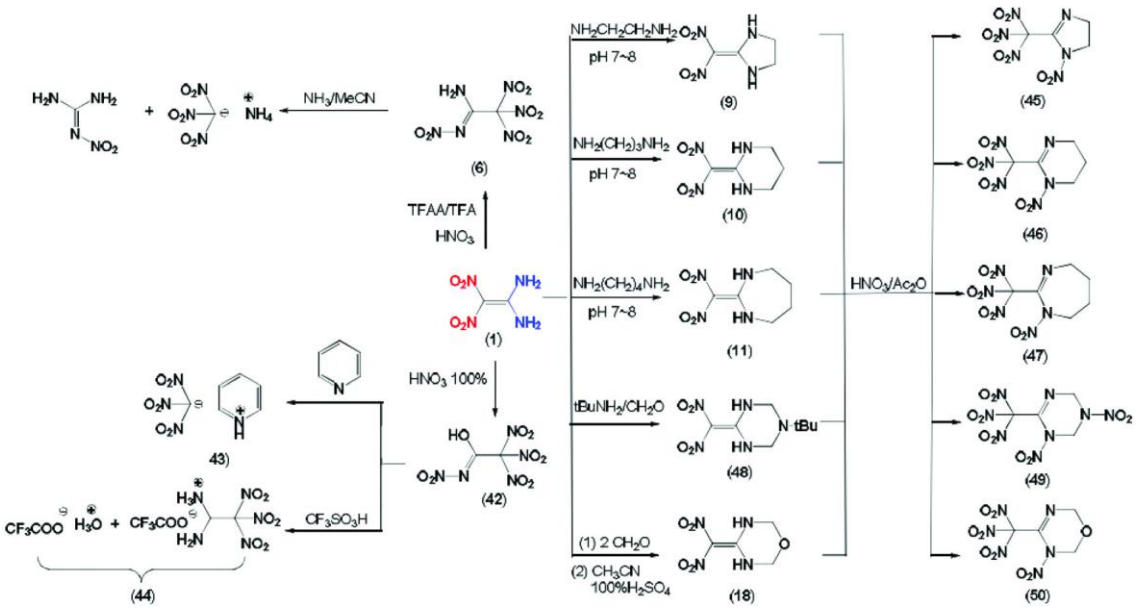

Scheme 9. Polynitro derivatives of FOX-7. Reprinted from ref. 122 with permission © 2016, The Royal Society of Chemistry.

Other High Energy Dense Oxidizers (HEDOs)

The challenge in the development of new HEDOs or improvement of those studied during the last few years is to seek a good compromise between performance and physicochemical properties, in this case between high specific impulse and high oxygen balance on one hand and acceptable thermal stability and low sensitivity on the other hand, in addition to low cost, simplicity of the synthesis, and low hazards.

HNIW or commonly known as CL-20 is regarded as one of the HEDOs for the next generation of propellants [35, 144-151]. It is found to be eco-friendlier as well as to reduce the propellant exhaust plume signature without generating combustion stability problems. Under ambient conditions, CL-20 has four polymorphs, α, β, γ, and ε, as shown in Fig. 13 [145]. These different polymorphs lead to various physicochemical features such as thermal stability, sensitivity, density, and performance, which govern its application. Thermodynamically, the ε-phase is the most thermodynamically stable and is considered as the favored phase for propulsion applications because of its highest density (2.04 g cm^{-3}).

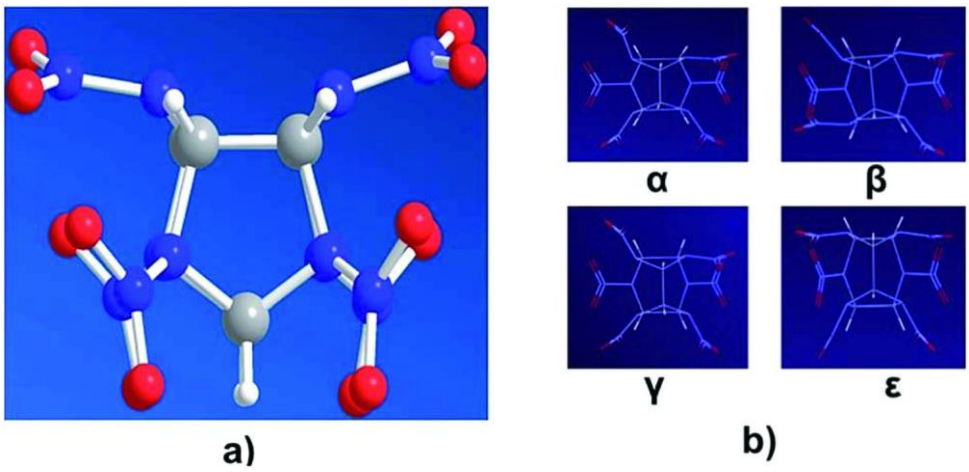

Figure 13. (a) Ball-and-stick model of ε-CL-20; (b) the four polymorphs of CL-20. Adapted from ref. 134 with permission © 2016, The Royal Society of Chemistry.

The synthesis of CL-20 is considered to be one of the most complicated chemical procedures. Several papers have been published demonstrating various procedures involving multiple steps and methodologies for the synthesis[144, 152]. However, HNIW has high impact and friction sensitivity as well as high production costs. Consequently, controlling the crystal density, decreasing the sensitivity and the production cost have received much attention in order to produce a promising candidate CL-20 for several energetic applications. In addition to Nair *et al.* [144], another interesting recent review paper by Viswanath *et al.* [152]

summarizes different synthesis strategies to produce CL-20 with reasonable properties and its characterization. The commonly known methods are based on the same starting material, hexabenzylhexaazaisowurtzitane (HBIW) [153]. Nevertheless, conversion of HBIW directly to CL-20 is a major challenge. A rather low yield of HNIW and high costs of the implemented nitronium tetrafluoroborate (NO_2BF_4) and nitrosonium tetrafluoroborate ($NOBF_4$) catalysts necessitate improvements of the HNIW synthesis method [1]. More recently, Simakova and Parmon [153] developed a new approach based on the two-step HBIW debenzylation with separately repeated use of the palladium-based catalyst in each catalytic stage. This approach is considered as a promising way to increase the catalyst productivity and to reduce the CL-20 production costs. All these improvement can certainly increase the number of its application as an AP substitute for solid rocket propulsion.

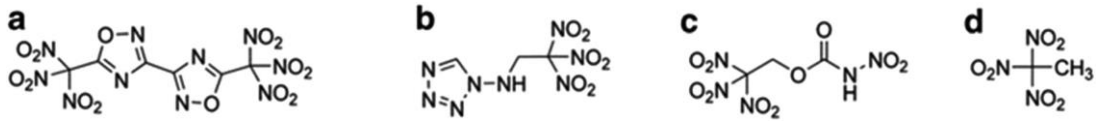

Scheme 10. Selected compounds synthesized by Klapötke group (a) 5,5'-bis-(trinitromethyl)-3,3'-bi-(1,2,4-oxadiazole), (b) 1-(trinitroethylamino) tetrazole, (c) 2,2,2-trinitroethyl nitrocarbamite, (d) trinitroethane.

Several groups worldwide have intensively investigated other potential chemicals to substitute the current widely used oxidizer (AP). Such compounds include azide, azo, nitro, amino functionalities ontriazine, azole, furazano, carbamite backbones to name a few[15, 17, 131, 154]. Some of the most promising classes of materials were poly-nitro moieties compounds. One of the well-known groups on the field is that of Klapötke, who investigated several classes of materials such as orthocarbonates, 2,5-disubstituted tetrazoles, bi-1,2,4-oxadiazoles, carbamites and nitrocarbamites (Scheme 10) [17, 155-157]. These different compounds demonstrated several advantages but also shortcomings for the suitability to use for propulsion purpose and as replacements for AP. Based on experiments and computing results, it was shown that propellants based on some of the synthesized chemicals broadly exceed the performance of AP-based ones, but fail to meet other requirements such as low sensitivities or thermal stability. More recently, the Klapötke group revealed that 2,2,2-trinitroethyl nitrocarbamite (TNENC) prepared using a simple synthesis procedure can be a potential replacement of AP [59]. This nitrocarbamite presents a melting temperature of 109 °C which is higher than that of ADN (93 °C) and a decomposition temperature of 153 °C which is higher than that of HNF (131 °C). Although it has a lower thermal stability and

friction sensitivity when compared to AP, it exhibits comparable properties and acceptable stability to that of ADN and HNF. Furthermore, this nitrocarbamite has a very positive high oxygen balance and present a specific impulse comparable to a composition using AP. Advantageously, the burning of TNENC with aluminum produces no toxic substances such as hydrogen chloride. however, it is worth noting that the main issue of this new oxidizer is its synthesis procedure that involves a toxic synthesis step using phosgene [59]. The same group has developed a new synthesis procedure to overcome this flaw [155]. Thus, a less hazardous synthesis route for 2,2,2-trinitroethyl carbamate, used to produce 2,2,2-trinitroethyl nitrocarbamite, is performed using chlorosulfonyl isocyanate in a one-step synthesis with a yield of 96% compared to the previously toxic procedure (71%).

Klapötke's group also revealed two different HEDOs that can replace AP in the homogenous and heterogeneous solid rocket propellants which are bis(2,2,2-trinitroethyl) oxalate (BTNEO) and 2,2,2-trinitroethyl formate (TNEF) [158, 159]. These new high energy dense oxidizers "oxalate and formate" have shown very good properties as green oxidizers for solid rocket propellants with melting temperatures of 115 °C and 127 °C, respectively, and decomposition temperatures of 186 °C and 192 °C, respectively. This means that they can be used in the production of solid propellants using the casting method because of the difference between their melting and decomposition temperatures, which is near 70 °C. Although they are perform less well than AP in the thermal and impact sensitivity, BTNEO showed a higher value than AP in friction sensitivity test [158].

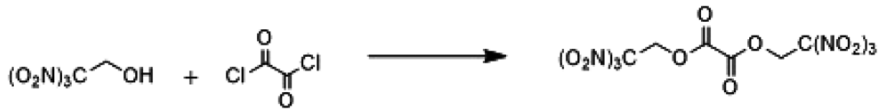

Scheme 11. Synthesis procedure of bis(2,2,2-trinitroethyl) oxalate.

In the same way, oxalate and formate oxidizers have a high density, which are 1.84 g cm^{-3} and 1.81 g cm^{-3}, respectively, with a high positive oxygen balance. Also, the specific impulse of these oxidizers which are 231 s and 228 s, respectively, are higher than that of AP. The synthesis of these oxidizers is easy (Schemes 11 and 12) and also their decomposition is eco-friendly.

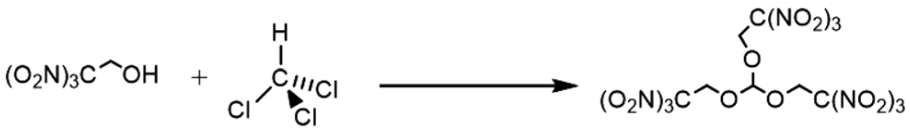

Scheme 12. Synthesis method of 2,2,2-trinitroethyl formate.

All these four different HEDOs showed clear homogenous smokeless burning with high burning rates when added to nitrocellulose (NC) as an oxidizer (Fig. 14) instead of the extremely dangerous sensitive nitroglycerine [160]. Klapötke's group synthesized these different HEDOs and fully characterized them. New formulations of green solid rocket propellants based on those oxidizers with different fuel binders are currently under study.

Figure 14. Homogenous smokeless burning of different green energetic compositions: (a) BTNEO/NC; (b) TNENCA/NC; (c) TNEF/NC.

Recently Shreeve's group [52] has investigated the synthesis of polynitro-substituted pyrazoles and triazoles as potential propellant oxidizers. The group revealed that 5-azido-3,4-dinitro-N-(2,2,2-trinitroethyl)-1H-pyrazol-1-amine (ANNPA), 3,5-dinitro-*N*-(2,2,2-trinitroethyl)-1H-pyrazol-1,4- diamine (DNNPDA), 3,4-dinitro-1H-pyrazole-1,5-diamine (DNPDN) and 3-nitro-*N*-(2,2,2-trinitroethyl)-1H-1,2,4-triazol-1-amine (NNTAA) can be considered as promising candidates as replacements oxidizers for AP. These compounds with an oxygen balance over 10% have good thermal stability, high density and favorable performance. More recently, Keshavarz *et al.* [61] have introduced novel tetrazole derivatives as performance energetic compounds, as an oxidizer in solid propellants. These tetrazols (5,5′ [(1Z,5Z)-3,4-dinitrohexaaza-1,5-diene-1,6-diyl]bis(1-nitro-1Htetrazole), (DNDNT); 3,3′,7,7′-tetranitro-3,3a,3′,3′a-tetrahydro7H,7′H-6,6′-bitetrazolo[1,5-e] pentazine, (TTBTE)) are considered as good candidates, because they have good thermal stability, good performance and less sensitivity.

Fan *et al.* [161] studied two new green tetrazole salts, hydroxylammonium 2-dinitromethyl-5-nitrotetrazolate (HADNMNT) and dihydroxylammonium 5,5'-bistetrazole-1,1'-diolate (TKX-50). Theoretically, it was revealed that HADNMNT is a promising oxidizer to replace AP in composite solid propellants. Safety tests demonstrated that TKX-50 shows excellent thermal stability and low mechanical sensitivities. The compatibility testes of TKX-50 with

HTPB, AP, RDX, and Al powder in vacuum stability tests were acceptable. Results from comparative investigation of TKX-50 and RDX as ingredient for composite solid propellants showed that TKX-50 formulations offer the advantages of high burning rate and low mechanical sensitivities.

Sinditskii *et al.* [162] focused his attention on high nitrogen energetic materials. Among polynitrogen energetic materials, 1,2,4,5-tetrazine derivatives are of particular interest for propulsion community because of their high density, thermostability, and remarkable insensitivity to electrostatic discharge, friction, and impact. High enthalpy of formation and good thermal stability of tetrazine cycle generate tetrazine-based energetic materials, which can be utilized as an insensitive, thermostable, environmentally friendly ingredient in various energetic material applications such as propellants and gas generating compositions. Investigations of combustion behavior revealed that most tetrazines are low-volatile components with high surface temperatures, which can play a dominant role of the condensed phase in combustion of several tetrazine derivatives.

Conclusions

With regard to the reference ingredient AP, which is the most used oxidizer in rocket science and is the compound to be replaced, it is notable that this chemical is an ionic material with properties which appear to be perfect, except for its toxicity. The currently developed substitutes need optimization to fully satisfy all of the requirements of ideal oxidizers. Thus, finding green, high-performing replacements for AP is a top priority internationally and need further endeavor to reach its aim.

For the near future, propellant formulations including green oxidizers are expected to advance the state-of-the-art of solid rocket propellants and reduce the environmental concerns caused by the use of AP. In the last few decades, several energetic oxidizers have appeared but most of them are far from being practically employed in real applications because of their various drawbacks. In this review, the most potential green oxidizers that show interesting properties and potential use in solid rocket propellantshave been focused on. In addition, the advantages and disadvantages of various green oxidizers have also discussed. The main challenges of green ingredients as propellant oxidizers and many of the attempts made to overcome these problems have been also highlighted.

To overcome the flaws of the current potential greenoxidizers such as PSAN, HNF and ADN, several procedures and methods of synthesis, crystallization and coating have been

recently developed to improve the physicochemical properties, decrease sensitivity, enhance compatibility, improve stabilityand performance, and reduce the roduction cost. Furthermore, the use of dual oxidizers, such as PSAN/AP or ADN/AP with less environmental impacts has been shown to be a god solution for improving the propellant formulations' performance. FOX-7 and its two derivatives TNAA and NTNAA were revealed to be very attractive and environmentally friendly replacement for AP with interesting roperties. CL-20 also proved to be a potential candidate as a replacement for AP. The development of other HEDOs such as TNENC, BTNEO, TNEF and TKX-50 has demonstrated that these candidates can meet the specific performance goal and allay the environmental concerns while presenting a helpful classification of hazards.

It is believed that the studies presented in this review will increase the interest of researchers on green oxidizers for solid rocket propulsion as well as provide a basic understanding of these green ingredients.

References

[1] L.T. DeLuca, *Eurasian Chem.-Technol. J.,* **2016**, 18 (3), 181-196.

[2] G.P. Sutton, O. Biblarz, *"Rocket Propulsion Elements"*. Canada: John Wiley & Sons, **2017**.

[3] J.-F. Guery, I.-S. Chang, T. Shimada, M. Glick, D. Boury, E. Robert, J. Napior, R. Wardle, C. Pérut, M. Calabro, *Acta Astronaut.,* **2010**, 66 (1), 201-219.

[4] L.T. DeLuca, L. Galfetti, F. Maggi, G. Colombo, L. Merotto, M. Boiocchi, C. Paravan, A. Reina, P. Tadini, L. Fanton, *Acta Astronaut.,* **2013**, 92 (2), 150-162.

[5] R.L. Geisler, R.A. Frederick, M. Giarra, in *"Encyclopedia of Aerospace Engineering"*. New York: John Wiley & Sons, **2010**.

[6] L.T. DeLuca, T. Shimada, V.P. Sinditskii, M. Calabro, *"Chemical Rocket Propulsion-A Comprehensive Survey of Energetic Materials"*. Switzerland: Springer, **2017**.

[7] L.T. DeLuca, in *"Chemical Rocket Propulsion"*. Switzerland: Springer, **2017**, pp. 1015-1032.

[8] H. Singh, in *"Chemical Rocket Propulsion"*. Switzerland: Springer, **2017**, pp. 127-138.

[9] N. Kubota, *"Propellants and Explosives: Thermochemical Aspects of Combustion"*. Weinheim, Germany: Wiley-VCH, **2015**.

[10] J.P. Agrawal, *"High Energy Materials: Propellants, Explosives and Pyrotechnics"*. Weinheim, Germany: John Wiley & Sons, **2010**.

[11] T. Brinck, *"Green Energetic Materials"*. Chichester: John Wiley & Sons, **2014**.

[12] K. Sellers, K. Weeks, W.R. Alsop, S.R. Clough, M. Hoyt, B. Pugh, J. Robb, *"Perchlorate: Environmental Problems and Solutions"*. New York: CRC press, **2006**.

[13] A. Larsson, N. Wingborg, In *"Advances in Spacecraft Technologies"*. Rijeka, Croatia: InTech, **2011**.

[14] M. Talawar, R. Sivabalan, T. Mukundan, H. Muthurajan, A. Sikder, B. Gandhe, A.S. Rao, *J. Hazard. Mater.*, **2009**, 161 (2), 589-607.

[15] T.M. Klapötke, *"Chemistry of High-Energy Materials"*. Berlin: Walter de Gruyter GmbH & Co KG, **2015**.

[16] N. Fischer, D. Izsák, T.M. Klapötke, S. Rappenglück, J. Stierstorfer, *Chem. - Eur. J.*, **2012**, 18 (13), 4051-4062.

[17] M.A. Kettner, T.M. Klapötke, in *"Chemical Rocket Propulsion"*. Switzerland: Springer, **2017**, pp. 63-88.

[18] S. Aldoshin, D. Lempert, T. Goncharov, A. Kazakov, S. Soglasnova, E. Dorofeenko, N. Plishkin, *Russ. Chem. Bull.*, **2016**, 65 (8), 2018-2024.

[19] M. Kohga, T. Naya, *J. Energ. Mater.*, **2015**, 33 (4), 288-304.

[20] P. Kumar, P.C. Joshi, R. Kumar, *Combust. Flame*, **2016**, 166, 316-332.

[21] M. Kohga, *Propellants Explos. Pyrotech.*, **2017**, 42, 665-670.

[22] C. Zhang, Y.J. Luo, Q.J. Jiao, B. Zhai, X.Y. Guo, *Propellants Explos. Pyrotech.*, **2014**, 39 (5), 689-693.

[23] G.D. Hugus, E.W. Sheridan, **2013**, US8444785.

[24] K. Balbudhe, A. Roy, S. Chakravarthy, *Proc. Combust. Inst.*, **2015**, 35 (2), 2471-2478.

[25] Y. Lan, J. Zhai, D. Li, R. Yang, *Propellants Explos. Pyrotech.*, **2014**, 39 (1), 18-23.

[26] T. Shindo, A. Wada, H. Maeda, H. Watanabe, H. Takegahara, *Acta Astronaut.*, **2017**, 131, 92-95.

[27] R.A. Sheldon, *Green Chem.*, **2017**, 19 (1), 18-43.

[28] H.F. Sneddon, *Green Chem.*, **2016**, 18 (19), 5082-5085.

[29] P. Anastas, N. Eghbali, *Chem. Soc. Rev.*, **2010**, 39 (1), 301-312.

[30] A. Mehrkesh, A.T. Karunanithi, *ACS Sustainable Chem. Eng.*, **2013**, 1 (4), 448-455.

[31] R. Aggarwal, I.K. Patel, *Int. J. Latest Trends Eng. Technol.*, **2015**, 6 (1), 83-87.

[32] P. Surmacz, *J. KONES*, **2016**, 23, 337-344.

[33] K.J. Stober, A. Thomas, B.J. Evans, B.J. Cantwell, in *52nd AIAA/SAE/ASEE Joint Propul. Conf.*, **2016**, p. 4991.

[34] S. Reshmi, H. Hemanth, S. Gayathri, C.R. Nair, *Polymer*, **2016**, 92, 201-209.

[35] A. Dey, A.K. Sikder, M.B. Talawar, S. Chottopadhyay, *Cent. Eur. J. Energ. Mater.*, **2015**, 12 (2), 377-399.

[36] D.M. Badgujar, M.B. Talawar, P.P. Mahulikar, *Propellants Explos. Pyrotech.*, **2016**, 41 (1), 24-34.

[37] J. Johansson, N. Latypov, S. EK, M. SKARSTIND, H. Skifs, **2017**, US0008768.

[38] T.M. Deppert, D.R. Smith, C. Shanholtz, **2017**, US3137438.

[39] N. Winterton, *Clean Technol. Environ. Policy*, **2016**, 18 (4), 991-1001.

[40] C. Eldsäter, E. Malmström, *Green Energ. Mater.*, **2014**, 205-234.

[41] G. da Silva, S.C. Rufino, K. Iha, *J. Aerosp. Technol. Manage.*, **2013**, 5 (2), 139-144.

[42] A.S. Gohardani, J. Stanojev, A. Demairé, K. Anflo, M. Persson, N. Wingborg, C. Nilsson, *Prog. Aeronaut. Sci.*, **2014**, 71, 128-149.

[43] G. Singh, *"Recent Advances on Energetic Materials"*. New York: Nova Scientific Publishers, **2015**.

[44] G. Tang, S. Tian, Z. Zhou, Y. Wen, A. Pang, Y. Zhang, D. Zeng, H. Li, B. Shan, C. Xie, *J. Phys. Chem. C*, **2014**, 118 (22), 11833-11841.

[45] D. Trache, F. Maggi, I. Palmucci, L.T. DeLuca, K. Khimeche, M. Fassina, S. Dossi, G. Colombo, *Arab. J. Chem.*, **2015**, DOI: 10.1016/j.arabjc.2015.11.016

[46] A. Mezroua, K. Khimeche, M.H. Lefebvre, M. Benziane, D. Trache, *J. Therm. Anal. Calorim.*, **2014**, 116 (1), 279-286.

[47] M. Zou, X. Wang, X. Jiang, L. Lu, *J. Solid State Chem.*, **2014**, 213, 235-241.

[48] Z. Yang, F. Gong, L. Ding, Y. Li, G. Yang, F. Nie, *Propellant, Explos. Pyrotech.*, **2017**, 42, 1-8.

[49] R. Tunnell, M. Ashcroft, R. Dale, D. Tod, W.G. Proud, *Propellant, Explos. Pyrotech.*, **2014**, 39 (4), 504-510.

[50] S. Chaturvedi, P.N. Dave, *J. Saudi Chem. Soc.*, **2013**, 17 (2), 135-149.

[51] V. Boldyrev, *Thermochim. Acta*, **2006**, 443 (1), 1-36.

[52] P. Yin, J. Zhang, C. He, D.A. Parrish, M.S. Jean'ne, *J. Mater. Chem. A*, **2014**, 2 (9), 3200-3208.

[53] T.T. Vo, D.A. Parrish, J.n.M. Shreeve, *J. Am. Chem. Soc.*, **2014**, 136 (34), 11934-11937.

[54] J. Jos, S. Mathew, *Crit. Rev. Solid State Mater. Sci.*, **2016**, 1-29.

[55] L.T. Deluca, F. Maggi, S. Dossi, V. Weiser, A. Franzin, V. Gettwert, T. Heintz, *Chin. J. Explos. Propellants*, **2013**, 36 (6), 1-14.

[56] S. Chaturvedi, P.N. Dave, *J. Energ. Mater.*, **2013**, 31 (1), 1-26.

[57] Q.J. Axthammer, B. Krumm, T.M. Klapötke, *J. Phys. Chem. A*, **2017**, 121 (18), 3567-3579.

[58] X. Zhang, X. Gong, *Can. J. Chem.*, **2016**, 95 (2), 199-206.

[59] Q.J. Axthammer, T.M. Klapötke, B. Krumm, R. Moll, S.F. Rest, *Z. Anorg. Allg. Chem.*, **2014**, 640 (1), 76-83.

[60] N. Fischer, D. Fischer, T.M. Klapötke, D.G. Piercey, J. Stierstorfer, *J. Mater. Chem.*, **2012**, 22 (38), 20418-20422.

[61] M.H. Keshavarz, Y.H. Abadi, K. Esmaeilpour, S. Damiri, M. Oftadeh, *Propellants Explos. Pyrotech.*, **2017**, 42 (5), 492-498.

[62] E.G. Mahadevan, *"Ammonium Nitrate Explosives for Civil Applications: Slurries, Emulsions and Ammonium Nitrate Fuel Oils"*. Weinheim, Germany: John Wiley & Sons, **2013**.

[63] U. Teipel, *"Energetic Materials: Particle Processing and Characterization"*. Weinheim, Germany: John Wiley & Sons, **2006**.

[64] C. Oommen, S. Jain, *J. Hazard. Mater.*, **1999**, 67 (3), 253-281.

[65] D.A. Kelley, **1996**, US5527498.

[66] J.-K. Kim, S.-I. Choi, E.J. Kim, J.H. Kim, K.-K. Koo, *Ind. Eng. Chem. Res.*, **2010**, 49 (24), 12632-12637.

[67] B.I. Elzaki, Y.J. Zhang, *Materials*, **2016**, 9 (7), 502-509.

[68] W. Pittman, Z. Han, B. Harding, C. Rosas, J. Jiang, A. Pineda, M.S. Mannan, *J. Hazard. Mater.*, **2014**, 280, 472-477.

[69] J.C. Oxley, J.L. Smith, E. Rogers, M. Yu, *Thermochim. Acta*, **2002**, 384 (1-2), 23-45.

[70] A.A. Vargeese, K. Muralidharan, *Appl. Catal. A: General*, **2012**, 447, 171-177.

[71] M. Kohga, S. Handa, *J. Energ. Mater.*, **2017**, 36 (1), 93-110.

[72] A.A. Vargeese, K. Muralidharan, V. Krishnamurthy, *Propellants Explos. Pyrotech.*, **2015**, 40 (2), 260-266.

[73] T. Lee, J.W. Chen, H.L. Lee, T.Y. Lin, Y.C. Tsai, S.-L. Cheng, S.-W. Lee, J.-C. Hu, L.-T. Chen, *Chem. Eng. J.*, **2013**, 225, 809-817.

[74] M. Yang, X. Chen, Y. Wang, B. Yuan, Y. Niu, Y. Zhang, R. Liao, Z. Zhang, *J. Hazard. Mater.*, **2017**, 337, 10-19.

[75] S. Cagnina, P. Rotureau, G. Fayet, C. Adamo, *Phys. Chem. Chem. Phys.*, **2013**, 15 (26), 10849-10858.

[76] J.C. Oxiey, S.M. Kaushik, N.S. Gilson, *Thermochim. Acta*, **1992**, 212, 77-85.

[77] K. Farhat, W. Cong, Y. Batonneau, C. Kappenstein, in *45th AIAA/ASME/SAE/ASEE Joint Propul. Conf. Exhibit*, **2009**, p. 4963.

[78] A.A. Vargeese, K. Muralidharan, *J. Hazard. Mater.*, **2011**, 192 (3), 1314-1320.

[79] Z.-X. Xu, G.-S. Xu, X.-Q. Fu, Q. Wang, *Nanomater. Nanotechnol.*, **2016**, 6, 1-10.

[80] B. Lurie, C. Lianshen, *Combust. Explos. Shock Waves*, **2000**, 36 (5), 607-617.

[81] M. Atamanov, I. Noboru, T. Shotaro, R. Amrousse, M. Tulepov, A. Kerimkulova, M. Hobosyan, K. Hori, K. Martirosyan, Z. Mansurov, *Combust. Sci. Technol.*, **2016**, 188, 2003-2011.

[82] L.T. DeLuca, I. Palmucci, A. Franzin, V. Weiser, V. Gettwert, N. Wingborg and M. Sjöblom, *J. Solid Rocket Technol.*, **2016**, 39, 765-774.

[83] M. Kohga, S. Handa, *J. Energ. Mater.*, **2017**, 35 (3), 276-291.

[84] M. Kohga, S. Handa, *J. Energ. Mater.*, **2018**, 36 (1), 93-110.

[85] M.Y. Nagamachi, J.I.S. Oliveira, A.M. Kawamoto, L.D. Rita de Cássia, *J. Aerosp. Technol. Manag.*, **2011**, 1 (2), 153-160.

[86] N. Ermolin, V. Fomin, *Combust. Explos. Shock Waves*, **2016**, 52 (5), 566-586.

[87] S. Venkatachalam, G. Santhosh, K. Ninan Ninan, *Propellants Explos. Pyrotech.*, **2004**, 29 (3), 178-187.

[88] E. Landsem, T.L. Jensen, F.K. Hansen, E. Unneberg, T.E. Kristensen, *Propellants Explos. Pyrotech.*, **2012**, 37 (6), 691-698.

[89] W. Kim, Y. Kwon, Y.M. Jo, Y.C. Park, *J. Energ. Mater.*, **2017**, 35 (1), 44-52.

[90] U. Teipel, T. Heintz, H.H. Krause, *Propellants Explos. Pyrotech.*, **2000**, 25 (2), 81-85.

[91] S. Benazet, G. Jacob, **2010**, US7789980.

[92] T. Heintz, H. Pontius, J. Aniol, C. Birke, K. Leisinger, W. Reinhard, *Propellants Explos. Pyrotech.*, **2009**, 34 (3), 231-238.

[93] F. Muscatelli, J. Renouard, J.-M. Bouchez, **2013**, US8491736.

[94] R. Raghavan, S. Jacob, *Propellants Explos. Pyrotech.*, **2013**, 38 (2), 273-277.

[95] S. Benazet, G. Jacob, **2010**, US7789980.

[96] G. Ting, Q. Li-Jun, Y. Rui, H. Lan, J. Yue-Ping, F. Hao, *J. Inorg. Mater.*, **2014**, 29 (8), 869-874.

[97] N. Ermolin, V. Fomin, *Combust. Explos. Shock Waves*, **2016**, 52 (5), 566-586.

[98] H. Matsunaga, H. Habu, A. Miyake, *J. Therm. Anal. Calorim.*, **2014**, 116 (3), 1227-1232.

[99] Y.-i. Izato, M. Koshi, A. Miyake, H. Habu, *J. Therm. Anal. Calorim.*, **2017**, 127 (1), 255-264.

[100] L.T. DeLuca, I. Palmucci, A. Franzin, V. Weiser, V. Gettwert, N. Wingborg, M. Sjöblom, *J. Solid Rocket Technol.*, **2016**, 39 (6), 765-774.

[101] S.H. Sonawane, M. Anniyappan, J. Athar, S. Banerjee, A.K. Sikder, *RSC Adv.*, **2016**, 6 (10), 8495-8502.

[102] E. Landsem, T.L. Jensen, T.E. Kristensen, F.K. Hansen, T. Benneche, E. Unneberg, *Propellants Explos. Pyrotech.*, **2013**, 38 (1), 75-86.

[103] M.Y. Nagamachi, J.I.S. Oliveira, A.M. Kawamoto, C.L. Dutra, *J. Aerosp. Technol. Manag.*, **2009**, 1 (2), 153-160.

[104] U. Teipel, T. Heintz, H. Krober, *Powder Handl. Process.*, **2001**, 13 (3), 283-288.

[105] T. Heintz, H. Pontius, J. Aniol, C. Birke, K. Leisinger, W. Reinhard, *Propellants Explos. Pyrotech.*, **2009**, 34 (3), 231-238.

[106] S. Sonawane, M. Anniyappan, J. Athar, A. Singh, M. Talawar, R. Sinha, S. Banerjee, A. Sikder, *Propellants Explos. Pyrotech.*, **2017**, 42 (4), 386-393.

[107] T.H. Hagen, T.L. Jensen, E. Unneberg, Y.H. Stenstrøm, T.E. Kristensen, *Propellants Explos. Pyrotech.*, **2015**, 40 (2), 275-284.

[108] J. de Flon, S. Andreasson, M. Liljedahl, C. Oscarson, M. Wanhatalo, N. Wingborg, in *47th AIAA/ASME/SAE/ASEE Joint Propul. Conf. Exhibit*, California, USA, **2011**, p. 6136.

[109] V. Weiser, A. Franzin, L.T. DeLuca, S. Fischer, V. Gettwert, S. Kelzenberg, S. Knapp, A. Raab, E. Roth, N. Eisenreich, in *"Chemical Rocket Propulsion"*. Switzerland: Springer, **2017**, pp. 253-270.

[110] S. Cerri, M.A. Bohn, K. Menke, L. Galfetti, *Propellants Explos. Pyrotech.*, **2014**, 39 (2), 192-204.

[111] N. Wingborg, in *51st AIAA/SAE/ASEE Joint Propul. Conf.*, Florida, USA, **2015**, p. 4222.

[112] C. Tagliabue, V. Weiser, A. Imiolek, A. Bohn, T. Heintz, V. Gettwert, in *47th Int. Annu. Conf. ICT*, Karlsruhe, Germany, **2016**, pp. 36/1-36/15.

[113] J.F. Lutz, *Angew. Chem. Int. Ed.*, **2007**, 46 (7), 1018-1025.

[114] D. Badgujar, M. Talawar, S. Asthana, P. Mahulikar, *J. Hazard. Mater.*, **2008**, 151 (2), 289-305.

[115] P. Dendage, D. Sarwade, S. Asthana, H. Singh, *J. Energ. Mater.*, **2001**, 19 (1), 41-78.

[116] U. Nair, S. Asthana, A.S. Rao, B. Gandhe, *Def. Sci. J.*, **2010**, 60 (2), 137-151.

[117] Y.-H. Joo, B.S. Min, *New J. Chem.*, **2014**, 38 (1), 50-54.

[118] H.-Y. Lu, J.-R. Li, D.-L. Yang, Q. Zhang, D.-X. Shi, *Chin. Chem. Lett.*, **2015**, 26 (3), 365-368.

[119] C. Yan, P. Ding, H. Yang, C. Lu, G. Cheng, *Ind. Eng. Chem. Res.*, **2016**, 55 (41), 11029-11034.

[120] P. Ding, H. Wang, L. Wen, G. Cheng, C. Lu, H. Yang, *Ind. Eng. Chem. Res.*, **2014**, 53 (36), 13851-13855.

[121] J. Kim, M.J. Kim, B.S. Min, *J. Korean Soc. Propuls. Eng.*, **2015**, 19 (4), 69-76.

[122] J. Athar, M. Ghosh, P.S. Dendage, R.S. Damse, A.K. Sikder, *Propellants Explos. Pyrotech.*, **2010**, 35 (2), 153-158.

[123] T.M. Deppert, D.R. Smith, C. Shanholtz, **2016**, US9505666.

[124] M.J. Tummers, A.E. Van der Heijden, E.H. Van Veen, *Combust. Flame*, **2012**, 159 (2), 882-886.

[125] D. Trache, K. Khimeche, M. Benziane, A. Dahmani, *J. Therm. Anal. Calorim.*, **2013**, 112 (1), 215-222.

[126] D. Trache, K. Khimeche, R. Benelmir, A. Dahmani, *Thermochim. Acta*, **2013**, 565 8-16.

[127] S. Sonawane, M. Anniyappan, J. Athar, A. Singh, M.B. Talawar, R.K. Sinha, S. Banerjee, A.K. Sikder, *Propellants Explos. Pyrotech.*, **2017**, 42 (4), 386-393.

[128] H. Schoyer, W. Welland-Veltmans, J. Louwers, P. Korting, A. Van der Heijden, H. Keizers, R. Van den Berg, *J. Propul. Power*, **2002**, 18 (1), 138-145.

[129] X. Xu, M. Liu, Y. Yin, C. Zheng, P. Deng, D. Xue, *Green Chem.*, **2016**, 18 (5), 1364-1367.

[130] A. Van der Heijden, A. Leeuwenburgh, *Combust. Flame*, **2009**, 156 (7), 1359-1364.

[131] M. Göbel, T.M. Klapötke, *Adv. Funct. Mater.*, **2009**, 19 (3), 347-365.

[132] A.J. Bellamy, in *"High Energy Density Materials"*. Berlin: Springer, **2007**, pp. 1-33.

[133] H. Gao, J.M. Shreeve, *Angew. Chem. Int. Ed.,* **2015**, 54 (21), 6335-6338.

[134] Y. Zhang, Q. Sun, K. Xu, J. Song, F. Zhao, *Propellants Explos. Pyrotech.,* **2016**, 41, 35-52.

[135] H. Gao, M.S. Jean'ne, *RSC Adv.,* **2016**, 6 (61), 56271-56277.

[136] N.V. Latypov, J. Bergman, A. Langlet, U. Wellmar, U. Bemm, *Tetrahedron,* **1998**, 54 (38), 11525-11536.

[137] B. Florczak, *Cent. Eur. J. Energ. Mater.,* **2008**, 5 (3-4), 103-111.

[138] Z. Chen, Z. Li, N. Yao, W.D. Lei, *Chin. J. Energ. Mater.,* **2010**, 18, 316-319.

[139] D. Lempert, E. Dorofeenko, Y. Shu, *Russ. J. Phys. Chem. B,* **2016**, 10 (3), 483-489.

[140] T.L. Jensen, E. Unneberg, T.E. Kristensen, *Propellants Explos. Pyrotech.,* **2017**, 42 (4), 381-385.

[141] T. Zhou, Y. Li, K. Xu, J. Song, F. Zhao, *New J. Chem.,* **2017**, 41 (1), 168-176.

[142] Q. Sun, Y. Zhang, K. Xu, Z. Ren, J. Song, F. Zhao, *J. Chem. Eng. Data,* **2015**, 60 (7), 2057-2061.

[143] T.T. Vo, J. Zhang, D.A. Parrish, B. Twamley, J.M. Shreeve, *J. Am. Chem. Soc.,* **2013**, 135 (32), 11787-11790.

[144] U. Nair, R. Sivabalan, G. Gore, M. Geetha, S. Asthana, H. Singh, *Combust. Explos. Shock Waves,* **2005**, 41 (2), 121-132.

[145] C. Guo, D. Wang, B. Gao, J. Wang, B. Luo, G. Yang, F. Nie, *RSC Adv.,* **2016**, 6 (2), 859-865.

[146] A. Atwood, T. Boggs, P. Curran, T. Parr, D. Hanson-Parr, C. Price, J. Wiknich, *J. Propul. Power,* **1999**, 15 (6), 740-747.

[147] X.-L. Xing, F.-Q. Zhao, S.-N. Ma, S.-Y. Xu, L.-B. Xiao, H.-X. Gao, R.-Z. Hu, *J. Therm. Anal. Calorim.,* **2012**, 110 (3), 1451-1455.

[148] U. Nair, G. Gore, R. Sivabalan, C. Divekar, S.N. Asthana, H. Singh, *J. Propul. Power,* **2004**, 20 (5), 952-955.

[149] R. Kurva, G. Gupta, S. Jawalkar, L. Vipin, P. Kulkarni, *Adv. Sci. Eng. Med.,* **2016**, 8 (7), 543-551.

[150] L. Ding, F.-Q. Zhao, Q. Pan, H.-X. Xu, *J. Anal. Appl. Pyrolysis,* **2016**, 121, 121-127.

[151] W.Q. Pang, L.T. De Luca, H.X. Xu, X.Z. Fan, Y.H. Li, W.X. Xie, Y. Li, *Int. J. Energ. Mater. Chem. Propul.,* **2016**, 15 (1), 49-64.

[152] J.V. Viswanath, K. Venugopal, N.S. Rao, A. Venkataraman, *Def. Technol.,* **2016**, 12 (5), 401-418.

[153] I.L. Simakova, V.N. Parmon, in *"Chemical Rocket Propulsion"*. Switzerland: Springer, **2017**, pp. 697-724.

[154] Z.Y. Han, Y.Z. Yang, Z.M. Du, Z.Y. Li, Q. Yao, Y.H. Wang, Z.Y. Hu, *Propellants Explos. Pyrotech.,* **2017**, 42 (3), 276-283.

[155] Q.J. Axthammer, B. Krumm, T.M. Klapötke, *J. Org. Chem.,* **2015**, 80 (12), 6329-6335.

[156] M. Kettner, T.M. Klapötke, *Chem. Commun.,* **2014**, 50 (18), 2268-2270.

[157] M.A. Kettner, T.M. Klapötke, *Chem. – Eur. J.,* **2015**, 21 (9), 3755-3765.

[158] T.M. Klapötke, B. Krumm, R. Scharf, *Eur. J. Inorg. Chem.,* **2016**, 2016 (19), 3086-3093.

[159] T.M. Klapötke, B. Krumm, R. Moll, S.F. Rest, *Z. Anorg. Allg. Chem.,* **2011**, 637, 2103-2110.

[160] M. Abd-Elghany, T.M. Klapötke, B. Krumm, J. Stierstorfer, in *20th Int. Seminar New Trend. Res. Energ. Mater.*, Pardubice, Czech Republic, **2017**, pp. 468-473.

[161] X. Fan, F. Bi, M. Zhang, J. Li, W. Pang, B. Wang, Z. Ge, in *"Chemical Rocket Propulsion"*. Switzerland: Springer, **2017**, pp. 165-177.

[162] V.P. Sinditskii, V.Y. Egorshev, G.F. Rudakov, S.A. Filatov, A.V. Burzhava, in *"Chemical Rocket Propulsion"*. Switzerland: Springer, **2017**, pp. 89-125.

Thermal Behavior and Decomposition Kinetics of Bis(2,2,2-trinitroethyl)-oxalate as a High Energy Dense Oxidizer and its Mixture with Nitrocellulose

Published in *Propellants Explos. Pyrotech.* **2017**, 42(12), 1373-1381 (DOI: 10.1002/prep.201700179) **"Inside cover picture"**

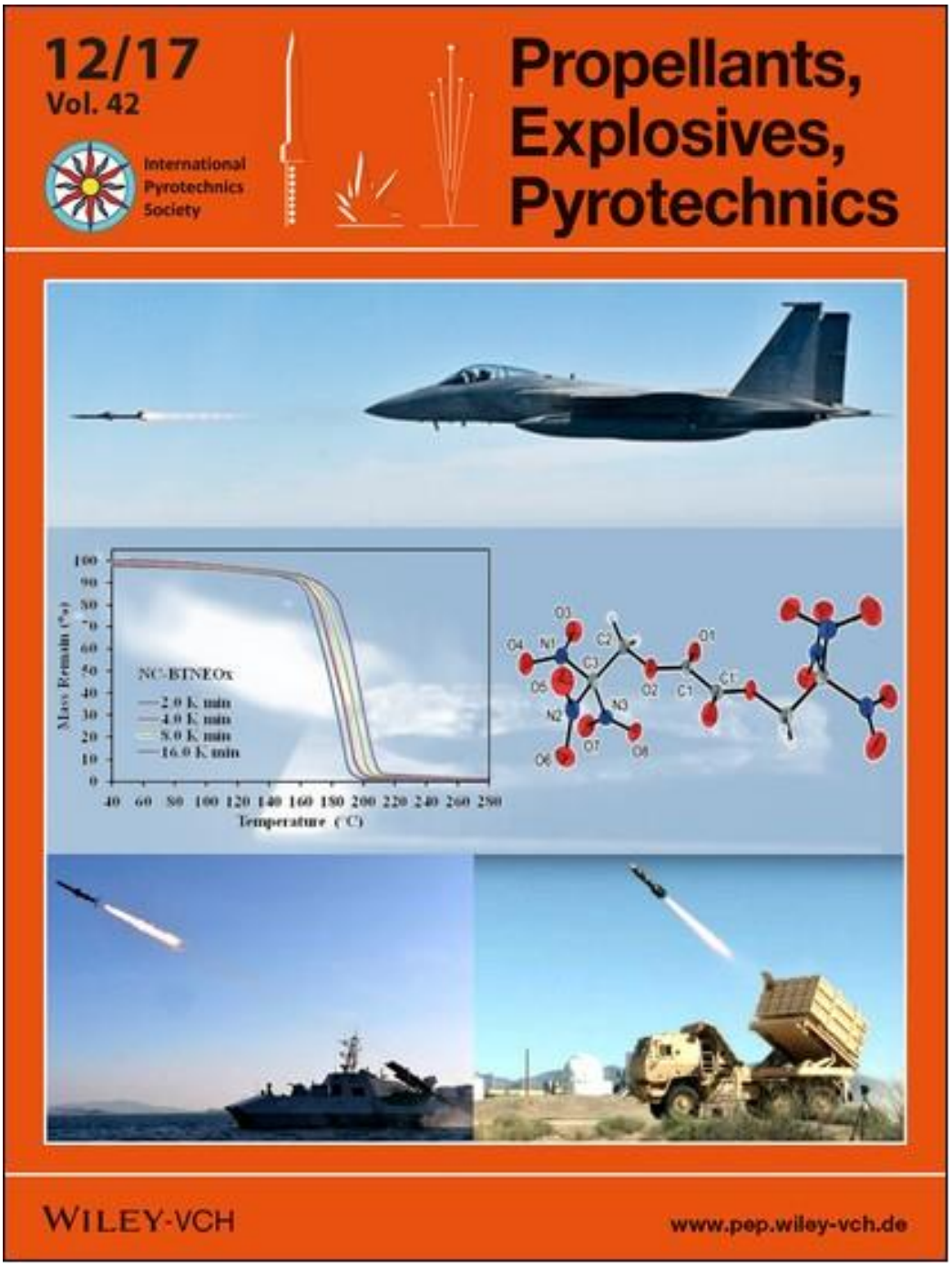

Thermal Behavior and Decomposition Kinetics of Bis(2,2,2-trinitroethyl)-oxalate as a High Energy Dense Oxidizer and its Mixture with Nitrocellulose

Published in *Propellants Explos. Pyrotech.* **2017**, 42(12), 1373-1381 (DOI: 10.1002/prep.201700179)

Abstract: A new propellant formulation (NC-BTNEOx) based on bis(2,2,2-trinitroethyl)oxalate (BTNEOx) as a high energy dense oxidizer (HEDO) mixed with nitrocellulose (NC) matrix was prepared and studied. BTNEOx was prepared and characterized by nuclear magnetic resonance (NMR) and X-ray diffraction (XRD). Photos of the prepared formulation obtained by scanning electron microscope (SEM) clarified a good mixing of the nitrocellulose (NC) matrix with BTNEOx. A smokeless burning was observed and recorded for the prepared NC-BTNEOx by a high speed camera. The thermal behavior and decomposition kinetics of the NC matrix, BTNEOx and their mixture have been investigated nonisothermally by using thermogravimetric analysis (TGA) and Differential scanning calorimetry (DSC). Isoconversional (model-free) methods; Kissinger, Ozawa and Flynn-Wall (OFW) and Kissinger-Akahira-Sunose (KAS), were used to determine the kinetic parameters of the studied samples. The results proved that BTNEOx has melting temperature at 104.1 °C and maximum peak temperature at 200.6 °C, also it has effective activation energy in the range of 107–110 kJ mol^{-1}. The prepared NC-BTNEOx has no endothermic peak and has exothermic peak at 201.7 °C which means that a composite might be formed due to the mixing of BTNEOx with NC. The prepared NC-BTNEOx has effective activation energy in the range of 172–180 kJ mol^{-1}. BTNEOx required more study to proof the possibility of replacing the nitroglycerine in a smokeless double base propellant.

Introduction

The main ingredients in traditional Double-base propellants (DBP) are nitrocellulose (NC) as a binder plasticized by the nitroglycerine (NG) which is entrapped into the fibers of NC. DBPs are considered one of the oldest propellant families which was developed as a result of the development of propulsion [1, 2]. During time and storage of DBPs, several chemical and physical processes might take place in the propellant grains (the consumption of the

stabilizer, migration, evaporation and decomposition of NG, etc.). These processes cause change in the performance of propellants and might cause a self-ignition [2]. The development in the field of rocket propellants is to increase the energy level of the propellants in addition to solve the decomposition problems of NG and it's extremely impact sensitivity [2-5].

Several researchers have studied the possibility of adding some additives such as aluminum or nitramines in order to achieve a composite modified double-base propellants (CMDB) [4, 6-9]. Researchers are currently focused on discovering new green and safe energetic materials which can replace NG in DBPs or ammonium perchlorate (AP) in composite solid rocket propellants and enhance the energetic characteristics, sensitivities and thermal properties. High-energy dense oxidizers (HEDOs) might be used to replace AP in composite propellants. These compounds consist of C, H, N, and O, with high oxygen content. 2,2,2-Trinitroethanol (TNE) is one of the most suitable starting material with an oxygen balance of +13.3 and is easily synthesized through a Henry reaction [10]. Large number of compounds have been synthesized starting from TNE during the recent studies, but few information are known about the chemistry of TNE with oxalyl chloride [11].

BTNEOx is an interesting new HEDO which has been prepared by Klapötke group et al [12] by one step method, it has oxygen balance of +7.7, impact sensitivity of 10 J and friction sensitivity higher than 360 N. BTNEOx has much lower sensitivities than NG and has not been studied in any propellant formulation yet. Also the investigation of the thermal behavior of the energetic materials is necessary and important for the research and development to find a suitable new materials. Usually, thermal analysis is considered the best process of studying the thermal decomposition of energetic materials. The most common thermal analysis techniques such as thermogravimetric analysis (TGA), differential thermal analysis (DTA) and differential scanning calorimetry (DSC) have been used isothermally and non-isothermally in the study of the decomposition kinetics [13-24].

In this paper, preparation and characterization of BTNEOx as a HEDO have been presented. A propellant formulation (NC-BTNEOx) based on NC as a binder and BTNEOx as an oxidizer have been prepared. The thermal behavior and decomposition kinetics of the individual NC and BTNEOx in addition to NC-BTNEOx, which has not previously been reported in the literature, were studied using thermogravimetric analysis (TGA) and differential scanning calorimetry (DSC) techniques.

Experimental

Oxalyl chloride, Aluminium chloride and 1,2-dichloroethane were obtained from Sigma-Aldrich. 2,2,2-trinitroethanol was prepared in our laboratories as reported in ref. [10], while Nitrocellulose with 13.15% nitrogen content was provided by Nitrochemie Aschau GmbH. Oxalyl chloride (1.0 g, 7.9 mmol) was added to the solution of 2,2,2-trinitroethanol (5.7 g, 31.5 mmol) in 1,2-dichloroethane (10 ml) and $AlCl_3$ (0.1 g, 8.7 mmol) was added. The solution was heated under reflux for 5 h. After the reaction mixture cooled, a colorless solid crystals were precipitated. By filtration and washing by cold water, solid crystals are obtained. By recrystallization from chloroform yielded (BTNEOx) as a colorless crystals (27 % yield) [12].

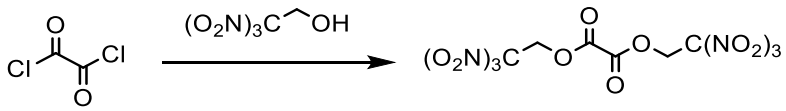

Scheme 1. Preparation of BTNEOx.

The propellant formulation has been prepared by casting technique where NC (after drying in oven at 60 ˚C for three days) was dissolved in the suitable amount of acetone for 40 minutes at room temperature. BTNEOx were added to the solution in three portions for 30 minutes with continuous stirring. The viscosity of the mixture should be the same during the addition of the oxidizer by adding a few ml of the solvent in case of increasing viscosity. The prepared propellant sample was left to be cured through evaporating the solvent in a vacuum oven at 50 ±2˚C to drive out the entrapped air. The prepared sample has 50 wt.% of BTNEOx and 50 wt.% of NC matrix.

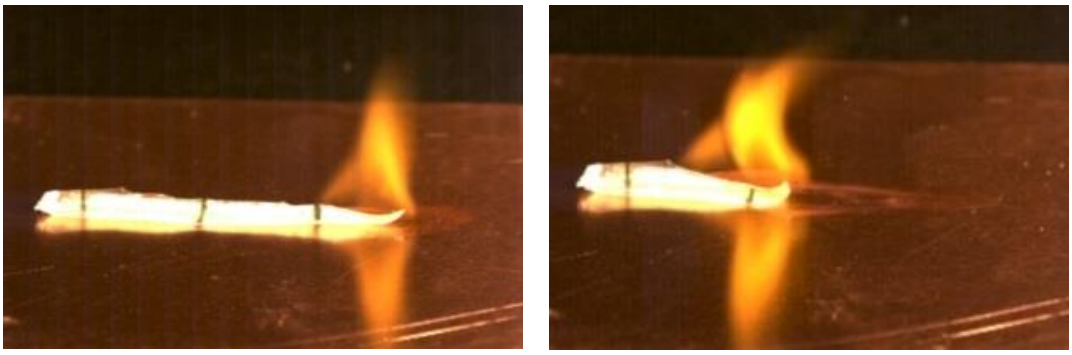

Figure 1. Burning of the prepared sample.

The new formulation (NC-BTNEOx) was prepared in the form of strand with 100 mm length, 10 mm width and 8 mm thickness. The strand was burned (in open-air) from one side and recording the burning by high speed camera. Fig. 1 shows a screen shots from the burning of the sample where completely smokeless gases were produced during a homogeneous burning.

The NMR spectra were recorded with a JEOL Eclipse 400 instrument, and the chemical shifts were determined with respect to the external standards Me_4Si (^1H, 399.8 MHz; ^{13}C, 100.5 MHz) and $MeNO_2$ (^{14}N, 28.8 MHz). Specific crystals were selected with a polarization microscope to be suitable for X-ray crystallography. The measurement was done using an Oxford XCalibur3 diffractometer. KappaCCD was used as a detector. The measurement was operated with Mo-K_α radiation ($\lambda = 0.7107$ Å). Direct method (SIR97) was used to solve the structure [25]. The result was refined by using the WINGX software package [26]. Finally, result was checked with the PLATON software [27]. Scanning electron microscope (SEM) model (FEI - Helios G3 UC) was used to study the morphology of the crystals.

The melting and decomposition points were measured with LINSEIS DSC – PT10 with samples of approximately 3 mg were placed in an aluminum pan with a pin-hole cover at a heating rate of 5 °C min^{-1} in a temperature range of 25 to 400 °C. The thermal decomposition kinetics of the samples were studied by using the results obtained by Thermogravimetric Analyzer (Perkin-Elmer, TGA 4000). The experimental conditions used to determine TG/DTG were; 1–3 mg samples were tested at different heating rates of 2, 4, 8 and 16 °C min^{-1} in the temperature range 30–600 °C under a flow of dynamic nitrogen of 20 ml min^{-1}.

Three different kinetic parameters should be determined for a complete kinetic description of the overall reaction which include the activation energy (E_a), pre-exponential factor (A) and kinetic model ($f(\alpha)$) of each individual process. Nowadays, a large number of analytical methods are available for the kinetic parameters of distinct solid-phase reactions evaluation. But on the other hand, the number of procedures for analysis of complex processes is much more limited. Either isoconversional or model-fitting methods can be used to determine the kinetic parameters isothermally or nonisothermally [28, 29].

The following equation is usually used for the kinetic studies of thermally excited reactions in solids:

$$d\alpha/dt = k(T)\, f(\alpha) \qquad (1)$$

Where α is the factional conversion, t is time, k(T) is the temperature dependent rate constant and f(α) is the reaction model. The temperature dependency of the rate constant is assumed to obey the Arrhenius expression:

$$k(T) = A \exp(-E/RT) \quad (2)$$

Where A is the pre-exponential factor, E is the activation energy and R is the universal gas constant. By using the integral form of Eqn. 1 used for isothermal conditions, it becomes:

$$g(\alpha) = \int_0^{\alpha} [f(\alpha)]^{-1} d\alpha = k(T)t \quad (3)$$

Where g(α) is the integrated form of the reaction model. The rate constants are calculated at several temperatures for each reaction model selected, and the Arrhenius parameters can be evaluated using the Arrhenius equation in its logarithmic form:

$$lnk(T) = lnA - E/RT \quad (4)$$

In the isoconversional method, it is assumed that the reaction model in Eqn. 1 is independent of the temperature. For the isothermal conditions, eqns. 3 and 4 can be combined to get:

$$-lnt_{\alpha,i} = ln[A/g(\alpha)] - E_{\alpha}/RT_i \quad (5)$$

Where E_α can be obtained from the slope for the plot of $-\ln t_{\alpha,i}$ vs. T_i^{-1}.

The activation energy (E_a) of the exothermic decomposition reaction of the prepared propellants samples can be calculated using Kissinger's method (see Eqn. 6) [30].

$$-\frac{Ea}{R} = \frac{d \ln(\beta/T_P^2)}{d(1/T_P)} \quad (6)$$

Where β is the heating rate and T_p is the peak temperature of the DTG thermogram at that rate. The activation energy is calculated from the slope of the straight line which obtained by plotting of $\ln(\beta/T_p^2)$ against $1/T_p$. Inaccurate values of E_a can be resulted from a such rough temperature integral approximation [31]. More accurate equation according to Starink [32] for E_a calculation which is commonly called the Kissinger–Akahira–Sunose (KAS) equation [33]:

$$ln\left(\frac{\beta_i}{T_{\alpha,i}^{1.92}}\right) = const - 1.0008\frac{E_\alpha}{RT_\alpha} \quad (7)$$

Also, Ozawa and Flynn–Wall (OFW) have developed an isoconversional calculation method for non-isothermal data (commonly referred to as the OFW method), in which taking the logarithm of the nonisothermal rate law to give the following equation [34]:

$$log\, g(\alpha) = log\frac{AE_a}{\beta R} + log\int_{\frac{E_a}{RT}}^{\infty}\frac{e^{\frac{-E_a}{RT}}}{\left(\frac{E_a}{RT}\right)^2}\, d\frac{E_a}{RT} \quad (8)$$

Substitution by using Doyle's approximation [35-37]:

$$log\int_{\frac{E_a}{RT}}^{\infty}\frac{e^{\frac{-E_a}{RT}}}{\left(\frac{E_a}{RT}\right)^2}\, d\frac{E_a}{RT} \approx -2.315 - 0.4567\frac{E_a}{RT} \quad (9)$$

Then OFW equation can be written as:

$$log\,\beta = log\frac{AE_a}{g(\alpha)R} - 2.315 - 0.457\frac{E_a}{RT} \quad (10)$$

Results and Discussion

BTNEOx was characterized by ^{1}H, ^{13}C and ^{14}N NMR spectroscopy in [D_6] acetone. The CH_2 resonance of the trinitroethyl moiety in 1H NMR spectra was appeared as a singlet δ =6.12 (s,4H,CH_2) ppm. In the spectra of ^{13}C NMR, the resonance for the carbonyl moiety was appeared at δ =153.79 [C(O)O] ppm, the carbon atoms for the trinitromethyl moiety are observed at δ =124.65 [$C(NO_2)_3$] ppm, and for the ethyl group was at δ =63.39 (CH_2) ppm. The ^{14}N NMR resonance for the trinitroethyl moiety was appeared as a sharp signal at δ = –35 [$C(NO_2)_3$] ppm. All these NMR spectra with the δ values were compared with those values from the reference [12] and were found to be identical.

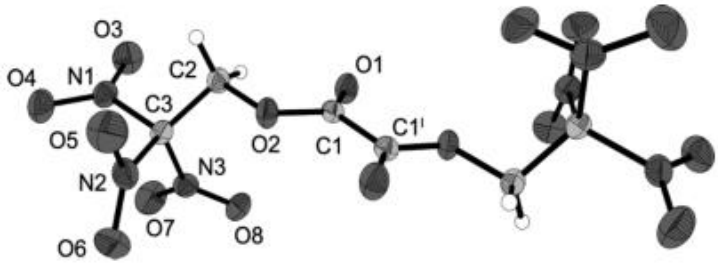

Figure 2. X-ray molecular structure of BTNEOx.

By recrystallization from chloroform, single crystals for X-ray diffraction measurements were obtained for the oxidizer (BTNEOx). The oxalate is crystallized in the monoclinic space group *P2₁ /c* containing four molecules in the unit cell, while the asymmetric unit consists of only two half molecules. The molecular structure of BTNEOx, as shown in Figure 2, is completed by a center of reflection in the center of the C1–C1' bond. It is common for oxalate structures that the C1–O2 bond is between an ordinary C–O single and double bonds

with a bond length of 1.343(2) Å [38]. The oxalate unit and each of the CH_2 groups are arranged in a perfectly planar manner. Trinitromethyl is just slightly twisted out of plane with a torsion angle of 156.7° (C1–O2–C2–C3). The structure is stabilized through the intramolecular attraction between N3 and O2 with an interatomic distance shorter than the sum of the van der Waals radii (2.73 Å). The nitro groups in the trinitromethyl unit arrange around the carbon atom like a propeller shape. In this way, the intramolecular interactions are formed between the partially positively charged nitrogen atoms and the partially negatively charged oxygen atoms, which give the geometry its stability [12].

The scanning electron microscope (SEM) was used to study the crystal morphology of the pure NC and the prepared BTNEOx in addition to the prepared propellant NC-BTNEOx. Fig. 3 presents the SEM photos of all the studied samples. It is clear that The studied NC consists of long fibers and after dissolving the NC fibers in acetone and evaporation of the solvent, the fibers were bonded with each other to form a homogeneous surface taking the shape of its mold after the casting process (Fig 3 (a,b)). The oxidizer (BTNEOx) has fine crystals which looks like sheets with small thickness (4-18 μm), length and width in the range of hundreds of μm (Fig 3 (c)). Photo of the prepared propellant NC-BTNEOx showed a good homogeneity between the crystals of the oxidizer and the NC fibers where the crystals of BTNEOx were plunged between the fibers and formed a homogeneous propellant sample (Fig3 (d)).

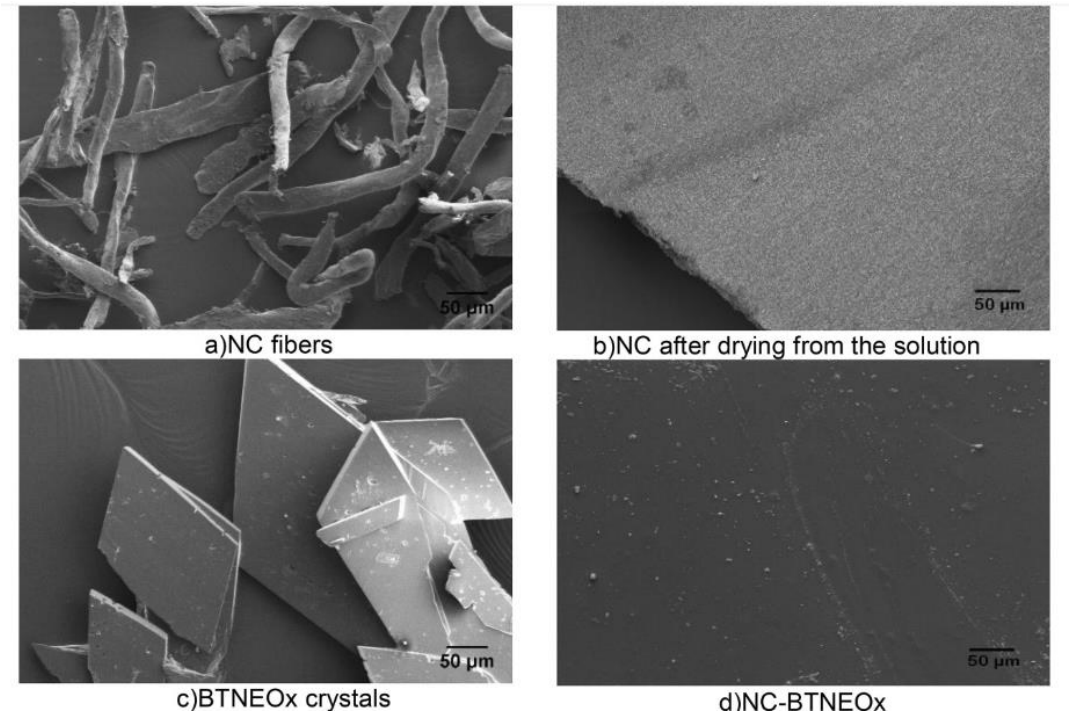

Figure 3. SEM of the oxidizer, NC matrix and NC-BTNEOx.

TG/DTG thermograms of NC, BTNEOx and NC- BTNEOx at four different heating rates 2, 4, 8, and 16℃ min^{-1} were presented in figures 4 and 5. The thermal decomposition of NC occurred in one sharp step, while the BTNEOx decomposed in many steps; it lost 20% of its weight in two early thermal decomposition steps (10% in each step) which refers to losing of two nitro groups before the main controlled thermal decomposition process occurred, which started at 143.8 °C (onset temperature) and ends at 199.9 °C (onset temperature at the end of decomposition peak) in case of 2 K min^{-1} heating rate.

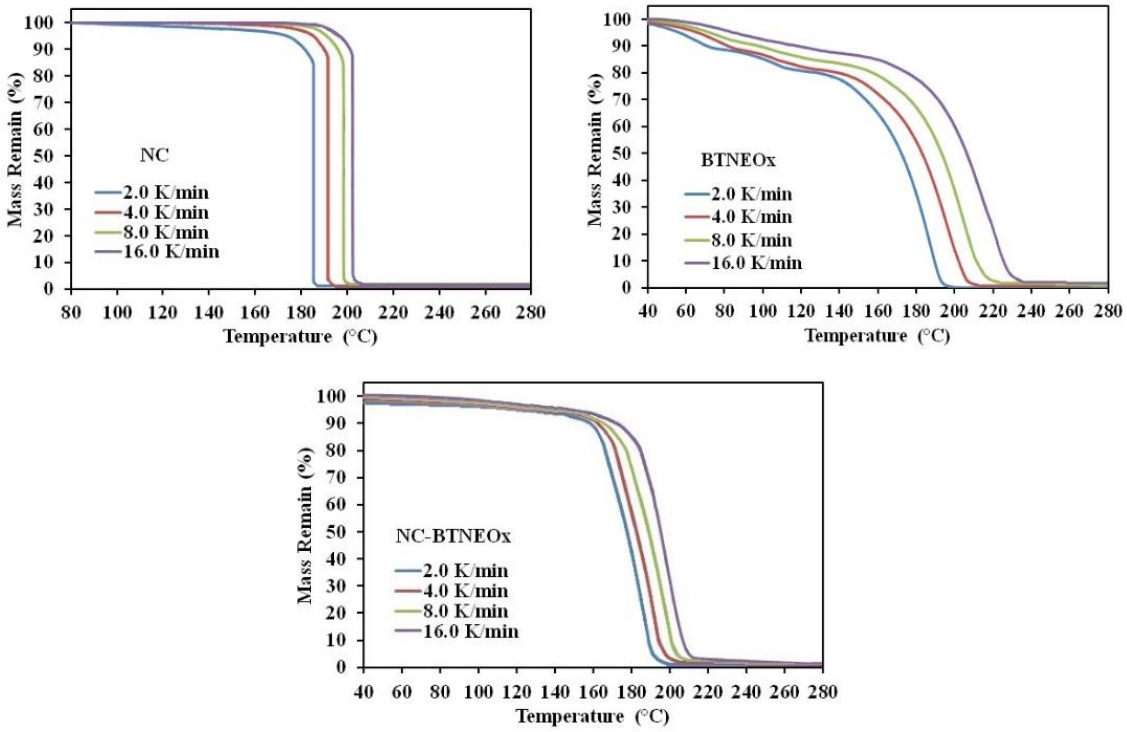

Figure 4. TG curves of NC, BTNEOx and the propellants sample NC-BTNEOx under different heating rates.

The TG thermogram of the prepared propellants samples (NC-BTNEOx) showed a homogenous controlled one step thermal decomposition reaction with decomposition temperature values lied between the NC as a matrix and BTNEOx as an oxidizer. The corresponding α-T curves are obtained from the mass remaining vs. temperature data (see Fig. 6).

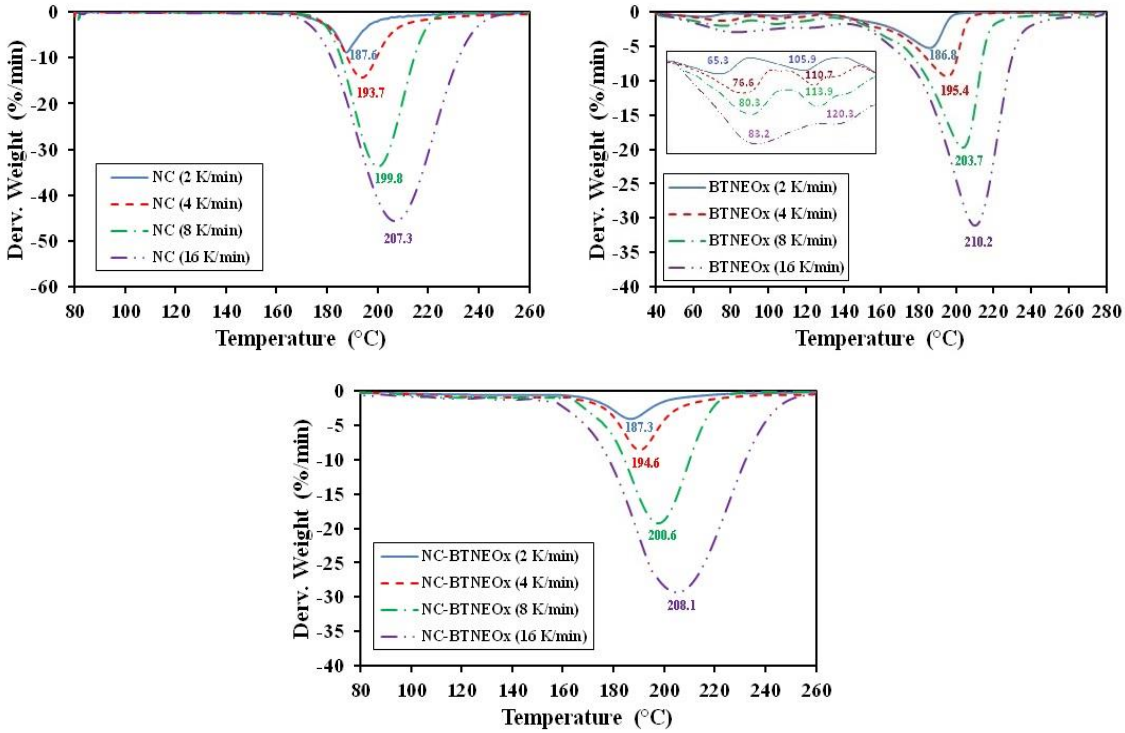

Figure 5. DTG curves for NC, BTNEOx and NC-BTNEOx under heating rates of 2, 4, 8 and 16 °C min^{-1}.

The DTG of the studied samples at the four different heating rates 2, 4, 8 and 16 ℃ min^{-1} showed that the max. peak decomposition temperature of NC-BTNEOx lied between that of NC and BTNEOx. Also it is clear from Fig. 5 that the two early thermal decomposition steps of the pure oxidizer BTNEOx were completely disappeared after preparing the propellant sample, which means that the crystals of the oxidizer were completely coated by the NC matrix. Furthermore, it might be possible that the oxidizer formed a composite with the NC binder and the mechanism of decomposition was changed. The decomposition temperatures obtained from TG curves and DTG peaks of NC, BTNEOx and NC-BTNEOx are listed in Table1. It is also clear that the onset decomposition temperatures and the initial mass loss temperatures of all the studied samples increase by increasing the heating rates.

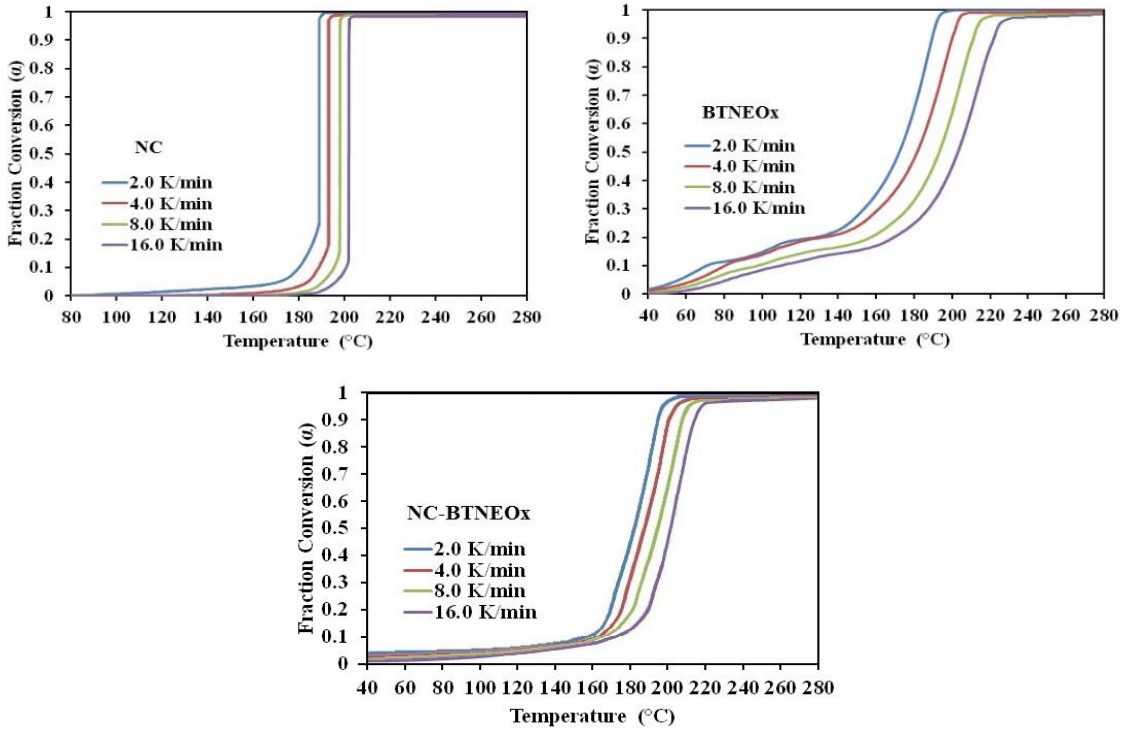

Figure 6. The α-T curves of NC, BTNEOx and NC-BTNEOx under heating rates of 2, 4, 8 and 16 °C min^{-1}.

Table 1. The non-isothermal TG/DTG data for NC, BTNEOx and NC-BTNEOx

Material	β ($K.min^{-1}$)	TG curves			DTG peaks	
		T_{ot} (°C)	T_i (°C)	Mass Loss (%)	T_p (°C)	T_{oe} (°C)
NC	2.0	177.74	182.19	99.74	187.57	198.11
	4.0	183.02	188.78	99.27	193.69	209.44
	8.0	191.75	193.85	99.53	199.76	218.54
	16.0	192.79	198.34	98.96	207.28	239.68
BTNEOx (main peak)	2.0	143.75	165.58	98.37	186.82	199.86
	4.0	151.97	177.91	97.68	195.41	204.23
	8.0	164.65	185.07	96.56	203.74	219.56
	16.0	181.68	200.38	94.88	210.19	238.79
NC-BTNEOx	2.0	156.70	164.07	99.32	187.29	198.11
	4.0	161.89	170.46	99.65	194.61	207.51
	8.0	169.32	179.38	98.72	200.58	220.46
	16.0	176.93	185.25	97.96	208.07	241.88

Note: T_{ot}: onset temperature of decomposition; T_{oe}: onset temperature of the end decomposition; T_i: initial thermal decomposition temperature; T_p: the peak temperature of mass loss rate; Mass Loss: from initial temperature to end temperature of DTG peak.

The effective activation energy was obtained by using the conventional Kissinger method. This method has a disadvantage which is the inability to determine the reaction steps or discuss the distinct activation energy E_a for each fraction conversion (α). Non-isothermal TGA technique was used to study the thermal decomposition kinetics where the activation energies of the samples were calculated from the slope of the straight line by plotting $\ln(\beta/T^2)$ versus 1/T at the four selected heating rates by applying Kissinger equation (eq. 6). The effective E_a of the NC matrix and BTNEOx was 187.5 kJ mol^{-1} and 109.4 kJ mol^{-1} respectively while the effective E_a of the propellants sample NC-BTNEOx was 179.5 kJ mol^{-1}. It means that the propellant sample has effective activation energy very close to the pure NC.

Ozawa and Flynn–Wall independently developed an isoconversional calculation method to calculate the activation energy E_a using nonisothermal data, which is commonly known as the OFW method [39]. The E_a is determined through a plot of log β versus $1/T$ at each α regardless of the employed model. The effective activation energies of NC matrix were varied from step to step of conversion with mean value of 182.2 kJ mol^{-1}. The mean value of E_a for the BTNEOx was **107.9** kJ mol^{-1}. Fig. 7 shows the effective activation energy for each step of conversion α for NC matrix, BTNEOx and for the NC-BTNEOx which has an effective E_a values very close to the NC with mean value of **172.2** kJ mol^{-1}, which means that the low effective activation energy of the oxidizer has not significant effect on the decomposition characteristics of the new propellant sample.

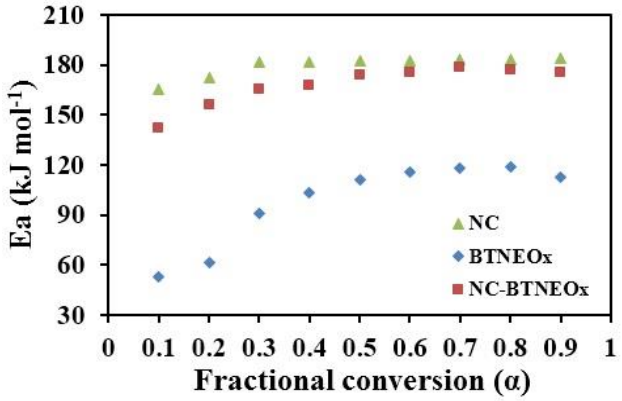

Figure 7. Activation energies for each conversion step (α) using OFW method.

Table 2. Effective activation energies (E_a) for NC, BTNEOx and the formulation NC-BTNEOx using different methods

Samples	Effective Activation Energy E_a (kJ mol^{-1})		
	Kissinger	OFW	KAS
NC	187.5	182.2	184.1
BTNEOx	109.4	107.9	108.3
NC-BTNEOx	179.5	172.2	176.9

The modified Kissinger–Akahira–Sunose (KAS) method could determine the activation energy for each degree of conversion using isoconversional way. Table 2 presents the values of effective activation energy for the whole samples using different methods. A good agreement was obtained by comparing the values using OFW method with those which obtained by using the modified KAS method. The effective activation energy for NC obtained by using KAS equation was 184.1 $kJ.mol^{-1}$, and for the oxidizer BTNEOx was 108.3 $kJ.mol^{-1}$ while the new propellant sample had a mean value of effective activation energy equal 176.9 $kJ.mol^{-1}$. The kinetic data are presented in Table 3. The mean values of effective activation energy using OFW and KAS methods were calculated in the interval of ($\alpha = 0.3–0.7$) as commonly suggested in literatures [13, 14, 20, 40] due to the large influence of the experimental conditions specially in case of TG/DTG on the data quality of the process "tails". Fig. 8 shows the relation between the pre-exponential factor A and the effective activation energy at each step of conversion and the effect of adding the oxidizer BTNEOx to the NC matrix which improve the normal distribution of the effective activation energy during each α that gives a homogeneous burning for the new propellants formula.

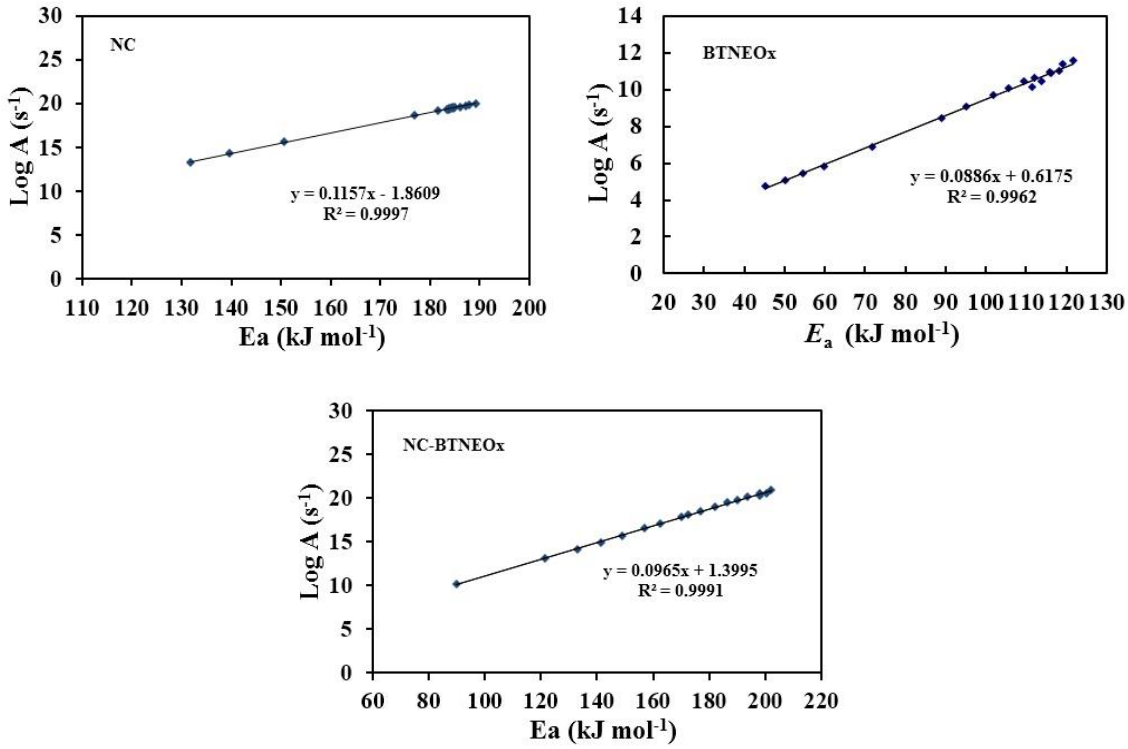

Figure 8. Log A vs E_a for each conversion step (α) using KAS method.

Table 3. Kinetic data of NC, BTNEOx and NC-BTNEOx obtained using the modified KAS method

α reacted	NC			BTNEOx			NC-BTNEOx		
	E_a	logA	r	E_a	logA	r	E_a	logA	r
0.1	139.6	14.28	0.9979	50.2	5.09	0.9953	121.6	13.15	0.9975
0.2	176.9	18.61	0.9989	59.9	5.83	0.9961	141.3	14.89	0.9986
0.3	183.4	19.35	0.9991	88.9	8.44	0.9991	157.2	16.57	0.9991
0.4	183.7	19.39	0.9986	101.8	9.71	0.9988	170.2	17.87	0.9985
0.5	184.2	19.44	0.9975	109.5	10.42	0.9992	177.0	18.52	0.9989
0.6	184.5	19.55	0.9958	119.7	11.41	0.9967	186.6	19.55	0.9982
0.7	184.9	19.58	0.9989	121.6	11.55	0.9973	193.6	20.18	0.9986
0.8	187.1	19.76	0.9991	118.0	11.01	0.9989	202.2	20.92	0.9990
0.9	189.2	19.98	0.9957	111.4	10.13	0.9984	197.9	20.26	0.9986
Mean	184.1	19.45		108.3	10.31		176.9	18.53	

The thermal behavior of the studied samples was obtained by using DSC at heating rate of 5 °C min^{-1}. The samples were encapsulated in an aluminum pan and measurements were performed under comparable conditions for the different samples. The thermogram of NC

matrix showed one sharp exothermic decomposition peak at 202.3 °C (see Fig. 9). On the other hand BTNEOx curve shows one endothermic melting peak at 104.1 °C and a rounded-form exothermic decomposition peak at 200.6 °C. While the curve of NC-BTNEOx showed only one well-formed exothermic peak at 201.7 °C without any endothermic melting peaks, which means that the new formula has different behavior compared with the pure oxidizer. This result indicated that a new composite might be formed during the mixing of the oxidizer with the NC.

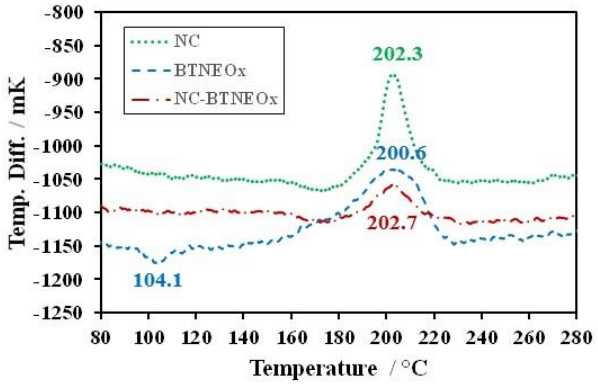

Figure 9. DSC thermogram for NC, BTNEOx and NC-BTNEOx at 5.0 K min^{-1} heating rate.

Table 4. The DSC exothermic peak data using non-isothermal DSC for NC, BTNEOx and NC-BTNEOx

Material	T_o (°C)	T_p (°C)	T_e (°C)
NC	180.9	202.3	216.4
BTNEOx	162.6	200.6	222.3
NC-BTNEOx	184.5	201.7	218.9

Note: T_o: decomposition onset temperature; T_p: peak temperature; T_e: the end decomposition onset temperature.

Conclusions

Bis(2,2,2-trinitroethyl)oxalate (BTNEOx) as a high energy dense oxidizer (HEDO) was successfully prepared and a new propellant formulation based on BTNEOx with NC was prepared and studied. The SEM photos proved that the BTNEOx crystals have different particle sizes in the form of sheets while the photo of NC-BTNEOx showed a good mixing of the ingredients. The high speed camera proved that the produced gases during the burning process are smokeless. The thermal study proved that BTNEOx was melted at 104.1 °C and its maximum decomposition peak was 200.6 °C while the prepared propellant had only

exothermic peak at 201.7 °C. This result proved that a new composite might be formed during the mixing of the oxidizer with the NC. Also the effective activation energy of the prepared propellant are very close to that of the pure NC. The three different methods used in this study showed effective activation energy of BTNEOx in the range of 107-110 kJ mol^{-1} while the prepared propellant was in the range of 172-180 kJ mol^{-1}. The results of the three methods are compatible with each other. The new oxidizer BTNEOx has low sensitivities compared with nitroglycerine and it has decomposition kinetics close to that of NC which means that it could be interesting to replace nitroglycerine in a smokeless double base propellant and its performance should be studied.

References

[1] H. AUSTRUY, in *"Solid Rocket Propulsion Technology"*. New York: Pergamon Press, **2012**, pp. 369-412.

[2] M. Sućeska, S.M. Mušanić, I.F. Houra, *Thermochim. Acta*, **2010**, 510 (1), 9-16.

[3] A. Chin, D.S. Ellison, S.K. Poehlein, M.K. Ahn, *Propellants Explos. Pyrotech.,* **2007**, 32 (2), 117-126.

[4] J. Agrawal, H. Singh, *Propellants Explos. Pyrotech.,* **1993**, 18 (2), 106-110.

[5] J. Agrawal, N. Agawane, R. Diwakar, R. Chandra, *Propellants Explos. Pyrotech.,* **1999**, 24 (6), 371-378.

[6] L.P. Arthur, **1975**, US3878003.

[7] N. Kubota, *"Propellants and Explosives: Thermochemical Aspects of Combustion"*. Weinheim, Germany: Wiley-VCH, **2015**.

[8] D.C. Sayles, **1990**, US4944816.

[9] X. Li, X. Liu, Y. Cheng, Y. Li, X. Mei, *J. Therm. Anal. Calorim.,* **2014**, 115 (1), 887-894.

[10] M.A. Epishina, I.V. Ovchinnikov, A.S. Kulikov, N.N. Makhova, V.A. Tartakovsky, *Mendeleev Commun.,* **2011**, 21 (1), 21-23.

[11] A. Ermakov, P. Bulatov, D. Vinogradov, V. Tartakovskii, *Russ. J. Org. Chem.,* **2004**, 40 (7), 1062-1063.

[12] T.M. Klapötke, B. Krumm, R. Scharf, *Eur. J. Inorg. Chem.,* **2016**, 2016 (19), 3086-3093.

[13] M. Abd-Elghany, T.M. Klapötke, A. Elbeih, S. Zeman, *J. Anal. Appl. Pyrolysis,* **2017**, 126, 267-274.

[14] A. Elbeih, M. Abd-Elghany, T.M. Klapötke, *Propellants Explos. Pyrotech.,* **2017**, 42 (5), 468-476.

[15] A. Elbeih, M. Abd-Elghany, T. Elshenawy, *Acta Astronaut.,* **2017**, 132, 124-130.

[16] M. Abd-Elghany, A. Elbeih, S. Hassanein, *Cent. Eur. J. Energ. Mater.,* **2016**, 13 (3), 349-356.

[17] M. Abd-Elghany, T.M. Klapötke, A. Elbeih, S. Hassanein, T. Elshenawy, *Chin. J. Explos. Propellants*, **2017**, 2 (4), 24-32.

[18] Y.-H. Wang, L.-L. Liu, L.-Y. Xiao, Z.-X. Wang, *J. Therm. Anal. Calorim.,* **2014**, 119 (3), 1673-1678.

[19] Q.-L. Yan, S. Zeman, F.-Q. Zhao, A. Elbeih, *Thermochim. Acta*, **2013**, 556, 6-12.

[20] Q.-L. Yan, S. Zeman, T.-L. Zang, A. Elbeih, *Thermochim. Acta*, **2013**, 574, 10-18.

[21] A. Elbeih, S. Zeman, J. Pachman, *Cent. Eur. J. Energ. Mater.*, **2013**, 10(3), 339-349.

[22] Q.-L. Yan, S. Zeman, R. Svoboda, A. Elbeih, *Thermochim. Acta,* **2012**, 547, 150-160.

[23] Q.-L. Yan, S. Zeman, A. Elbeih, *Thermochim. Acta*, **2012**, 537, 1-12.

[24] Q. Wang, L. Wang, X. Zhang, Z. Mi, *J. Hazard. Mater.,* **2009**, 172 (2), 1659-1664.

[25] A. Altomare, M.C. Burla, M. Camalli, G.L. Cascarano, C. Giacovazzo, A. Guagliardi, A.G. Moliterni, G. Polidori, R. Spagna, *J. Appl. Crystallogr.,* **1999**, 32 (1), 115-119.

[26] L.J. Farrugia, *J. Appl. Crystallogr.,* **1999**, 32 (4), 837-838.

[27] A.L. Spek, *Acta Crystallog. Section D: Biolog. Crystallog.,* **2009**, 65 (2), 148-155.

[28] A. Khawam, D.R. Flanagan, *J. Pharm. Sci.,* **2006**, 95 (3), 472-498.

[29] M. Abd-Elghany, A. Elbeih, S. Hassanein, in *18th Int. Seminar New Trend. Res. Energ. Mater*, Pardubice, Czech Republic, **2015**, pp. 386-402.

[30] H.E. Kissinger, *Anal. Chem.,* **1957**, 29, 1702-1706.

[31] S. Vyazovkin, A.K. Burnham, J.M. Criado, L.A. Pérez-Maqueda, C. Popescu, N. Sbirrazzuoli, *Thermochim. Acta,* **2011**, 520 (1), 1-19.

[32] M. Starink, *Thermochim. Acta,* **2003**, 404 (1), 163-176.

[33] T. Akahira, T. Sunose, *Res. Report Chiba Inst. Technol. (Sci. Technol.),* **1971**, 16, 22-31.

[34] S. Vyazovkin, D. Dollimore, *J. Chem. Inf. Comput. Sci.,* **1996**, 36 (1), 42-45.

[35] C. Doyle, *Appl. Polym. Sci.*, **1961**, 5, 285–292.

[36] C. Doyle, *Appl. Polym. Sci.*, **1962**, 6, 639–642.

[37] C. Doyle, D. Charles, *Nature*, **1965**, 1-12.

[38] S. Joseph, R. Sathishkumar, S. Mahapatra, G.R. Desiraju, *Acta Crystallog. Section B: Struct. Sci.*, **2011**, 67 (6), 525-534.

[39] T. Ozawa, *Bull. Chem. Soc. Jpn.*, **1965**, 38, 1881-1886.

[40] Q.-L. Yan, S. Zeman, A. Elbeih, A. Zbynek, *Cent. Eur. J. Energ. Mater.*, **2013**, 10 (4), 509-528.

Investigation of 2,2,2-trinitroethyl-nitrocarbamate as a High Energy Dense Oxidizer and its Mixture with Nitrocellulose (Thermal Behavior and Decomposition Kinetics)

Published in *J. Anal Appl. Pyrol.* **2017**, 12, 397-404 (DOI: 10.1016/j.jaap.2017.09.010)

Abstract: Thermal behavior and decomposition kinetics of the new interesting high energy dense oxidizer (HEDO) 2,2,2-trinitroethyl-nitrocarbamate (TNENC) and its propellant formulation based on nitrocellulose (NC) as a binder was investigated using nonisothermal thermogravimetric analyzer (TGA) and differential scanning calorimetry (DSC). TNENC has been prepared and characterized by nuclear magnetic resonance (NMR). X-ray diffraction (XRD) was used to study the molecular structure of TNENC. Scanning electron microscope (SEM) was used to check the homogeneity of the new propellant formulation (NC-TNENC). The burning behavior of the prepared NC-TNENC was recorded by high speed camera to observe the smoke produced. A high specific impulse (I_s = 244.46 s) was obtained from the characteristics calculation of the new propellant formulation by using EXPLO5_V6.03 software. The kinetic parameters of the studied samples were determined by using isoconversional (model-free) methods Kissinger, Ozawa and Flynn–Wall (OFW) and Kissinger–Akahira–Sunose (KAS). The results proved that TNENC melts at temperature of 110.5 °C and has a maximum decomposition peak temperature at 166.4 °C, also it has activation energy in the range of 104-106 kJ mol^{-1}. The prepared NC-TNENC didn't show any endothermic peak and its exothermic peak was at 200.8 °C which means that a composite might be formed during the chemical mixing of TNENC with NC. The activation energy of the prepared NC-TNENC was in the range of 176-181 kJ mol^{-1}. TNENC required experimental performance measurements to proof the possibility of replacing the nitroglycerine in a smokeless double base propellant.

Introduction

Double-base propellants (DBP) which are commonly consists of the nitrocellulose (NC) as a binder plasticized by the nitroglycerine (NG) that is entrapped into the fibers of NC are considered as a one of the oldest propellant families which was developed as a result of the development of propulsion [1, 2]. Within the time and during storage of the DBP, several

chemical and physical processes might take place in the propellant grains which included (the consumption of the stabilizer, migration, evaporation and decomposition of NG, etc.). These processes cause change in the stability and the performance of propellants and might cause a self-ignition for the propellants [2]. The development in the field of rocket propellants depends on increasing the energy level of the propellants in addition to solve the NG decomposition problems and it's extremely impact sensitivity [2-5]. Several researchers have studied the possibility of adding some additives such as aluminum or nitramines (HMX, RDX, etc.) to achieve a composite modified double-base propellants (CMDB) [4, 6-9]. Advanced nitramines were prepared and characterized in order to determine the possibility of their application on the field of energetic materials [10-12]. Researches nowadays are focused on the synthesis of a new green safe energetic materials which can replace NG in double base propellants or ammonium perchlorate (AP) in composite solid rocket propellants in order to enhance the energetic characteristics, sensitivities and thermal properties. High-energy dense oxidizers (HEDOs) might be used to replace AP in composite propellants. HEDOs contain high oxygen content and consist of C, H, N, and O elements. 2,2,2-Trinitroethanol (TNE) is one of the most important and suitable starting material with an oxygen balance (ΩCO) of 30.9 % and is easily synthesized through a Henry reaction [13]. TNE was the starting material for a large number of compounds which have been synthesized during the recent studies [14, 15]. 2,2,2-trinitroethyl-nitrocarbamate (TNENC) is an interesting new HEDO which has been prepared by Klapötke's group [14], it has oxygen balance of +14.9, impact sensitivity of 10 J and friction sensitivity of 96 N. TNENC has lower sensitivities than NG and has not been studied in any propellant formulation yet. Also the investigation of the thermal behavior and decomposition kinetics of the energetic materials are necessary and important for the research and development to find a suitable new materials. Usually, thermal analysis is considered the best process to study the thermal decomposition of energetic materials. The most common thermal analysis techniques such as thermogravimetric analyzer (TGA), differential thermal analysis (DTA) and differential scanning calorimetry (DSC) have been used isothermally and non-isothermally in the study of the decomposition kinetics [16-25]. The thermal behavior of TNENC has not been studied yet.

In this work, preparation and characterization of TNENC as a HEDO have been presented. A propellant formulation (NC-TNENC) based on NC as a binder and TNENC as an oxidizer have been prepared. The thermal behavior and decomposition kinetics of the individual NC

and TNENC in addition to NC-TNENC were studied using TGA and DSC techniques. The kinetic parameters of the NC, TNENC and the new propellant NC-TNENC were determined by using different isoconversional methods for calculation.

Experimental

Nitrocellulose (13.15% N) was provided by Nitrochemie Aschau GmbH., conc. sulfuric acid, acetonitrile, fuming nitric acid, chlorosulfonyl isocyanate and ethyl acetate were obtained from Sigma-Aldrich. 2,2,2-trinitroethanol and 2,2,2-trinitroethyl-carbamate has been prepared in our laboratories as reported in ref. [13, 14]. 2,2,2-trinitroethanol (0.76 g, 4.2 mmol) was dissolved in acetonitrile, chlorosulfonyl isocyanate (CSI) (0.64 g, 4.5 mmol) was added with cautious at 0 °C. The mixture was stirred at room temperature for 1.5 h, then the reaction mixture was cooled in an ice bath and water (50 ml) was added slowly. After stirring for 10 min. at room temperature, the precipitate was filtered to get a colorless 2,2,2-trinitroethyl-carbamate. The second step begins by adding 2,2,2-trinitroethyl-carbamate (0.25 g, 1.1 mmol) in small portions with caution at 0 °C into a mixed acid of conc. sulfuric acid (1 ml) and fuming nitric acid (99.5%, 1 ml). The solution was stirred for 2 h at 0 °C and then for another 2 h. at ambient temperature. After quenching the mixture in ice-water (200 ml), extracted with ethyl acetate and then drying over magnesium sulfate. By removing the solvent and recrystallization from carbon tetrachloride, we get 0.3 g (99 % yield) of 2,2,2-trinitroethyl-nitrocarbamate.

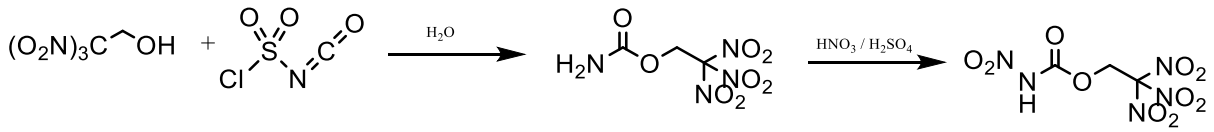

Scheme 1. Preparation of TNENC.

NC was dried at 60 °C for three days, then it was dissolved in a sufficient amount of acetone for 40 minutes at room temperature. TNENC was added in three portions to the solution of NC for 30 minutes during mixing. In order to keep the viscosity of the mixture the same as started, a few ml of solvent should be added (in case of increasing viscosity). The prepared propellant samples were poured in a specific mold and the solvent was evaporated in a vacuum oven at 50 ± 2 °C to drive out the entrapped air. The weight percentage of the prepared samples were 50 wt.% of TNENC and 50 wt.% of NC matrix.

The burning of the new propellant formulation (NC-TNENC) which was prepared in the form of a strand with 100 mm length, 10 mm width and 8 mm thickness from one side (in open-air) showed a smokeless and homogeneous burning. Figure 1 shows the burning behavior of the new propellant formulation which was recorded by high speed camera.

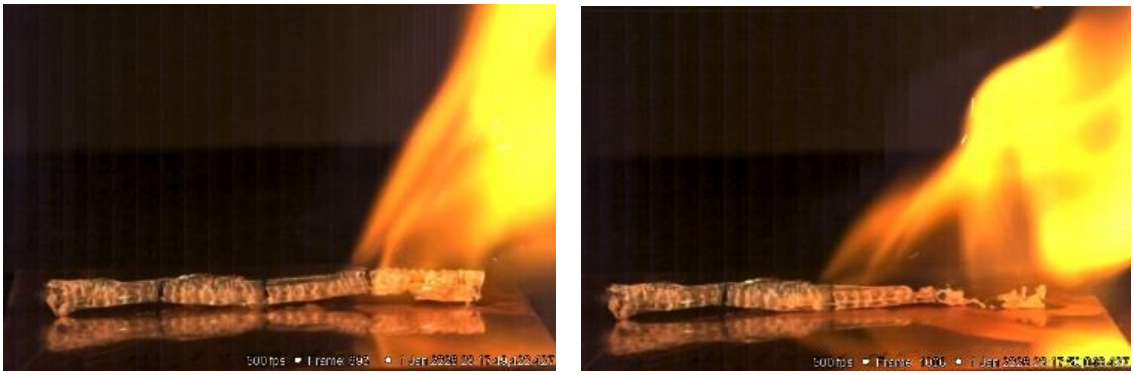

Figure 1. Burning of the new prepared propellant formulation.

The NMR spectra were recorded with a JEOL Eclipse 400 instrument, and the chemical shifts were determined with respect to the external standards Me_4Si (^1H, 399.8 MHz; ^{13}C, 100.5 MHz) and $MeNO_2$ (^{14}N, 28.8 MHz). Specific crystals were selected with a polarization microscope to be suitable for X-ray crystallography. The measurement was done using an Oxford XCalibur3 diffractometer. KappaCCD was used as a detector. The measurement was operated with Mo-K_α radiation (λ = 0.7107 Å). Direct method (SIR97) was used to solve the structure [26]. The result was refined by using the WINGX software package [27]. Finally, result was checked with the PLATON software [28]. The morphology of the studied crystals as well as the homogeneity of the prepared propellant were studied by using SEM (FEI - Helios G3 UC). The thermal decomposition kinetics of the samples were studied using Thermogravimetric Analyzer (Perkin-Elmer, TGA 4000). The experimental conditions used are as following: (TG/DTG: 1–3 mg samples were examined at different heating rates of 2, 4, 8 and 16 °C min^{-1} in the temperature range 30–600 °C under a flow of dynamic nitrogen of 20 ml min^{-1}). The thermal behavior was determined by using LINSEIS DSC – PT10 with samples of approximately 3 mg placed in an aluminum pan with a pin-hole cover at a heating rate of 5 °C min^{-1} in a temperature range of 25 to 400 °C.

The kinetic analysis could be obtained through the determination of the kinetic triplets which are the activation energy (E_a), pre-exponential factor (A) and kinetic model ($f(\alpha)$). These three kinetic parameters should be determined for complete description of the kinetics for

each reaction step. A large number of analytical methods are available nowadays which can be used to determine the kinetic parameters of distinct solid-phase reactions evaluation. The kinetic parameters can be determined either isothermally or nonisothermally by using two main methods which are: Isoconversional (model-free) and model-fitting methods [29, 30]. The kinetic studies of thermally excited reactions in solids is usually used the following equation:

$$d\alpha/dt = k(T)f(\alpha) \quad (1)$$

Where α is the factional conversion, t is time, k(T) is the temperature dependent rate constant and f(α) is the reaction model. The temperature dependency of the rate constant is assumed to obey the Arrhenius expression:

$$k(T) = A \exp(-E/RT) \quad (2)$$

Where A is the pre-exponential factor, E is the activation energy and R is the universal gas constant. By using the integral form of Eqn. 1 which for isothermal conditions, it becomes:

$$g(\alpha) = \int_0^{\alpha} [f(\alpha)]^{-1} d\alpha = k(T)t \quad (3)$$

Where g(α) is the integrated form of the reaction model. The rate constants are calculated at several temperatures for each reaction model selected, and the Arrhenius parameters can be evaluated using the Arrhenius equation in its logarithmic form:

$$lnk(T) = lnA - E/RT \quad (4)$$

In the isoconversional method, it is assumed that the reaction model in Eqn. 1 is independent of the temperature. For the isothermal conditions, eqns. 3 and 4 can be combined to get:

$$-lnt_{\alpha,i} = ln[A/g(\alpha)] - E_{\alpha}/RT_i \quad (5)$$

Where E_α can be obtained from the slope for the plot of $-\ln t_{\alpha,i}$ vs. T_i^{-1}.

The activation energy (E_a) of the exothermic decomposition reaction of the prepared propellants samples can be calculated by easy way using Kissinger's method (see Eqn. 6) [31].

$$-\frac{Ea}{R} = \frac{d\ln(\beta/T_P^2)}{d(1/T_P)} \quad (6)$$

Where β is the heating rate and T_p is the DTG peak temperature at that rate. By plotting of $\ln(\beta/T_p^2)$ versus $1/T_p$, the activation energy can be calculated from the slope of this straight

line. Such rough temperature integral approximation may cause an inaccurate calculated values of E_a [32]. More accurate equation was presented according to Starink [33] for E_a calculation which is commonly called the Kissinger–Akahira–Sunose (KAS) equation [34]:

$$ln\left(\frac{\beta_i}{T_{\alpha,i}^{1.92}}\right) = const - 1.0008\frac{E_\alpha}{RT_\alpha} \quad (7)$$

Ozawa and Flynn–Wall (OFW) used a nonisothermal data and developed an isoconversional calculation method (commonly referred to as the OFW method), in which taking the logarithm of the nonisothermal rate law to give the following equation [35]:

$$log\, g(\alpha) = log\frac{AE_a}{\beta R} + log\int_{\frac{E_a}{RT}}^{\infty}\frac{e^{\frac{-E_a}{RT}}}{\left(\frac{E_a}{RT}\right)^2}\, d\frac{E_a}{RT} \quad (8)$$

By substitution using Doyle's approximation [36-38]:

$$log\int_{\frac{E_a}{RT}}^{\infty}\frac{e^{\frac{-E_a}{RT}}}{\left(\frac{E_a}{RT}\right)^2}\, d\frac{E_a}{RT} \approx -2.315 - 0.4567\frac{E_a}{RT} \quad (9)$$

Then OFW equation can be written as:

$$log\,\beta = log\frac{AE_a}{g(\alpha)R} - 2.315 - 0.457\frac{E_a}{RT} \quad (10)$$

Results

TNENC was characterized by ^{1}H, ^{13}C and ^{14}N NMR spectroscopy in [D_6] acetone. In the ^{1}H spectra the CH_2 group was observed at δ = 5.63 (s, 2 H, CH_2) ppm, while the NH group was appeared at δ = 10.92 (s, 1 H, NH. For ^{13}C NMR was the appearance of the trinitromethyl group at δ = 122.81 ($C(NO_2)_3$) ppm, and δ = 145.5 ppm for (CO_2N) and the CH_2 group was observed at δ = 62.21 (CH_2) ppm.^{14}N NMR showed the trinitromethyl group at δ = –36.15 ($C(NO_2)_3$) ppm, and the nitramine group was observed at δ = –55.1 (NNO_2) ppm. By comparing the results with the reference [14], it was found that the results are nearly the same.

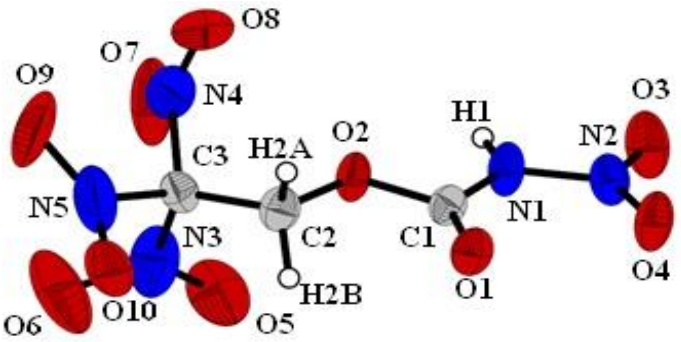

Figure 2. X-ray molecular structure for TNENC.

Due to the phase transition that was shown at about – 62 °C, which leads to a micro-fracture of the single crystal that made a measurement impossible, the data collection of the compound TNENC had to be performed at higher temperature. So, the data collection was carried out at – 30 °C. Nitrocarbamate moiety of TNENC shows a perfect planarity as shown by the angles sum around the C1 and the two nitrogen atoms N1 and N2, where the angle sum for each is 360°. The N1–N2 bond of the nitramine moiety is 1.373 Å, which indicates the intrinsic of a double bond character, that achieved by the delocalization of the nitrogen lone pair. The carbonyl group shows also a slight shortening (1.182 Å). The trinitroethyl moiety is stabilized by the interactions between N⋯O atoms (N3⋯O7, N4⋯O9, N5⋯O6). TNENC shows two traditional hydrogen bonds, which links the hydrogen that attached to N1 with the two oxygen atoms ($O1^{i}$, $O4^{i}$). The significantly strongest interaction is between the carbonyl (O1) and the NH group. The improper hydrogen bond with carbon as donor (CH⋯O) can be observed from figure 2. The extensive hydrogen-bonding between the methylene (C2–H2A/B) and adjoining nitro groups may help to explain the good thermal stability (see Table 1) [14, 39].

Table 1. Hydrogen bond lengths and angles of TNENC

D–H⋯*A*	D–H	H⋯*A*	D⋯*A*	D–H⋯*A*
N1–H1⋯$O1^{i}$	0.82	2.015	2.797	159.8
N1–H1⋯$O4^{i}$	0.82	2.634	3.117	119.3
C2–H2B⋯$O3^{ii}$	0.99 [a)]	2.711	3.635	154.1
C2–H2B⋯$O4^{ii}$	0.99 [a)]	2.516	3.424	157.2
C2–H2A⋯$O10^{iii}$	0.99 [a)]	2.607	3.448	143.9

a)Normalized C–H length 0.99 Å. Symmetry codes of acceptors molecules: (*i*) x,½-y, -½+z; (*ii*) 1-x, -½+y, 1½-z; (*iii*) –x, -y, 1-z.

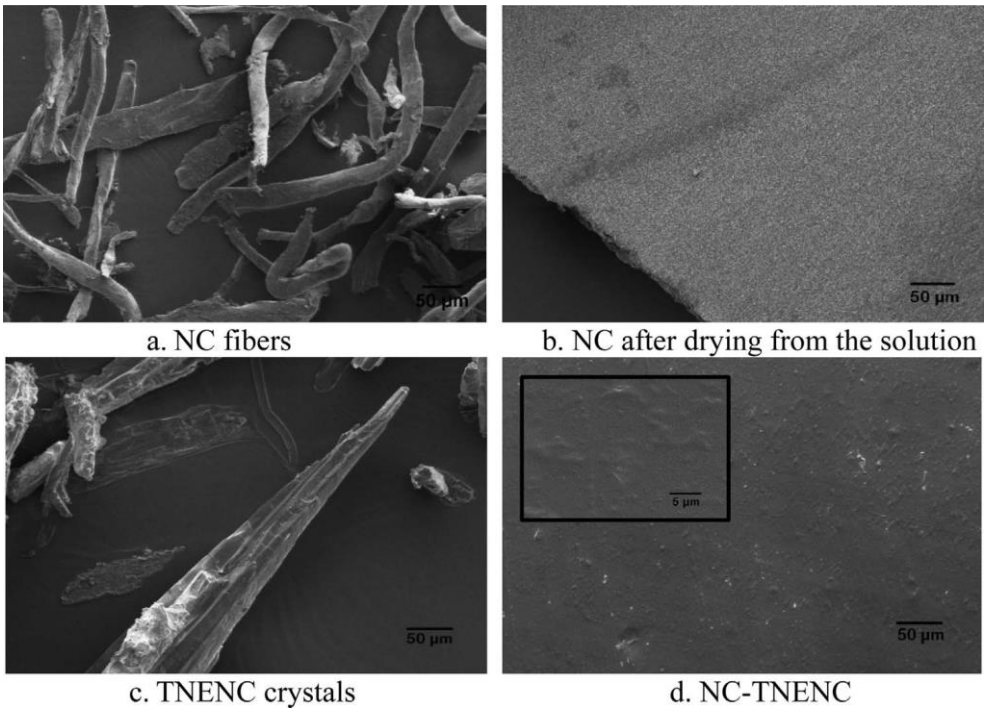

Figure 3. SEM of the oxidizer, NC matrix and NC-TNENC.

SEM results showed that the matrix of NC consists of long fibers which were completely changed to the form of a sheet after obtaining it from a solution containing acetone as a solvent, the fibers were bonded to each other and give a homogeneous surface which took the shape of its mold after the casting process as shown in Fig. 3. Colorless needle crystals of the TNENC were obtained from the preparation process and after the mixing with NC, a clear homogeneity was appeared of NC matrix with TNENC as shown in Fig. 3d. The crystals of the oxidizer and the NC fibers are completely disappeared and mixed together with a very smooth surface of the prepared samples. This result clarifies the homogeneous burning process of the propellant as shown in Fig. 1.

TG/DTG thermograms of NC, TNENC and NC-TNENC were recorded at four different heating rates 2, 4, 8, and 16 K min^{-1} and were presented in Fig. 4 and Fig. 5. It is clear from the TG thermograms presented on Fig. 4 that the NC decomposes thermally in one sharp step, while TNENC showed a controlled thermal decomposition process which was occurred in one decomposition step. The effect of the TNENC on the thermal decomposition of NC can be noticed from the TG thermogram of the prepared propellant sample (NC-TNENC), which enhanced the sharp thermal decomposition step of NC to a homogenous controlled one step thermal decomposition reaction with a slight effect on the thermal decomposition temperature of the NC.

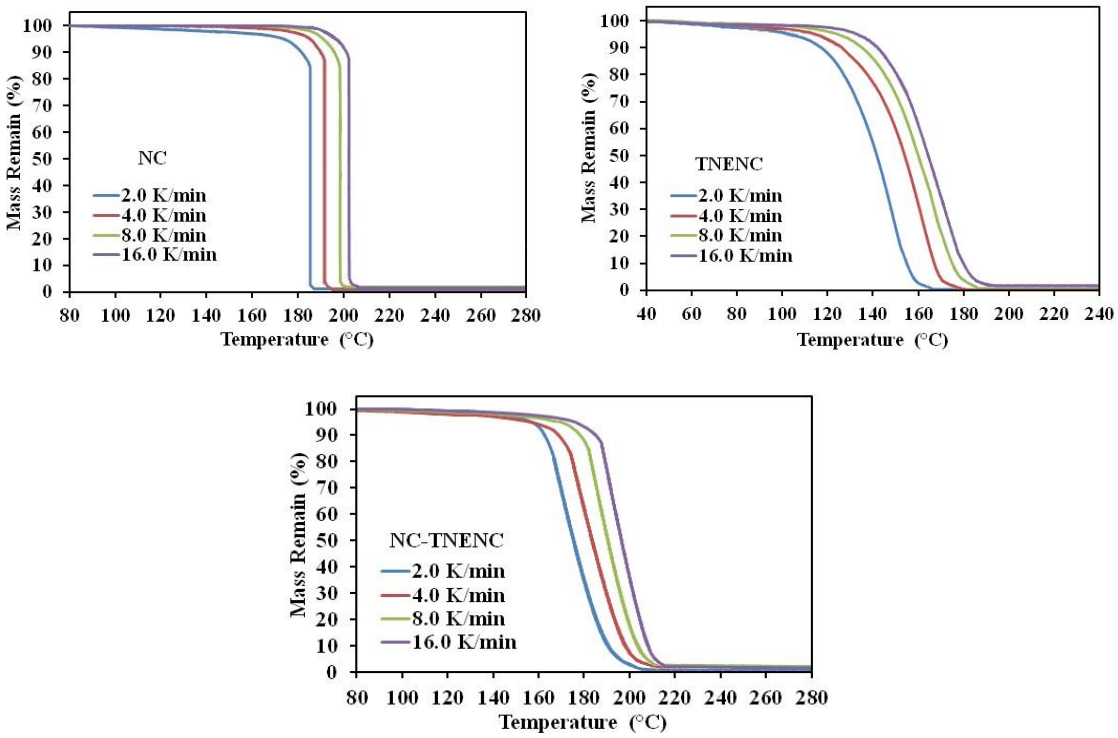

Figure 4. TG thermograms of NC and NC-TNENC under different heating rates.

Also there are small mass loss exist during the heating process and before starting the onset fast decomposition, this might be due to the evaporation of the residual solvent. At heating rates 2 K min^{-1}, the initial decomposition of NC was at 183.2 °C and the maximum decomposition peak was at 187.6 °C, which means that a quick decomposition occurred for NC. In case of NC-TNENC, the initial decomposition was at 165.1 °C while the maximum decomposition peak was at 185.4 °C (20 °C difference), this result proved that the TNENC oxidizer acts as a cooler and reduced the decomposition process of NC, also the new propellant had a different characteristics from both the individual TNENC and NC.

The onset decomposition temperature and the initial mass loss temperature of the studied samples increase with increasing the heating rates. The DTG thermogram (Fig. 5) of the studied samples at the four different heating rates showed that the decomposition peak temperature of NC-TNENC is very close to that of the pure NC, although the oxidizer TNENC decomposes at lower temperature. Furthermore, a complex might be formed between the oxidizer and the NC binder which changed the decomposition mechanism.

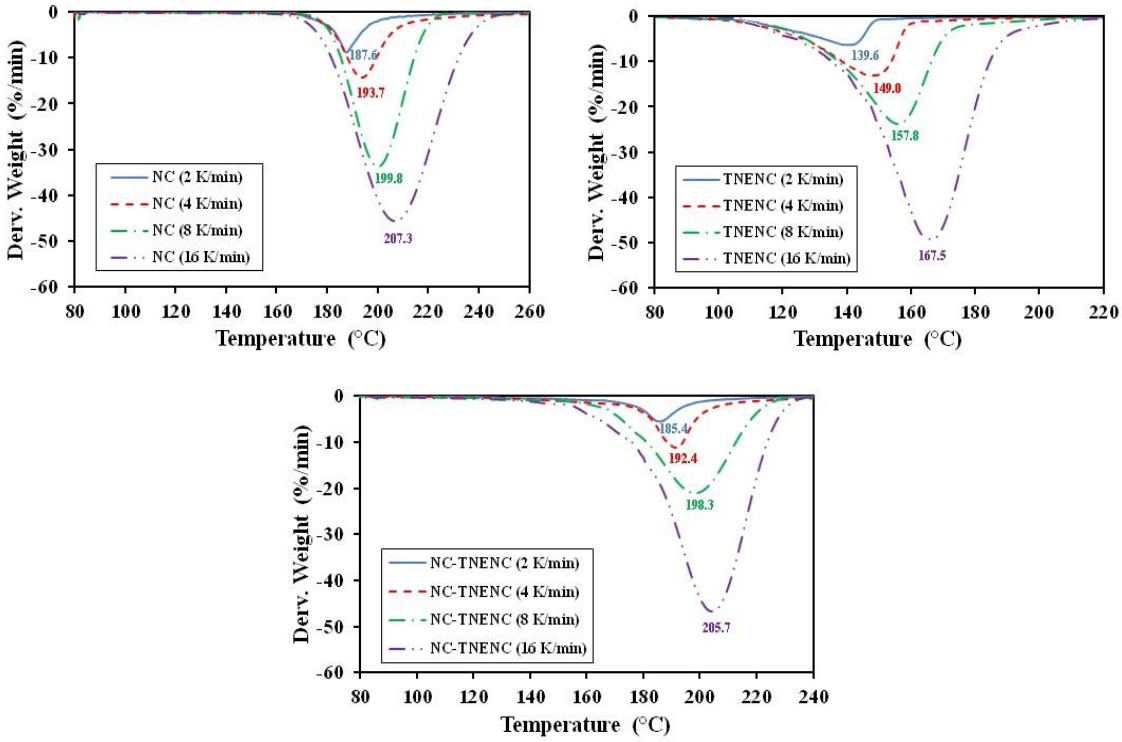

Figure 5. DTG curves for NC, TNENC and NC-TNENC under heating rates of 2, 4, 8 and 16 K min^{-1}.

Table 2. The nonisothermal TG/DTG data for NC, TNENC and NC-TNENC

Material	β (K min^{-1})	TG curves			DTG peaks	
		T_{ot} (°C)	T_i (°C)	Mass Loss (%)	T_p (°C)	T_{oe} (°C)
NC	2.0	179.8	183.2	99.7	187.6	198.1
	4.0	186.0	189.8	99.3	193.7	209.4
	8.0	193.8	196.9	99.5	199.8	218.5
	16.0	195.8	202.3	99.0	207.3	231.7
TNENC	2.0	117.9	128.8	98.5	139.6	148.3
	4.0	126.4	139.2	97.4	149.0	160.6
	8.0	138.6	146.1	96.6	157.8	174.4
	16.0	142.0	154.8	94.2	167.5	198.7
NC-TNENC	2.0	160.3	165.1	99.2	185.4	199.6
	4.0	171.2	176.8	98.6	192.4	210.3
	8.0	178.6	181.2	98.0	198.3	227.2
	16.0	182.3	185.1	97.5	205.7	236.1

Note: T_{ot}: onset temperature of decomposition; T_{oe}: onset temperature of the end decomposition; T_i: initial thermal decomposition temperature; T_p: the peak temperature of mass loss rate; Mass Loss: from initial temperature to end temperature of DTG peak.

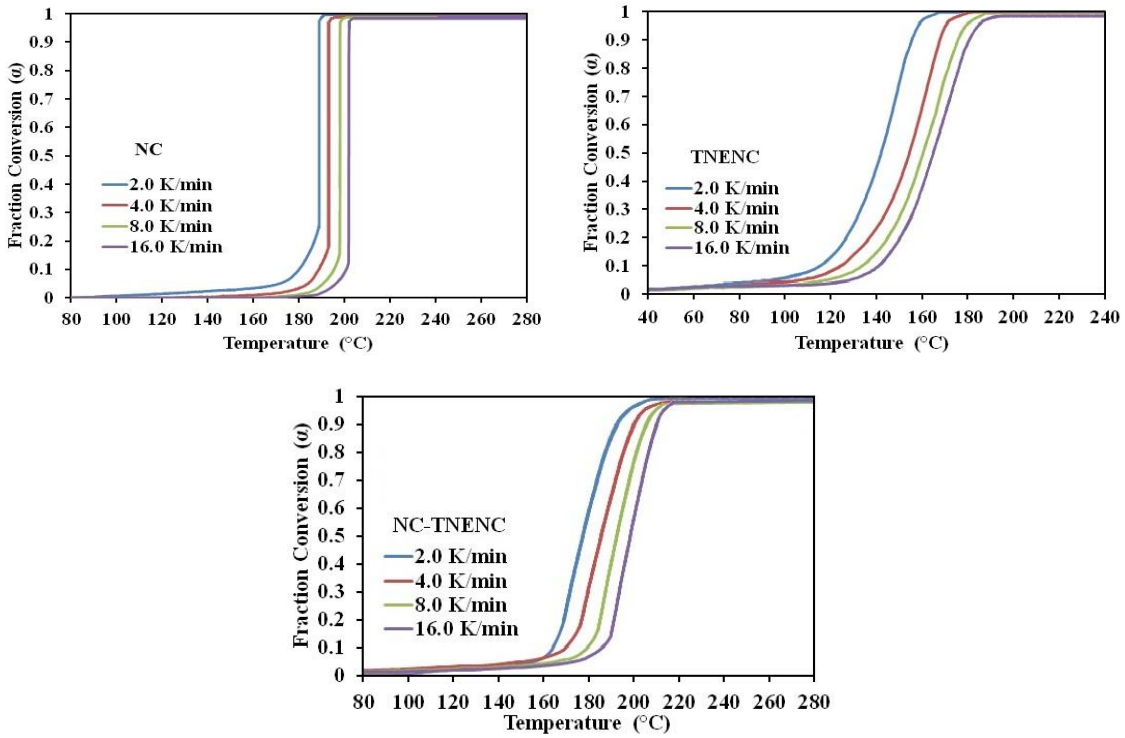

Figure 6. The α-T curves of NC and NC-TNENC under heating rates of 2, 4, 8 and 16 K min^{-1}.

Fig. 6 showed the corresponding α-T curves which were obtained from the mass remaining vs. temperature data. The results confirm the quick mass loss of the individual NC and the decrease in the rate of the mass loss after mixing of NC with TNENC.

The conventional Kissinger method was used to obtain the activation energy E_a of the studied samples. The thermal decomposition kinetics were studied using nonisothermal TGA technique. The activation energy of the studied samples were calculated by applying Kissinger equation (eq. 6) from the slop of the straight line from plotting $\ln(\beta/T^2)$ versus 1/T at the four selected heating rates, where T is the decomposition peak temperature which obtained from the DTG thermogram (Fig. 6). The activation energy of the NC matrix and TNENC was 187.5 kJ mol^{-1} and 106.2 kJ mol^{-1} respectively while the activation energy of the propellants sample NC-TNENC was 181.3 kJ mol^{-1}. From this result, it is shown that the propellant sample has a high activation energy value and very close to that of the pure NC, which give the propellant good stability. Due to the disadvantage of this method which is the inability to determine the reaction steps or discuss the distinct activation energy for each fraction conversion (α) another methods of kinetic parameters calculation was applied.

OFW is an isoconversional calculation method which is independently developed by Ozawa and Flynn–Wall to calculate the activation energy E_a using nonisothermal data [40]. The

activation energy E_a is determined from the slop of the straight line through a plot of log β versus $1/T$ at each α regardless of the employed model. The activation energy for each step of reaction α shows the thermal decomposition behavior of the studied samples. Fig. 7 shows the activation energy variations for the studied samples from step to step of reaction. The activation energy of NC was found to be 182.2 kJ mol^{-1} (average value). Jutier et al stated that the activation energy of NC depends on the nitrogen content in addition to the source of the cellulose used for the preparation of NC [41]. Juties found that the activation energy of NC (13.5% nitrogen content) was 184 ± 8 kJ mol^{-1} using Ozawa method which is almost the same as our measurements (less than 1 % difference). The oxidizer TNENC has a low activation energy with mean value of **104.1** kJ mol^{-1}, there is no published value for the activation energy of TNENC in literature for comparison. The new propellant sample showed activation energy with average value of **176.4** kJ mol^{-1} which is slightly lower than that of the NC. It means that the effect of TNENC oxidizer on the activation energy of the new propellant can be neglected and the behavior of the new propellant looks similar to that of NC.

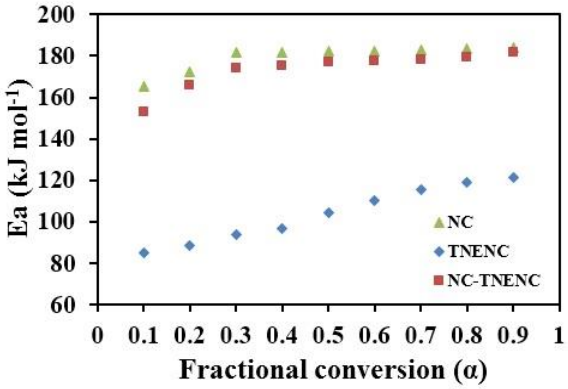

Figure 7. Activation energies for each conversion step (α) using OFW method.

The modified Kissinger–Akahira–Sunose (KAS) method was used to determine the activation energy at each degree of conversion. Table 3 present the kinetic parameter values of the different studied samples based on KAS method. The average activation energy value of NC was 184.1 kJ.mol^{-1}, for the oxidizer TNENC was 105.1 kJ.mol^{-1} and the new propellant sample was 178.9 kJ.mol^{-1}. The mean activation energy values using OFW and KAS methods were calculated in the interval of (α = 0.3 – 0.7) as commonly suggested in literatures [16, 19, 20, 42] due to the large influence of the experimental conditions specially in case of TG/DTG on the data quality of the process “tails”. The pre-exponential factor A

and the activation energy E_a relationship was presented in Fig. 8 at each step of conversion where the effect of adding the oxidizer TNENC to the NC matrix improved the normal distribution of the activation energy during each α and gives a homogeneous burning for the new propellants formula.

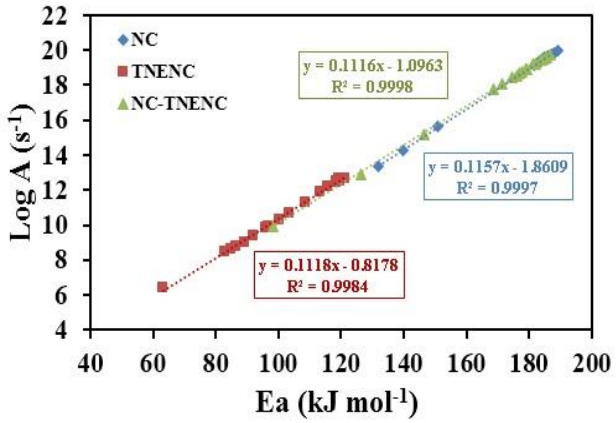

Figure 8. Log A vs E_a for each conversion step (α) using KAS method.

Table 3. Kinetic data of NC, TNENC and NC-TNENC obtained using the modified KAS method

α reacted	NC			TNENC			NC-TNENC		
	E_a	logA	r	E_a	logA	r	E_a	logA	r
0.1	139.6	14.28	0.9979	82.9	8.45	0.9968	126.4	12.93	0.9984
0.2	176.9	18.61	0.9989	86.4	8.80	0.9974	168.7	17.75	0.9968
0.3	183.4	19.35	0.9991	91.9	9.36	0.9987	174.6	18.43	0.9979
0.4	183.7	19.39	0.9986	96.9	9.93	0.9983	176.8	18.66	0.9988
0.5	184.2	19.44	0.9975	103.6	10.72	0.9991	178.9	18.88	0.9981
0.6	184.5	19.55	0.9958	113.2	11.91	0.9989	181.2	19.20	0.9990
0.7	184.9	19.58	0.9989	119.4	12.64	0.9978	183.5	19.43	0.9973
0.8	187.1	19.76	0.9991	118.3	12.42	0.9985	184.9	19.52	0.9982
0.9	189.2	19.98	0.9957	121.1	12.69	0.9974	186.7	19.71	0.9967
Mean	184.1	19.45		105.0	10.91		178.9	18.89	

From table 3, it was observed that the activation energy of TNENC slightly increase as the fractional conversion increase where it reached at 90% conversion to 121.1 kJ mol^{-1}. The new propellant has activation energy 126.4 kJ mol^{-1} at 10% conversion, then a clear increase in the activation energy observed at 20% conversion (38 kJ mol^{-1} increase in the activation energy) accompanied by a balanced slight increase in the activation energy until the end of

the conversion. This result might be due to the presence of residue of the solvent which affect the activation energy of the propellant at the beginning of the conversion, then a stable increase started from 20% conversion until the end of the conversion. The same trend observed for NC, which could be due to the same reason. The presence of the new oxidizer with the NC caused slight decrease of the activation energy of NC but in the same trend. It is also known that the decomposition of composite explosives is a complex process and the variation of the activation energies of NC-TNENC and the individual materials could be also due to the possible effect of the complexity of decomposition.

In order to compare the results obtained by the three different methods, the values of activation energy of all the studied samples were presented in table 4. A good agreement was observed between the results obtained by OFW method and those obtained by KAS method with maximum difference of 1.5%, while the maximum difference between the results obtained by OFW and those obtained by Kissinger was 3%. It means that the results of the three methods are close to each other and the activation energy of the new propellant NC-TNENC is in the range of 176 to 182 kJ $mol^{-1}$with respect to the different methods and the researchers can depend on these results in the future.

Table 4. Activation energies (E_a) for NC, TNENC and the formulation NC-TNENC using different methods

Sample	Activation Energy E_a (kJ mol^{-1})		
	Kissinger	OFW	KAS
NC	187.5	182.2	184.1
TNENC	106.2	104.1	105.1
NC-TNENC	181.3	176.4	178.9

DSC was used to obtain the thermal behavior of the studied samples at heating rate of 5 K min^{-1}. The samples were encapsulated in an aluminum pan with a pin-hole cover and measurements were performed under comparable conditions for the different samples. In fig. 9 the thermogram of NC matrix showed one exothermic decomposition peak at 202.3 °C. On the other hand TNENC curve shows an endothermic melting peak at 110.5 °C and decomposed with an exothermic peak at 166.4 °C. While the curve of NC-TNENC showed only one exothermic peak at 200.8 °C without any endothermic melting peaks, which means that the new propellant formula has different thermal behavior compared with the pure oxidizer. This result indicated that a new complex might be formed during the mixing of the

oxidizer with the NC. Brodman et al stated that NC makes a chemical complex by mixing with RDX or HMX which was discussed in their US patent [43], also a π complex intermediate was formed between diphenyl amine (DPA) and NC due to the high free-radical intensity possessed by the propellant composition [3]. Sovizi et al [44] stated that the decomposition parameters might be affected by the particle size of NC and the maximum decomposition peak temperature decreases as the particle size of NC decreases. He proved that the maximum peak decomposition temperature of micro-NC at heating rate of 5 K min^{-1} was 201.8 °C which is very close to our result at the same heating rate (202.3 °C). Pourmortazavi et al studied the effect of nitrogen content of NC on its decomposition [45], he proved that the decomposition peak temperature decreases as the nitrogen content increases. The results of DSC proved that the thermal behavior of the new prepared oxidizer TNENC has been changed completely due to its mixing with NC which proof the advantage of using TNENC as oxidizer with NC.

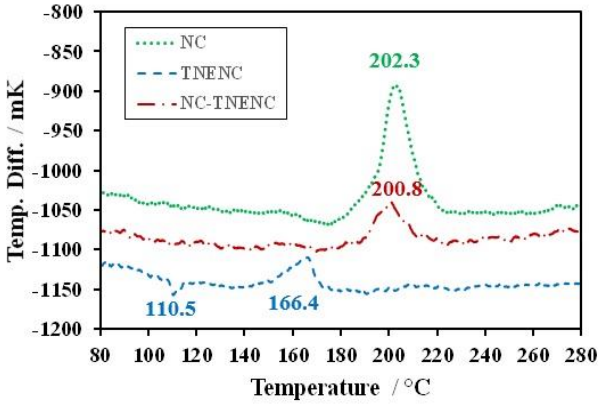

Figure 9. DSC thermogram for NC, TNENC and NC-TNENC at 5.0 K min^{-1} heating rate.

Table 5. The DSC data using non-isothermal DSC for NC, TNENC and NC-TNENC

Sample	Exothermic peak			Endothermic peak	
	T_o (°C)	T_p (°C)	T_e (°C)	T_{eo} (°C)	T_{ep} (°C)
NC	180.9	202.3	216.4	---	---
TNENC	151.6	166.4	174.3	108.7	110.5
NC-TNENC	191.4	200.8	211.3	---	---

Note: T_o: decomposition onset temperature; T_p: decomposition peak temperature; T_e: the end decomposition onset temperature; T_{eo}: melting onset temperature; T_{ep}: melting peak temperature.

Conclusions

2,2,2-trinitroethyl-nitrocarbamate (TNENC) is a new interesting high energy dense oxidizer (HEDO) which can be easily and safely prepared as a powder by comparing with the dangerous liquid NG. A new propellant formula based on TNENC with NC was prepared. The SEM photos proved that the oxidizer TNENC had a good homogeneous mixing with NC. The high speed camera proved that burning process of the new propellant formula was smokeless. The thermal study proved that the TNENC has melting peak at 110.5 °C and has a maximum decomposition peak temperature of 166.4 °C at heating rate 5 K min^{-1}, while the prepared propellant has higher maximum decomposition peak temperature at 200.8 °C without any melting peak. This result proved that a new composite might be formed during the mixing process, also the activation energy of the prepared propellant was very close to that of the NC. The kinetic study by the different three methods showed activation energy of TNENC in the range of 104-106 ± 0.2 kJ mol^{-1}, while the prepared propellant showed a higher activation energy values in the range of 176-181 ± 0.3 kJ mol^{-1}. The new oxidizer TNENC has a much lower sensitivity than NG in addition to the high specific impulse (I_s = 244.46 s) of its propellant composition (NC-TNENC) calculated by EXPLO5_V6.03 software which means that it could be used to replace the NG in the smokeless double base propellant and its performance should be studied experimentally.

References

[1] H. AUSTRUY, in *"Solid Rocket Propulsion Technology"*. New York: Pergamon Press, **2012**, pp. 369-412.

[2] M. Sućeska, S.M. Mušanić, I.F. Houra, *Thermochim. Acta*, **2010**, 510 (1), 9-16.

[3] A. Chin, D.S. Ellison, S.K. Poehlein, M.K. Ahn, *Propellants Explos. Pyrotech.*, **2007**, 32 (2), 117-126.

[4] J. Agrawal, H. Singh, *Propellants Explos. Pyrotech.*, **1993**, 18 (2), 106-110.

[5] J. Agrawal, N. Agawane, R. Diwakar, R. Chandra, *Propellants Explos. Pyrotech.*, **1999**, 24 (6), 371-378.

[6] L.P. Arthur, **1975**, US3878003.

[7] N. Kubota, *"Propellants and Explosives: Thermochemical Aspects of Combustion"*. Weinheim, Germany: Wiley-VCH, **2015**.

[8] D.C. Sayles, **1990**, US4944816.

[9] X. Li, X. Liu, Y. Cheng, Y. Li, X. Mei, *J. Therm. Anal. Calorim.*, **2014**, 115 (1), 887-894.

[10] A. Elbeih, J. Pachman, S. Zeman, W. Trzcinski, M. Suceska, *Propellants Explos. Pyrotech.*, **2013**, 38 (2), 238-243.

[11] A. Elbeih, S. Zeman, M. Jungova, P. Vavra, Z. Akstein, *Propellants Explos. Pyrotech.*, **2012**, 37(6), 676-684.

[12] A. Elbeih, S. Zeman, M. Jungova, Z. Akstein, *Cent. Eur. J. Energ. Mater.*, **2012**, 9(2), 131-138.

[13] M.A. Epishina, I.V. Ovchinnikov, A.S. Kulikov, N.N. Makhova, V.A. Tartakovsky, *Mendeleev Commun.*, **2011**, 21 (1), 21-23.

[14] Q.J. Axthammer, T.M. Klapötke, B. Krumm, R. Moll, S.F. Rest, *Z. Anorg. Allg. Chem.*, **2014**, 640 (1), 76-83.

[15] T.M. Klapötke, B. Krumm, R. Scharf, *Eur. J. Inorg. Chem.*, **2016**, 2016 (19), 3086-3093.

[16] M. Abd-Elghany, T.M. Klapötke, A. Elbeih, S. Zeman, *J. Anal. Appl. Pyrolysis*, **2017**, 126, 267-274.

[17] Y.-H. Wang, L.-L. Liu, L.-Y. Xiao, Z.-X. Wang, *J. Therm. Anal. Calorim.*, **2014**, 119 (3), 1673-1678.

[18] Q.-L. Yan, S. Zeman, F.-Q. Zhao, A. Elbeih, *Thermochim. Acta*, **2013**, 556, 6-12.

[19] Q.-L. Yan, S. Zeman, T.-L. Zang, A. Elbeih, *Thermochim. Acta*, **2013**, 574, 10-18.

[20] A. Elbeih, M. Abd-Elghany, T.M. Klapötke, *Propellants Explos. Pyrotech.*, **2017**, 42 (5), 468-476.

[21] Q.-L. Yan, S. Zeman, R. Svoboda, A. Elbeih, *Thermochim. Acta*, **2012**, 547, 150-160.

[22] A. Elbeih, S. Zeman, J. Pachman, *Cent. Eur. J. Energ. Mater.*, **2013**, 10(3) 339-349.

[23] Q.-L. Yan, S. Zeman, A. Elbeih, *Thermochim. Acta*, **2012**, 537, 1-12.

[24] M. Abd-Elghany, T.M. Klapötke, A. Elbeih, S. Hassanein, T. Elshenawy, *Chin. J. Explos. Propellants*, **2017**, 2 (4), 24-32.

[25] Q. Wang, L. Wang, X. Zhang, Z. Mi, *J. Hazard. Mater.*, **2009**, 172 (2), 1659-1664.

[26] A. Altomare, M.C. Burla, M. Camalli, G.L. Cascarano, C. Giacovazzo, A. Guagliardi, A.G. Moliterni, G. Polidori, R. Spagna, *J. Appl. Crystallog.*, **1999**, 32 (1), 115-119.

[27] L.J. Farrugia, *J. Appl. Crystallog.*, **1999**, 32 (4), 837-838.

[28] A.L. Spek, *Acta Crystallographica Section D: Biological Crystallography*, **2009**, 65 (2), 148-155.

[29] A. Khawam, D.R. Flanagan, *J. Pharm. Sci.*, **2006**, 95 (3), 472-498.

[30] M. Abd-Elghany, A. Elbeih, S. Hassanein, in *18th Int. Seminar New Trend. Res. Energ. Mater*, Pardubice, Czech Republic, **2015**, pp. 386-402.

[31] H.E. Kissinger, *Anal. Chem.*, **1957**, 29, 1702-1706.

[32] S. Vyazovkin, A.K. Burnham, J.M. Criado, L.A. Pérez-Maqueda, C. Popescu, N. Sbirrazzuoli, *Thermochim. Acta,* **2011**, 520 (1), 1-19.

[33] M. Starink, *Thermochim. Acta,* **2003**, 404 (1), 163-176.

[34] T. Akahira, T. Sunose, *Res. Report Chiba Inst. Technol. (Sci. Technol.),* **1971**, 16, 22-31.

[35] S. Vyazovkin, D. Dollimore, *J. Chem. Inf. Comp. Sci.*, **1996**, 36 (1), 42-45.

[36] C. Doyle, *Appl. Polym. Sci.*, **1961**, 5, 285–292.

[37] C. Doyle, *Appl. Polym. Sci.*, **1962**, 6, 639–642.

[38] C.D Doyle, D. Charles, *Nature*, **1965**, 1-12.

[39] R.J. Butcher, R.D. Gilardi, C. George, J. Flippen-Anderson, *J. Chem. Crystallog.*, **1996**, 26 (6), 381-388.

[40] T. Ozawa, *Bull. Chem. Soc. Jpn.,* **1965**, 38, 1881-1886.

[41] J.-J. Jutier, R.E. Prud'homme, *Thermochim. Acta,* **1986**, 104, 321-337.

[42] Q.-L. Yan, S. Zeman, A. Elbeih, A. Zbynek, *Cent. Eur. J. Energ. Mater.,* **2013**, 10 (4), 509-528.

[43] B.W. Brodman, M.P. Devine, S. Schwartz, **1977**, US4033798.

[44] M.R. Sovizi, S. Hajimirsadeghi, B. Naderizadeh, *J. Hazard. Mater.,* **2009**, 168 (2), 1134-1139.

[45] S. Pourmortazavi, S. Hosseini, M. Rahimi-Nasrabadi, S. Hajimirsadeghi, H. Momenian, *J. Hazard. Mater.,* **2009**, 162 (2), 1141-1144.

Higher Performance and Safer Handling:Formulation Based on 2,2,2-Trinitroethyl Formate and Nitrocellulose

Published in *ChemPlusChem*. **2018**, 83(3), 128-131 (DOI: 10.1002/cplu.201800088)

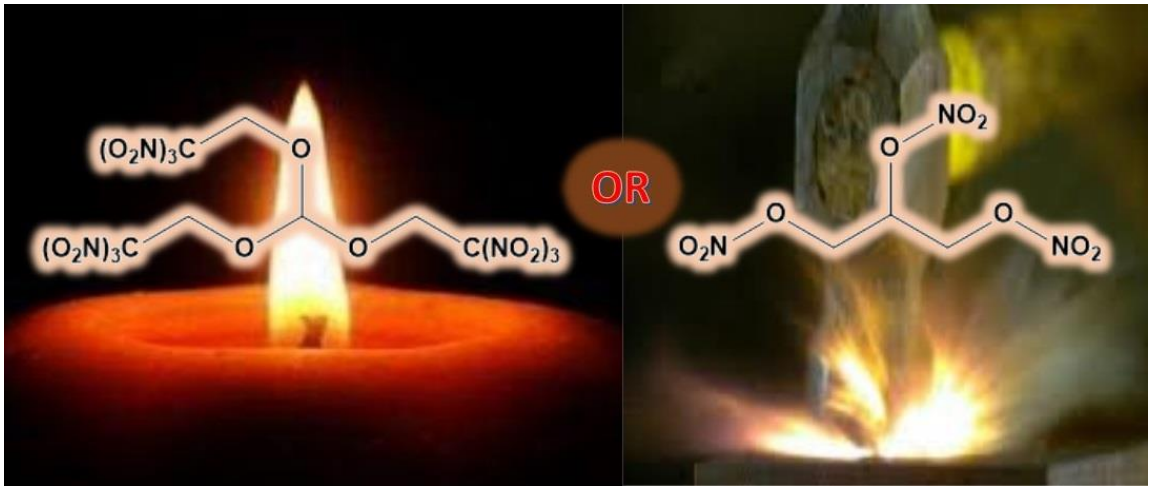

Abstract: A new green propellant formulation based on the high-energy dense oxidizer (HEDO) 2,2,2-trinitroethyl formate (TNEF) and nitrocellulose (NC) was prepared and thermally investigated using non-isothermal thermogravimetric analysis (TGA) and differentialscanning calorimetry (DSC). Scanning electronmicroscopy (SEM) was used to check the crystals of the oxidizer and the homogeneity of the new propellant formulation (NC-TNEF). The burning behavior of NC-TNEF was recorded by high-speed camera to observe the smoke produced. A high specific impulse (I_s = 257.4 s) was obtained from the characteristics calculation of the new propellant formulation by using EXPLO5_V6.03 software. The NC-TNEF mixture did not show any endothermic peak and its exothermic peak was at 204.6 °C, which means that acomposite might be formed. The activation energy of the NC-TNEF was in the range of 184–190 kJ mol^{-1}. NC-TNEF has a higher performance and a lower hazard compared with the double-base propellant.

Introduction

Solid propellants have a wide range of applications in tactical rockets, space launcher boosters and even amateur hobby rockets [1-9]. Solid rocket propellants divided into two categories: homogenous (double-base) propellants and heterogeneous (composite)

propellants. Double-base propellants (DBP) which are commonly consists of the nitrocellulose (NC) as a binder plasticized by the nitroglycerine (NG) are considered as a one of the oldest solid propellant families which was developed as a result of the development of propulsion [10]. Within the time and during storage of the DBP, several physical and chemical processes take place in the propellant grains which included (the consumption of the stabilizer, migration, evaporation and decomposition of NG, etc.). The stability and the performance of propellants were affected and changed due to these processes and might cause a self-ignition for the propellants [11]. The researchers are working on solving the NG decomposition problems and it's high impact sensitivity [12, 13]. The possibility of addition of some additives such as aluminum or nitramines (RDX, HMX, etc.) was studied [14-17]. Researches nowadays are focused on the synthesis of new green safe energetic materials that can replace NG in DBP to overcome the over-mentioned problems, and to enhance the energetic characteristics [18, 19]. 2,2,2-Trinitroethanol (TNE) which is easily synthesized through a Henry reaction [20], is one of the interesting starting material for preparation of large number of compounds [21]. 2,2,2-trinitroethyl formate (TNEF) is an interesting HEDOs. It was firstly prepared in 1967 [22], recently it was synthesized by other methods [23, 24]. It has been used in various energy materials [25, 26]. It has oxygen balance of (Ω CO_2) of 10.1 %, impact sensitivity of 5 J and friction sensitivity of 96 N [24]. TNEF has lower sensitivities, higher density and oxygen balance than NG and has not been studied in any propellant formulation yet.

In addition, the investigation of the thermal behavior and decomposition kinetics of the energetic materials are necessary to find suitable new materials. The most common thermal analysis techniques such as thermogravimetric analysis (TGA) and differential scanning calorimetry (DSC) have been used to study the decomposition kinetics of many energetic materials [27-35]. Although TNEF is a new interesting HEDO, but it has not been thermally studied yet. In this work, synthesis and characterization of TNEF have been presented. A propellant formulation (NC-TNEF) have been prepared. The thermal behavior and decomposition kinetics of the individual NC and TNEF in addition to NC-TNEF were studied using TGA and DSC techniques. The kinetic parameters of the samples were determined by using different isoconversional methods for calculation.

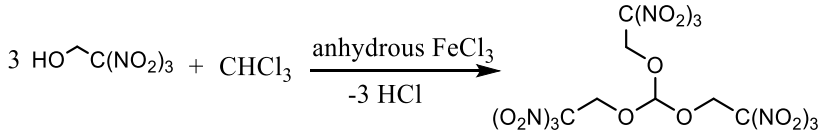

Scheme 1. Synthesis of TNEF.

Experimental

TNEF has been successfully synthesized from TNE and chloroform by using anhydrous Iron trichloride as a catalyst. It was characterized by ^{1}H, ^{13}C, and ^{14}N NMR and FTIR and compared with the reference [24]. The results showed highly synthesized purity of the TNEF. NC (13.15% N) was provided by Nitrochemie Aschau GmbH. Dried NC (at 60 °C for three days) was dissolved in a sufficient amount of acetone for 40 minutes at room temperature. TNEF was added in three portions to the solution of NC for 30 minutes during mixing (150 rpm). Because of the acetone high volatility, few ml of acetone should be added during the mixing process to keep the viscosity of the mixture at the same level. The prepared propellant samples were poured in a specific mold and the solvent was evaporated in a vacuum oven at 50 ±2 °C to drive out the entrapped air. The weight percentage of the prepared samples were 50 wt.% of TNEF and 50 wt.% of NC matrix.

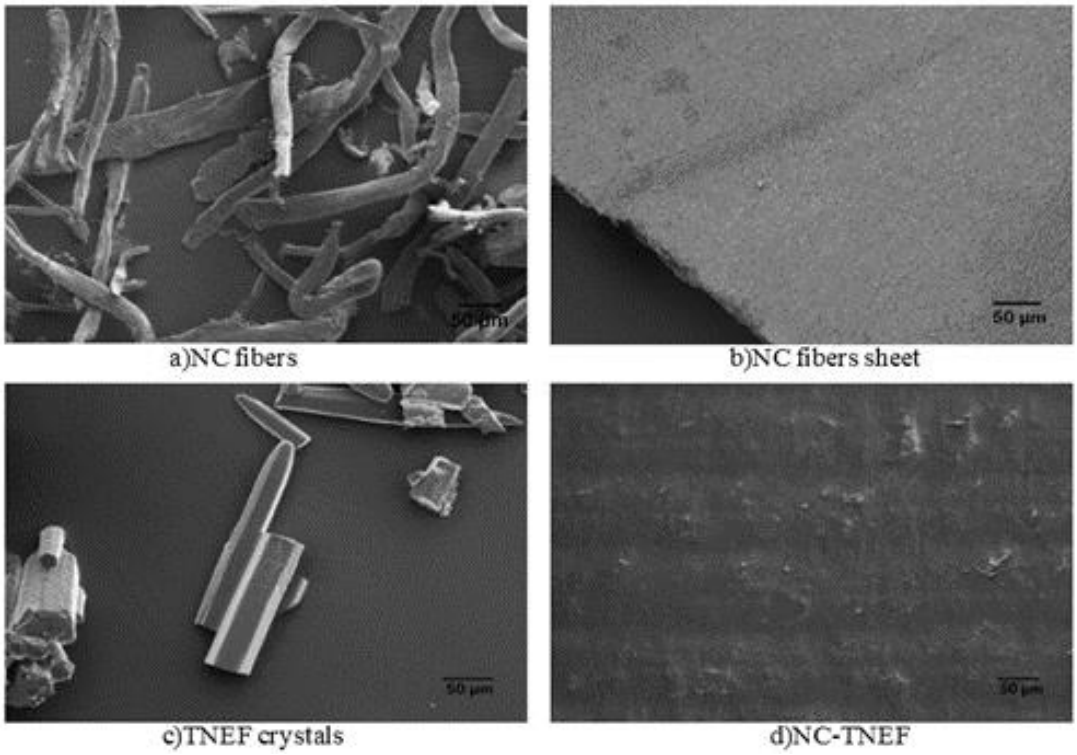

Figure 1. SEM of the oxidizer, NC and the new formulation (NC-TNEF).

Results

SEM results showed that the long fibers of NC were changed to the sheet form after recrystallization from acetone solution. The fibers were bonded together and were formed a homogeneous surface that took the shape of its mold after the casting process as shown in

Fig. 1b. Colorless hexagonal rods (60-200 µm length and 30 µm thickness) crystals of the TNEF were obtained from the preparation process (Fig. 1c). Fig. 1d shows a clear homogeneity of NC matrix with TNEF in the prepared propellant sample. The crystals of the oxidizer and the NC fibers are mixed together with a smooth colorless surface. This result may clarifies the homogeneous and smokeless burning process of the propellant recorded by high-speed camera as shown in Fig. 2.

Figure 2. Burning of the repared formulation.

TG/DTG thermograms of NC-TNEF under four different heating rates 2, 4, 8, and 16 K min^{-1} was presented in Fig. 3. The thermal decomposition of NC occurs in one sharp step, while the TNEF has a higher decomposition temperature than NC matrix (see supporting information). The TG/DTG thermogram of the NC-TNEF showed a controlled one-step thermal decomposition reaction with higher decomposition temperature than pure NC, which improves the thermal decomposition temperature of the new smokeless propellants compared to NC. The characteristic parameters of NC, TNEF and NC-TNEF are listed in Table 1 shows the effect of increasing the heating rate on the thermal behavior of the studied sample. Conventional Kissinger method was applied to calculate the kinetic parameters (see supporting information). The activation energies of NC, TNEF and NC-TNEF were 187.5, 198.4 and 190.7 kJ mol^{-1} respectively.

Table 1. Characteristic parameters of the TG/DTG of NC, TNEF and NC-TNEF

Material	β [a] (K.min^{-1})	TG curves			DTG peaks	
		T_{ot} [b] (°C)	T_i [d] (°C)	% mass loss [f]	T_p [e] (°C)	T_{oe} [c] (°C)
NC	2.0	179.74	183.19	99.74	187.57	198.81
	4.0	186.02	189.78	99.27	193.69	212.44
	8.0	193.75	196.85	99.53	199.76	220.54
	16.0	195.79	202.34	98.96	207.28	239.68
TNEF	2.0	168.66	180.37	99.62	196.87	203.46
	4.0	174.27	187.41	99.14	203.46	218.57
	8.0	181.11	194.16	98.53	209.78	231.28
	16.0	187.96	201.75	97.98	216.21	246.94
NC-TNEF	2.0	179.81	188.04	99.13	191.69	201.52
	4.0	192.29	195.63	98.75	198.27	214.68
	8.0	199.53	202.71	98.09	205.08	225.35
	16.0	204.01	208.32	97.36	211.21	241.87

[a] heating rate. [b] onset temperature of decomposition. [c] onset temperature of the end decomposition. [d] initial thermal decomposition temperature. [e] the peak temperature of mass loss rate. [f] from initial temperature to end temperature of DTG peak.

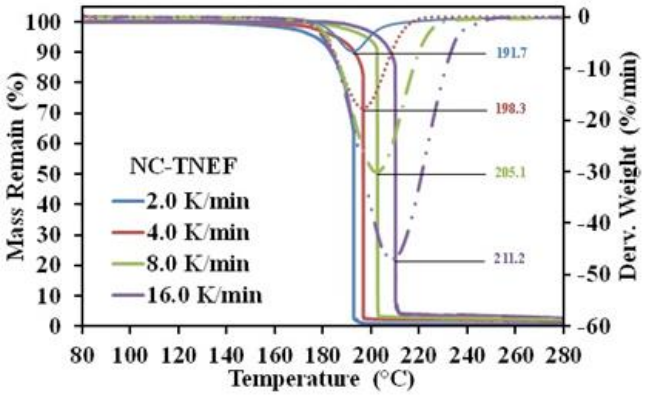

Figure 3. TG/DTG thermogram of the new formulation.

Also, Ozawa and Flynn–Wall (OFW) developed an isoconversional calculation method to calculate the activation energy (E_a) at each fraction conversion (α) using nonisothermal data [36]. The E_a of NC is varied from step to step of conversion with mean value of 182.2 kJ mol^{-1}, while TNEF showed a higher value of activation energy with mean value of 192.6 kJ mol^{-1}. Fig. 4 shows the activation energy at each step of conversion α for the studied samples.

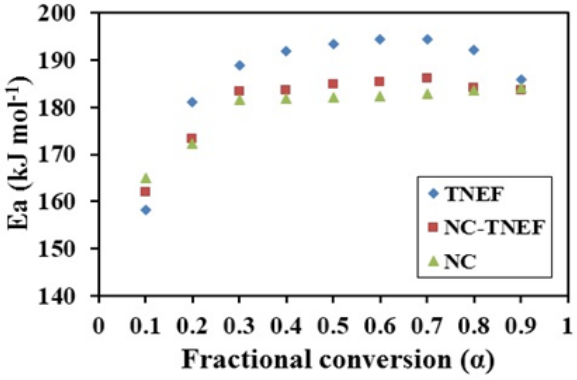

Figure 3. Activation energies at each α using OFW method.

DSC was used to determine the thermal behavior of the studied samples at 5 K min^{-1}. Fig. 5 shows one exothermic decomposition peak at 202.3 °C for the NC matrix. Otherwise, TNEF shows a small endothermic melting peak at 126.7 °C and an exothermic decomposed peak at 210.2 °C. Which are very close to the value of melting temperature (127.6 °C) that determined by Hill *et al* [22]. NC-TNEF showed only one exothermic peak at 204.6 °C. This result indicates that a new homogenous hydrogen-bonded complex of nitrocellulose and the oxidizer might be formed as a result of the dissolving of NC and the oxidizer in a selected solvent, followed by the evaporation of the solvent. Brodman et al stated that NC makes a chemical complex by mixing it with RDX or HMX [37], also a π complex intermediate was formed between diphenyl amine and NC due to the high free-radical intensity possessed by the propellant composition [38]. Sovizi et al [39] stated that the decomposition parameters might be affected by the particle size of NC and the maximum decomposition peak temperature of micro-NC at 5 °C min^{-1} was 201.8 °C, which is very close to our result at the same heating rate. The results of DSC proved that the thermal behavior of TNEF has been changed completely due to its mixing with NC, which proof the advantage of using TNEF as oxidizer with NC.

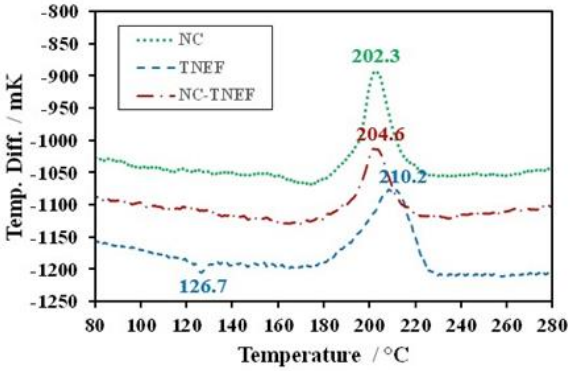

Figure 5. DSC thermogram of the studied samples at heating rate of 5 K min^{-1}.

The impact and friction sensitivities of TNEF have values of 5 J and 96 N respectively at 50% probability of initiation. These results proved that TNEF has low sensitivity compared with NG. Moreover, the specific impulse calculated by EXPLO5 V_6.03 of the prepared NC-TNEF is 257.4 s that is much higher than the traditional DBP based on NC and NG. These results proved that replacement of NG by TNEF leads to decrease the hazard of the DBP and increase the specific impulse.

Conclusions

2,2,2-trinitroethyl formate is an interesting HEDO that can be easily prepared as a powder, and easier to handle than the dangerous liquid NG. A new propellant formula based on TNEF with NC was prepared. The SEM photos proved a good homogeneous mixing of TNEF with NC. A smokeless homogenous burning process was recorded with a high-speed camera. The thermal study proved that the prepared propellant NC-TNEF has a maximum decomposition peak temperature at 204.6 °C, which is higher than that of NC. The results prove that a new composite might be formed during the mixing process. The kinetic study showed the activation energy of TNEF in the range of 193 to 198 ± 0.4 kJ mol^{-1}, while it was 185 to 191 ± 0.4 kJ mol^{-1} for NC-TNEF propellant. The new oxidizer TNEF has a much lower sensitivity than NG in addition to the high specific impulse of its propellant composition. These results confirm that TNEF could be used to replace the NG in the smokeless double base propellant and its performance should be studied experimentally.

References

[1] L.T. DeLuca, *Eurasian Chem.-Technol. J.,* **2016**, 18 (3), 181-196.

[2] G.P. Sutton, O. Biblarz, *"Rocket Propulsion Elements"*. Hoboken: John Wiley & Sons, **2017**.

[3] J.-F. Guery, I.-S. Chang, T. Shimada, M. Glick, D. Boury, E. Robert, J. Napior, R. Wardle, C. Pérut, M. Calabro, *Acta Astronaut.,* **2010**, 66 (1), 201-219.

[4] L.T. DeLuca, L. Galfetti, F. Maggi, G. Colombo, L. Merotto, M. Boiocchi, C. Paravan, A. Reina, P. Tadini, L. Fanton, *Acta Astronaut.,* **2013**, 92 (2), 150-162.

[5] R. Blockley, W. Shyy, *"Encyclopedia of Aerospace Engineering"*. Wiley Online Library, **2010**.

[6] L.T. DeLuca, T. Shimada, V.P. Sinditskii, M. Calabro, *"Chemical Rocket Propulsion: A Comprehensive Survey of Energetic Materials"*. Switzerland: Springer, **2017**.

[7] D. Trache, T.M. Klapötke, L. Maiz, M. Abd-Elghany, L.T. DeLuca, *Green Chem.*, **2017**, 19 (20), 4711-4736.

[8] L.T. DeLuca, in *"Chemical Rocket Propulsion"*. Switzerland: Springer, **2017**, pp. 1015-1032.

[9] H. Singh, in *"Chemical Rocket Propulsion"*. Switzerland: Springer, **2017**, pp. 127-138.

[10] H. AUSTRUY, in *"Solid Rocket Propulsion Technology"*. New York: Pergamon Press, **2012**, 369-412

[11] M. Sućeska, S.M. Mušanić, I.F. Houra, *Thermochim. Acta*, **2010**, 510 (1), 9-16.

[12] J. Agrawal, H. Singh, *Propellants Explos. Pyrotech.*, **1993**, 18 (2), 106-110.

[13] J. Agrawal, N. Agawane, R. Diwakar, R. Chandra, *Propellants Explos. Pyrotech.*, **1999**, 24 (6), 371-378.

[14] L.P. Arthur, **1975**, US3878003.

[15] N. Kubota, *"Propellants and Explosives: Thermochemical Aspects of Combustion"*. Weinheim, Germany: Wiley-VCH, **2015**.

[16] D.C. Sayles, **1990**, US4944816.

[17] X. Li, X. Liu, Y. Cheng, Y. Li, X. Mei, *J. Therm. Anal. Calorim.*, **2014**, 115 (1), 887-894.

[18] I.V. Kuchurov, M.N. Zharkov, L.L. Fershtat, N.N. Makhova, S.G. Zlotin, *ChemSusChem*, **2017**, 10, 3914-3946.

[19] Q. Zhang, J.M. Shreeve, *Chem. Rev.*, **2014**, 114 (20), 10527-10574.

[20] M.A. Epishina, I.V. Ovchinnikov, A.S. Kulikov, N.N. Makhova, V.A. Tartakovsky, *Mendeleev Commun.*, **2011**, 21 (1), 21-23.

[21] T.M. Klapötke, B. Krumm, R. Scharf, *Eur. J. Inorg. Chem.*, **2016**, 2016 (19), 3086-3093.

[22] M.E. Hill, **1967**, US3306939.

[23] A.B. Sheremetev, I.L. Yudin, *Mendeleev Commun.*, **2005**, 15 (5), 204-205.

[24] T.M. Klapötke, B. Krumm, R. Moll, S.F. Rest, *Z. Anorg. Allg. Chem.*, **2011**, 637, 2103-2110.

[25] M.L. Chan, A.D. Turner, **1991**, US5009728.

[26] N.N. Makhova, A.B. Sheremetev, I.V. Ovchinnikov, I.L. Yudin, A.S. Ermakov, P.V. Bulatov, D.B. Vinogradov, D.B. Lempert, G.B. Manelis, in 35th *Int. Annu. Conf. ICT*, Karlsruhe, Germany, **2004**, pp. 140/1-140/11.

[27] M. Abd-Elghany, T.M. Klapötke, A. Elbeih, *Propellants Explos. Pyrotech.,* **2017**, 42 (12), 1373-1381.

[28] Y.-H. Wang, L.-L. Liu, L.-Y. Xiao, Z.-X. Wang, *J. Therm. Anal. Calorim.,* **2014**, 119 (3), 1673-1678.

[29] Q.-L. Yan, S. Zeman, F.-Q. Zhao, A. Elbeih, *Thermochim. Acta,* **2013**, 556, 6-12.

[30] M. Abd-Elghany, A. Elbeih, S. Hassanein, *Cent. Eur. J. Energ. Mater.,* **2016**, 13 (3), 349-356.

[31] Q. Wang, L. Wang, X. Zhang, Z. Mi, *J. Hazard. Mater.,* **2009**, 172 (2), 1659-1664.

[32] Q.-L. Yan, S. Zeman, R. Svoboda, A. Elbeih, *Thermochim. Acta,* **2012**, 547, 150-160.

[33] M. Abd-Elghany, T.M. Klapötke, A. Elbeih, *J. Anal. Appl. Pyrolysis,* **2017**, 128, 397-404.

[34] Q.-L. Yan, S. Zeman, A. Elbeih, *Thermochim. Acta,* **2012**, 537, 1-12.

[35] M. Abd-Elghany, T.M. Klapötke, A. Elbeih, S. Zeman, *J. Anal. Appl. Pyrolysis,* **2017**, 126, 267-274.

[36] T. Ozawa, *Bull. Chem. Soc. Jpn.,* **1965**, 38, 1881-1886.

[37] B.W. Brodman, M.P. Devine, S. Schwartz, **1977**, US4033798.

[38] A. Chin, D.S. Ellison, S.K. Poehlein, M.K. Ahn, *Propellants Explos. Pyrotech.,* **2007**, 32 (2), 117-126.

[39] M.R. Sovizi, S.S. Hajimirsadeghi B. Naderizadeh, *J. Hazard. Mater.,* **2009**, 168 (2), 1134-1139.

Supporting Information

1. Chemicals

Nitrocellulose (13.15% N) was provided by Nitrochemie Aschau GmbH., Chloroform, anhydrous iron(III) chloride and diethyl ether, which were obtained from Sigma-Aldrich; 2,2,2-trinitroethanol (TNE) which was prepared in our laboratories (AK Klapötke).

2. Experimental Techniques

The NMR spectra of TNEF were recorded with a JEOL Eclipse 400 instrument, and the chemical shifts were determined with respect to the external standards Me4Si (1H, 399.8 MHz; 13C, 100.5 MHz) and MeNO2 (14N, 28.8 MHz).

The IR spectra were recorded by a Perkin–Elmer Spectrum FTIR spectrometer equipped with a Smiths DuraSamplIR II attenuated total reflectance (ATR) device. The spectra was obtained at ambient temperature.

Determination of sensitivities to different stimuli was studied; impact sensitivity (IS) was performed by BAM falling hammer test (T 316 SS) according to STANAG 4489 32. and the friction sensitivity (FS) was measured by a BAM friction tester (ODG 632 GmbH) according to STANAG 4487 33.

The thermal decomposition kinetics of the samples were studied using Thermogravimetric Analyzer (Perkin-Elmer, TGA 4000). The experimental conditions which were used are as following: (TG/DTG: 1–3 mg samples were examined at different heating rates of 2, 4, 8 and 16 K min^{-1} in the temperature range 30–600 °C under a flow of dynamic nitrogen of 20 ml min^{-1}). The melting and decomposition points were measured with LINSEIS DSC – PT10 with samples of approximately 3 mg placed in an aluminum pan with a pin-hole cover at a heating rate of 5 K min^{-1} in a temperature range of 25 to 400 °C.

EXPLO5 thermodynamic code version_6.03 has been used to determine the combustion characteristics of the new propellant, NC-TNEF. The combustion conditions are based on the ideal gas equation of state with under isobaric combustion with combustion chamber pressure of 70 atm. The specific impulse of the propellant was recorded.

3. TG/DTG Thermograms of NC and TNEF

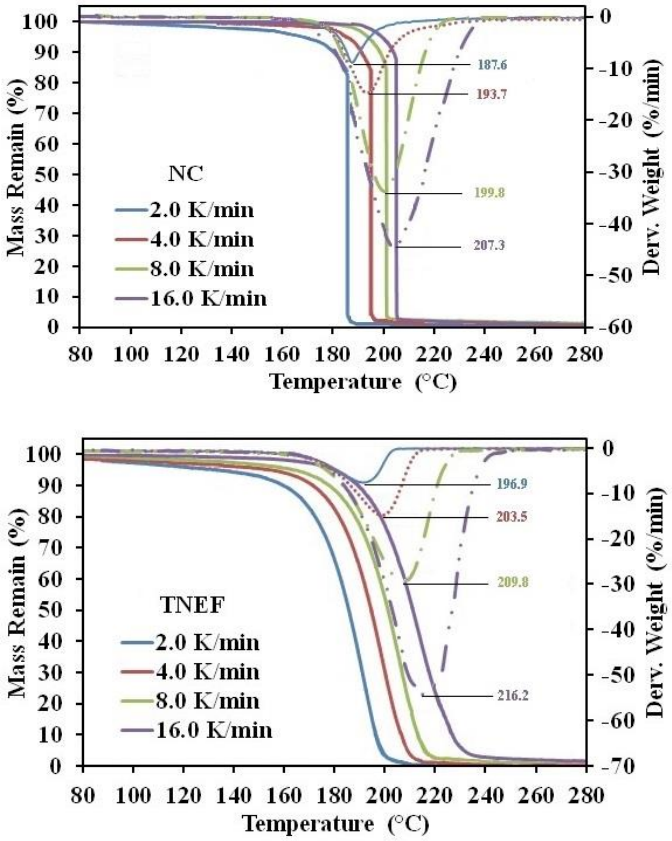

4. Kinetic Analysis

The kinetic triplets which are the activation energy (E_a), pre-exponential factor (A) and kinetic model ($f(\alpha)$) represent the kinetic analysis. For complete description of the kinetics, these three kinetic parameters should be determined for each reaction step. Nowadays, a large number of analytical methods that can be used to determine the kinetic parameters of distinct solid-phase reactions evaluation are available. The kinetic parameters can be determined either isothermally or nonisothermally by using two main methods which are: Isoconversional (model-free) and model-fitting methods.

Calculation of the Activation Energy:

The activation energy (E_a) of the exothermic decomposition reaction of the prepared propellants samples can be calculated by easy way using Kissinger's method.

$$-\frac{Ea}{R} = \frac{d\ln(\beta/T_P^2)}{d(1/T_P)}$$

Where β is the heating rate and T_p is the DTG peak temperature at that rate. By plotting of $\ln(\beta/T_p^2)$ versus $1/T_p$, the activation energy can be calculated from the slope of this straight line.

Ozawa and Flynn–Wall (OFW) used a nonisothermal data and developed an isoconversional calculation method (commonly referred to as the OFW method), in which taking the logarithm of the nonisothermal rate law and substituting using Doyle's approximation to give the following equation.

$$log\,\beta = log\frac{AE_a}{g(\alpha)R} - 2.315 - 0.457\frac{E_a}{RT}$$

Environmentally Safe (Chlorine-Free): New Green Propellant Formulation Based on 2,2,2trinitroethyl-formate and HTPB

Published in *RSC Advances*. **2018**, 8(21), 11771-11777 (DOI: 10.1039/c8ra01515e)

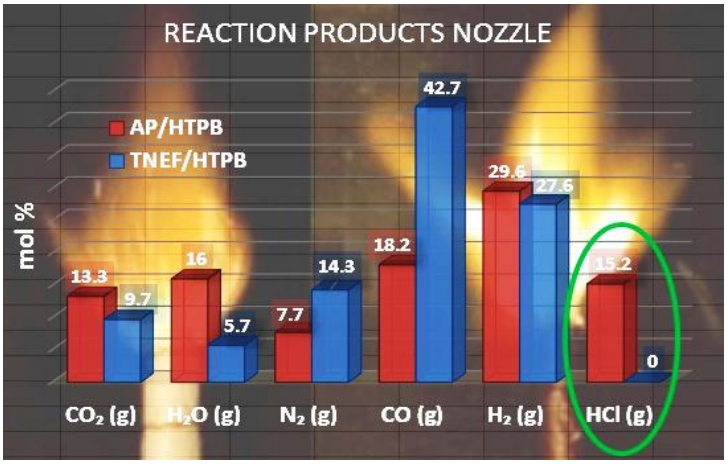

Abstract: A new green (chlorine-free) high energy dense oxidizer (HEDO) 2,2,2-trinitroethyl-formate (TNEF) and its propellant formulation based on the hydroxyl-terminated polybutadiene (HTPB) as a binder was prepared and studied. The new oxidizer TNEF was successfully prepared and characterized by nuclear magnetic resonance (NMR) and FTIR spectrometer. Scanning electron microscopy (SEM) was used to check the crystal morphology of the oxidizer. A high specific impulse (I_s = 250.1 s) was obtained from the characteristics calculation of the new oxidizer instead of (I_s = 156.9 s) for the commonly used ammonium perchlorate (AP) by using EXPLO5_V6.03 software. The burning behavior and the burning rate were determined by using a high speed camera. TNEF and the propellant formulations were studied by using nonisothermal thermogravimetric analysis (TGA) and the kinetic parameters of the studied samples were determined by using isoconversional (model-free) methods "Kissinger, Ozawa and Flynn–Wall (OFW) and Kissinger–Akahira–Sunose (KAS)". The results proved that the new oxidizer and its formulation based on HTPB have chlorine-free decomposition products and have higher performance characteristics than the traditional propellants.

Introduction

Due to the large merits of high compatibility, low viscosity and the superior mechanical properties, hydroxyl-terminated polybutadiene (HTPB) became one of the most commonly used polymeric binders in several fields specially in the field of composite solid rocket propellants [1]. For the simplicity, reliability and lower propulsion system cost of the solid propellants, they have immense range of applications in tactical rockets, submarine-based ballistic missiles, space launcher boosters and even amateur hobby rockets [2, 3]. These propellants are composed of a polymeric matrix that loaded with a solid powder oxidizer and possibly of a metal powder which plays the role of a secondary fuel component. Despite of its smoke combustion and toxic gaseous products, still ammonium perchlorate (AP) is the most widely used oxidizer for composite solid propellants [4-6].

Composite solid propellants that based on AP and HTPB are well known for their good performance characteristics and relatively low cost of manufacturing, but their limitations regarding toxicity and environmental impact are also well documented. Perchlorate contamination is becoming a more widespread concern in many countries all over the world [7-12]. At high concentrations, perchlorate can affect thyroid gland functions. Away from influencing the thyroid activity in humans, AP produce large amount of hydrochloric acid (HCl) during its combustion. Future propellants should not have such major hazards that cause diverse harmful to the crew or ground handling personnel. Green propellant formulations (chlorine-free) would highly reduce the risks of toxicity, operational handling complexity, spacecraft contamination, and environmental contamination hazardous.

Many researchers are working on solving the toxicity problems of AP without affecting the propellant performance [13]. To achieve this target, numerous researches have been studied based on adding some additives such as metals or nitramines (RDX, HMX, etc.) [14-18]. Several groups worldwide have intensively investigated other compounds to substitute AP to overcome its toxicity problems and to enhance the energetic characteristics, sensitivities and thermal properties [19-21]. These compounds are based on orthocarbonates, tetrazoles, carbamates, nitro-carbamates, formates, pyrazoles and triazoles [22-24]. Henry *et al* [25] has synthesized 2,2,2-Trinitroethanol (TNE), which is important and suitable starting material for a numerous compounds which have been synthesized during the recent studies [26]. 2,2,2-trinitroethyl-formate (TNEF) is a new interesting high energy dense oxidizer (HEDO) that has density of 1.81 g cm^{-3}, oxygen balance of (ΩCO_2) of 10.1 %, impact sensitivity of 5 J and friction sensitivity of 96 N [27].

TNEF is a chlorine-free HEDO, which might have high performance and has not been studied in any propellant formulation yet. Moreover, studying of the thermal behavior and kinetics of reaction for the new energetic materials are essential to find suitable new applicable applications [28-36]. In this paper, preparation and characterization of TNEF were presented. Propellant formulations based on HTPB as a binder and TNEF and AP as oxidizers have been prepared. EXPLO5 V_6.03 has been used to study the burning characteristics and decomposition products of the samples. The burning rate of the propellants was measured. The thermal behavior and decomposition kinetics of the individual HTPB and TNEF in addition to the two propellant formulations were studied using TGA technique. Different isoconversional methods for calculation were applied to determine the kinetic parameters of the HTPB, TNEF and the new propellant formulations.

Experimental

Hydroxyl-terminated polybutadiene (HTPB, R-45M of ARCO Co.) as a pre-polymer with a hydroxyl content of 0.84 meq g^{-1}, hexamethylene diisocyanate (HMDI) as a curing agent with an NCO equivalence value of 11.83 meq g^{-1}, chloroform, anhydrous iron (III) chloride and diethyl ether, which were obtained from Sigma-Aldrich; 2,2,2-trinitroethanol (TNE) which was prepared in our laboratories (AK Klapötke).

The synthesis of the air- and moisture-sensitive materials were done in an inert atmosphere of dry nitrogen using Schlenk techniques [37]. The chloroform was freshly distilled prior to use. 2,2,2-trinitroethanol (10 g, 56.0 mmol) was dissolved in dry chloroform (20 mL), anhydrous iron(III) chloride (0.8 g, 4.92 mmol) was added under careful exclusion of moisture. The mixture was heated under reflux at 85 °C for 5 days. After cooling, the content of reaction was poured into diethyl ether (100 mL). The ether solution was washed with cold water (3 x 100 mL) and dried over magnesium sulfate. After removing the solvent, a creamy coloured crude product was obtained, which was recrystallized from dichloromethane to yield 7.6 g (74% yield) of colorless crystals of 2,2,2-trinitroethyl-formate.

The preparation process is based on mixing of the oxidizer (TNEF, 80 wt. %) with the pre-polymer (HTPB) in a 200 mL vertical mixer for 40 minutes at 40 °C under vacuum to drive out entrapped air. Then, the curative (HMDI) was added at 55 °C. Mixing process remained for another 30 minutes. Finally, the prepared propellant samples were put in a specific mold and were cured in a vacuum oven at 60 ± 2 °C for seven days. The weight percentage of the binder system was 20 wt. %. The AP/HTPB formulation was prepared by the same method.

The NMR spectra were recorded for TNEF by a JEOL Eclipse 400 instrument, and the chemical shifts were determined with respect to the external standards Me_4Si (^1H, 399.8 MHz; ^{13}C, 100.5 MHz) and $MeNO_2$ (^{14}N, 28.8 MHz). Elemental analysis of C, H, N were performed with an Elementar Vario EL Analysis. The IR spectra were recorded at ambient temperature by a Perkin–Elmer Spectrum BX-FTIR spectrometer equipped with a Smiths DuraSamplIR II attenuated total reflectance (ATR) device. Determination of sensitivities to different stimuli was studied by BAM falling hammer test to determine the impact sensitivity (IS) according to STANAG 4489 [38] and BAM friction tester (ODG 632 GmbH) for the determination of the friction sensitivity (FS) according to STANAG 4487 [39]. EXPLO5 thermodynamic code version_6.03 has been used to determine the combustion characteristics of the propellant samples. The combustion conditions are based on the ideal gas equation of state with 70 atm combustion chamber pressure and under isobaric combustion. The specific impulse of the propellant samples were recorded. The burning rate of the studied propellants was measured by using a high-speed camera [40]. Model (visario g2 1500) with frame measurements (1.000 fps). The propellant samples were prepared in the form of cylinders with dimension of 100 mm length and 8 mm diameter and the burning rate was measured at atmospheric pressure (0.1 MPa). Each sample was measured triple times and the mean value was recorded (with max. error 2.8%). Thermogravimetric Analysis (Perkin-Elmer, TGA 4000) was used to study the thermal decomposition kinetics of the samples under the following experimental conditions: (TG/DTG: 1–3 mg samples were examined at different heating rates of 1, 3, 5 and 7 K min^{-1} in the temperature range 30–500 °C under nitrogen flow of 20 ml min^{-1}).

Results

The characteristics calculations of TNEF as a new green high-energy dense oxidizer and TNEF/HTPB propellants formulation that have been tested by using EXPLO5 V_6.03 thermodynamic code showed interesting results comparing with that of AP and AP/HTPB. Fig. 1 shows the calculated mole percentage of reaction gaseous products at the nozzle exit for the most common AP/HTPB propellant formulation and the new green TNEF/HTPB propellant formulation. It is clear that AP/HTPB produce more than 15% toxic hydrochloric acid ($HCl_{(g)}$) during the burning process. On the other hand, the new green propellant formulation TNEF/HTPB has no $HCl_{(g)}$ in the burning gaseous products. In addition, TNEF has specific impulse (I_s = 250.1 s) and characteristic exhaust velocity (C^* = 1408 m s^{-1}) which

are higher than that of AP (I_s = 156.9 s) and (C^* = 947 m s^{-1}). Moreover the new green propellant formulation TNEF/HTPB has also higher values of specific impulse (I_s = 231.5 s) and characteristic exhaust velocity (C^* = 1425 m s^{-1}) than the values of AP/HTPB (I_s = 228.2 s) and (C^* = 1404 m s^{-1}) respectively.

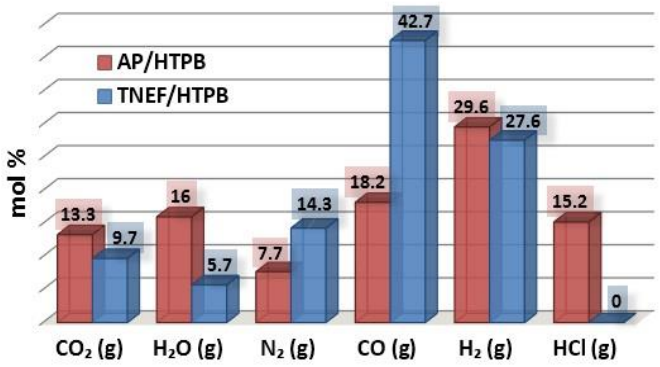

Figure 1. Reaction gaseous products at nozzle exit.

TNEF was prepared as discussed in the experimental part, with a yield of 74%. The obtained crystals were colorless and SEM was used to study its crystal morphology. Hexagonal rods crystals with sharp edges were observed having approximate dimension of 70-200 µm length and 30 µm thickness as shown in Fig. 2. The crystals have smooth surface without cracks, while the sharp edges might affect the sensitivity characteristics of TNEF. The impact sensitivity was measured and found to be 5.4 J (50% probability of initiation) which is slightly higher than the traditional explosive RDX, while the friction sensitivity was 106 N.

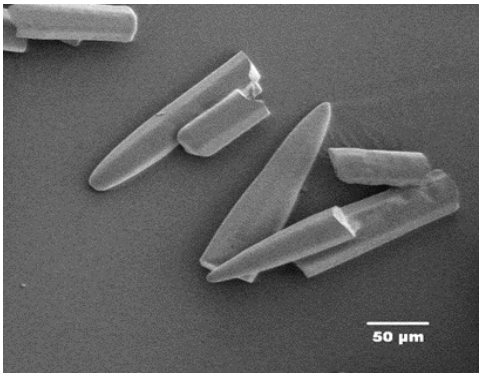

Figure 2. SEM of 2,2,2-trinitroethyl-formate.

Results of the elemental analysis of TNEF in addition to the NMR spectroscopy and IR spectra are presented in the supplementary information (ESI). According to the combustion theory [41], the decomposed gases diffusion process of the AP particles and the surrounding

HTPB at burning surface controls the combustion mode of AP/HTPB composite propellants [42-45]. The decomposed gases from the decomposition process of the AP particles and the HTPB binder react to produce heat on and above the burning surface. The HTPB binder as a fuel and the AP particles as an oxidizer diffuse and mix above the burning surface to form diffusional premixed flame (Diffusion zone) and produce final combustion products such as CO_2, H_2O, N_2, CO, H_2 and HCl. The conductive heat feedback from the burning surface increase the temperature in the condensed phase from the initial propellant temperature (T_0) to the burning surface temperature (T_s). Then, increasing of the temperature occurs in the gas phase due to the exothermic reaction over the burning surface and reaches the final combustion temperature (T_g) (see Fig. 3).

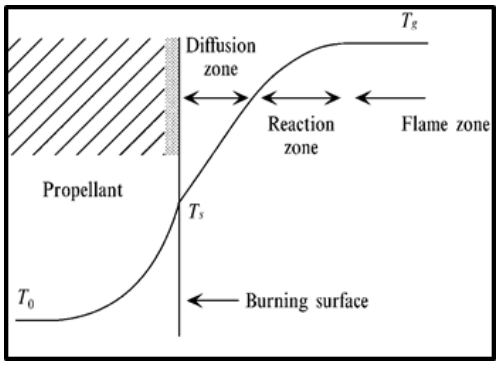

Figure 3. Combustion wave structure of an AP composite propellant [41].

The burning of the prepared samples (TNEF/HTPB and AP/HTPB) showed a uniform cigarette burning as shown in Fig.4. The combustion process of the studied samples are controlled by the diffusion process of the decomposed gases of the oxidizer particles and the surrounding binder at the burning surface of the propellant. This zone (diffusion zone) is just above the burning surface and it seems to be dark where a series of degradation reactions occurs rapidly. It is clear that the diffusion zones of the two propellant formulations have almost the same thickness, which indicate that the new oxidizer (TNEF) is also diffuse in the HTPB matrix during the first burning stage of the new propellant formula. The decomposed gases reacted (oxidation reaction occurred) and produced heat above the burning surface. This zone is the reaction zone where a highly illuminated zone appeared as shown in Fig. 4.

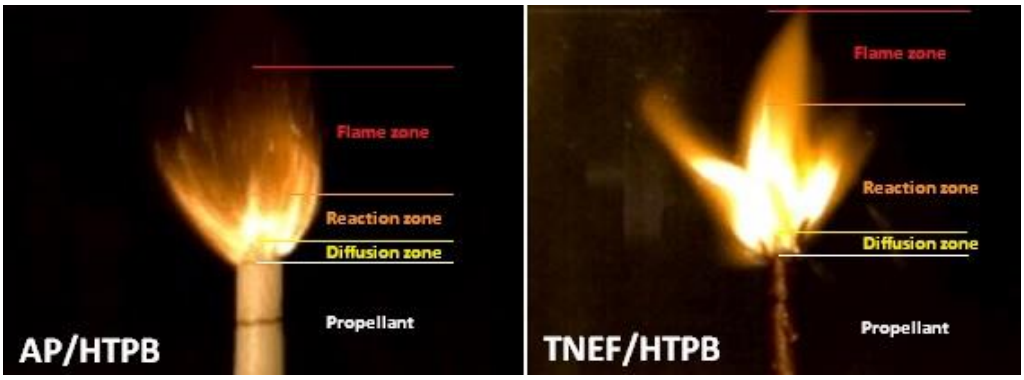

Figure 4. Burning behavior of the propellant samples.

The thickness of the reaction zone of the new propellant formula is more than twice that of the traditional propellant formula and the intensity of brightness is higher. It means that the reaction between the fuel HTPB and the oxidizer TNEF is vigorous reaction. This may clarify the higher performance characteristics of the new propellant formulation than that of the traditional one. The final combustion products are formed above the reaction zone where thermal equilibrium of the combustion products happened, and this zone is known by the flame zone. The thickness of the flame zone of AP/HTPB propellant is more than that of the TNEF/HTPB. This result might be due to the high amount of gaseous products produced over the reaction zone during the combustion of AP/HTPB compared with that of TNEF/HTPB propellant in addition to the presence of $HCl_{(g)}$ as a main gaseous product in case of the AP/HTPB burning which increase the flame zone with smoke of $HCL_{(g)}$.

The burning rate of TNEF/HTPB and AP/HTPB was measured by using high-speed camera as discussed in the experimental part. It was found that the burning rate of AP/HTPB propellant is 2.70 mm s^{-1}, while the burning rate of the new propellant formulation TNEF/HTPB is 2.86 mm s^{-1}. These results proved that TNEF/HTPB is a promising propellant formulation, which has higher burning rate than the traditional propellant AP/HTPB and the calculated burning characteristics are also higher. As a result, the decomposition kinetics of the two formulations was studied using thermal analysis technique. TG curves of TNEF, HTPB, TNEF/HTPB and AP/HTPB under four different heating rates 1, 3, 5, and 7 K min^{-1} were presented in Fig. 5. It is shown that a single decomposition step has been observed for TNEF that starts at 188.8 °C (onset temperature) and ends at 217.8 °C (onset temperature at the end of decomposition peak) in case of 5 K min^{-1} heating rate.

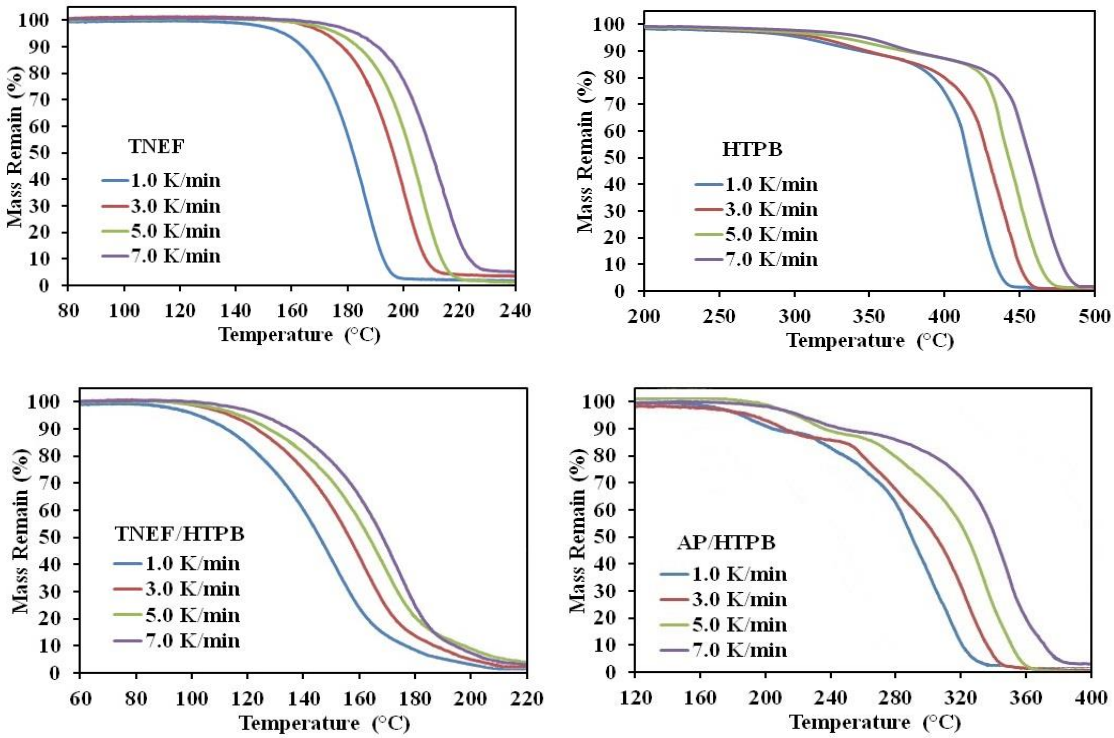

Figure 5. TGA thermograms of the studied samples.

HTPB decomposes on two stages starts at 330.0 °C for the first stage with mass loss ratio of 15% and at 441.3 °C for the second decomposition stage with final mass loss of about 97%, which means that HTPB can almost decompose to gaseous products completely. The new green propellants formulation showed a controlled homogenous one thermal decomposition step starts at 169.5 °C in case of 5 K min^{-1} heating rate, which can be the slow decomposition of TNEF that release large amount of heat, which leads to accelerate the thermal decomposition process of HTPB.

In addition, produce few gaseous products that cannot be released quickly. The reaction between these entrapped gaseous products release large amount of heat, which leads to accelerate the thermal decomposition process. TG thermogram of the AP/HTPB propellants showed two thermal decomposition stages that starts at 194.1 °C for the first stage. In the second stage, many kinds of oxidizing gases are generated and the thermal decomposition process accelerates due to release of large amount of heat. The characteristic parameters of the TG curves and DTG peaks of the studied samples are listed in Table 1, which shows that the onset decomposition temperature and the initial mass loss temperature of the samples increased with increasing the heating rates. It is also obvious that the thermal decomposition reaction process of the common propellant formula that based on AP is more complicated

than that of the new propellant formula, which is based on the new green high-energy dense oxidizer. It is clear that the decomposition temperature of the new propellant is lower than the traditional propellant (AP/HTPB) at each studied heating rate.

Table 1. TG/DTG data of the TNEF, HTPB, TNEF/HTPB and AP/HTPB

Material	β [K.min^{-1}]	TG curves		DTG peaks	
		T_o [°C]	Mass Loss [%]	T_p [°C]	T_e [°C]
TNEF	1.0	169.0	98.79	186.6	196.1
	3.0	184.5	97.67	200.3	211.8
	5.0	188.8	99.54	206.2	217.8
	7.0	192.1	97.06	209.6	221.0
HTPB	1.0(1st)	301.2	14.81	322.5	357.8
	1.0(2nd)	417.5	84.29	423.6	437.6
	3.0(1st)	319.3	15.22	342.1	379.4
	3.0(2nd)	432.7	84.07	442.9	465.6
	5.0(1st)	338.4	13.89	353.4	392.2
	5.0(2nd)	436.5	84.83	455.2	477.9
	7.0(1st)	346.2	14.56	361.3	408.6
	7.0(2nd)	442.0	84.08	461.6	485.7
TNEF/HTPB	1.0	139.8	99.13	163.7	171.2
	3.0	160.9	98.65	175.4	184.5
	5.0	169.5	96.09	182.9	192.3
	7.0	176.0	97.36	188.3	196.8
AP/HTPB	1.0(1st)	168.0	11.82	189.9	193.6
	1.0(2nd)	289.6	85.81	298.0	323.9
	3.0(1st)	185.7	14.06	211.8	230.5
	3.0(2nd)	303.4	84.59	322.9	344.8
	5.0(1st)	194.1	12.68	228.2	235.7
	5.0(2nd)	309.7	86.52	335.1	361.4
	7.0(1st)	208.3	11.13	237.0	245.2
	7.0(2nd)	317.1	85.29	349.8	366.8

Note: T_o: onset decomposition temperature; T_e: onset temperature of the end decomposition; T_p: the peak temperature of mass loss rate; Mass Loss: from initial temperature to end temperature of DTG peak, (1st) first decomposition peak, (2nd) second decomposition peak.

The thermal decomposition reaction kinetics of all the studied samples are discussed using the conventional Kissinger method, which is based on the shift of decomposition peak temperature by changing the heating rate. The activation energies for the samples were calculated from the slope of the straight line by plotting $\ln(\beta/T^2)$ versus 1/T for the four selected heating rates by applying Kissinger equation (see ESI). The activation energy of the new oxidizer TNEF was found to be 146.4 kJ mol^{-1}, while for the TNEF/HTPB was 125.6 kJ mol^{-1}. The traditional propellants sample AP/HTPB had two activation energies 72.1 kJ mol^{-1} and 103.9 kJ mol^{-1} for the first and second steps of reaction respectively, which were lower than that of the new green propellant formula. Although the simplicity of this method, but it has a disadvantage, which is the inability to determine the reaction steps or discuss the distinct activation energy for each fraction conversion (α).

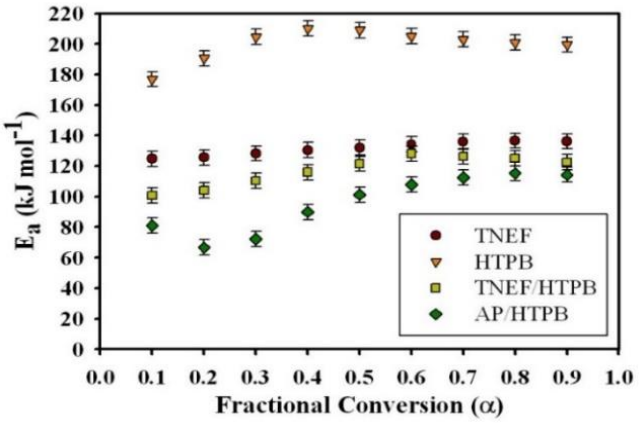

Figure 6. Activation energies at each conversion step (α) using OFW method.

Table 2. Kinetic data of TNEF, HTPB, TNEF/HTPB and AP/HTPB obtained using the modified KAS method

α reacted	TNEF			HTPB			TNEF/HTPB			AP/HTPB		
	E_a	logA	r	E_a	logA	r	E_a	logA	r	E_a	logA	r
0.1	123.8	12.08	0.9993	176.2	10.86	0.9933	99.3	10.35	0.9893	76.8	5.09	0.9694
0.2	124.7	11.98	0.9989	189.1	11.68	0.9991	102.6	10.33	0.9944	61.3	3.18	0.9744
0.3	127.3	12.15	0.9991	203.1	12.57	0.9954	109.0	10.82	0.9958	66.9	3.53	0.9802
0.4	129.6	12.31	0.9986	209.4	12.96	0.9985	114.8	11.28	0.9968	85.3	5.13	0.9781
0.5	131.6	12.45	0.9994	208.6	12.83	0.9992	120.8	11.78	0.9972	97.1	6.10	0.9874
0.6	133.6	12.60	0.9988	204.2	12.43	0.9987	127.3	12.30	0.9976	103.9	6.61	0.9865
0.7	135.4	12.72	0.9989	202.0	12.19	0.9993	125.2	12.01	0.9987	108.7	6.95	0.9909
0.8	136.0	12.71	0.9991	199.5	11.93	0.9989	123.4	11.67	0.9977	111.4	7.09	0.9934
0.9	135.5	12.55	0.9984	197.9	11.69	0.9981	119.6	11.43	0.9985	110.4	6.85	0.9952
Mean	131.5	12.45		205.5	12.60		119.4	11.64		92.4	5.66	

Ozawa and Flynn–Wall developed an isoconversional calculation method which is commonly known as the OFW method to calculate the activation energy E_a through a plot of log β versus 1/T at each α regardless of the employed model using nonisothermal data (see ESI) [46]. It was found that the activation energy of TNEF is varied from step to step of conversion with mean value of 132.1 kJ mol^{-1}. The new green propellant formula TNEF/HTPB showed a higher value of activation energy than that of the traditional AP/HTPB propellant with mean value of 120.4 kJ mol^{-1}. Fig. 6 shows the activation energy at each step of conversion α for TNEF, HTPB, TNEF/HTPB and AP/HTPB. The activation energy of the first stage thermal decomposition of AP/HTPB was 73.9 kJ mol^{-1}, while for the second stage was 96.7 kJ mol^{-1}. The activation energies of the fuel binder, HTPB, are higher than all the studied samples while its propellant based on the new oxidizer, TNEF, has the same behavior as the pure TNEF. The activation energies of the new propellant are higher than that of the traditional propellant (AP/HTPB). In order to confirm these results, another method named Kissinger–Akahira–Sunose (KAS) was also used to determine the activation energy at each degree of conversion using isoconversional method. Table 2 presents the kinetic data values of the studied samples using KAS method of calculation. By comparing the values using OFW method with those obtained by using the modified KAS method, a good agreement was detected. The activation energy of TNEF obtained by KAS equation (see ESI) was found to be 131.5 kJ mol^{-1}. The new propellant formula has a mean value of activation energy equal 119.4 kJ mol^{-1}, which is higher than that of the traditional propellants formula AP/HTPB (92.4 kJ mol^{-1}). As commonly suggested in literatures, the mean values of activation energy using OFW and KAS methods were calculated in the interval of (α = 0.3–0.7) due to the large influence of the experimental conditions specially in case of TG/DTG on the data quality of the process “tails” [47-50].

Conclusions

2,2,2-trinitroethyl-formate (TNEF) is a new interesting (chlorine-free) green high-energy dense oxidizer (HEDO), which can be easily prepared from 2,2,2-Trinitroethanol (TNE). The burning characteristics calculated for the new green propellant formula based on TNEF with HTPB was higher than that of traditional propellant based on AP/HTPB. The TNEF/HTPB propellant does not produce any toxic $HCl_{(g)}$ in the burning process that makes it environmentally safe comparing with the traditional propellant formula AP/HTPB which produce about 15% $HCl_{(g)}$ (mol%). The measured burning rate of TNEF/HTPB (2.86 mm s^{-}

^{1}) was higher than AP/HTPB (2.70 mm s^{-1}). A uniform cigarette burning was observed for both of the studied propellant samples with nearly the same diffusion zone and higher intensity of brightness in case of TNEF/HTPB which is compatible with the calculated results. The kinetic study by the different three methods showed activation energy of TNEF in the range of 131-146 ± 0.5 kJ mol^{-1}, while the activation energy of TNEF/HTPB propellant is in the range of 119-126 ± 0.4 kJ mol^{-1}, which is higher than that of AP/HTPB (88-97 ± 0.3 kJ mol^{-1}). The new TNEF/HTPB formulation is an interesting propellant composition which might be candidate to replace the toxic traditional composite solid rocket propellant AP/HTPB.

References

[1] K.K. Kuo, M. Summerfield, *"Fundamentals of Solid-Propellant Combustion"*. New York: American Institute of Aeronautics and Astronautics, **1984**.

[2] L.T. DeLuca, in *"Chemical Rocket Propulsion"*. Switzerland: Springer, **2017**, pp. 1015-1032.

[3] H. Singh, in *"Chemical Rocket Propulsion"*. Switzerland: Springer, **2017**, pp. 127-138.

[4] E. Price, S. Chakravarthy, J. SAMBAMURTHl, R. Sigman, *Combust. Sci. Technol.*, **1998**, 138, 63-83.

[5] M.R. Sovizi, G. Fakhrpour, A.R. Madram, *J. Therm. Anal. Calorim.*, **2017**, 129 (1), 401-410.

[6] M. Rodríguez-Pesina, J. García-Domínguez, F. García-Hernández, L.M. Flores-Vélez, O. Domínguez, *Mater. Sci. Appl.*, **2017**, 8 (6), 436-447.

[7] B. Gu, J.D. Coates, *"Perchlorate: Environmental Occurrence, Interactions and Treatment"*. Boston: Springer Science & Business Media, **2006**.

[8] B.C. Blount, L. Valentin-Blasini, J.D. Osterloh, J.P. Mauldin, J.L. Pirkle, *J. Exposure Sci. Environ. Epidemiol.*, **2007**, 17 (4), 400-407.

[9] C. Vigreux-Besret, A. Mahé, G. Ledoux, A. Garnier, C. Rosin, A. Baert, M. Joyeux, P.-M. Badot, P. Panetier, G. Rivière, *Food Addit. Contam.: Part A*, **2015**, 32 (7), 1148-1155.

[10] M. Sijimol, M. Mohan, D. Dineep, *Energ. Ecol. Environ.*, **2016**, 1 (3), 148-156.

[11] M.V. Maffini, L. Trasande, T.G. Neltner, *Curr. Environ. Health Rep.*, **2016**, 3 (2), 107-117.

[12] B. Chanbasha, H. Nsubuga, **2017**, US9664645.

[13] D. Trache, T.M. Klapötke, L. Maiz, M. Abd-Elghany, L.T. DeLuca, *Green Chem.*, **2017**, 19 (20), 4711-4736.

[14] M. Celina, L. Minier, R. Assink, *Thermochim. Acta*, **2002**, 384 (1), 343-349.

[15] Z. Ma, F. Li, H. Bai, *Propellants Explos. Pyrotech.*, **2006**, 31 (6), 447-451.

[16] R. Dubey, P. Srivastava, I. Kapoor, G. Singh, *Thermochim. Acta*, **2012**, 549, 102-109.

[17] J.A. Styborski, M.J. Scorza, M.N. Smith, M.A. Oehlschlaeger, *Propellants Explos. Pyrotech.*, **2015**, 40 (2), 253-259.

[18] T. Kuwahara, *Propellants Explos. Pyrotech.*, **2015**, 40 (5), 765-771.

[19] M. Göbel, T.M. Klapötke, *Adv. Funct. Mater.*, **2009**, 19 (3), 347-365.

[20] T.M. Klapötke, *"Chemistry of High-Energy Materials"*. Germany: Walter de Gruyter GmbH & Co KG, **2017**.

[21] M.A. Kettner, T.M. Klapötke, in *"Chemical Rocket Propulsion"*. Switzerland: Springer, **2017**, pp. 63-88.

[22] P. Yin, J. Zhang, C. He, D.A. Parrish, M.S. Jean'ne, *J. Mater. Chem. A*, **2014**, 2 (9), 3200-3208.

[23] M.A. Kettner, T.M. Klapötke, *Chem. - Eur. J.*, **2015**, 21 (9), 3755-3765.

[24] M.H. Keshavarz, Y.H. Abadi, K. Esmaeilpour, S. Damiri, M. Oftadeh, *Propellants Explos. Pyrotech.*, **2017**, 42 (5), 492-498.

[25] M.A. Epishina, I.V. Ovchinnikov, A.S. Kulikov, N.N. Makhova, V.A. Tartakovsky, *Mendeleev Commun.*, **2011**, 21 (1), 21-23.

[26] T.M. Klapötke, B. Krumm, R. Scharf, *Eur. J. Inorg. Chem.*, **2016**, 2016 (19), 3086-3093.

[27] T.M. Klapötke, B. Krumm, R. Moll, S.F. Rest, *Z. Anorg. Allg. Chem.*, **2011**, 637, 2103-2110.

[28] M. Abd-Elghany, T.M. Klapötke, A. Elbeih, *Propellants Explos. Pyrotech.*, **2017**, 42 (12), 1373-1381.

[29] Y.-H. Wang, L.-L. Liu, L.-Y. Xiao, Z.-X. Wang, *J. Therm. Anal. Calorim.*, **2014**, 119 (3), 1673-1678.

[30] Q.-L. Yan, S. Zeman, F.-Q. Zhao, A. Elbeih, *Thermochim. Acta*, **2013**, 556, 6-12.

[31] M. Abd-Elghany, A. Elbeih, S. Hassanein, *Cent. Eur. J. Energ. Mater.*, **2016**, 13 (3), 349-356.

[32] Q. Wang, L. Wang, X. Zhang, Z. Mi, *J. Hazard. Mater.*, **2009**, 172 (2), 1659-1664.

[33] Q.-L. Yan, S. Zeman, R. Svoboda, A. Elbeih, *Thermochim. Acta*, **2012**, 547, 150-160.

[34] M. Abd-Elghany, T.M. Klapötke, A. Elbeih, *J. Anal. Appl. Pyrolysis*, **2017**, 128, 397-404.

[35] Q.-L. Yan, S. Zeman, A. Elbeih, *Thermochim. Acta*, **2012**, 537, 1-12.

[36] A. Elbeih, S. Zeman, J. Pachman, *Cent. Eur. J. Energ. Mater.*, **2013**, 10(3), 339-349.

[37] D.F. Shriver, M.A. Drezdzon, *"The Manipulation of Air-Sensitive Compounds"*. New York: John Wiley & Sons, **1986**.

[38] S.A. NATO, *Impact Sensitivity Tests*, **1999**, STANAG 4489.

[39] S.A. NATO, *Explosives, Friction Sensitivity Tests*, **2002**, STANAG 4487.

[40] L. Zhang, R. Tian, Z. Zhang, *Aerosp. Sci. Technol.*, **2017**, 62, 31-35.

[41] N. Kubota, *"Propellants and Explosives: Thermochemical Aspects of Combustion"*. Weinheim, Germany: WILEY-VCH, **2002**.

[42] K.N. Ramohalli, in *"Fundamentals of Solid-Propellant Combustion"*. New York: American Institute of Astronautics and Aeronautics, **1984**, pp. 409-477.

[43] G. Lengelle, J. Duterque, J. Trubert, in *"Solid Propellant Chemistry, Combustion, And Motor Interior Ballistics"*,. Portland, USA: American Institute of Astronautics and Aeronautics, **2000**, pp. 287-334.

[44] M.W. Beckstead, R. Derr, C. Price, *AIAA J.*, **1970**, 8 (12), 2200-2207.

[45] T. Kuwahara, N. Kubota, *Combust. Sci. Technol.*, **1986**, 47, 81-91.

[46] T. Ozawa, *Bull. Chem. Soc. Jpn.*, **1965**, 38, 1881-1886.

[47] A. Elbeih, M. Abd-Elghany, T.M. Klapötke, *Propellants Explos. Pyrotech.*, **2017**, 42 (5), 468-476.

[48] Q.-L. Yan, S. Zeman, A. Elbeih, A. Zbynek, *Cent. Eur. J. Energ. Mater.*, **2013**, 10 (4), 509-528.

[49] M. Abd-Elghany, T.M. Klapötke, A. Elbeih, S. Zeman, *J. Anal. Appl. Pyrolysis*, **2017**, 126, 267-274.

[50] Q.-L. Yan, S. Zeman, T.-L. Zang, A. Elbeih, *Thermochim. Acta*, **2013**, 574, 10-18.

Thermo-analytical Study of 2,2,2-trinitroethyl-formate As a New Oxidizer and its Propellant Based on a GAP Matrix in Comparison with Ammonium Dinitramide

Published in *J. Anal Appl. Pyrol.* **2018**, 133, 30-38 (DOI: 10.1016/j.jaap.2018.05.004)

Abstract: A new high energy dense oxidizer (HEDO) 2,2,2-trinitroethyl-formate (TNEF) was prepared and characterized by nuclear magnetic resonance (NMR). A new propellant based on glycidyl azide polymer (GAP) and TNEF was prepared. Thermo-analytical study of TNEF in comparison with ammonium dinitramide (ADN) and their propellant formulations based on GAP were investigated. The decomposition gaseous products and the combustion characteristics of the propellants were determined by using thermodynamic code (EXPLO5_V6.03). Scanning electron microscope (SEM) technique was applied to clarify the crystal morphology of the oxidizers in addition to the homogeneity of the propellants ingredients. Impact and friction sensitivities of the oxidizers and the GAP binder were measured. Differential scanning calorimetry (DSC) and thermogravimetric analysis (TGA) techniques were used to study the pyrolysis of the oxidizers as well as the prepared propellants. The decomposition kinetics were determined by Kissinger and Kissinger–Akahira–Sunose (KAS) methods The thermal degradation of ADN is faster than TNEF oxidizer. ADN and TNEF have melting temperatures at 95.5 °C and 127.1 °C and maximum decomposition temperature at 183.5 °C and 210.1 °C respectively. In addition, TNEF has activation energy in the range of 131–146 kJ mol^{-1}, while ADN has activation energy in the range of 114–117 kJ mol^{-1}. TNEF has specific impulse (250.1 s) higher than ADN (202.4 s). TNEF is a promising oxidizer to be used in composite solid rocket propellants.

Introduction

Solid rocket propellants (SRP) have a wide range of applications in space launcher boosters, airplane ejection seats, tactical rockets and even amateur hobby rockets [1]. Due to the simplicity, reliability and low cost of propulsion system of the SRP, they are preferred over liquid and hybrid propellants [2, 3]. Composite solid rocket propellants (CSRP) are composed of an oxidizer embedded in a polymeric matrix where a metal powder might be included as a secondary fuel to increase the specific impulse. One of the most usable

propellant formulation for more than 60 years contains hydroxyl-terminated polybutadiene (HTPB) as polymeric matrix, ammonium perchlorate (AP) as oxidizer and aluminum (Al) as metal powder [2, 4-6]. In 1972, a new trend of energetic binders such as 3,3-Bis(azidomethyl)oxetane (BAMO), poly 3-nitratomethyl-3-methyl oxetane (poly NIMMO) and glycidyl azide polymer (GAP) was appeared, which enhanced the properties of composite rocket propellant to a great extent [7]. On the other hand, many scientists and researchers are working to develop new oxidizers for replacing AP because of its toxicity. AP-based propellants produce large amount of hydrochloric acid ($HCl_{(g)}$) as a gaseous product during its burning that contaminate the atmosphere. In addition, Urbansky *et al.* stated that the drinking water obtained from southwestern USA might include perchlorate anion (ClO_4^-), which cause a problem in some regions of the United States [8]. Also, the formation of aluminum oxide (Al_2O_3) from the combustion of CSRP is a source of toxicity to humans, animals and plants [9, 10]. Synthesis of new compounds is one of the priorities for the scientists all over the world [11, 12] in addition to testing of new formulations [13-15] to overcome the toxicity of the traditional SRP and to fulfill the requirements of CSRP that impart high performance, thermal stability and environmentally safe during the manufacture process. Many CSRP formulations based on GAP as energetic binder and different high energy materials as oxidizers have been studied during last year's [16-20]. ADN is one of the most promising green oxidizer to be used in SRP with GAP (which has high performance characteristics and good thermal stability) [21-28]. 2,2,2-trinitroethyl-formate (TNEF) is a new interesting high-energy dense oxidizer (HEDO) that has been prepared by Klapötke's group [29]. It has high performance parameters and good thermal stability. Actually, there is no information about the application of TNEF neither as a plastic bonded explosive nor as a composite solid rocket propellant [30-33]. In addition, the thermal behavior and reaction kinetics of the new oxidizer (TNEF) have not been studied yet. As a result, TNEF were prepared and characterized. In addition, a new CSRP formulations based on TNEF/GAP was prepared and the thermal decomposition kinetics of both TNEF and its propellant formulation were studied. ADN and the traditional propellant based on ADN/GAP were studied for comparison.

Experimental

Glycidyl azide polymer (GAP diol L-996, 3M, St. Paul, MN. (Molecular weight (Mn): 2900 g/mol). Hexamethylene diisocyanate (HMDI) as a curing agent with an NCO equivalence

value of 11.83 meq g^{-1}, 1,1,1-Tris(hydroxymethyl)propane as a crosslinking agent, Dibutyltin dilaurate as a catalyst, Chloroform and Anhydrous iron(III) chloride were obtained from Sigma-Aldrich. Ammonium dinitramide (ADN) and 2,2,2-trinitroethanol were prepared in our laboratories. ADN was prepared by nitration of potassium sulfamate according to the method discussed in ref [34]. 2,2,2-trinitroethanol (12.5 g, 70.0 mmol) was dissolved in dry chloroform (25 mL), anhydrous iron (III) chloride (1.0 g, 6.15 mmol) was added carefully to avoid the moisture. The mixture was heated under reflux in an oil bath at 85 °C for 120 h. The content of reaction, after cooling, was poured into diethyl ether (300 mL). The ether solution was washed with cold water (3 x 100 mL) and dried over magnesium sulfate. After removing the solvent, a creamy coloured crude product was left., which was recrystallized from dichloromethane to yield 9.5 g (74% yield) of colorless crystals of 2,2,2-trinitroethyl-formate.

GAP was mixed with crosslinking agent (1,1,1-Tris(hydroxymethyl)propane) and dibutyltin dilaurate was added, the mixture was stirred under vacuum in a vertical mixer (500 mL) for 30 minutes at 40 °C. TNEF was added in three portions and stirred for another 30 minutes. Then, the mixture was cured by adding HMDI at 50 °C and mixing process remained for another 30 minutes. Finally, the prepared propellant samples were poured in a specific mold and were cured in a vacuum oven at 60 ± 2 °C for seven days. The weight percentage of the oxidizer to the binder system was 86:14 wt %. The ADN/GAP formulation was prepared by the same method using oxidizer to binder system ratio 84:16 wt % respectively. The selected percentage of each propellant will be discussed later in the theoretical calculation results.

JEOL Eclipse 400 instrument was used to determine the NMR spectra of TNEF. The chemical shifts were obtained based on the external standards Me_4Si (^1H, 399.8 MHz; ^{13}C, 100.5 MHz) and $MeNO_2$ (^{14}N, 28.8 MHz). Impact sensitivity was measured by using BAM falling hammer test obtained from OZM Company, while the friction sensitivity was determined by using BAM friction test [35-37]. The morphology of the studied crystals as well as the homogeneity of the prepared propellant were studied by using SEM (FEI - Helios G3 UC). EXPLO5 thermodynamic code version_6.03 was used to determine the combustion characteristics of the propellant samples. The combustion conditions are based on the ideal gas equation of state with 70 atm combustion chamber pressure and under isobaric combustion. The gaseous products and the specific impulse of the propellant samples were calculated. The thermal decomposition kinetics of the samples were studied using Thermogravimetric Analysis (Perkin-Elmer, TGA 4000) where 1–3 mg samples were

examined at different heating rates of 1, 3, 5 and 7 K min^{-1} in the temperature range 30–500 °C under a flow of dynamic nitrogen of 20 ml min^{-1}). The thermal behavior was determined by using LINSEIS DSC – PT10 with samples of approximately 3 mg placed in an aluminum pan with a pin-hole cover at a heating rate of 5 K min^{-1} in a temperature range of 25 to 400 °C.

The determination of the kinetic triplets which are pre-exponential factor (*A*), kinetic model (*f*(α)) and the activation energy (E_a) are very important for the kinetic analysis, which should be determined for complete description of the kinetics. Many analytical methods are available nowadays that can be used to determine the kinetic parameters of solid-phase reactions. Model-fitting and isoconversional (model-free) methods are considered the two main methods to determine the kinetic parameters, which can be used either isothermally or nonisothermally [38-41].

The activation energy (E_a) of the decomposition reaction of the samples can be calculated from Kissinger's method (eqn. 1) [42].

$$-\frac{Ea}{R} = \frac{d\ln(\beta/T_P^2)}{d(1/T_P)} \quad (1)$$

Where β is the heating rate and T_p is the DTG peak temperature at that rate. The activation energy can be calculated from the slop of the straight line of $\ln(\beta/T_p^2)$ versus $1/T_p$. Such rough integral approximation of the temperature may cause an inaccurate calculated values of E_a [43, 44]. More accurate equation was presented according to Starink [45] to calculate E_a which is commonly called the Kissinger–Akahira–Sunose (KAS) equation [46]:

$$ln\left(\frac{\beta_i}{T_{\alpha,i}^{1.92}}\right) = const - 1.0008\frac{E_\alpha}{RT_\alpha} \quad (2)$$

Results

The performance characteristics of the new competitor oxidizer (TNEF) and its GAP-based propellant formulation were calculated by using EXPLO5 V_6.03. The theoretical calculations of the best formulation based on ADN/GAP and TNEF/GAP are presented in Fig. 1. The optimum weight percentage of each oxidizer in the propellant formulation was selected to prepare the propellant formulation. It is clear that ADN with 84 wt% presents the highest specific impulse of the ADN/GAP propellant while TNEF with 86-88 wt% has the highest specific impulse of all the TNEF/GAP studied formulations. As a result, percentage of the oxidizer selected in the preparation of ADN/GAP propellant formulation was 84 wt%, while the TNEF percentage in the prepared TNEF/GAP propellant was 86 wt%.

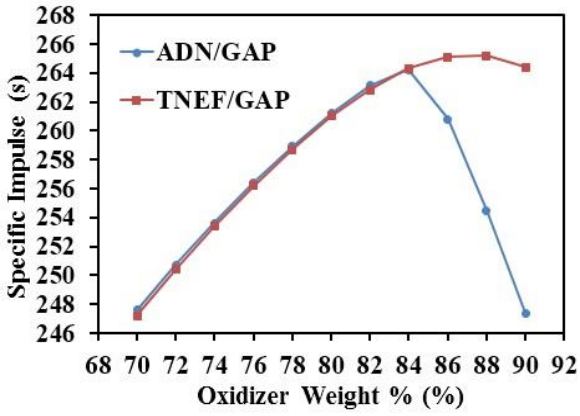

Figure 1. Relation between the oxidizer weight percentage in each propellant and its specific impulse.

In order to check the gaseous products produced from the combustion of each propellant, Fig. 2 shows the calculated mole percentage of the reaction gaseous products at the nozzle exit for the TNEF/GAP propellant formulation in comparison with the ADN/GAP propellant. It is clear that the TNEF/GAP propellant produced percentage of CO_2 higher than ADN/GAP propellant (more than double the amount produced from ADN/GAP propellant). While the percentage of $H_2O_{(g)}$ is higher in case of ADN/GAP. As a result, it was predicted that the energy produced from the combustion of TNEF/GAP should be higher than that produced from ADN/GAP (heat of formation of CO_2 is higher than that of $H_2O_{(g)}$). In addition, the new oxidizer TNEF has specific impulse (I_s = 250.1 s) and characteristic exhaust velocity (C^* = 1408 m s^{-1}), which are higher than that of ADN (I_s = 202.4 s) and (C^* = 1243 m s^{-1}) respectively, which give it a feature of high combustion characteristics.

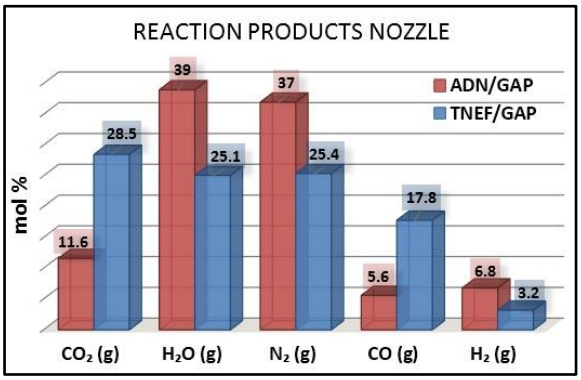

Figure 2. Reaction gaseous products at the nozzle exit.

The new oxidizer (TNEF) was characterized by ^1H, ^{13}C, and ^{14}N NMR spectroscopy. The $CH_2C(NO_2)_3$ singlet moiety in the ^1H NMR spectra can be determined at δ = 5.49 ppm in [D_6] acetone. The methylene groups carbon resonances (CH_2) could be observed at 63.7

ppm, while the carbon atom of the formate group was identified at 113.6 ppm and the trinitromethyl groups $C(NO_2)_3$ at 124.7 ppm in the ^{13}C NMR spectra. The nitrogen atom of $C(NO_2)_3$ group was found at –33.1 ppm in ^{14}N NMR spectra.

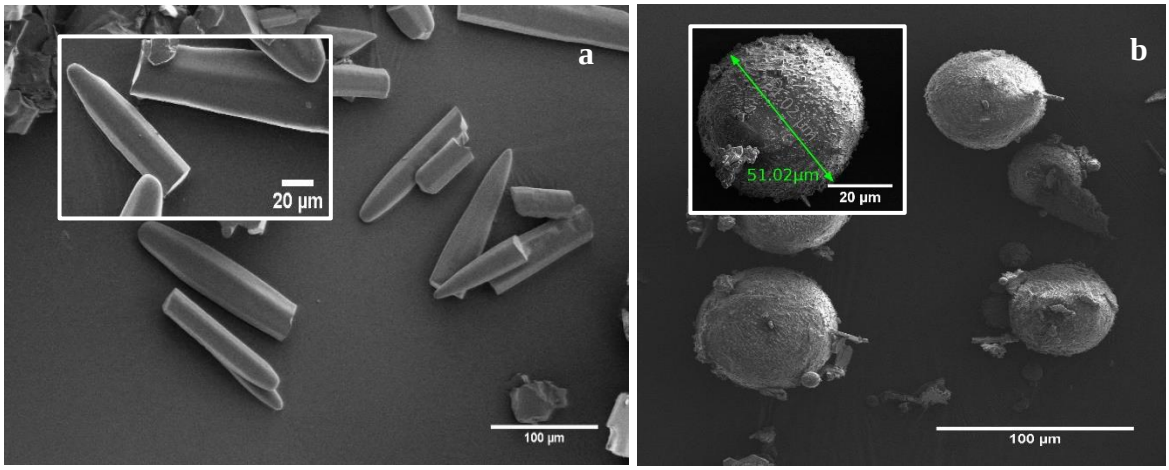

Figure 3. SEM of TNEF a) before and b) after recrystallization.

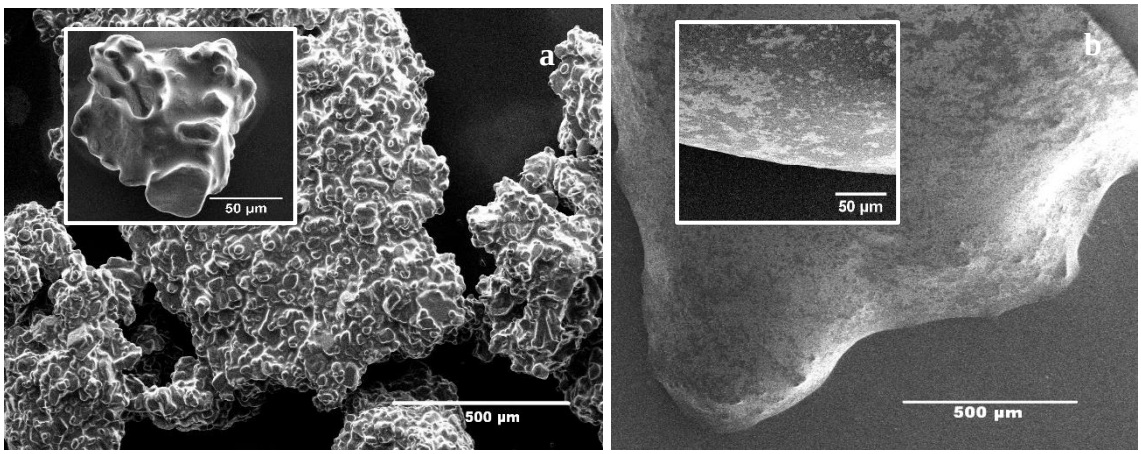

Figure 4. SEM of a) ADN/GAP and b) TNEF/GAP.

SEM was used in order to study the crystal morphology of the obtained TNEF. The prepared TNEF has irregular crystals with sharp edges. As a result, solvent/anti-solvent recrystallization techniques were applied to improve the morphology of TNEF. Three different solvents (acetonitrile, acetone and chloroform) and two anti-solvents (water and hexane) were used. It was concluded that the system based on acetone as a solvent and water as anti-solvent with ratio 1:10 volume percentage respectively was the best selection to obtain spherical crystals. The obtained crystals have average particle size of 50 µm with rough surface and uniform shape as shown in Fig. 3. After mixing of TNEF with the GAP polymeric matrix, it was observed that the crystals of TNEF were almost disappeared and a

homogenous mixture of TNEF/GAP propellant was obtained as shown in Fig. 4b. In case of ADN/GAP propellant, the irregular shape of ADN crystals were collected with each other (aggregation of ADN crystals) and coated by the GAP polymeric matrix as shown in Fig. 4a. By comparing the SEM photos of TNEF/GAP and ADN/GAP propellants, the homogenous mixing of TNEF/GAP is clear and it might be possible to predict the smooth burning behavior of TNEF/GAP propellant. In case of ADN/GAP propellant if the GAP matrix does not fill the entire space between the ADN crystals, the burning behavior could be uncontrolled due to the presence of voids. On the other side, it is predicted that the homogeneity of the prepared propellants will affect their thermal degradation process.

The sensitivity of the individual materials was studied where the results of impact and friction sensitivities measurements are presented in Table 1. The reported values are the 50% probability of initiation obtained by the Probit method [47].

Table 1. Sensitivity results of the studied individual energetic materials

Sensitivity	TNEF (raw)	TNEF (recryst.)	ADN	GAP	TNEF/GAP	ADN/GAP
Impact (J)	4.6	7.8	4.9	8.4	9.2	7.5
Friction (N)	92	106	280	>360	>360	>360

Here, the impact sensitivity resulted from uniaxial compression and friction sensitivity resulted from shear slide at certain constant volume for all the studied samples are presented. It is clear that the impact sensitivity of TNEF has been significantly decreased after the recrystallization process. While a small effect on the friction sensitivity appeared. This result is compatible with the results of SEM, where the spherical crystals of TNEF has lower sensitivity to impact than the raw crystals. The AND was used without recrystallization. The prepared propellants have low friction sensitivity (> 360 N), while the impact sensitivity of TNEF/GAP is lower than ADN/GAP, this result is also confirmed by the SEM photo of TNEF/GAP propellant which shows homogeneous mixture of the TNEF/GAP propellant formulation.

TG/DTG thermograms of TNEF, ADN, TNEF/GAP and ADN/GAP were recorded at four different heating rates 1, 3, 5, and 7 K min^{-1} (see Fig. 5 and Fig. 6).

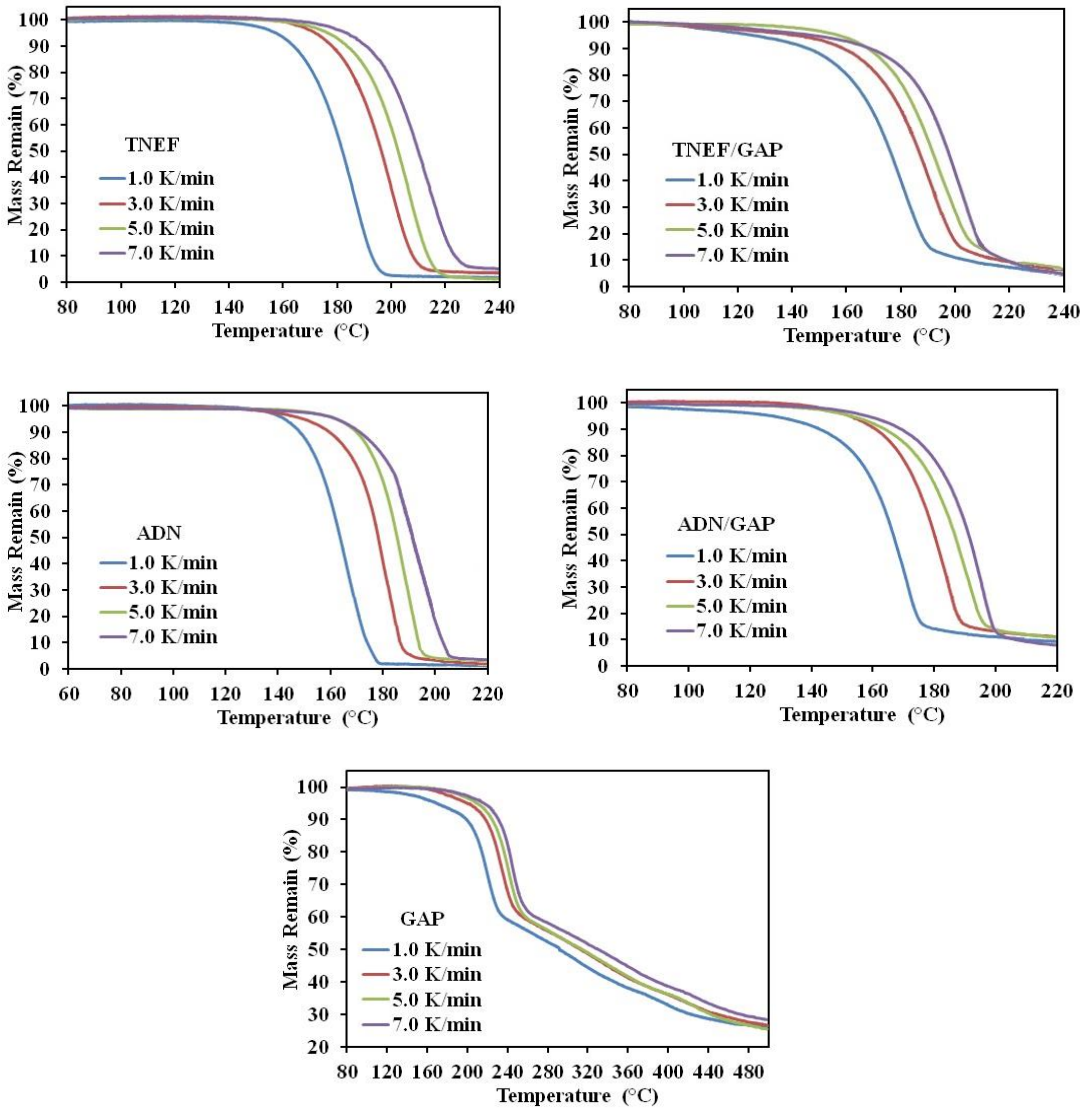

Figure 5. TG thermograms of TNEF, ADN, GAP, TNEF/GAP and ADN/GAP under different heating rates.

From the TG thermograms (Fig. 5), it is clear that TNEF starts its mass loss at temperature higher than that of ADN. The DTG curves presented on Fig. 6 showed maximum decomposition peaks at 206.2 °C for TNEF and 187.5 °C for ADN at 5 K min^{-1} heating rate. One-step decomposition process was observed for both TNEF and ADN. Regarding to the GAP binder, two steps decomposition stages were observed. The GAP polymer has rate of mass loss less than 75% where the mechanism of decomposition of the two decomposition stages are different. This might be due to the azido group decomposition at the first peak followed by the degradation of the main structure of the polymer [48]. It was stated in ref [48] that several explosives are dissolved in GAP matrix and may form complex where the explosives with high rigidity should have high thermal reactivity of the corresponding

GAP/PBX. In this study, the homogenous propellant TNEF/GAP has lower decomposition temperature than the pure oxidizer TNEF, this might be due to the dissolving of TNEF in the GAP matrix which affect its thermal stability and decreased the decomposition temperature of the pure TNEF. The onset decomposition temperature of TNEF was 190.7 °C while the prepared TNEF/GAP has onset decomposition temperature at 170.3 °C using 5 K min^{-1} heating rate. On the other side, the decomposition temperature of the propellant based on ADN/GAP is higher than that of the pure ADN. It means that the GAP matrix increased the decomposition temperature of the pure ADN. These results are compatible with the results of SEM, where ADN crystals were coated by the GAP matrix which improve the thermal decomposition of ADN.

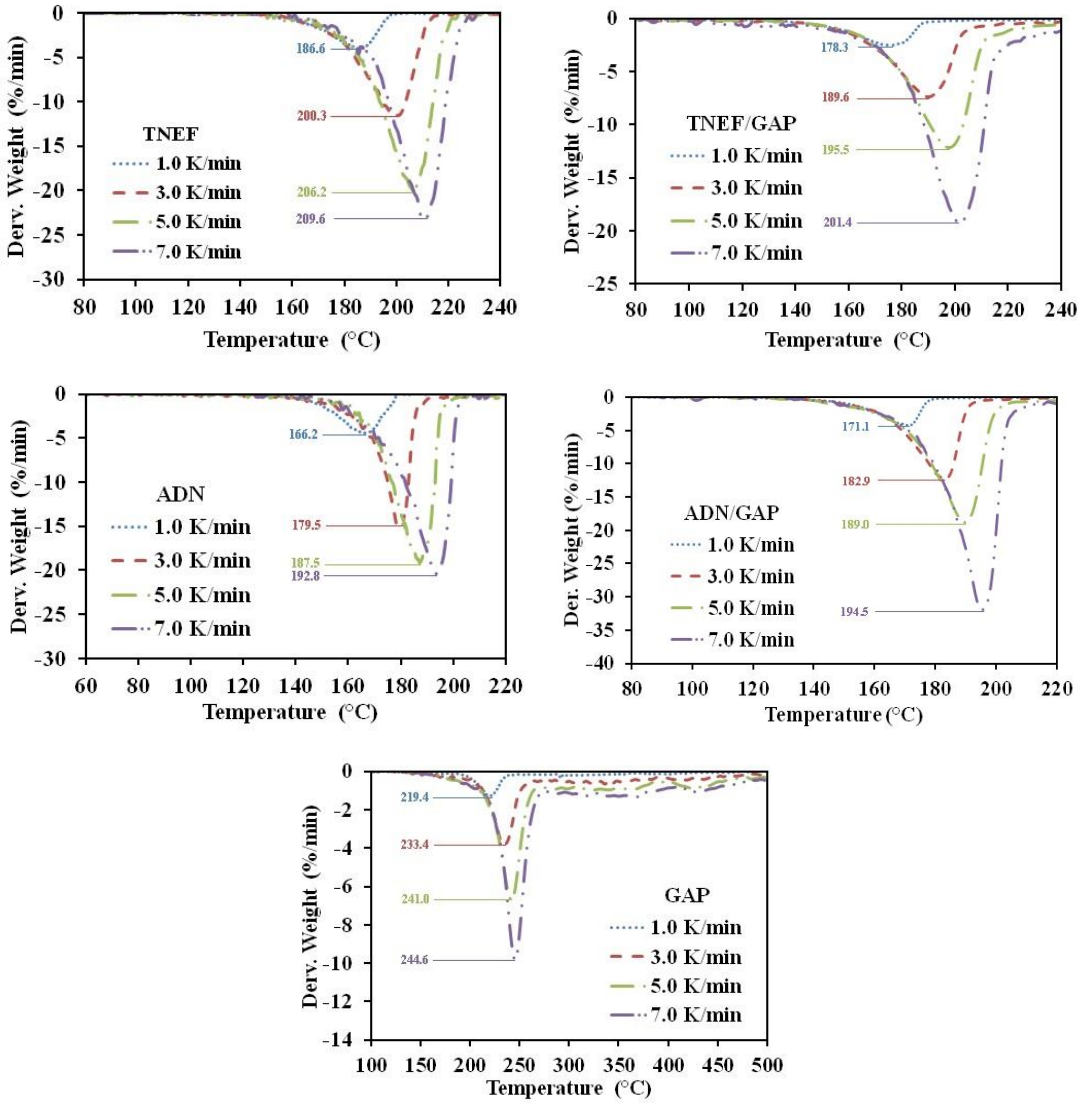

Figure 6. DTG curves of TNEF, ADN, GAP, TNEF/GAP and ADN/GAP under heating rates of 1, 3, 5 and 7 K min^{-1}.

From figure 6, it is clear that the onset decomposition temperature and the initial mass loss temperature of the studied samples increase by increasing the heating rates. On comparing the thermal decomposition results of TNEF/GAP and ADN/GAP propellants, it was observed that the new propellant based on TNEF has higher decomposition temperature compared with the traditional propellant based on ADN at each individual heating rate. The decomposition process of obtained propellant TNEF/GAP was unpredicted and it might be due to the dissolving of TNEF on GAP matrix or formation of complex between TNEF and GAP matrix, which affect the decomposition behavior of the propellant.

Table 2. The nonisothermal TG/DTG data of TNEF, ADN, GAP, TNEF/GAP and ADN/GAP

Material	β ($K\ min^{-1}$)	TG curves			DTG peaks	
		T_{ot} (°C)	T_i (°C)	Mass Loss (%)	T_p (°C)	T_{oe} (°C)
TNEF	1.0	170.8	182.3	98.6	186.6	188.9
	3.0	184.9	193.5	96.8	200.3	205.1
	5.0	190.7	202.6	99.1	206.2	210.9
	7.0	195.3	206.8	95.0	209.6	218.3
ADN	1.0	155.1	158.8	98.7	166.2	171.7
	3.0	169.4	172.2	97.1	179.5	183.1
	5.0	176.6	179.1	96.6	187.5	192.5
	7.0	186.4	188.8	94.1	192.8	196.5
GAP	1.0	198.2	201.6	72.7	219.4	235.0
	3.0	219.3	227.4	71.9	233.4	250.2
	5.0	224.4	232.3	74.8	241.0	257.3
	7.0	230.0	235.8	70.6	244.6	262.8
TNEF/GAP	1.0	151.8	164.3	93.3	178.3	184.0
	3.0	167.2	176.8	91.2	189.6	199.3
	5.0	170.3	183.5	90.8	195.5	209.0
	7.0	178.3	192.2	94.5	201.4	215.6
ADN/GAP	1.0	153.3	157.6	88.9	171.1	174.7
	3.0	167.0	171.7	85.4	182.9	188.2
	5.0	174.5	179.3	85.6	189.0	195.9
	7.0	181.3	185.9	90.2	194.5	200.4

Note: T_{ot}: onset decomposition temperature; T_{oe}: onset temperature of the end decomposition; T_i: initial thermal decomposition temperature; T_p: the maximum peak temperature; Mass Loss: from initial temperature to end temperature.

The thermal decomposition kinetics of the individual oxidizers as well as the propellant formulations were studied using nonisothermal TGA technique and their activation energies were determined using the conventional Kissinger method by applying Kissinger equation (eq. 1). The activation energy were obtained from the slop of the straight line from plotting $\ln(\beta/T^2)$ versus 1/T at the four selected heating rates, where T is the decomposition peak temperature which obtained from the DTG thermogram (Fig. 6). The activation energies of the TNEF and ADN were 146.4 kJ mol^{-1} and 117.2 kJ mol^{-1} respectively, while the activation energies of the propellant samples TNEF/GAP and ADN/GAP were 145.1 kJ mol^{-1} and 134.1 kJ mol^{-1} respectively. From this result, it is clear that the new oxidizer TNEF and its propellant TNEF/GAP have higher activation energy values than that of the ADN and its GAP-based propellant formulation, which give the advantage for TNEF.

The activation energy at the different fractional conversion was determined by using modified Kissinger–Akahira–Sunose (KAS) method. The Kinetic parameters of the individual energetic materials (ADN, TNEF, GAP) in addition to the prepared propellants (TNEF/GAP and ADN/GAP) are presented in Table 3 and 4. Fig. 7 shows the variations of the activation energy for the studied samples from reaction step to another. The mean values of activation energies were calculated at α interval from 0.3 to 0.7 due to the increased of inaccuracy from the tail peak of DTG [49-51].

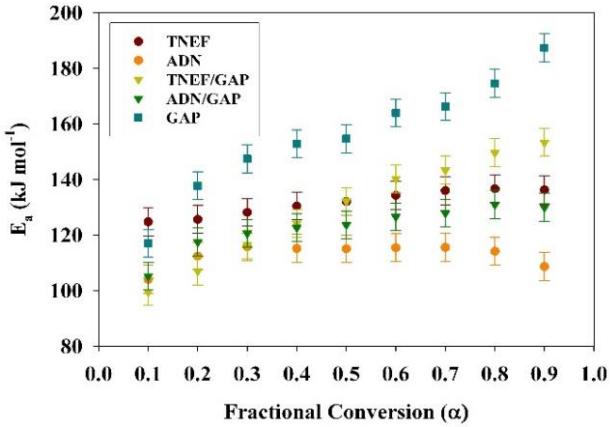

Figure 7. Activation energies for each fractional conversion (α) using KAS method.

The mean value of the activation energy of TNEF was found to be 132.1 kJ mol^{-1}, which is higher than ADN (115.3 kJ mol^{-1}). In case of ADN, the activation energy increased until 0.3 fractional conversion, then it starts to be nearly constant until 0.7 fractional conversion followed by decreasing at the end of the reaction conversion. The propellant based on

ADN/GAP has the same behavior as ADN until 0.3 fractional conversion with higher activation energies but it continue to increase slightly as the fractional conversions increase until it reached nearly 130 kJ mol^{-1} at 0.8 fractional conversion. On the other side, the activation energy of TNEF increases as the fractional conversion increases. At 0.1 fractional conversion, the activation energy of TNEF is 124 kJ mol^{-1} and slightly increases until reached maximum value at 0.8 fractional conversion (136 kJ mol^{-1}).

Table 3. Kinetic data of the new oxidizer (TNEF) and ADN obtained using the modified KAS method

α reacted	TNEF			ADN		
	E_a (kJ mol^{-1})	logA (s^{-1})	r	E_a (kJ mol^{-1})	logA (s^{-1})	r
0.1	123.8	12.08	0.998	102.3	9.98	0.978
0.2	124.7	11.98	0.998	111.1	10.89	0.990
0.3	127.3	12.15	0.999	114.2	11.15	0.993
0.4	129.6	12.31	0.998	113.8	11.01	0.997
0.5	131.6	12.45	0.999	113.9	10.94	0.999
0.6	133.6	12.60	0.998	114.1	10.91	0.999
0.7	135.4	12.72	0.998	114.2	10.84	0.998
0.8	136.0	12.71	0.997	112.6	10.59	0.998
0.9	135.5	12.55	0.996	106.8	9.79	0.998
Mean	131.5	12.45		114.0	10.97	

The new propellant TNEF/GAP has different behavior, an obvious increase in the activation energy with increasing of the fractional conversion. TNEF/GAP has activation energies ranging from 98-154 kJ mol^{-1}. By comparing the activation energies of the studied samples with the GAP binder, it is clear that GAP binder has the highest activation energy of all the studied samples at the same reaction conversion. The significant reduction of the activation energies at each conversion shows the effect of the decomposition of GAP binder (nitrene) [48] on the studied oxidizers and it might be due to the dissolution of the oxidizers in the intermediate decomposition products of the propellants, which cause the autocatalytic degradation products. It is well known that the decomposition of energetic materials represents a complex process and the difference in the activation energies of propellants and their individual components might be due to the complexity of the decomposition behavior.

Table 4. Kinetic data of the polymeric binder and the two propellant formulations obtained using the modified KAS method

α reacted	GAP			TNEF/GAP			ADN/GAP		
	E_a (kJ mol^{-1})	logA (s^{-1})	r	E_a (kJ mol^{-1})	logA (s^{-1})	r	E_a (kJ mol^{-1})	logA (s^{-1})	r
0.1	115.0	9.94	0.997	97.6	9.50	0.996	103.5	10.21	0.986
0.2	136.8	12.03	0.992	105.4	10.10	0.998	116.3	11.53	0.988
0.3	146.9	12.93	0.998	115.2	11.10	0.998	119.5	11.76	0.997
0.4	152.5	13.35	0.998	123.1	11.88	0.998	121.6	11.90	0.998
0.5	154.4	12.85	0.999	131.8	12.80	0.998	122.9	11.96	0.999
0.6	163.4	13.08	0.998	140.0	13.65	0.999	125.7	12.21	0.999
0.7	165.2	12.15	0.997	143.3	13.87	0.999	127.1	12.29	0.998
0.8	176.5	13.33	0.993	149.7	14.40	0.998	130.2	12.57	0.997
0.9	186.3	14.18	0.987	153.5	14.61	0.997	128.9	11.91	0.986
Mean	156.5	12.87		130.7	12.66		123.4	12.02	

The values of the activation energy of the studied samples by the different methods are presented in Table 5. The results obtained by Kissinger methods is slightly higher than that obtained by KAS method except for GAP binder. The maximum difference between the two methods is less than 12 %. The average activation energy of TNEF and its propellant is very close to each other and lower than the GAP binder. While the average activation energy of ADN is lower than its propellant where ADN/GAP has average activation energy lies between the activation energy of both GAP and ADN).

Table 5. Activation energies (E_a) for TNEF, ADN, GAP, TNEF/GAP and ADN/GAP using the different methods

Sample	Activation Energy E_a (kJ mol^{-1})	
	Kissinger	KAS
TNEF	146.4	131.5 ± 3.8
ADN	117.2	114.0 ± 2.6
GAP	152.8	156.5 ± 11.4
TNEF/GAP	145.1	130.7 ± 8.2
ADN/GAP	134.1	123.4 ± 5.3

The DSC thermograms of all the studied samples studied at heating rate 5 K min^{-1} are presented in Figure 8. In case of the pure ADN, a melting peak (endothermic) appeared at 95.5 °C as a max. peak followed by onset exothermic decomposition peak at 165.9 °C and maximum decomposition peak at 183.5 °C. While ADN/GAP propellant has melting peak at 93.1 °C, which is lower than that of ADN. The decrease of the melting temperature of the mixture may be due to the use of technical GAP which might acts as impurity and decreased the melting temperature of the pure ADN. In addition, the maximum peak decomposition temperature of ADN/GAP is 186.4 °C, which is higher than that of the pure ADN. This might be due to the high decomposition temperature of the pure GAP (245.7 °C max. peak temperature at heating rate 5 K min^{-1}) which acts as inhibitor in this case and increased the decomposition temperature of the propellant ADN/GAP. Table 6 includes the data of DSC measurements for the studied samples at heating rate of 5 K min^{-1}. In addition, it was found that the oxidizer TNEF has endothermic melting peak at 127.1 °C and followed by onset decomposition peak at 189.6 °C and maximum decomposition peak at 210.1 °C. It is obvious that TNEF has higher thermal stability compared with the oxidizer ADN. Regarding to the new propellant TNEF/GAP it was found that the maximum decomposition temperature of the propellant is lower than the pure TNEF by nearly 15 °C. It means that GAP binder decreased the decomposition temperature of TNEF even that GAP has decomposition temperature at 245.7 °C. This result confirms that TNEF might be dissolved in the polymeric matrix, which affects its thermal stability. Still the new propellant has decomposition temperature higher than the traditional propellant based on ADN/GAP.

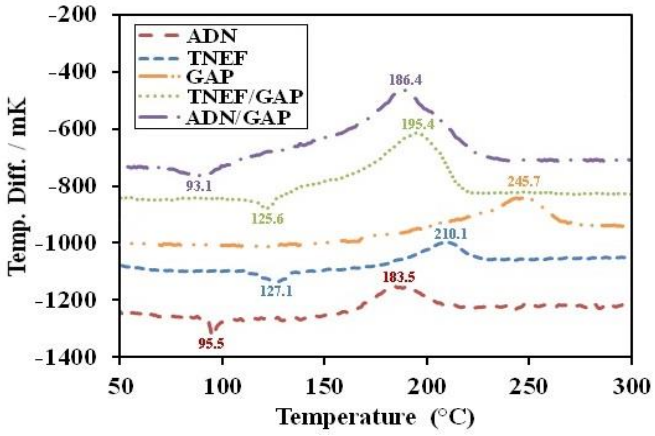

Figure 8. DSC thermogram of TNEF, ADN, TNEF/GAP and ADN/GAP at 5 K min^{-1} heating rate.

Table 6. The DSC data using non-isothermal DSC of TNEF, ADN, TNEF/GAP and ADN/GAP

Sample	Exothermic peak			Endothermic peak	
	T_o (°C)	T_p (°C)	T_e (°C)	T_{mo} (°C)	T_{mp} (°C)
TNEF	189.6	210.1	223.0	122.7	127.1
ADN	165.9	183.5	207.9	92.0	95.5
GAP	217.9	245.7	261.7	---	---
TNEF/GAP	178.4	195.4	209.6	121.3	125.6
ADN/GAP	169.8	186.4	200.8	89.6	93.1

Note: T_o: onset decomposition temperature; T_p: decomposition peak temperature; T_e: the end decomposition temperature; T_{mo}: melting onset temperature; T_{mp}: melting peak temperature.

Conclusions

2,2,2-trinitroethyl-formate (TNEF) is a new interesting competitor as a high energy dense oxidizer (HEDO) which has higher performance characteristics and thermal stability than the common ammonium dinitramide (ADN). The thermochemical calculations showed that TNEF has specific impulse of 250.1 s, which is higher than that of ADN (202.1 s). In addition, it has green decomposition gaseous products (chlorine-free) comparing with other common used oxidizer (ammonium perchlorate AP). The impact sensitivity of TNEF was improved through an easy and fast recrystallization process to decrease its impact sensitivity than ADN. The SEM photos showed high homogeneity degree of TNEF after recrystallization process with the energetic GAP matrix in comparison with the ADN oxidizer. The thermal study proved the higher thermal stability of TNEF that melts at 127.1 °C and decomposes at 210.1 °C in comparison with ADN that melts at 95.5 °C and decomposes at 183.5 °C. The kinetic study showed activation energy of TNEF (in the range of 132-146 ± 0.5 kJ mol^{-1}) higher than that of ADN (in the range of 114-117 ± 0.2 kJ mol^{-1}). TNEF is a promising high-energy dense oxidizer, which might have applications in future.

References

[1] D. Trache, T.M. Klapötke, L. Maiz, M. Abd-Elghany, L.T. DeLuca, *Green Chem.*, **2017**, 19, 4711-4736.

[2] L.T. DeLuca, in *"Chemical Rocket Propulsion"*. Switzerland: Springer, **2017**, pp. 1015-1032.

[3] H. Singh, in *"Chemical Rocket Propulsion"*. Switzerland: Springer, **2017**, pp. 127-138.

[4] A. Mezroua, K. Khimeche, M.H. Lefebvre, M. Benziane, D. Trache, *J. Therm. Anal. Calorim.,* **2014**, 116 (1), 279-286.

[5] D. Trache, F. Maggi, I. Palmucci, L.T. DeLuca, *J. Therm. Anal. Calorim.,* **2018**, 132 (3), 1601-1615.

[6] D. Trache, F. Maggi, I. Palmucci, L.T. DeLuca, K. Khimeche, M. Fassina, S. Dossi, G. Colombo, *Arab. J. Chem.,* **2015**, DOI: 10.1016/j.arabjc.2015.11.016

[7] A. Provatas, **2000**, (DSTO-TR-0966 Australia).

[8] E.T. Urbansky, *Environ. Sci. Pollut. Res.,* **2002**, 9 (3), 187-192.

[9] K. Sellers, K. Weeks, W.R. Alsop, S.R. Clough, M. Hoyt, B. Pugh, J. Robb, *"Perchlorate: Environmental Problems and Solutions"*. New York: CRC press, **2006**.

[10] M. Talawar, R. Sivabalan, T. Mukundan, H. Muthurajan, A. Sikder, B. Gandhe, A.S. Rao, *J. Hazard. Mater.,* **2009**, 161 (2), 589-607.

[11] M.A. Kettner, T.M. Klapötke, in *"Chemical Rocket Propulsion"*. Switzerland: Springer, **2017**, pp. 63-88.

[12] T.M. Klapötke, *"Chemistry of High-Energy Materials"*. Germany: Walter de Gruyter GmbH & Co KG, **2017**.

[13] G.D. Hugus, E.W. Sheridan, **2013**, US8444785.

[14] M. Kohga, *Propellants Explos. Pyrotech.,* **2017**, 42 (6), 665-670.

[15] M. Abd-Elghany, T.M. Klapötke, A. Elbeih, *J. Anal. Appl. Pyrolysis,* **2017**, 128, 397-404.

[16] S.-M. Shen, S.-W. Wang, Y.-S. Chiu, S.-I. Chen, F.-M. Chang, C.-C. Huang, *Thermochim. Acta,* **1993**, 216, 255-266.

[17] K. Menke, T. Heintz, W. Schweikert, T. Keicher, H. Krause, *Propellants Explos. Pyrotech.,* **2009**, 34 (3), 218-230.

[18] K. Menke, J. Böhnlein-Mauß, H. Schubert, *Propellants Explos. Pyrotech.,* **1996**, 21 (3), 139-145.

[19] W.Q. Pang, L.T. DeLuca, H.X. Xu, X.Z. Fan, F.Q. Zhao, W.X. Xie, in *"Chemical Rocket Propulsion"*. Switzerland: Springer, **2017**, pp. 403-423.

[20] G.-P. LI, M.-H. LIU, L.-H. SHEN, Y. Luo, *Chin. J. Explos. Propellants*, **2015**, 38 (2), 25-29.

[21] S. Cerri, M.A. Bohn, K. Menke, L. Galfetti, *Propellants Explos. Pyrotech.,* **2014**, 39 (2), 192-204.

[22] M.A. Bohn, S. Cerri, in *"Chemical Rocket Propulsion"*. Switzerland: Springer, **2017**, pp. 771-800.

[23] G. Santhosh, S. Venkatachalam, A. Francis, K. Krishnan, K. Catherine, K. Ninan, in *33rd Int. Annu. Conf. ICT*, Karlsruhe, Germany, **2002**, 64/1-64/14.

[24] A. Larsson, N. Wingborg, in *"Advances in Spacecraft Technologies"*. Croatia: InTech, **2011**.

[25] M.Y. Nagamachi, J.I.S. Oliveira, A.M. Kawamoto, R.d.C.L. Dutra, *J. Aerosp. Technol. Manag.,* **2009**, 1 (2), 153-160.

[26] D.E. Jones, Q.S. Kwok, M. Vachon, C. Badeen, W. Ridley, *Propellants Explos. Pyrotech.*, **2005**, 30 (2), 140-147.

[27] J. Agrawal, S. Walley, J. Field, *J. Propul. Power*, **1997**, 13 (4), 463-470.

[28] S.R. Chakravarthy, J.M. Freeman, E.W. Price, R.K. Sigman, *Propellants Explos. Pyrotech.*, **2004**, 29 (4), 220-230.

[29] T.M. Klapötke, B. Krumm, R. Moll, S.F. Rest, *Z. Anorg. Allg. Chem.,* **2011**, 637, 2103-2110.

[30] B. Gaur, B. Lochab, V. Choudhary, I. Varma, *J. Macromol. Sci., Part C: Polym. Rev.,* **2003**, 43 (4), 505-545.

[31] M. Eroğlu, O. Güven, *J. Appl. Polym. Sci.,* **1996**, 61 (2), 201-206.

[32] T. Wang, S. Li, B. Yang, C. Huang, Y. Li, *J. Phys. Chem. B,* **2007**, 111 (10), 2449-2455.

[33] A. Elbeih, T.Z. Wafy, T. Elshenawy, *Cent. Eur. J. Energ. Mater.*, **2017**, 14 (1), 77-89.

[34] W. Kim, Y. Kwon, Y.M. Jo, Y.C. Park, *J. Energ. Mater.,* **2017**, 35 (1), 44-52.

[35] M. Suceska, *"Test Methods for Explosives"*. New York: Springer, **2012**.

[36] S.A. NATO, **1999**, STANAG 4489.

[37] S.A. NATO, **2002**, STANAG 4487.

[38] A. Khawam, D.R. Flanagan, *J. Pharm. Sci.,* **2006**, 95 (3), 472-498.

[39] M. Abd-Elghany, T.M. Klapötke, A. Elbeih, *Propellants Explos. Pyrotech.,* **2017**, 42 (12), 1373-1381.

[40] D. Trache, *Carbohydr. polym.,* **2016**, 151, 535-537.

[41] D. Trache, A. Abdelaziz, B. Siouani, *J. Therm. Anal. Calorim.,* **2017**, 128 (1), 335-348.

[42] H.E. Kissinger, *Anal. Chem.*, **1957**, 29, 1702-1706.

[43] S. Vyazovkin, A.K. Burnham, J.M. Criado, L.A. Pérez-Maqueda, C. Popescu, N. Sbirrazzuoli, *Thermochim. Acta,* **2011**, 520 (1), 1-19.

[44] D. Trache, K. Khimeche, A. Mezroua, M. Benziane, *J. Therm. Anal. Calorim.*, **2016**, 124 (3), 1485-1496.

[45] M. Starink, *Thermochim. Acta*, **2003**, 404 (1), 163-176.

[46] T. Akahira, T. Sunose, *Res. Report Chiba Inst. Technol. (Sci. Technol.),* **1971**, 16, 22-31.

[47] J. Šelešovský, J. Pachmáň, *Cent. Eur. J. Energ. Mater.*, **2010**, 7 (3), 269-278.

[48] A.K. Hussein, S. Zeman, A. Elbeih, *Thermochim. Acta*, **2018**, 660, 110-123.

[49] M. Abd-Elghany, T.M. Klapötke, A. Elbeih, S. Zeman, *J. Anal. Appl. Pyrolysis*, **2017**, 126, 267-274.

[50] S. Zeman, Q.-L. Yan, A. Elbeih, *Cent. Eur. J. Energ. Mater.*, **2014**, 11 (3), 395-404.

[51] Q.-L. Yan, S. Zeman, P. Sánchez Jiménez, T.-L. Zhang, L. Pérez-Maqueda, A. Elbeih, *J. Phys. Chem. C*, **2014**, 118 (40), 22881-22895.